ANNUAL REPORT

East Texas and Western Louisiana Coastal Erosion Study

Year 3

Robert A. Morton, James C. Gibeaut, and William A. White
Assisted by Radu Boghici and Kevin Lyons

Prepared for the U.S. Department of Interior
U.S. Geological Survey

Cooperative Agreement No. 14-08-0001-A0912

Bureau of Economic Geology
Noel Tyler, Director
The University of Texas at Austin
Austin, Texas 78713-8924

October 1994

CONTENTS

Addenda (attached)

Report Organization

The following report summarizes the major accomplishments achieved by the Bureau of Economic Geology during the third year study (FY 93-94) of coastal erosion and wetlands loss along the southeastern Texas coast. The report covers activities between July 1, 1993, and August 31, 1994. Major accomplishments are reported for each work element and task identified in the cooperative agreement. Documents summarizing the major accomplishments and containing the important scientific conclusions are included as Addenda 1-5.

Work Element 1: Coastal Erosion Analysis

The coastal erosion work element is intended to (1) establish a computerized database of historical shoreline positions (1882-1982), (2) update the database using the most recent shoreline information (1990's), (3) analyze historical trends of shoreline movement in the context of the regional geologic framework and human modifications, (4) synthesize the physical and habitat characteristics of different shoreline types, (5) establish a network of field monitoring sites for surveying coastal changes, and (6) prepare documents of shoreline change suitable for coastal planning and resource management.

Task 1: Shoreline Mapping. During the third year of study we completed mapping of the Gulf shoreline on 1990 aerial photographs obtained from the Texas Department of Transportation. The photographs cover approximately three-fourths of the project area (High Island to Brown Cedar Cut). Mapped shorelines were digitized and stored in the Bureau ARC/INFO geographic information system for comparison with previously defined shoreline positions to determine changes and trends. Magnitudes and rates of shoreline movement for the most recent time period (1982-1990) were determined at transect sites spaced approximately 5,000 ft apart along the shore. Plots of cumulative shoreline movement through time were prepared, trends were analyzed, and the most recent representative trends and time periods were selected for additional computations. Results of this work have been submitted to the Texas General Land Office for incorporation into their Coastal Zone Management plan.

The only segment where the 1990's shoreline update remains to be done is from Sabine Pass to High Island. Further work regarding shoreline movement along the southeastern Texas Coast is pending more recent low-altitude aerial photographs. The most recent photographs of the remaining area are too small (1:62,500) to accurately depict the shoreline. The U.S. Fish and Wildlife Service indicates that it plans to take 1:24,000 photographs of the upper Texas Coast

possibly in the fall of 1994 as part of an inventory of sea grasses. If these photographs become available, they will be used to complete the coastal erosion analysis of the study area.

We also examined the relationship between wetland loss and accelerated relative sea-level rise resulting from human-induced subsidence and faulting along the upper Texas coast. Wetland loss in the Galveston Bay and Sabine Lake estuaries, and interfluvial area between the estuaries was analyzed. In the interfluvial area, brackish marshes that have been converted to open water along an active fault were mapped and digitized to determine the extent of losses. Synthesis of data on wetland losses along the upper Texas coast shows that more than 11,700 ha of vegetated wetlands have been replaced by shallow subaqueous flats and open water. Salt, brackish, and fresh marshes and fluvial woodlands have been affected. Major losses have occurred in fluvial-deltaic areas along the Neches and Trinity rivers. Although many processes or activities may contribute to wetland loss, human-induced subsidence resulting from ground-water withdrawal is a major process affecting wetlands along the upper Texas coast. Additionally, submergence of wetlands is associated, locally, with faulting and subsidence apparently related to hydrocarbon production. A paper on this analysis was completed and submitted to the *Journal of Coastal Research.* The title of the paper by W. A. White and T. A. Tremblay is "Submergence of Wetlands as a Result of Human-Induced Subsidence and Faulting along the Upper Texas Gulf Coast" **(Addendum 1)**.

In addition, results of studies detailing the spatial and temporal changes in marsh distribution in the Galveston Bay System were presented at the 15th Annual Meeting of the Society of Wetland Scientists held in Portland, Oregon, May 30-June 3, 1994. This paper was partially funded by the USGS Coastal Erosion Project. Among the findings presented were (1) approximately 20 percent of salt, brackish, and fresh marsh habitats have been lost in the Galveston Bay system since the early 1950's, and (2) a major cause of the loss is accelerated rates of subsidence due to ground-water withdrawal.

Task 2: Geomorphic Characterization. During year 3, geomorphological characteristics and classifications of the Gulf shoreline, interior bay shores, and the Intracoastal Waterway were combined with other criteria to produce shoreline type maps for oil spill response and contingency planning. Also, we conducted an overflight covering all of the shores of the study area (Gulf and inland coastal water bodies) in conjunction with Miles Hayes of Research Planning Inc. (RPI). This work was supported primarily by the Texas Natural Resources Inventory Program, but it relied heavily on prior geomorphological mapping conducted as part of the USGS Coastal Erosion project.

SIGNIFICANT RESULTS. We prepared a report that summarizes and illustrates significant wetland losses within the Galveston-Trinity Bay system and the Sabine Lake estuarine system

(Addendum 1). The report concludes that most of these losses are caused by land-surface subsidence, reductions in fluvial sediment supply to the flood basins and river deltas, and wave erosion around the open shores of the major bays and Gulf of Mexico. Results of Galveston Bay wetland-loss studies were presented at the Society of Wetland Scientists annual meeting, and an abstract entitled "Marsh Loss in the Galveston Bay System, Texas," by W. A. White, T. A. Tremblay, and E. G. Wermund was published in the conference proceedings.

Results of the joint BEG/RPI shoreline type mapping project will be provided to the Texas General Land Office and NOAA in an electronic format.

Work Element 2: Regional Geologic Framework

Work element 2 investigated the geologic origin and evolution of the principal subenvironments that are present along the southeastern Texas coast. This is being accomplished by establishing a chronostratigraphic framework for the coastal systems and reconstructing the evolution of coastal environments during the post-glacial rising phase and highstand in sea level. This work element will also provide data on the physical characteristics and natural habitats of the various shoreline types in the context of shoreline stability.

Task 1: Stratigraphic Analysis. The study area encompasses a diverse assemblage of depositional environments ranging from non-marine fluvial systems and transitional coastal systems to the marine continental shelf. During year 3, we used vibracores, faunal assemblages, isotopic dates, and seismic surveys to investigate the late Quaternary and Holocene stratigraphy of several of these environments. These data were used to construct cross sections illustrating the various coastal and non-marine facies. Eventually we plan to construct a detailed sea-level curve for the late Holocene and Modern time periods. Results of these investigations will provide a basis for predicting future magnitudes and rates of land loss.

Subtask 1: Data Inventory and Compilation. In year 3 we constructed cross-valley topographic profiles and refined stratigraphic cross sections of major alluvial valleys and bayhead deltas of the southeastern Texas coast including the Sabine, Neches, Trinity, and San Jacinto Rivers. The stratigraphic cross sections were constructed using descriptions of foundation borings acquired for geotechnical investigations. The cross sections, which depict sedimentary facies, relative age relationships, and major unconformities, illustrate the lithostratigraphy of the late Quaternary valley fill. Depositional environments interpreted from the cross sections show a progressive marine influence in downstream regions and fluvial influence in upstream regions. Buried fluvial terraces were identified from the cross sections and from the work of Pearson et al. (1986), which

encompasses the region immediately offshore from Sabine Pass. Stratigraphic cross sections of the Sabine-Neches entrenched valley were used to locate seismic profiles and to select sites for possible vibracores during the summer field work.

Foundation boring descriptions were obtained for the Trinity River crossings at Romayor and at Moss Hill from the Texas Department of Transportation. Cross sections constructed from these data extended the shallow subsurface control upstream to the exposed terraces of the Deweyville, which are also observed along the Sabine and Neches Rivers.

We compiled approximately 130 radiocarbon dates, sample depths, and interpreted depositional environments for the study area from published reports including Nelson and Bray (1970), Pearson et al. (1986), and Thomas (1990). Maps for each depositional environment were prepared showing the locations, depths, and ages of samples corresponding to that environment. These maps will be interpreted to determine if they show any systematic shifts in depositional environments during the late Pleistocene-Holocene rise in sea level.

Subtask 2: Field Studies. During year 3, we prepared, photographed and described 15 deep subsurface cores in the entrenched valley fill of the Neches River, the chenier plain of southeastern Texas, and the coastal wetland interfluve between the Sabine and Trinity River systems. The hollow-stem auger cores taken by the Bureau of Economic Geology drill rig penetrated Holocene washover and marsh deposits that comprise the coastal interfluve between the Sabine and Galveston entrenched valleys. Vibracores previously taken in the McFaddin National Wildlife Refuge will be compared with the auger cores taken from the same general area.

SIGNIFICANT RESULTS. Descriptions of the auger cores were completed and are presented in **Addendum 2.** Preliminary interpretations of depositional environments were made on the basis of detailed descriptions, and preliminary stratigraphic cross sections were prepared for the interfluve, chenier plain, and incised valley areas. A wood sample from a deep boring in the Neches entrenched valley near Sabine Pass was submitted to Beta Analytic, Inc. for ^{14}C analysis. Results of the test indicate that the lower alluvial valley of the Sabine/Neches system was flooded about 8800 years ago. An organic sample from the Sabine Bank deposits in the Gulf of Mexico, which was also submitted to Beta Analytic, yielded a date of about 7800 BP. Additional datable materials (shells, wood, peat) have been identified and will be analyzed for ^{14}C in 1995.

Work Element 3: Coastal Processes

Understanding coastal processes is the key to understanding coastal erosion and predicting future coastal changes. Therefore, this work element involves numerous tasks that attempt to

quantify basin energy, sediment motion, and the forcing functions that drive the coastal system. Objectives of this work element are to evaluate the magnitudes and rates of the relative rise in sea level during geological and historical time, to provide a basis for assessing wave and current energy as well as sediment transport, to assess climatic and meteorological influences on coastal processes, to evaluate the impacts of storms on shoreline stability and instantaneous erosion potential, and to begin quantifying the coastal sediment budget.

Task 2: Sediment Transport. We obtained from the National Weather Service (NWS) paper records of meteorological data for the Galveston weather station and digital data for the Houston Intercontinental Airport. The data set includes 10 years of hourly wind speed, wind direction, and barometric pressure. The records extend from 1983 (pre-Hurricane Alicia) through 1993. Computer programs were written to extract, analyze, and plot the data from the NWS files. Preliminary time-series plots were displayed to illustrate daily average wind speed, daily average wind direction, daily average pressure, and selected hourly pressures (at the time of Hurricane Alicia) to check for data quality and formats. The preliminary plots and tables show the data to be in excellent condition with only a very small percentage of missing data. We also obtained the NOAA Marine Environmental Buoy Database for the Gulf of Mexico on CD ROM. This database includes meteorological, wave, and oceanographic data from the Coastal-Marine Automated Network (C-MAN) stations operated by the NOAA National Data Buoy Center. We will compare these data with the more complete record from Houston Intercontinental Airport.

Task 3: Sediment Budget. This task will evaluate the primary sediment sources (updrift erosion and fluvial sediment supply) and the principal sinks (beach accretion, onshore washover, dune construction, and offshore deposition). Some additional sediment losses occur at tidal inlets, and some unknown quantity is trapped in the deep-draft navigation channels. Material periodically dredged from the ship channels deserves further evaluation as a potential source of beach nourishment material. During the third year of study, we continued to analyze the 10-year post-Alicia record of beach profile data at seven sites between Galveston Island and Follets Island. Emphasis was placed on volumetric changes and the alongshore gains and losses in sand attributed to cross shore and alongshore transport processes. Results indicate a broad range of beach responses immediately after and 10 years after the storm ranging from continuous erosion to continuous accretion. Additional analyses were conducted to compare rates of shoreline movement calculated from beach surveys with those derived from aerial photographs. Results of this analysis showed that storms commonly accelerate rates of shoreline movement and the accelerations can dramatically affect predicted shoreline positions based on short-term rates of shoreline movement.

SIGNIFICANT RESULTS. A summary report presenting the findings of the beach profile comparison on Galveston Island and Follets Island was accepted and published by the Journal of Coastal Research. The report, entitled "Stages and Durations of Post-storm Beach Recovery, Southeastern Texas Coast, U.S.A.," is included as **Addendum 3**. These same beach profiles also are being used to track time-dependent volumetric and morphological changes of the beaches. Results of that study have been submitted for publication in the Proceedings volume of the Large-Scale Coastal Behavior Conference. The manuscript, entitled "Meso-Scale Transfer of Sand during and after Storms: Implications for Prediction of Shoreline Movement," is included as **Addendum 4**. In this paper we illustrate how sediment transport directions can be derived from the hourly wind data, a technique that greatly improves our ability to understand the changes in beach volume. The paper also suggests that rates of shoreline movement are accelerated after a major storm.

Work Element 4: Prediction of Future Coastal Response

Task 1: Mathematical Analysis of Rates of Change. In year 3 development continued on the Shoreline Shape and Projection Program (SSAP) that will aid in determining future shoreline positions. The program will project future shoreline positions based on established methods that compute shoreline rates-of-change and a new method that involves comparing the shape of the projected shoreline with the expected shape. SSAP is being developed in FORTRAN for the Windows operating environment and is designed to easily accept historical shoreline data from a Geographic Information System (GIS) and to return projected shorelines to the GIS.

Work on SSAP in year 3 involved checking the algorithms that compute shoreline rates-of-change. Rate-of-change calculations from the literature and Bureau publications were compared with calculations from SSAP. Results from a computer program provided by Mike Fenster of the University of Virginia (UVA) were also compared. All comparisons have been favorable even though there were some slight differences with the UVA program and results published by Fenster et al. 1993, in the Journal of Coastal Research. The cause of these differences has been traced to variations in the methods of calculations and errors in the literature.

SIGNIFICANT RESULTS. The program variables were documented to assist in subsequent program trouble shooting, additions, and upgrades. Variable names, types, uses, and occurrences have been traced through the program's subroutines and presented in a table.

Work Element 5: Sand Resources Investigations

During year 3 we obtained the wave refraction model RCPWAVE provided by the U.S. Army Corps of Engineer's Coastal Engineering Research Center. Results from the model will be compared to large-scale (5 km) geomorphic features of the southeast Texas shoreline from East Matagorda Bay to Sabine Pass. Also we constructed a rectilinear bathymetric grid covering the study area, which is 300 km long and extends 100 km offshore to depths of 30 m. Grid cells measure 500 m alongshore and 125 m normal to shore forming a grid with 600 by 800 cells. Digital bathymetric data used to construct the grid were obtained from Mark Hanson of the U.S. Geological Survey in St. Petersburg, Florida. We used a combination of bathymetric data from surveys dating from the 1930's to the 1970's. Care was taken to use the latest available data for a particular area. Preliminary plots of the compiled bathymetry were printed to check for missing data and for quality control.

Of the eight vibracores (3 to 6 m deep) collected from Sabine Bank in cooperation with the MMS Sand Assessment project, several cores were selected for subsampling the mud unit beneath the sand body and beneath the interpreted ravinement surface. The samples were made available to a graduate student in the University of Texas Department of Geological Sciences for identification of the microfauna and interpretation of the depositional environment based on faunal assemblages and salinity regimes.

SIGNIFICANT RESULTS. Preliminary analyses of the foraminifera assemblages indicate that the muddy sediments beneath the ravinement surface at the base of Sabine Bank were deposited in a nearshore open marine environment, which confirms our interpretation of an inner shelf shallow-water depositional setting of the sand bank.

Work Element 6: Technology Transfer

The technology transfer work element provides for timely reporting of project results and makes the interpretations and conclusions available to users as needed. It also establishes a repository to preserve raw data and materials that would be a significant source of information for future studies.

SIGNIFICANT RESULTS. In year 3, a paper entitled "Geo-Indicators of Coastline and Wetland Changes" was presented at the International Union of Geological Sciences Workshop on Geological Indicators of Rapid Environmental Change. The workshop was held at Corner Brook, Newfoundland, Canada. A copy of the paper, which has been submitted for publication in the workshop proceedings volume, is included as **Addendum 5**.

References

Fenster, M. S., Dolan, R., and Elder, J. F., 1993, A new method for predicting shoreline positions from historical data: Journal of Coastal Research, v. 9, p. 147-171.

Nelson, H. F., and Bray, E. E., 1970, Stratigraphy and history of the Holocene sediments in the Sabine-High Island area, Gulf of Mexico, in Morgan, J. P., and Shaver, R. H., editors, Deltaic sedimentation, modern and ancient: Society of Economic Paleontologists and Mineralogists Special Publication 15, p. 48-77.

Pearson, C. E., Kelley, D. B., Weinstein, R. A., and Gagliano, S. M., 1986, Archaeological investigations on the outer continental shelf: a study within the Sabine River valley, offshore Louisiana and Texas: Coastal Environments, Inc., Report prepared for Mineral Management Service, 314 p.

Thomas, M. A., 1990, The impact of long-term and short-term sea level changes on the evolution of the Wisconsinan-Holocene Trinity/Sabine incised valley system Texas continental shelf: unpub. Ph.D. dissertation, Rice University, Houston Texas, 247 p.

Addendum 1. Submergence of Wetlands as a Result of Human-Induced Subsidence and Faulting along the Upper Texas Gulf Coast

Journal of Coastal Research	10	4	00–00	Fort Lauderdale, Florida	Fall 1994

Submergence of Wetlands as a Result of Human-Induced Subsidence and Faulting along the upper Texas Gulf Coast

William A. White and Thomas A. Tremblay

Bureau of Economic Geology
The University of Texas at Austin
University Station, Box X
Austin, TX 78713, U.S.A.

ABSTRACT

WHITE, W.A. and TREMBLAY, T.A., 1994. Submergence of wetlands as a result of human-induced subsidence and faulting along the upper Texas Gulf Coast. *Journal of Coastal Research*, 10(4), xxx–xxx. Fort Lauderdale (Florida), ISSN 0749-0208.

Loss of wetlands in the northern Gulf of Mexico has been attributed to numerous processes and is of continuing concern. This paper synthesizes and examines the distribution and extent of wetland losses along the upper Texas coast in relation to subsidence and faulting associated with underground fluid production. Since the 1930's, these processes have been of primary importance along the upper Texas coast, contributing to the conversion of thousands of hectares of vegetated coastal wetlands to either open water or shallow subaqueous flats. Relatively large wetland losses have occurred in salt, brackish, and fresh marshes and woodlands in the Galveston Bay and Sabine Lake estuarine systems on the upper Texas coast. Throughout Galveston Bay, approximately 10,700 ha of wetland habitat has been permanently inundated, with major losses occurring on the north and west sides of the bay system, including 3,600 ha in fluvial-deltaic areas along the San Jacinto and Trinity Rivers. More than 5,000 ha of vegetated wetlands have been submerged along the lower reaches of the Neches River since the 1950's. Although many processes or activities can lead to loss of wetlands, there is evidence that the major contributing factor in this change along the upper Texas coast is human-induced subsidence caused by ground-water withdrawal. In addition, submergence of wetlands in some areas is associated with more localized faulting and subsidence apparently related to hydrocarbon production. Human-induced subsidence and faulting accelerate rates of relative sea-level rise so they greatly exceed rates of wetland vertical accretion. In fluvial-deltaic areas, where there is the potential for fluvial sediment deposition to offset submergence, upstream dams and reservoirs trap sediments and prevent their delivery to coastal wetlands. Although rates of submergence and wetland loss generally increased from the 1930's to 1980's, rates have declined in some areas since the 1970's, a trend that possibly tracks diminishing rates of human-induced subsidence.

ADDITIONAL INDEX WORDS: *Faults, Galveston Bay, marsh loss, marsh sedimentation, relative sea-level rise, Sabine Lake, subsidence rates.*

INTRODUCTION

The most extensive losses of coastal wetlands in the United States over the past two decades have occurred along the coast of the northern Gulf of Mexico. Almost 60 percent of the wetland losses are due to conversion of salt and brackish marshes to open water (DAHL *et al.*, 1991). Extreme loss of coastal wetlands have been reported in Louisiana (GAGLIANO *et al.*, 1981; BRITSCH and DUNBAR, 1993) and in Texas (WHITE *et al.*, 1985, 1987, 1993), where approximately 58 percent of the Nation's salt and brackish marshes are located (FIELD *et al.*, 1991).

Wetland losses in Louisiana have been severe (BRITSCH and DUNBAR, 1993), with their extent and causes reasonably well known (TURNER and CAHOON, 1988; PENLAND *et al.*, 1990; WILLIAMS *et al.*, 1993). Such is not the case in Texas. Only recently through comprehensive studies of wetlands along the Texas coast (WHITE and CALNAN, 1991; WHITE *et al.*, 1993) has a more quantitative understanding of wetland losses been determined on a regional scale. In Louisiana, a combination of natural and artificial causes of wetland loss have been identified, including compactional subsidence, delta abandonment, sea-level rise, severe storms, geosynclinal downwarping, long-term climate change, construction of dams and levees for flood control, dredging of canals, mineral extraction, and subsurface fluid withdrawal (PENLAND *et al.*, 1990; WILLIAMS *et al.*, 1993). Most of these processes have also affected Texas coastal wetlands, but one process is of primary importance—subsurface fluid withdrawal. In Louisiana, this process is considered of local importance (TURNER and CAHOON, 1988), but along the upper Texas coast, subsurface fluid withdrawal, a process that has accelerated subsidence, is considered a primary cause of wetland submergence and loss of

93132 received 8 December 1993; accepted in revision 6 May 1994.

93132

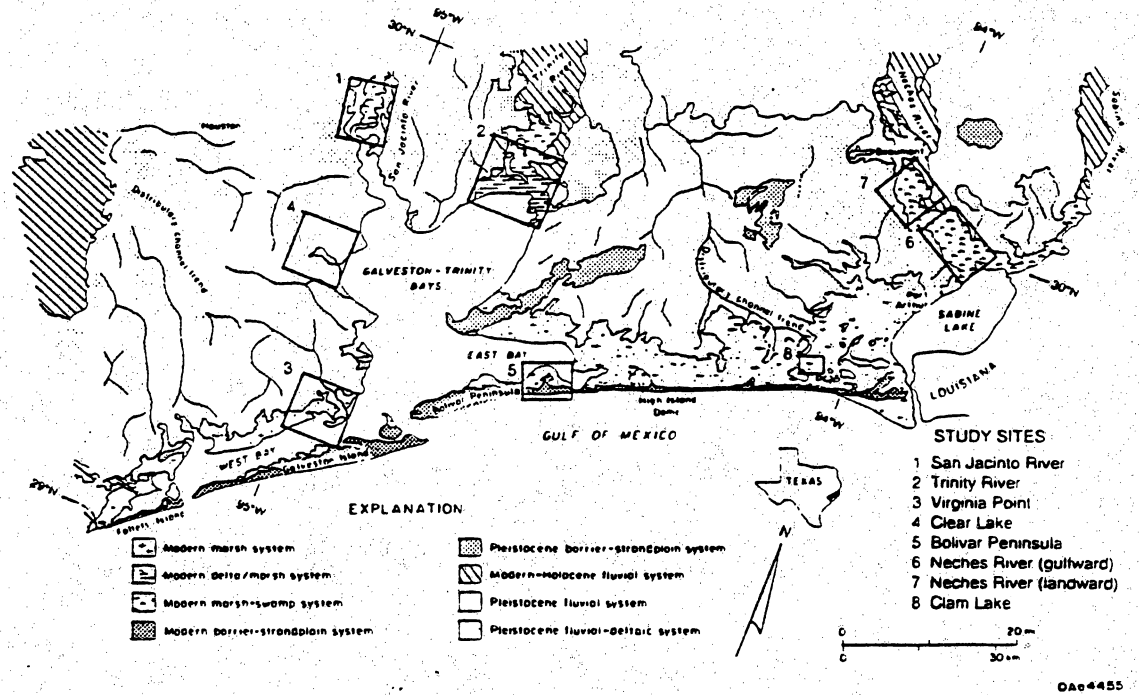

Figure 1. Study sites in relation to upper Quaternary depositional systems. Modified from FISHER *et al.* (1972, 1973).

emergent vegetation (WHITE *et al.*, 1993). This paper examines the relationship between wetland loss and accelerated relative sea-level rise resulting from human-induced subsidence and faulting along the upper Texas coast.

Geologic Setting

The regional geologic framework of the upper Texas coast consists of two major estuaries, Sabine Lake and Galveston Bay, and a complex array of Holocene and Pleistocene depositional systems (FISHER *et al.*, 1972, 1973) (Figure 1). The estuaries formed when valleys entrenched by major rivers during Wisconsinan glaciation and sea-level lowstand were flooded during the post-glacial sea-level rise (LEBLANC and HODGSON, 1959). The shallowness of the estuaries (< 3 m) indicates that the entrenched valleys, incised to depths locally exceeding 30 m (KANE, 1959; REHKEMPER, 1969), have been largely filled with Holocene sediment. Inland parts of the various river valleys, where entrenchment was not as deep and fluvial sediment supply is abundant, have been completely filled. In the case of the Trinity River, a bayhead delta has prograded over estuarine muds at the head of Trinity Bay.

Prominent depositional features along the upper Texas coast include a modern strandplain-chenier system (FISHER *et al.*, 1973) in an interfluvial area southwest of Sabine Lake, and an extensive barrier island and peninsula complex that separates the bays and lagoons of Galveston Bay from the Gulf of Mexico (Figure 1). Major fluvial systems include the San Jacinto and Trinity Rivers in the Galveston Bay system and the Neches and Sabine Rivers that flow into Sabine Lake (Figure 1).

Distribution of Wetlands

Brackish and salt marshes are extensive along the upper Texas coast (WHITE *et al.*, 1985, 1987). Brackish marshes, which commonly include *Spartina patens, Distichlis spicata, Spartina spartinae, Alternanthera philoxeroides, Phragmites australis, Scirpus maritimus,* and *Scirpus olneyii*, cover broad areas between Sabine Lake and Galveston Bay landward of the barrier-strandplain-chenier system. Other occurrences along the lower alluvial valleys and deltas of the Trinity and Neches Rivers, and on landward margins of

East and West Bays (Figure 1). Salt marshes, which are composed of *Spartina alterniflora*, *Batis maritima*, *Salicornia* spp., *Distichlis spicata*, *Monanthochloe littoralis*, *Scirpus maritimus*, *Juncus roemerianus*, and at higher elevations *Spartina patens*, fringe the Galveston Bay system principally along the mainland and back-island shores of West Bay and the shores of Bolivar Peninsula in East Bay (WHITE and PAINE, 1992). Fresh marshes, fluvial woodlands and swamps occur along more inland reaches of the Sabine, Neches, Trinity, and San Jacinto Rivers (Figure 1).

Wetlands have developed on various Holocene and Pleistocene land forms. Thicknesses of Holocene sediments underlying wetlands range from more than 40 m at the southwest end of Bolivar Peninsula, which lies above the entrenched Pleistocene valley, to less than 1 m where marshes have developed on flooded Pleistocene surfaces along the inland margins of the marsh system. Thickness of Holocene sediments in the major fluvial-deltaic areas is generally less than 15 to 20 m, and in the interfluvial area between Sabine Lake and Galveston Bay, it is generally less than 10 m (based on unpublished soils borings).

Methods of Documenting Wetland Losses and Relationships to Subsidence

In studies of wetland losses from which this synthesis is derived, aerial photographs taken in the 1930's, 1950's, 1970's, and 1980's, supported by field surveys, were used to determine changes in wetland distribution. Two major map units were used in the analysis (1) vegetated areas and (2) open water and unvegetated flats. Units delineated on photographs were transferred to base maps from which spatial and temporal changes were determined primarily through digitization and entry of data into a geographic information system (WHITE *et al.*, 1993) and secondarily with a grid system used to measure mapped areas (WHITE *et al.*, 1985, 1987). Losses throughout the entire Galveston Bay system have been documented (Figure 2), but only major losses have been quantified in the Sabine Lake estuarine system and in the interfluvial area between Sabine Lake and Galveston Bay (Figure 1). Wetland areas undergoing submergence were examined with respect to subsidence patterns (GABRYSCH, 1984; GABRYSCH and BONNET, 1975; GABRYSCH and COPLIN, 1990) to define spatial and temporal relationships between submergence and subsidence and to identify significant differences between documented subsidence rates and possible wetland vertical accretion rates.

WETLAND LOSSES, AREAL EXTENT AND DISTRIBUTION

Extensive areas of salt, brackish, and locally fresh marshes have been converted to areas of open water and flats as interior wetlands were submerged and shorelines retreated from erosion. These kinds of losses are most pronounced in salt and brackish marshes in the Galveston Bay system (Figure 2) and in brackish to fresh marshes along the Neches River valley inland from Sabine Lake. Losses have also occurred in brackish marshes in the interfluvial area southwest of Sabine Lake. A total of eight sites, including two in the Neches River valley, are examined in this paper (Figure 1).

Galveston Bay System

The Galveston Bay System ranks as the seventh largest estuary in the United States (MCKINNEY *et al.*, 1989), encompassing almost 163,000 ha of estuarine open water and an additional 52,800 ha of marsh (WHITE *et al.*, 1993). Brackish and salt marshes compose about 83 percent of the marsh system, with fresh marshes making up the remaining 17 percent. From the 1950's to 1989, approximately 10,700 ha of marsh was converted to open water and flats (WHITE *et al.*, 1993). Major areas impacted include wetlands in the San Jacinto and Trinity River valleys, Virginia Point (an area south of Texas City), Bolivar Peninsula, and nearshore areas along west Galveston Bay (Figure 2 and Table 1).

San Jacinto River

In the lower San Jacinto River valley at the head of Galveston Bay, more than 570 ha of fluvial woodlands, swamps, and fresh to brackish marshes were replaced by open water between 1956 and 1979 (WHITE *et al.*, 1985; Figure 3). Aerial photographs taken in the 1930's, 1950's, and 1980's show that water progressed up the San Jacinto River valley, displacing wetlands and uplands (WHITE and CALNAN, 1991). During the 26-year period between 1930 and 1956, emergent areas decreased by 590 ha, and between 1956 and 1986, by 1,259 ha (Table 1). The rate of vegetated-area loss (fluvial woodlands, swamps, and marshes) in-

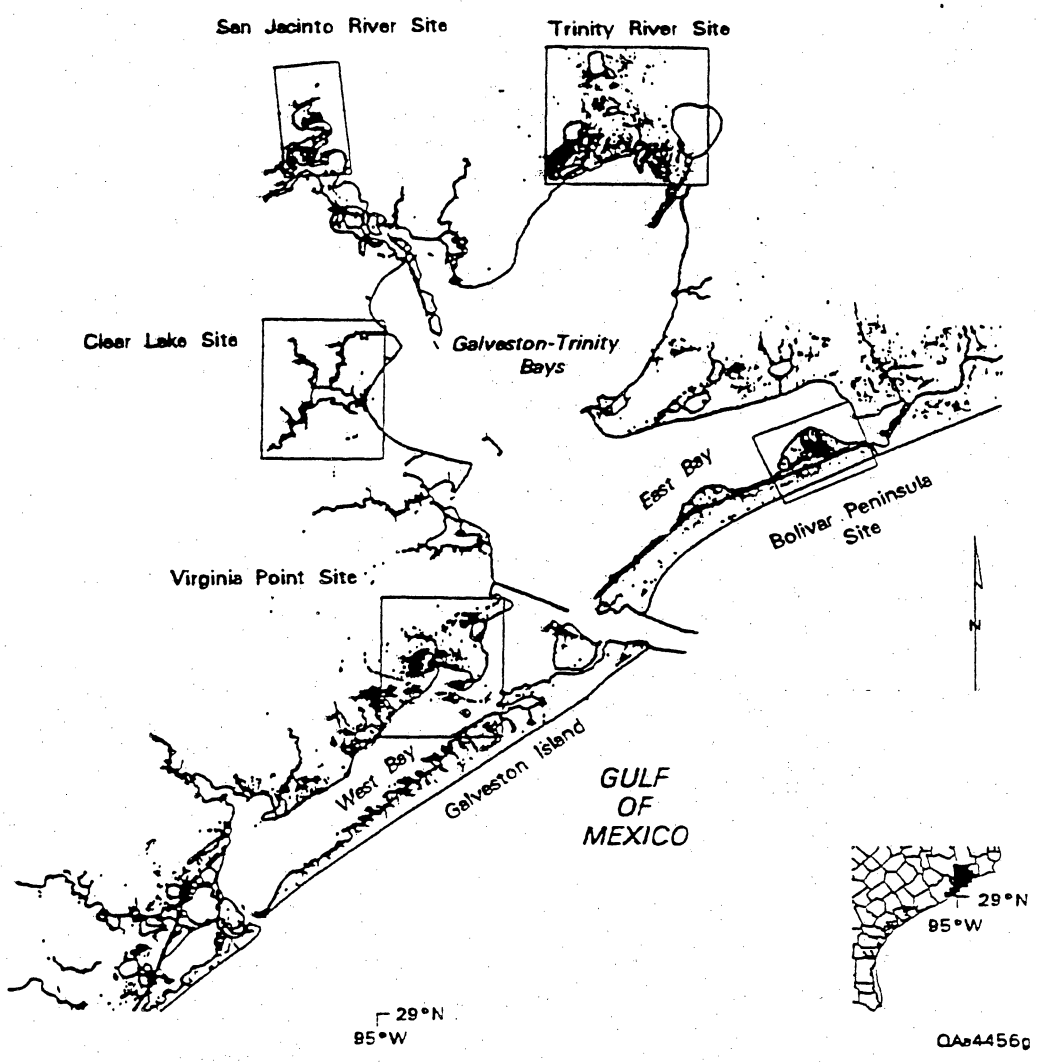

Figure 2. Study sites in the Galveston Bay system in relation to marsh areas (in black) that were converted to open water and flats between the 1950's and 1989. Modified from WHITE *et al.* (1993).

creased from about 23 ha yr^{-1} to more than 40 ha yr^{-1} during these two periods.

Trinity River

The Trinity River delta, at the head of Trinity Bay, is the only natural bay-head delta in Texas that has undergone significant progradation in recent historic times. Historical analysis of the Trinity River delta using aerial photographs taken in 1930, 1956, 1974, and 1988 (WHITE and CALNAN, 1991) shows that delta progradation continued from 1930 to 1956, when approximately 600 ha of marsh was added to the delta. This trend in marsh gain was reversed between 1956 and 1974, when 1,445 ha of mostly marshland was converted to open water and unvegetated flat. Vegetated wetlands continued to shrink by an additional 90 ha between 1974 and 1988. Although some wetland losses around the Trinity River delta have resulted from bay shoreline erosion (PAINE and MORTON, 1986), the most extensive losses have occurred in interior marshes. From 1953 to 1989, wetland losses exceeded 1,742 ha in the delta and

Table 1. *Submergence of vegetated wetlands along the upper Texas coast. See Figure 1 for site locations. All but interfluvial area compiled from* WHITE et al. *(1985, 1987, and 1993), and* WHITE and CALNAN *(1991).*

Location	Period	Gain or Loss (hectares)
Galveston Bay System		
San Jacinto River	1930–1956	−590
	1956–1986	−1,259
Trinity River	1930–1956	+596
	1956–1974	−1,445[1]
	1974–1988	−89
Trinity River	1953–1989	−1,742[2]
Virginia Point	1952–1989	−1,470
Clear Lake	1952–1989	−355
Bolivar Peninsula	1952–1989	−600
Sabine Lake Estuarine System		
Neches River		
Site 6 (see Figure 1)	1956–1978	−3,811
Site 7 (see Figure 1)	1938–1956	−340
	1956–1987	−1,306
Interfluvial area (Clam Lake)	1930–1956	0
	1956–1987	−277
Total losses (Trinity River data includes only 1953–1989)		−11,750

[1] Includes approximately 600 ha of marsh submerged by a power plant cooling reservoir

[2] This area (from WHITE *et al.*, 1993) includes more alluvial valley than the preceding site along the Trinity River. It also includes the power plant cooling reservoir, which accounts for 600 ha of marsh loss

lower reaches of the Trinity River alluvial valley (WHITE *et al.*, 1993, Figure 2).

Virginia Point

Wetland losses near Virginia Point, located on the inland margin of West Bay south of Texas City (Figure 2), are among the most extensive in the Galveston Bay system. Approximately 1,470 ha of primarily regularly flooded salt marsh was replaced by open water and mud flats between the early 1950's and 1989 (WHITE *et al.*, 1993). Wetland losses in the Virginia Point area have previously been reported by JOHNSTON and ADER (1983), and WHITE *et al.*, (1985).

Western Margins of Galveston Bay (Clear Lake)

The Clear Lake study site, which encompasses the lake and tributaries on the western margin of Galveston Bay (Figure 2), is an example of wetland submergence along bayous and creeks connecting to Galveston Bay. In the Clear Lake area, approximately 355 ha of vegetated wetland habitat was converted to open water and flats between the 1950's and 1980's (WHITE *et al.*, 1993). Ninety-one percent of the emergent wetlands located along Armand Bayou, which discharges into Clear Lake, disappeared between the early 1950's and 1979 (MCFARLANE, 1991).

Bolivar Peninsula

A relatively large salt marsh occurs on the relict tidal inlet/washover fan complex on the bayward side of Bolivar Peninsula in East Bay (Figure 2). Aerial photographs taken in 1930 indicate that the marsh system was well vegetated and interior marshes had not yet begun to deteriorate. By 1956 open water had begun to replace vegetated areas, and between 1956 and 1979, approximately 600 ha of emergent vegetation was replaced primarily by shallow subaqueous flats and open water (Figure 4).

Sabine Lake Estuarine System and Interfluvial Area

Sabine Lake is about one-eighth of the size of Galveston Bay in terms of area of estuarine open water (DIENER, 1975), but an extensive marsh complex occurs in the strandplain-chenier system southwest of the lake extending westward in the interfluvial area that separates the two bay systems. Additional wetlands are located inland from the lake along the modern rivers (Figure 1).

Neches River

The Neches River, which discharges at the head of Sabine Lake, is the site of a large marsh-swamp complex that has developed on fluvial and fluvial-deltaic deposits within the entrenched valley (FISHER *et al.*, 1973). The most extensive loss of contiguous wetlands on the Texas coast has occurred within the Neches River valley (WHITE *et al.*, 1987; WHITE and CALNAN, 1991). Two areas along a 25-km reach of the Neches lower valley have been investigated (Figure 1). Vegetated wetlands in both areas underwent substantial losses after the 1950's. Between the mid-1950's and 1978, 3,810 ha of marsh was displaced primarily by open water along an approximately 16-km stretch of the lower Neches River valley (Figure 5). The rate of loss was almost 160 ha yr^{-1}. Additional losses in fresh-water marshes, woodlands, and swamps have occurred upstream from this site (WHITE and CALNAN, 1991). At the upstream site, emer-

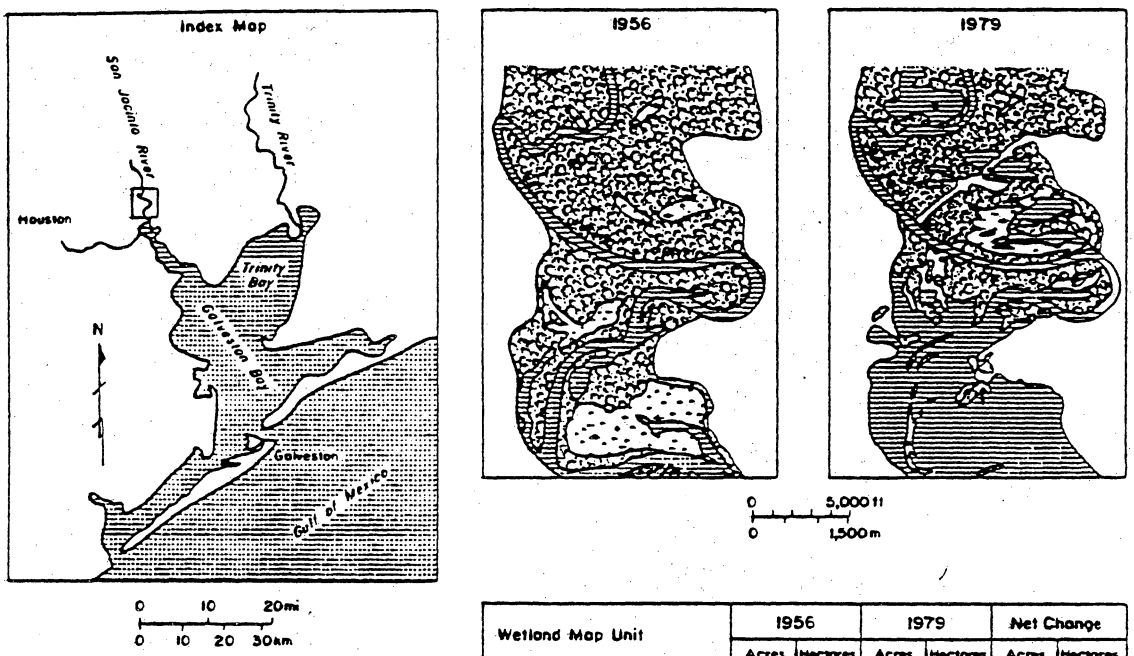

Wetland Map Unit	1956		1979		Net Change	
	Acres	Hectares	Acres	Hectares	Acres	Hectares
Water	875	355	2,295	930	+1,420	+575
Fluvial Woodlands & Swamps	3,480	1,410	2,090	845	-1,390	-565
Fresh to Brackish Marsh	650	265	300	120	-350	-145

OA 937

Figure 3. Changes in the distribution of wetlands between 1956 and 1979 within a subsiding segment of the San Jacinto River near Houston, Texas. The difference in net changes in water and vegetated wetlands is due principally to devegetation of wetlands from other processes such as pipeline construction and mining of sand resources. From WHITE *et al.* (1985).

gent vegetation decreased by about 340 ha between 1938 and 1956, and by approximately 1,300 ha between 1956 and 1987. These losses translate into averages rates of 19 ha yr^{-1} for the earlier period and 42 ha yr^{-1} for the latter period.

Interfluvial Area (Clam Lake)

Losses in vegetated wetlands are not restricted to estuaries and fluvial-deltaic systems. In the interfluvial area southwest of Sabine Lake, conversion of emergent vegetation to open water occurred in the broad brackish-marsh complex. This marsh complex has developed on a relatively thin wedge of Holocene sediments (generally < 10 m thick; unpublished Bureau of Economic Geology soil borings) landward of the modern barrier/strandplain system (Figure 1). The area of marsh loss investigated is near Clam Lake, which is about 19 km southwest of Sabine Lake and approximately 4 km inland from the Gulf shoreline. Additional marsh loss has occurred within this interfluvial area nearer to Sabine Lake, but these losses have not been quantified.

Almost 280 ha of brackish marsh was converted to open water between the mid 1950's and 1987 in the area immediately northeast of Clam Lake. In fact, most of the conversion had occurred by 1978. Coalescing ponds formed landward of a northeast-southwest-oriented lineament (WHITE *et al.*, 1987).

MAJOR CAUSES OF WETLAND LOSS

Conversion of vegetated wetlands to water and barren flats may result from several interactive

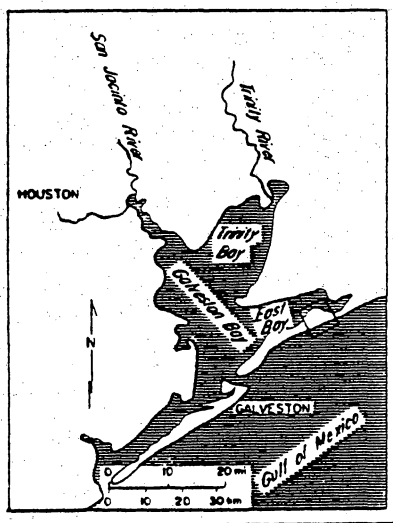

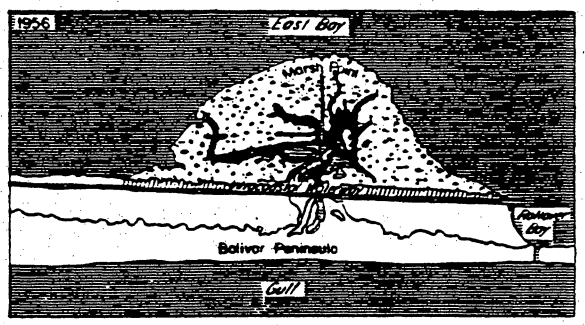

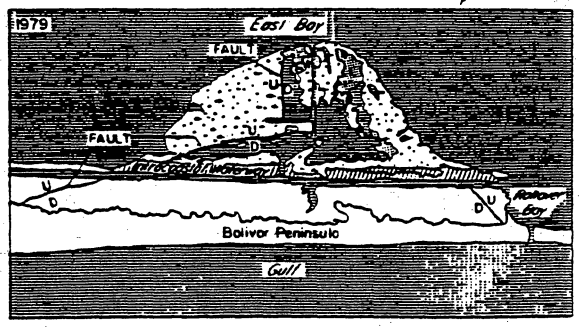

Wetland Map Unit	1956		1979		Net Change	
	Acres	Hectares	Acres	Hectares	Acres	Hectares
Water	140	57	1130	458	+990	+401
Marsh	3480	1409	2560	1037		
Marsh-covered tidal channels	640	259				
TOTAL MARSH	4120	1669	2560	1037	-1560	-632
Barren tidal flats			270	109	+270	+109
Dredged spoil/uplands	520	211	720	292	+200	+81
TOTAL	4780	1936	4680	1896	-100*	-40*

*Most of the loss in total area is probably due to erosion of marsh along the margins of East Bay. Historical monitoring indicates that this shoreline is undergoing erosion at rates of up to 311 (1m) per year (Penland and Morton, 1986)

(Areas were calculated using a square-count method; smallest squares used were equivalent to 6.4 acres or 2.6 hectares).

OA 1774

Figure 4. Changes in distribution of wetlands between 1956 and 1979 near Marsh Point on the bayward side of Bolivar Peninsula. Increases in the areal extent of open water and decreases in the areal extent of marsh are apparently related to localized subsidence and active faults (D = downthrown side of fault, U = upthrown side). From WHITE *et al.* (1985).

processes, including natural and artificial changes in hydrology, intrusion of salt water into fresh areas, reductions or alterations in sediment supply and dispersal, dredging of canals, climatic changes, subsidence, and high rates of relative sea-level rise (TURNER and CAHOON, 1988; PENLAND *et al.*, 1990; WILLIAMS *et al.*, 1993). Submergence of wetlands in many areas indicates that wetland vertical accretion rates are not sufficient to offset rates of relative sea-level rise (BAUMANN and DELAUNE, 1982). Although marsh vertical accretion rates tend to track rates of relative sea-level rise (NIXON, 1980; STEVENSON *et al.*, 1985), the upper limit, based on organic matter production, is estimated to be 14 to 16 mm yr^{-1} (BRICKER-URSO *et al.*, 1989). In Louisiana, marsh vertical accretion rates, which are among the highest on the Gulf Coast, range from about 13 mm yr^{-1} in levee areas to less than 8 mm yr^{-1} in backmarshes (HATTON *et al.*, 1983). Rates of relative sea-level rise exceed vertical accretion rates in many areas, and marshes are being replaced by open water (DELAUNE *et al.*, 1983; HATTON *et al.*, 1983; BAUMANN *et al.*, 1984). Although the imbalance between rates of vertical accretion and relative sea-level rise can be expressed as an accretion deficit and corresponding loss in elevation, REED and CAHOON (1993) suggest that direct determinations of elevation provides a better measure of the elevation change and the relationship between subsidence and accretion. Low elevations, which lead to increased frequency and duration of flooding,

can result in deterioration and eventual loss of vegetation (REED and CAHOON, 1992). Vegetation loss may be a result of plant dieback or soil erosion below the living root zone (NYMAN *et al.*, 1993).

Along the upper Texas coast numerous interactive processes of natural and artificial origin are undoubtedly involved in the submergence and deterioration of wetlands. Regional human-induced subsidence and faulting, which have greatly accelerated rates of relative sea-level rise, appear to be the primary processes affecting wetlands in areas where losses are most pronounced.

Human-Induced Subsidence

Holocene sediment sequences underlying wetlands in Texas are not as thick as in Louisiana, and therefore coastwide natural compactional subsidence is not as high (RAMSEY and PENLAND, 1989). However, regional human-induced subsidence caused by subsurface fluid production has been extensive and has affected a relatively large area in the Galveston Bay system (Figure 6). Rates of "natural" compactional subsidence and eustatic sea-level rise, which together may range up to 13 mm yr^{-1} along the upper Texas coast (SWANSON and THURLOW, 1973; LYLES *et al.*, 1988), are greatly exceeded by human-induced subsidence with rates of up to almost 120 mm yr^{-1} from 1964 to 1973 (GABRYSCH and BONNET, 1975). The major cause of human-induced subsidence is the withdrawal of underground fluids, principally ground water, oil, and gas (PRATT and JOHNSON, 1926; WINSLOW and DOYEL, 1954; GABRYSCH, 1969; YERKES and CASTLE, 1969; KREITLER, 1977; PAINE, 1993).

In the Houston-Galveston area, there has been up to 3 m of land-surface subsidence from large-scale ground-water withdrawal since 1906 (GABRYSCH and COPLIN, 1990). The subsidence "bowl" encompasses an area of approximately 943,500 ha where a minimum of 30 cm of subsidence has occurred (Figure 6). The large Houston subsidence bowl merges with a secondary depression bowl centered on Texas City (Figure 6). From the early 1940's to late 1970's, rates of subsidence were exceptionally high, more than 75 mm yr^{-1} in the area of maximum subsidence (GABRYSCH and COPLIN, 1990). Since the late 1970's rates in some areas, notably the eastern part of the subsidence bowl and Texas City, have declined substantially due to the curtailment of ground-water pumpage (GABRYSCH and COPLIN, 1990).

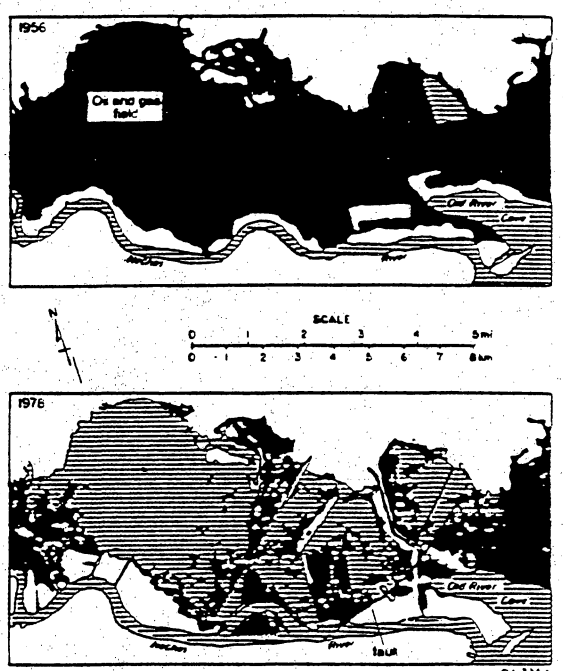

Map Unit	1956		1978		Net Change*	
	Acres	Hectares	Acres	Hectares	Acres	Hectares
Water	2,560	1,037	11,070	4,483	+8,510	+3,446
Marsh	15,740	6,375	6,330	2,564	−9,410	−3,811

* Loss of additional 900 acres (365 hectares) of marsh primarily due to spoil disposal.

Figure 5. Changes in the distribution of wetlands between 1956 and 1978 in the lower Neches River Valley at the head of Sabine Lake. Site 6 on the Neches River shown in Figure 1. The fault crossing this area has apparently contributed to the changes (D = downthrown side, U = upthrown side). From WHITE *et al.* (1987).

Faulting

Subsidence in some areas has occurred along active faults that intersect wetlands. The major zone of surface faulting along the Texas coast is in the Houston-Galveston area where 150 linear km of faulting has been reported (BROWN *et al.*, 1974). Surface faults correlate with, and appear to be extensions of, subsurface faults in many areas (WEAVER and SHEETS, 1962; VAN SICLEN, 1967; KREITLER, 1977). Most of the surface faulting in the Houston metropolitan area has apparently taken place during the last few decades, largely due to fluid withdrawal (water, oil, and gas), which has reinitiated and accelerated fault activity (REID, 1973; KREITLER, 1977; VERBEEK and CLANTON, 1981).

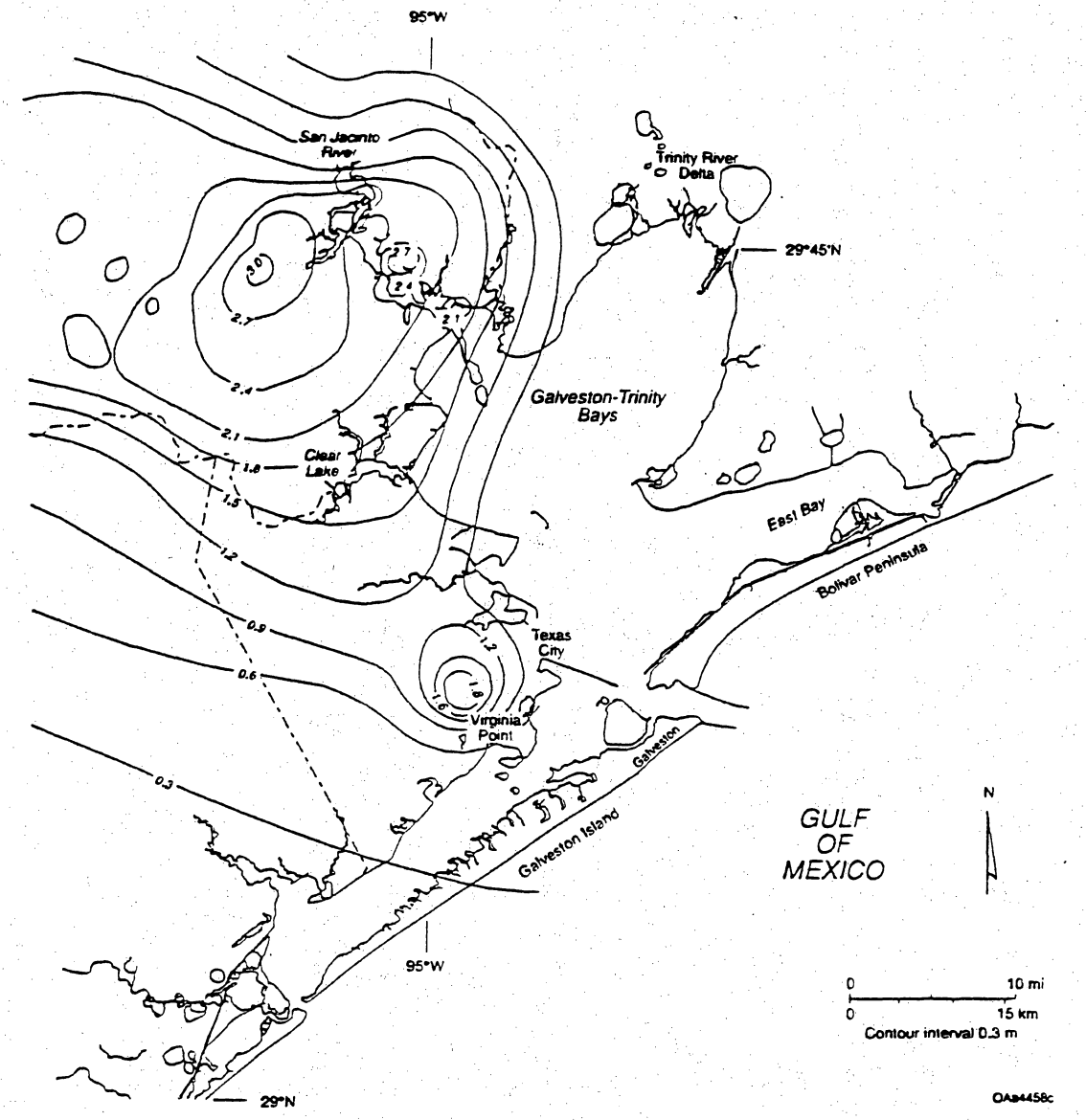

Figure 6. Land-surface subsidence in the Galveston Bay area, 1906 to 1987. Subsidence contours in meters are from GABRYSCH and COPLIN (1990).

The range in measurable vertical displacement of surface traces of faults is from 0 to 3.9 m (REID, 1973). Rates of fault movement commonly range between 5 mm yr^{-1} and 20 mm yr^{-1} (VERBEEK and CLANTON, 1981) but may exceed 40 mm yr^{-1} (VAN SICLEN, 1967; REID, 1973). Movement along surface faults apparently occurs episodically (REID, 1973). Highways, railroads, industrial complexes, airports, homes, and other structures placed on active faults in the Houston area have undergone millions of dollars worth of damage annually (VERBEEK and CLANTON, 1981).

As vertical displacement occurs along a fault that intersects a marsh, more frequent and eventually permanent inundation of the surface on the downthrown side of the fault can lead to replace-

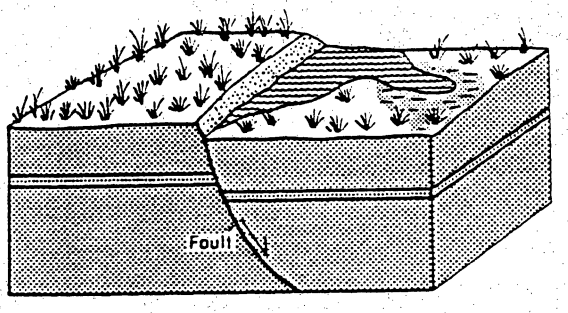

FIGURE 7. Block diagram of changes in wetlands that may occur along an active surface fault. There is generally an increase in low marshes, shallow subaqueous flats, and open water on the downthrown side of the fault relative to the upthrown side. From WHITE *et al.* (1993).

ment of marsh vegetation by open water (Figure 7). The loss of vegetation on the downthrown side of the fault but not the upthrown side indicates that the rate of relative sea-level rise exceeds the rate of marsh sedimentation on the downthrown side. More than 25 active faults that cross wetlands along the upper Texas coast (Freeport area to Sabine Pass) have been identified on aerial photographs. Most of the identified faults are in the Galveston Bay area (WHITE *et al.*, 1985). Not all the active faults are associated directly with oil and gas production.

Relationship Between Wetland Submergence and Subsidence and Faulting

Galveston Bay System

San Jacinto River. Although some wetland losses can be attributed to mining of sand in the San Jacinto River alluvial valley, most of the loss in marshes and fluvial woodlands is due to subsidence caused by ground-water withdrawal (GABRYSCH, 1984). Submergence along the San Jacinto River valley is pronounced because of its proximity to the center of maximum subsidence (Figure 6). Between 1964 and 1973, approximately 0.6 m of subsidence occurred in this area, which translates into rates as high as 67 mm yr^{-1} (Table 2). As subsidence occurs, submergence of wetlands and uplands progresses inland along the axis of the entrenched valley (Figure 3).

Lake Houston, with a sediment trapping efficiency of 87 percent (U.S. DEPARTMENT OF AGRICULTURE, 1959) and located only 16 km upstream from the mouth of the San Jacinto River, has undoubtedly reduced the amount of fluvial sediments reaching coastal wetlands. Nevertheless, the magnitude of land-surface subsidence in the river valley has been so great that it is unlikely aggradation rates could keep pace with past subsidence rates even if Lake Houston and other lakes had not been constructed. More recent subsidence rates are dramatically lower (GABRYSCH and COPLIN, 1990), however, and reductions in fluvial sediment supply may become a more significant factor in wetland loss in the future.

Table 2. *Estimated rates of subsidence in wetlands undergoing submergence in the Galveston Bay system. Based on land-surface subsidence maps published by GABRYSCH, 1984, GABRYSCH and BONNET, 1975, and GABRYSCH and COPLIN, 1990.*

Site	Subsidence for Selected Periods (mm/yr)			
	1906–1943	1964–1973	1973–1978	1978–1987
San Jacinto River	5	67	46	8
Trinity River	?	10–14	8	?
Clear Lake	3	60	61	17
Virginia Point	2–5	14–34	12–30	8

Trinity River. Approximately 40 percent of the submergence of wetlands in the Trinity River delta and alluvial valley (Figure 2) resulted from construction of a power plant cooling reservoir (more than 1,010 ha in size) in the southwestern part of the delta. Most of the remaining 60 percent of marsh loss, however, was due to submergence apparently associated with subsidence and declining river sediment loads (Figure 8). Benchmark releveling surveys across the Trinity River alluvial valley (BALAZS, 1980) indicate that subsidence rates from 1973 to 1978 approached 8 mm yr^{-1}. A similar rate was estimated for the period 1943–1973 (Table 2), and adding the Gulf of Mexico regional sea-level rise of 2.4 mm yr^{-1} (GORNITZ and LEBEDEFF, 1987) yields a relative sea-level rise of more than 10 mm yr^{-1} at this Trinity River site. Estimated rates of marsh sedimentation over the past 50 years, based on ^{210}Pb analysis in three cores from marshes in the Trinity River delta, average 5.4 mm yr^{-1} and range as low as 4.2 mm yr^{-1} (WHITE and CALNAN, 1990). The rate of relative sea-level rise is almost two times the average rate of sedimentation, or vertical accretion.

Even though the dramatic reduction in fluvial sediments (Figure 8) has likely contributed to marsh loss, subsidence appears to be the controlling factor. Excluding losses resulting from the

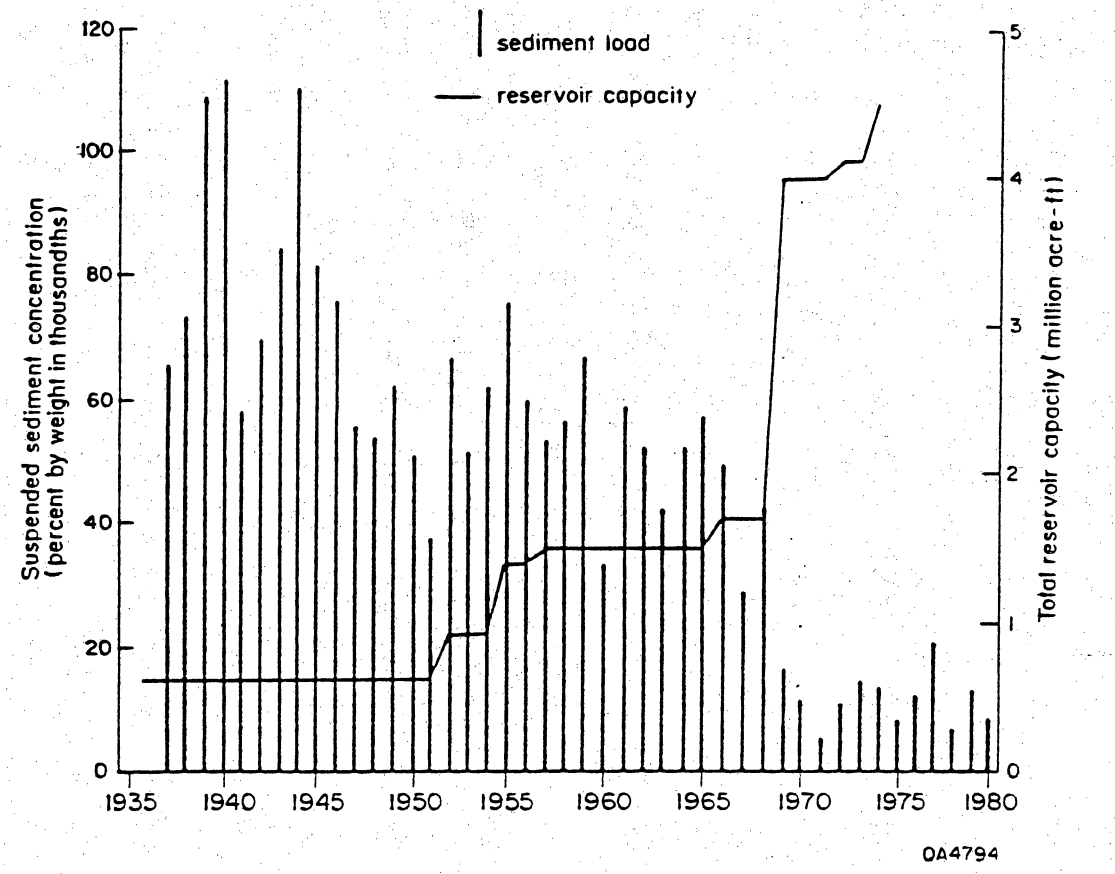

Figure 8. Suspended-sediment load (percent by weight) of the Trinity River at Romayor, and cumulative authorized water storage in reservoirs of the Trinity River basin. Note the dramatic decline in sediments after 1968 when Lake Livingston was completed on the Trinity River above the Romayor gaging station. From PAINE and MORTON (1986).

power plant cooling reservoir mentioned previously, the rate of marsh loss during the period 1974–1988 was approximately 70 percent lower than the rate in 1956–1974 (WHITE and CALNAN, 1990). This diminishing marsh-loss rate may be due to the sharp declines in subsidence rates on the east side of the Houston-Galveston subsidence bowl (Figure 6) after 1978. Subsidence rates declined in some areas by as much as 90 percent as a result of reductions in ground-water pumpage (GABRYSCH and COPLIN, 1990).

Virginia Point. Although some of the wetland loss near Virginia Point (Figure 2) can be attributed to dredging of channels and construction of industrial ponds near Texas City, the major cause is human-induced subsidence (Figure 9). The largest area of change is northwest of Jones Bay where salt marsh vegetation was replaced by open water in an area unaffected by dredged channels and reservoirs. The Virginia Point area is partly encompassed by a subsidence "bowl" centered on Texas City (Figure 6). Land-surface subsidence from 1906 to 1987 ranged from slightly less than 0.6 to 1.8 m (Figure 9). In the area northwest of Jones Bay, estimated rates of subsidence exceeded 14 mm yr^{-1} for the period of 1943 to 1987 (GABRYSCH and COPLIN, 1990). With the inclusion of the Gulf of Mexico regional sea-level rise of 2.4 mm yr^{-1} (GORNITZ and LEBEDEFF, 1987), the rate of relative sea-level rise is more than 16 mm yr^{-1}, which apparently was higher than marsh vertical accretion rates. Emergent vegetation did not continue its decline from 1979 to 1989 (WHITE *et al.*, 1993), perhaps reflecting a diminishing rate of

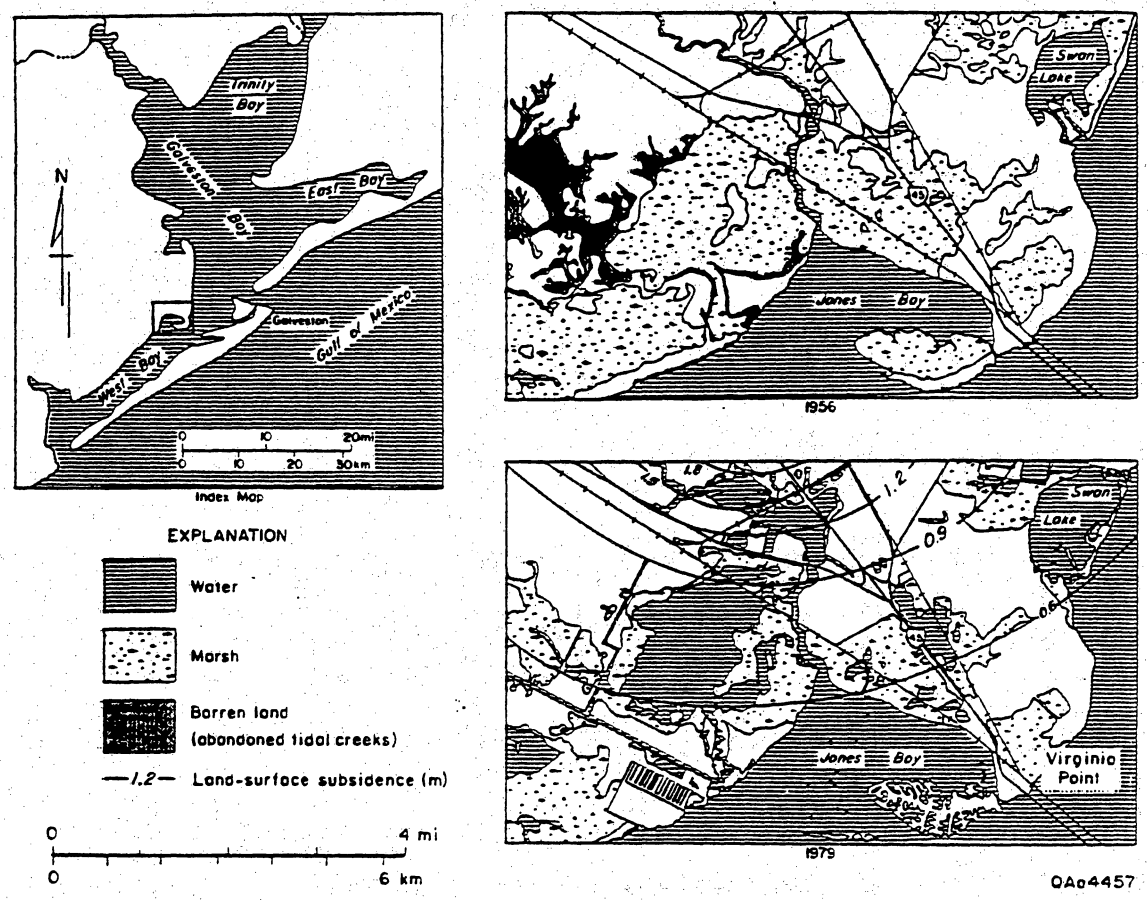

Figure 9. Changes in the distribution of wetlands between 1956 and 1979 in relation to subsidence in the Virginia Point quadrangle south of Texas City. Note the increase in open water in 1979. Contours show the amount of subsidence (in meters) that occurred between 1906 and 1987 based on maps from GABRYSCH and COPLIN (1990). Modified from WHITE *et al.* (1985).

subsidence (Table 2) as a result of reductions in ground-water pumpage in Texas City (GABRYSCH and COPLIN, 1990).

Western Margins of Galveston Bay (Clear Lake). Conversion of wetlands to water and flats in the Clear Lake area (League City 7.5-minute quadrangle) represents the trend occurring along the bayous and creeks located on the north and west sides of Galveston Bay, an area affected most by subsidence (Figure 6). The Clear Lake area had subsided between 1.5 and 2 m by 1987 (Figure 10). Rates of subsidence near the mouth of Clear Lake increased from less than 3 mm yr^{-1} in 1906–1943 to about 35 mm yr^{-1} in 1943–1973 to almost 60 mm yr^{-1} in 1964–1973 (PULICH and WHITE, 1991). The trend in this area has been one of expansion of open water and shallow flats at the expense of marshes and woodlands as subsidence promoted the encroachment of estuarine water up the valleys.

Bolivar Peninsula. The Bolivar Peninsula site is outside of the Houston subsidence bowl (Figures 2 and 6). Submergence of marshes on this relict tidal inlet/washover fan complex on the margins of East Bay are related to faulting and more localized subsidence (WHITE *et al.*, 1985). The location and orientation of two faults in this area (Figure 4) correlate with normal faults that have been mapped in the subsurface (Figure 11) (EWING, 1985; MORTON and PAINE, 1990). Analysis of aerial photographs indicates that the faults are active. Fault traces do not appear on aerial photographs taken in the 1930's, they are faintly visible on photographs taken in 1956, and they

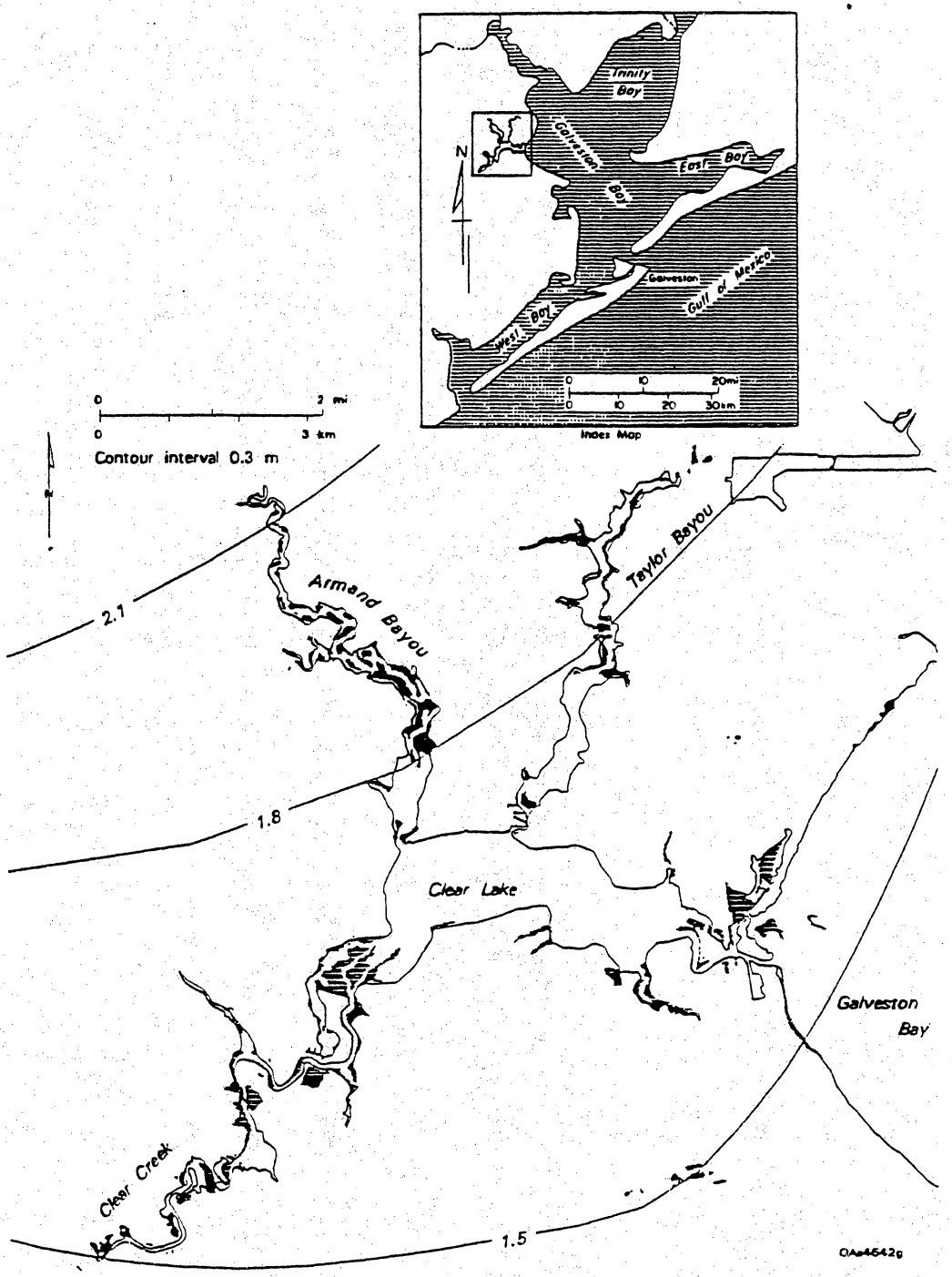

Figure 10. Relationship between subsidence and marsh submergence in the Clear Lake area. Marsh areas that were converted to open water and flats are shown in black. Modified from WHITE *et al.* (1993).

are strongly visible on photographs taken in 1979. A benchmark releveling profile along State Highway 87, which extends down Bolivar Peninsula, also indicates the faults are active; a marked increase in subsidence of from 6 mm yr^{-1} to 10 mm yr^{-1} occurred from the upthrown side to downthrown side of one of the faults crossed by the releveling survey (WHITE *et al.*, 1993). The subsidence rate at the highway was 10 mm yr^{-1} for the period of the survey 1936–1954. This rate could possibly be matched by marsh sedimentation, depending on sediment supply. However, displacement along the fault may be more pronounced toward East Bay where marshes on the downthrown side have been converted to open water. In addition, the rate of fault movement may have increased since 1954 when the benchmarks were releveled. Fault activation and subsidence at this site appear to be associated with hydrocarbon production and regional depressurization of subsurface formations by large-scale fluid withdrawal from the Caplen oil and gas field (EWING, 1985; KREITLER, *et al.*, 1988). Total fluid withdrawal (oil, gas, and formation water) from the Caplen field since its discovery in 1939 is approximately 30–40 million barrels to 1985, with most production from lower Miocene reservoirs at depths of 2,100 to 2,200 m (EWING, 1985). EWING (1985) noted that the association of oil and gas production and fault movement since the 1930's suggests a causal relationship.

Sabine Lake Estuary System and Interfluvial Area

Neches River. Reasons for submergence of marshes in the Neches River valley (Figure 5) are more complex than those for marsh submergence in the Galveston Bay area where the magnitude of subsidence has been so great. Although human-induced subsidence associated with ground-water and oil and gas production has been documented in the Sabine Lake area (RATZLAFF, 1980), it is more localized than around Galveston Bay. Unfortunately, benchmark releveling surveys do not cross the Neches River valley where the most extensive marsh loss has occurred. Additionally, numerous human alterations of the marsh system complicate the analysis. The river, which is located on the south side of the valley, was dredged for navigation purposes in the early 1900's. Since then, the channel has been straightened, deepened, and maintained as a deep-draft shipping route. Dredged material has been dumped on natural levees along the channel. Two oil and gas fields with access channels and levees have been developed in the valley, and canals have been dredged across the valley for pipeline installation. In addition, intake and discharge canals for a power plant located on the north side of the valley cross the marsh system.

Displacement of marshes by open water and shallow subaqueous flats appears to be related to a combination of factors in addition to subsidence and faulting (WHITE *et al.*, 1987). Other factors include dredged canals, which can cause direct and indirect losses (SCAIFE *et al.*, 1983; TURNER and CAHOON, 1988), changes in hydrologic regime due to artificial channels and spoil disposal (SWENSON and TURNER, 1987), a decline in fluvial sediments supplied to this alluvial area as a result of reservoir development in the Neches River basin, and artificial levees (dredged spoil) that inhibit overbank flooding along the dredged portion of the river. GOSSELINK *et al.* (1979) attributed some of the habitat loss in the Sabine basin to a number of causes, including hydrologic and salinity modifications resulting from canals and upstream reservoirs.

Although factors contributing to marsh loss in the Neches River valley are complex and difficult to quantify adequately with existing data, the conversion of marsh to open water suggests that marsh aggradation rates are not keeping pace with the rate of relative sea-level rise. A similar conclusion was reached by DELAUNE *et al.* (1983) in a study of a brackish marsh in the Chenier Plain near Calcasieu Lake, Louisiana, about 50 km east of Sabine Lake. DELAUNE *et al.* (1983) reported that marsh area was being replaced by water at an increasing rate because marsh vertical accretion rates averaging 0.8 cm yr^{-1} were surpassed by submergence rates averaging 1.2 cm yr^{-1}. Among the human activities that possibly contributed to the transformation to open water were (1) ship channel construction (promoting salt intrusion and possibly sediment diversion) and (2) oil, gas, and groundwater withdrawals (accelerating subsidence) (DELAUNE *et al.*, 1983).

Subsidence rates in the Neches River valley are not known, but tide gage records at Sabine Pass, about 35 km gulfward of the Neches River valley, indicate a relative sea-level rise of 13.2 ± 3.2 mm yr^{-1} for the period 1960 to 1978 (LYLES *et al.*, 1988). Benchmark releveling surveys near the northernmost site indicate that at least 20 cm of subsidence has occurred in association with with-

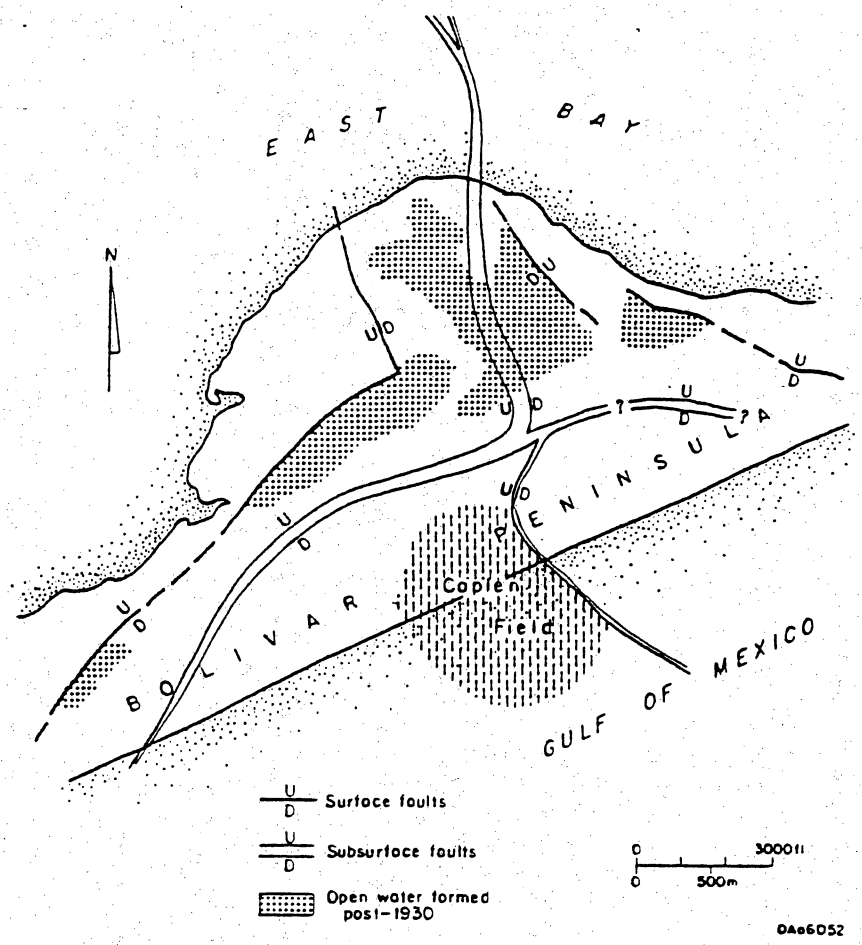

Figure 11. Relationship between subsurface and surface traces of faults at the Caplen Field on Bolivar Peninsula. Compare with Figure 4, which illustrates the marsh loss along faults in this area. Modified from EWING (1985).

drawal of underground fluids (RATZLAFF, 1980). Interpretation of marsh losses on aerial photographs shows that the most extensive submergence has occurred above oil and gas fields located in the Neches River valley. Oil production from the Port Neches field (Figure 5), most of which are from depths of about 1,800 m, has exceeded 30 million barrels since the field's discovery in 1928 (TEXAS RAILROAD COMMISSION, 1993). The field is associated with a moderate to deep-seated piercement salt dome with no surface expression (FISHER *et al.*, 1973). A fault, downthrown toward the field, bounds the southern margin of the most impacted area (Figure 5). Submergence of marshland has occurred more extensively on the downthrown side of the fault than on the upthrown side, suggesting that submergence rates exceed vertical accretion rates on the downthrown side.

Interfluvial Area (Clam Lake). Submergence of marsh vegetation near Clam Lake has occurred on the northwest side of a lineament interpreted as a fault (Figure 12). Coalescing ponds have formed since 1956 on the fault's downthrown side. The fault could not be located on aerial photographs taken in the 1930's or in 1956. However, it is distinct on 1978 and 1989 photographs (Figure 12). The appearance (configuration, alignment, and contrasting tones on each side) of this lineament is similar to that of surface faults reported by VERBEEK and CLANTON (1981) and WHITE *et al.* (1985). The fact that the fault does not appear on photographs taken in the 1930's

and 1950's but is distinct on later photographs indicates that the fault has been activated. The fault is downthrown to the northwest toward an oil and gas field north of Clam Lake. It is probable that the fault is the surface extension of a deep-seated fault that has been activated by hydrocarbon production similar to the Bolivar Peninsula site (Figure 11). Oil production from the Clam Lake field has exceeded 21 million barrels since its discovery in 1937 (TEXAS RAILROAD COMMISSION, 1993). Production is from a depth of approximately 700 m, and similar to the Port Neches field, it is associated with a moderate to deep-seated piercement salt dome (FISHER *et al.*, 1973). Some of the wetland loss near Clam Lake can be attributed to levees constructed across the marsh, but canals, except for those formed in borrow areas that parallel the levees, have not been dredged through the marsh and have not contributed to the marsh loss.

SUMMARY AND CONCLUSIONS

Synthesis of data on wetland losses documented from aerial photographic analysis of selected sites on the upper Texas coast indicates that thousands of hectares of vegetated coastal wetlands have been converted to open water and shallow subaqueous flats. Major areas affected include brackish to fresh marshes and woodlands in fluvial-deltaic areas along the San Jacinto, Trinity, and Neches Rivers, brackish and salt marshes in the Galveston Bay estuarine system, and brackish marshes in the interfluvial area between Sabine Lake and Galveston Bay.

More than 10,000 ha of wetlands throughout the Galveston Bay estuarine system have been affected by submergence. Losses are pronounced on the north and west side of the bay, including the San Jacinto and Trinity River fluvial-deltaic areas where together almost 3,600 ha of vegetated area has been replaced by open water and flats since the 1930's. Locally on the west side of Galveston Bay at Virginia Point, approximately 1,400 ha of salt marsh was converted to open water and flat between 1952 and 1989. In the Neches River fluvial-deltaic area near the head of Sabine Lake, more than 5,000 ha of emergent vegetation has been lost since the 1950's. Submergence of salt and brackish marshes also occurred on the bayward side of Bolivar Peninsula and in the interfluvial area between Sabine Lake and Galveston Bay.

As exemplified in Louisiana where causes for wetland loss are relatively well known, many processes may lead to the conversion of vegetated wetlands to open water and shallow flats: compactional subsidence and sea-level rise, delta abandonment, erosion from severe storms, dredging of canals, construction of levees and dams that alter hydrology and sediment supply, saltwater intrusion, and underground fluid withdrawal, among others. Whereas these processes also affect Texas coastal wetlands, there is evidence that the major contributing factors in wetland submergence on the upper Texas coast are subsidence and faulting associated with underground fluid production. Rates of "natural" subsidence and eustatic sea-level rise are greatly exceeded by rates of human-induced subsidence in the Galveston-Houston area where a subsidence "bowl" formed primarily from ground-water withdrawal encompasses more than 1×10^6 ha. In wetland areas undergoing submergence, rates of relative sea-level rise due primarily to human-induced subsidence range from 10 to more than 60 mm yr^{-1}. For comparison, maximum rates of marsh vertical accretion documented along the Gulf Coast in Louisiana, where the highest rates have been reported, are near 13 mm yr^{-1} in streamside marshes and less than 8 mm yr^{-1} in backmarshes. Rates of vertical accretion in backmarshes in the Trinity River fluvial-deltaic system in Texas average less than 6 mm yr^{-1}.

Wetland loss associated with faulting and subsidence has occurred in several locations, including Bolivar Peninsula in East Galveston Bay, the Neches River Valley at the head of Sabine Lake, and the interfluvial area between Sabine Lake and Galveston Bay. Emergent vegetation is converted to open water and shallow subaqueous flats on the downthrown side of faults where the rate of downward vertical movement and sea-level rise apparently exceeds marsh vertical accretion rates. There is evidence that fault movement in the areas investigated is related to hydrocarbon production.

Near the mouths of coastal rivers where there is the potential for sediment deposition to offset submergence, upstream dams and reservoirs trap a large percentage of sediment and prevent its delivery to coastal wetlands. Artificial channels and levees further inhibit available sediment from reaching wetlands.

Although rates of wetland loss doubled locally from the 1930's–1950's compared to the 1950's–1970/80's, rates declined in some areas after the 1970's. These reductions in wetland loss in the Galveston Bay system may be related to dramatic reductions in rates of human-induced subsidence as a result of curtailment of ground-water pumpage after the 1970's.

ACKNOWLEDGEMENTS

Funding for this paper was provided by the U.S. Geological Survey as part of a cooperative study with the Bureau of Economic Geology on coastal erosion of East Texas. Much of the information on wetland losses along the Texas coast are the result of wetland studies sponsored by the Environmental Protection Agency and Texas Natural Resources Conservation Commission (formerly Texas Water Commission) through the Galveston Bay National Estuary Program (GBNEP), and by the Texas Water Development Board, and Texas Parks and Wildlife Department.

Investigations of wetland trends in the Galveston Bay system as part of GBNEP were a cooperative effort between the Bureau of Economic Geology and U.S. Fish and Wildlife Service (E. G. Wermund and L. R. Handley, Co-principal Investigators). The authors thank S. Jeffress Williams of the U.S. Geological Survey and Robert A. Morton of the Bureau of Economic Geology for reviewing the draft manuscript and providing very useful comments for its revision. We also wish to thank Patrice Porter, Diane Spinney, David Stephens, and Michele Bailey of the Bureau of Economic Geology for assistance in figure preparation and digitization. Publication authorized by the director, Bureau of Economic Geology, The University of Texas at Austin.

LITERATURE CITED

BALAZS, E.I.M. 1980. The 1978 Houston-Galveston and Texas Gulf Coast vertical control surveys. *NOAA Technical Memorandum NOS NGS 27*. Rockville, Maryland, 61 p.

BAUMANN, R.H. and DELAUNE, R.D., 1982. Sedimentation and apparent sea-level rise as factors affecting land loss in coastal Louisiana. *In*: BOESCH, D.F. (ed.), *Proceedings of the Conference on Coastal Erosion and Wetland Modification in Louisiana: Causes, Consequences, and Options*. Washington, D.C.: U.S. Fish and Wildlife Service, Biological Services Program, FWS/OBS-82/59, pp. 2–13.

BAUMANN, R.H.; DAY, J.W., JR., and MILLER, C.A., 1984. Mississippi deltaic wetland survival: Sedimentation versus coastal submergence. *Science*, 224, 1093–1095.

BRICKER-URSO, S.; NIXON, S.W.; COCHRAN, J.K.; HIRSCHBERG, D.J., and HUNT, C., 1989. Accretion rates and sediment accumulation in Rhode Island salt marshes. *Estuaries*, 12, 300–317.

BRITSCH, L.D. and DUNBAR, J.B., 1993. Land loss rates: Louisiana coastal plain. *Journal of Coastal Research*, 9, 324–338.

BROWN, L.F., JR.; MORTON, R.A.; MCGOWEN, J.H.; KREITLER, C.W., and FISHER, W.L., 1974. *Natural Hazards of the Texas Coastal Zone*. Austin, Texas: The University of Texas at Austin, Bureau of Economic Geology, 13p., 7 maps.

DAHL, T.E.; JOHNSON, C.E., and FRAYER, W.E., 1991. *Wetlands, Status and Trends in the Conterminous United States Mid-1970's to Mid-1980's*. Washington, D.C.: U.S. Department of the Interior, U.S. Fish and Wildlife Service, 23p.

DELAUNE, R.D.; BAUMANN, R.H., and GOSSELINK, J.G., 1983. Relationships among vertical accretion, coastal submergence, and erosion in a Louisiana Gulf Coast marsh. *Journal of Sedimentary Petrology*, 53, 147–157.

DIENER, R.A., 1975. *Cooperative Gulf of Mexico Estuarine Inventory and Study—Texas*: Area description. Seattle, Washington: National Oceanic and Atmospheric Administration, Technical Report, National Marine Fisheries Service Circular 393, 129p.

EWING, T.E., 1985. Subsidence and surface faulting in the Houston-Galveston area, Texas—Related to deep fluid withdrawal?. *In*: DORFMAN, M.H. and MORTON, R.A (eds.), *Geopressured-Geothermal Energy: Proceedings of the 6th U.S. Gulf Coast Geopressured-Geothermal Energy Conference*. New York: Pergamon, pp. 289–298.

FIELD, D.W.; REYER, A.J.; GENOVESE, P.V., and SHEARER, B.D., 1991. *Coastal Wetlands of the United States, An Accounting of a Valuable National Resource*. Rockville, Maryland: National Oceanic and Atmospheric Administration in Cooperation with the U.S. Fish and Wildlife Service, A special NOAA 20th anniversary report, 59p.

FISHER, W.L.; BROWN, L.F., JR.; MCGOWEN, J.H., and GROAT, C.G., 1973. *Environmental Geologic Atlas of the Texas Coastal Zone—Beaumont-Port Arthur Area*. Austin, Texas: The University of Texas at Austin, Bureau of Economic Geology, 93p., 9 maps.

FISHER, W.L.; MCGOWEN, J.H.; BROWN, L.F., JR., and GROAT, C.G., 1972. *Environmental Geologic Atlas of the Texas Coastal Zone—Galveston-Houston Area.* Austin, Texas: The University of Texas at Austin, Bureau of Economic Geology, 91p., 9 maps.

GABRYSCH, R.K., 1969. Land-surface subsidence in the Houston-Galveston region, Texas. *Proceedings, International Symposium on Land Subsidence, Publication No. 88,* Tokyo, Japan, AIHS, pp. 43–54.

GABRYSCH, R.K., 1984. Ground-water withdrawals and land-surface subsidence in the Houston-Galveston region, Texas, 1906–1980. *Texas Department of Water Resources Report 287,* Austin, Texas, 64p.

GABRYSCH, R.K. and BONNET C.W., 1975. Land-surface subsidence in the Houston-Galveston region, Texas. *Texas Water Development Board Report 188,* Austin, Texas, 19p.

GABRYSCH, R.K. and COPLIN, L.S., 1990. Land-surface subsidence resulting from ground-water withdrawals in the Houston-Galveston region, Texas, through 1987. *U.S. Geological Survey Report of Investigations No. 90-01,* Washington, D.C., 53p.

GAGLIANO, S.M.; MEYER-ARENDT, K.J., and WICKER, K.M., 1981. Land loss in the Mississippi River deltaic plain. *Gulf Coast Association of Geological Societies Transactions,* 31, 271–273.

GORNITZ, V. and LEBEDEFF, S., 1987. Global sea-level changes during the past century. *Society of Economic Paleontologists and Mineralogists, Special Publication No. 41,* 3–16.

GOSSELINK, J.G.; CORDES, C.L., and PARSONS, J.W., 1979. *An Ecological Characterization Study of the Chenier Plain Coastal Ecosystem of Louisiana and Texas.* Washington, D.C.: U. S. Fish and Wildlife Service, Office of Biological Services, FWS/OBS-78/9 through 78/11, 3 vols.

HATTON, R.S.; DELAUNE, R.D., and PATRICK, W.H., JR., 1983. Sedimentation, accretion, and subsidence in marshes of the Barataria Basin, Louisiana. *Limnology and Oceanography,* 28, 494–502.

JOHNSTON, J.B. and ADER, R.A., 1983. The use of a GIS for Gulf of Mexico wetland change. *In:* MAGOON, O. T. and CONVERSE, H. (eds.), *Coastal Zone '83,* Volume I. New York: American Society of Civil Engineers, pp. 362–371.

KANE, H.E., 1959. Late Quaternary geology of Sabine Lake and vicinity, Texas and Louisiana. *Gulf Coast Association of Geological Societies Transactions,* 9, 225–235.

KREITLER, C.W., 1977. Faulting and land subsidence from ground-water and hydrocarbon production, Houston-Galveston, Texas. *Bureau of Economic Geology Research Note 8,* The University of Texas at Austin, Austin, Texas, 22p.

KREITLER, C.W.; WHITE, W.A., and AKHTER, M.S., 1988. Land subsidence associated with hydrocarbon production, Texas Gulf Coast (abs.). *American Association of Petroleum Geologists Bulletin,* 72, 208.

LEBLANC, R.J. and HODGSON, W.D., 1959. Origin and development of the Texas shoreline. *In:* RUSSELL, R.J., (chm.), *Second Coastal Geography Conference.* Louisiana State University, Coastal Studies Institute, Baton Rouge, Louisiana, pp. 57–101.

LYLES, S.D.; HICKMAN, L.E., JR., AND DEBAUGH, H.A., JR., 1988. *Sea Level Variations for the United States.* Rockville, Maryland: National Oceanic and Atmospheric Administration, National Ocean Service, 182p.

MCFARLANE, R.W., 1991. An environmental inventory of the ~~Christmas Bay~~ Coastal Preserve. *Galveston Bay National Estuary Program, GBNEP-7,* Webster, Texas, 95p.

MCKINNEY, L.D.; HIGHTOWER, M.; SMITH, B.; BECKETT, D., and GREEN A., 1989. Management issues: Galveston Bay. *In:* Galveston Bay: Issues, Resources, Status, and Management. U.S. Department of Commerce, National Oceanic and Atmospheric Administration, *Estuary-of-the Month Seminar Series No. 13,* Washington, D.C., pp. 79–87.

MORTON, R.A. and PAINE, J.G., 1990. Coastal land loss in Texas—An overview. *Gulf Coast Association of Geological Societies Transactions,* 40, 625–634.

NIXON, S.W., 1980. Between coastal marshes and coastal waters—A review of twenty years of speculation and research on the role of salt marshes in estuarine productivity and water chemistry. *In:* HAMILTON, PETER and MACDONALD, K.B. (eds.), *Estuarine and Wetland Processes.* New York: Plenum Press, 437–525.

NYMAN, J.A.; CARLOSS, M.; DELAUNE, R.D., and PATRICK, W.H., JR., Are landscape patterns related to marsh loss processes. *In:* MAGOON, O.T.; WILSON, W.S.; CONVERSE, H., and TOBIN, L.T. (eds.), *Coastal Zone '93, Proceedings of the Eighth Symposium on Coastal and Ocean Management.* New York: American Society of Civil Engineers, 337–348.

PAINE, J.G., 1993. Subsidence of the Texas coast: Inferences from historical and late Pleistocene sea levels. *Tectonophysics,* 222, 445–458.

PAINE, J.G. and MORTON, R.A., 1986. Historical shoreline changes in Trinity, Galveston, West, and East Bays, Texas Gulf Coast. *Bureau of Economic Geology Geological Circular 86-3,* The University of Texas at Austin, 58p.

PENLAND, S.; ROBERTS, H.H.; WILLIAMS, S.J.; SALLENGER, A.H., JR.; CAHOON, D.R.; DAVIS, D.W., and GROAT, C.G., 1990. Coastal land loss in Louisiana. *Gulf Coast Association of Geological Societies Transactions,* 40, 685–699.

PRATT, W.E. and JOHNSON, D.W., 1926. Local subsidence of the Goose Creek oil field. *Journal of Geology,* 34, 577–590.

PULICH, W.M. and WHITE, W.A., 1991. Decline of submerged vegetation in the Galveston Bay system: Chronology and relationships to physical processes. *Journal of Coastal Research,* 7, 1125–1138.

RAMSEY, K.E. and PENLAND, S., 1989. Sea-level rise and subsidence in Louisiana and the Gulf of Mexico. *Gulf Coast Association of Geological Societies Transactions,* 39, 491–500.

RATZLAFF, K.W., 1980. Land-surface subsidence in the Texas coastal region. Washington, D.C. *U.S. Geological Survey Open-File Report 80-969,* 19p.

REED, D.J. and CAHOON, D.R., 1992. The relationship between marsh surface topography, hydroperiod, and growth of *Spartina alterniflora* in a deteriorating Louisiana salt marsh. *Journal of Coastal Research,* 8, 77–87.

REED, D.J. and CAHOON, D.R., 1993. Marsh submergence vs. marsh accretion: Interpreting accretion deficit data in coastal Louisiana. *In*: MAGOON, O.T.; WILSON, W.S.; CONVERSE, H., and TOBIN, L.T. (eds.), *Coastal Zone '93, Proceedings of the Eighth Symposium on Coastal and Ocean Management*. New York: American Society of Civil Engineers, pp. 243–257.

REHKEMPER, L.J., 1969. Sedimentology of Holocene estuarine deposits, Galveston Bay. *In*: LANKFORD, R.R. and ROGERS, J.J.W. (eds.), *Holocene Geology of the Galveston Bay Area*. Houston, Texas: Houston Geological Society, pp. 12–52.

REID, W.M, 1973. Active Faults in Houston, Texas. Unpublished Ph.D. Dissertation, The University of Texas at Austin, Austin, Texas, 122p.

SCAIFE, W.W.; TURNER, R.E., and COSTANZA, R., 1983. Coastal Louisiana recent land loss and canal impacts. *Environmental Management*, 7, 433–442.

STEVENSON, J.C.; WARD, L.G., and KEARNEY, M.S., 1985. Vertical accretion in marshes with varying rates of sea level rise. *In*: WOLFE, T.A. (ed.), *Estuarine Variability*. Orlando, Florida: Academic Press, Inc., 241–259.

SWANSON, R.L. and THURLOW, C.I., 1973. Recent subsidence rates along the Texas and Louisiana coasts as determined from tide measurements. *Journal of Geophysical Research*, 78, 2665–2671.

SWENSON, E.M. and TURNER, R.E., 1987. Spoil banks: Effects on a coastal marsh water-level regime. *Estuarine, Coastal and Shelf Science*, 24, 599–609.

TEXAS RAILROAD COMMISSION, 1993. *Oil and Gas Division Annual Report, 1992, Volume 1*. Austin, Texas: Railroad Commission of Texas, 440p.

TURNER, R.E. and CAHOON, D.R. (eds.), 1988. *Causes of Wetland Loss in the Coastal Central Gulf of Mexico, Volume II: Technical Narrative*. New Orleans, Louisiana: U.S. Department of the Interior, Minerals Management Service, OCS Study/MMS 87-0120, 400p.

U.S. DEPARTMENT OF AGRICULTURE, 1959. Inventory and use of sedimentation data in Texas. Austin, Texas: *Texas Board of Water Engineers, Bulletin 5912*, 85p.

VAN SICLEN, D., 1967. The Houston fault problem. *Proceedings of the American Institute of Professional Geologists*, 3rd Annual Meeting, Texas Section, pp. 9–31.

VERBEEK, E.R., and CLANTON, U.S., 1981. Historically active faults in the Houston metropolitan area. Texas. *In*: ETTER, E. M. (ed.), *Houston Area Environmental Geology: Surface Faulting, Ground Subsidence, Hazard Liability*. Houston, Texas: Houston Geological Society, pp. 28–68.

WEAVER, P. and SHEETS, M., 1962. Active faults, subsidence and foundation problems in the Houston, Texas, area. *Geology of the Gulf Coast and Central Texas, Houston Geological Society Guidebook*, Houston, Texas, pp. 254–265.

WHITE, W.A., and CALNAN, T.R., 1990. *Sedimentation and Historical Changes in Fluvial-Deltaic Wetlands along the Texas Gulf Coast with Emphasis on the Colorado and Trinity River Deltas*. The University of Texas at Austin, Bureau of Economic Geology, final report prepared for the Texas Parks and Wildlife Department, Austin, Texas, 124p., 7 Appendices.

WHITE, W.A., and CALNAN, T.R., 1991. Submergence of vegetated wetlands in fluvial-deltaic areas, Texas Gulf Coast. *In*: *Coastal Depositional Systems, Gulf of Mexico*. Society of Economic Paleontologists and Mineralogists, Gulf Coast Section, Twelfth Annual Research Conference, Houston, Texas, pp. 278–279.

WHITE, W.A. and PAINE, J.G., 1992. Wetland plant communities, Galveston Bay system. *Galveston Bay National Estuary Program, GBNEP-16*, Webster, Texas, 124p.

WHITE, W.A.; CALNAN, T.R.; MORTON, R.A.; KIMBLE, R.S.; LITTLETON, T.G.; MCGOWEN, J.H.; NANCE, H.S., and SCHMEDES, K.E., 1985. *Submerged Lands of Texas, Galveston-Houston Area: Sediments, Geochemistry, Benthic Macroinvertebrates, and Associated Wetlands*. Austin, Texas: The University of Texas at Austin, Bureau of Economic Geology, Special publication, 145p.

WHITE, W.A.; CALNAN, T.R.; MORTON, R.A.; KIMBLE, R.S.; LITTLETON, T.G.; MCGOWEN, J.H., and NANCE, H.S., 1987. *Submerged Lands of Texas, Beaumont-Port Arthur Area: Sediments, Geochemistry, Benthic Macroinvertebrates, and Associated Wetlands*. Austin, Texas: The University of Texas at Austin, Bureau Economic Geology Special Publication, 110p.

WHITE, W.A.; TREMBLAY, T.A.; WERMUND, E.G., JR., and HANDLEY, L.R., 1993. Trends and status of wetland and aquatic habitats in the Galveston Bay system, Texas. *Galveston Bay National Estuary Program, GBNEP-31*, Webster, Texas, 225p.

WILLIAMS, S.J.; PENLAND, S., and ROBERTS, H.H., 1993. Processes affecting coastal wetland loss in Louisiana deltaic plain: *In*: MAGOON, O.T.; WILSON, W.S.; CONVERSE, H., and TOBIN, L.T. (eds.), *Coastal Zone '93, Proceedings of the Eighth Symposium on Coastal and Ocean Management*. New York: American Society of Civil Engineers, pp. 211–219.

WINSLOW, A.G. and DOYEL, W.W., 1954. Land-surface subsidence and its relation to the withdrawal of ground water in the Houston-Galveston region, Texas. *Economic Geology*, 49, pp. 413–422.

YERKES, R.F. and CASTLE, R.O., 1969. Surface deformation associated with oil and gas field operations in the United States. *Proceedings, International Symposium on Land Subsidence, Publication No. 88*, Tokyo, Japan, AIHS, 1, pp. 55–66.

Figure 12. Aerial photograph of fault near Clam Lake. Topographically low marshes and open water increase in area on the downthrown side (D) of the fault relative to the upthrown side (U). Photograph taken by NASA in 1989. Location in Figure 1.

Figure 12. Aerial photograph of fault near Clam Lake. Topographically low marshes and open water increase in area on the downthrown side (D) of the fault relative to the upthrown side (U). Photograph taken by NASA in 1989. Location in Figure 1.

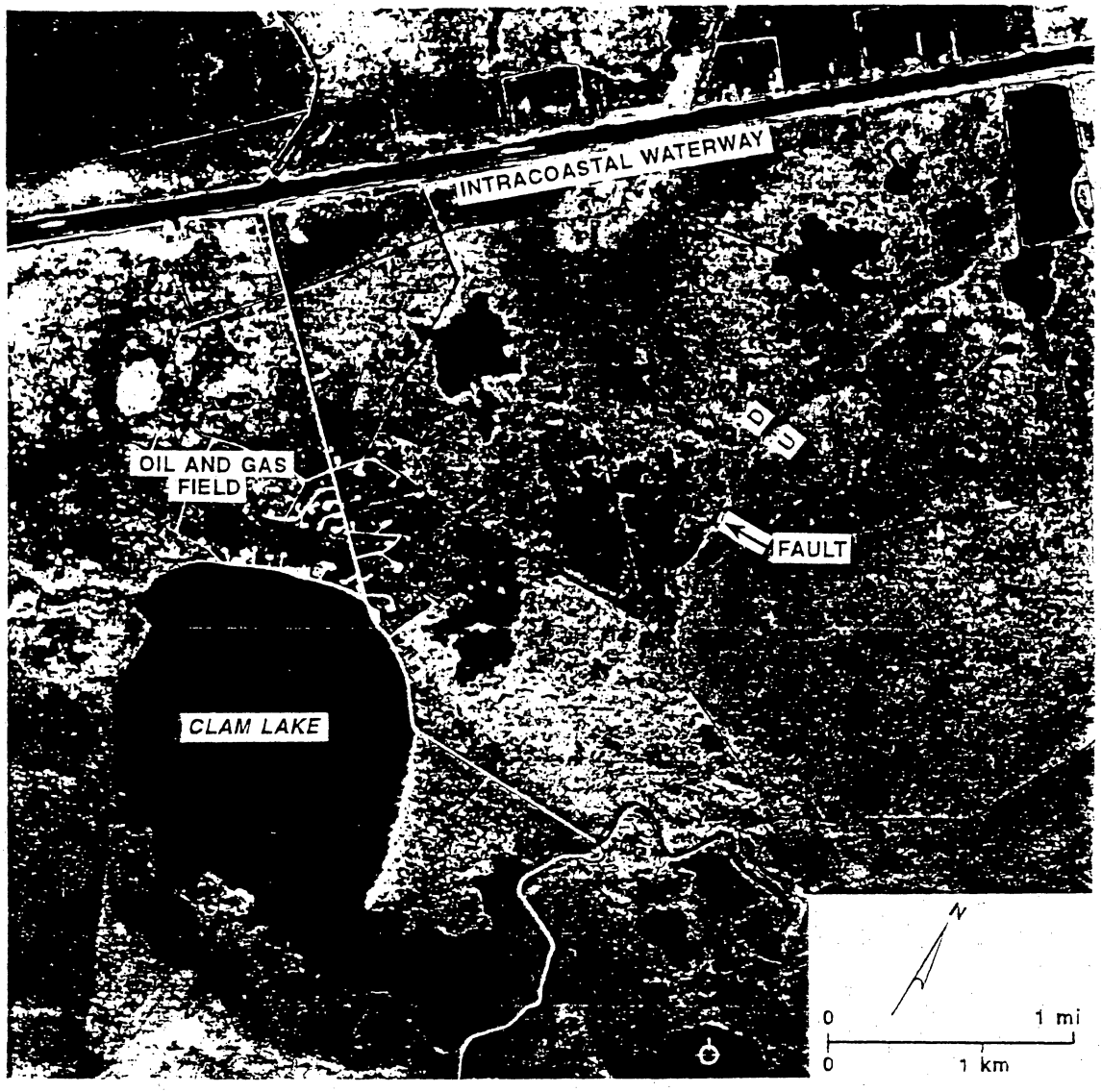
INTRACOASTAL WATERWAY
OIL AND GAS FIELD
D
U
FAULT
CLAM LAKE
N
0
1 mi
0
1 km

Addendum 2. Descriptions of Auger Cores, Southeastern Texas Coast

Descriptions of Auger Cores, Southeastern Texas Coast

Core Number	Latitude	Longitude	Depth (ft)	Environment
CE-2	29°35'26"	94°23'26"	24.2	interfluve
CE-3	29°35'07"	94°23'34"	19.0	interfluve
CE-4	29°32'56"	94°23'17"	34.15	interfluve
CE-5	29°37'21"	94°11'45"	23.9	interfluve
CE-6	29°40'02"	94°04'23"	28.9	interfluve
CE-7	29°41'49"	93°57'04"	44.5	chenier plain
CE-8	29°42'47"	93°54'45"	44.45	chenier plain
CE-9	29°43'58"	93°52'34"	29.3	chenier plain
CE-10	29°43'49"	93°53'02"	80.0	chenier plain
CE-11	29°44'21"	93°54'20"	34.1	incised valley
CE-12	29°44'52"	93°55'40"	33.9	incised valley
CE-13	29°45'58"	93°56'13"	95.4	incised valley
CE-14	30°00'32"	92°51'30"	30.4	incised valley
CE-15	30°00'11"	92°51'52"	59.3	incised valley

COASTAL EROSION PROJECT

Location: CE-2

Remarks:

Vibra Core ☐ _____
Piston Core ☐ _____
Rotary Core ☒ _____
Elevation: _____

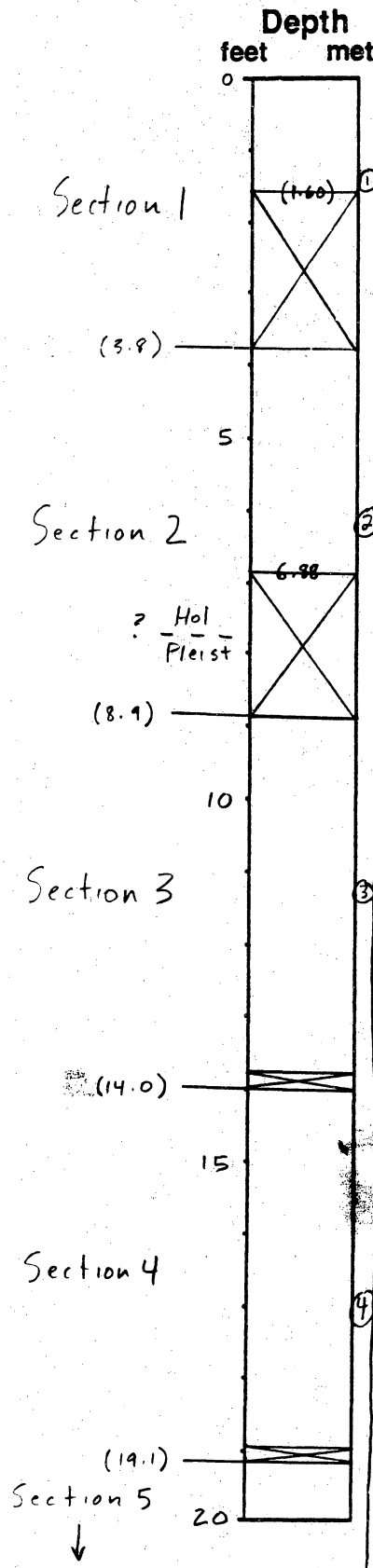

0 – .33': Light brownish gray (5 YR 6/1); muddy sand w/ abundant oyster shell fragments (Fill material)

.33 – 1.60': Mod. reddish orange (10 R 6/6); slightly muddy fine sand, crudely laminated, scattered oxidation (Fill material)

1.60 – 3.8': NO RECOVERY

3.8 – 4.24': Medium gray (N4); slightly silty soft clay; faint streaky lamination, fine-scale mottling

— sharp contact w/ concentrated organic debris —

4.24 – 6.53': Grayish black (N2); soft clay; faint streaky laminations, black organic debris, fine to medium scale medium gray (N4) mottling (similar mottling to above)

— sharp, very irregular contact —

6.53 – 6.72': Very pale orange (10 YR 8/2); very fine sand w/ discontinuous silty mud laminae

— sharp, very irregular contact —

6.72 – 6.84': Grayish black (N2); soft clay; fine scale, sand-filled small bioturbation traces

— sharp, very irregular contact —

6.84 – 6.88': Grayish orange (10 YR 7/4); fine sand (not much recovered)

6.88 – 8.9': NO RECOVERY

8.9 – 11.73': Med. light gray (N5); stiff silty clay; root traces (oxidized and non-oxidized)

— gradational contact —

11.73 – 13.81': Greenish gray (5 GY 6/1) w/ dark yellowish orange (10 YR 6/6) mottling; silty to sandy stiff clay, sandier at base; circular, oxidized burrows (¼" – ½" across), burrows more abundant at base; $CaCO_3$ nodules

13.81 – 14.0': NO RECOVERY

14.0 – 16.96': Greenish gray (5 GY 6/1) w/ dark yellowish orange (10 YR 6/6) mottling; clayey silt to clayey very fine sand (variable + heterogeneous) locally preserved fine laminations, otherwise extensively bioturbated — small root traces (?) to near vertical burrows to ¼" across (some sand-filled); abundant $CaCO_3$ nodules

— sharp contact —

16.96 – 17.04': Greenish gray (5 GY 6/1); silty clay; scattered small root traces

— sharp contact —

17.04 – 17.64': Grayish yellow (5 Y 8/4); very fine sand w/ scattered muddy laminae; some preserved laminations (inclined at base, horizontal at top), elsewhere sand-filled burrows obliterate laminations

— sharp erosional contact —

17.64 – 17.79': Greenish gray (5 GY 6/1); silty clay; sand-filled burrows

— gradational contact —

(Section 4 continued next page)

Location: CE-2

Remarks:

Vibra Core ☐ _____
Piston Core ☐ _____
Rotary Core ☒ _____
Elevation: _____

Depth
feet meters

Section 5

(24.2) (TD)
25

Description

17.79 - 18.16 : Grayish orange (10 YR 7/4); very fine sand w/ muddy laminae; some preserved sub-horizontal laminations, otherwise burrowed
— sharp erosional contact —
18.16 - 18.25 : Greenish gray (5 GY 6/1); silty clay w/ thin sandy laminae; sand-filled burrows
— sharp, irregular contact —
18.25 - 18.94 : Grayish yellow (5 Y 8/4); very fine sand w/ sandy mud laminae, muddy laminae decrease upward; horizontally laminated to ripple cross-bedded
18.94 - 19.1 : NO RECOVERY
19.1 - 19.85 : Grayish yellow (5 Y 8/4); very fine sand; massive
— gradational contact —
19.85 - 20.67 : Grayish yellow (5 Y 8/4); very fine sand; small (< 1/8") burrows filled w/ sandy clay
— sharp contract w/ clay drape —
20.67 - 22.38 : Grayish orange (10 YR 7/4); very fine sand; burrows (1/4 - 1/2") filled w/ sandy clay, burrow abundance decreases upward
22.38 - 22.84 : Grayish yellow (5 Y 8/4) to greenish gray (5 GY 6/1); very fine sand w/ muddy laminae to silty clay w/ very fine sand laminae sand-dominated at base, mud-dominated at top
— sharp contact —
22.84 - 23.13 : Greenish gray (5 GY 6/1); clay w/ wispy very fine sand laminae
— sharp irregular contact —
23.13 - 23.46 : Dark yellowish orange (10 YR 6/6); very fine sand; inclined laminations (ripple x-beds)
— sharp contact —
23.46 - 23.67 : Greenish gray (5 GY 6/1); clay; small sand-filled burro
— sharp contact —
23.67 - 23.88 : Grayish yellow (5 Y 8/4); very fine sand w/ irregular muddy laminae
— sharp contact —
23.88 - 23.98 : Greenish gray (5 GY 6/1); clay
— sharp contact —
23.98 - 24.2 : Grayish yellow (5 Y 8/4) to greenish gray (5 GY 6/1); very fine sand w/ horizontal sandy clay laminae

END CORE - TD

COASTAL EROSION [illegible]

Location: CE - 2A

Remarks: along HWY 124 in High Island area
redrill of CE-2

Vibra Core ☐
Piston Core ☐
Rotary Core ☒
Elevation:

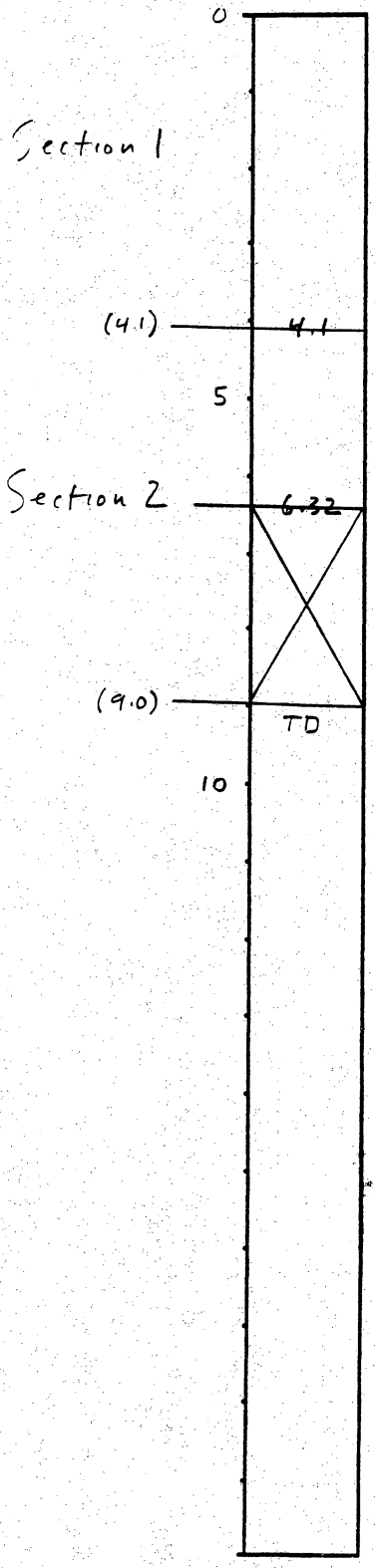

Description

0 - .42' : Dusky yel br (10 YR 2/2); hard silty clay; preserved organic matter (roots), small shell frags

— gradational contact —

1.42 - 3.29' : Mod. reddish br (10 R 4/6); clayey fine sand; disturbed chaotic texture, oyster shell frags at top (Fill material)

— sharp contact —

3.29 - 3.62 : Br. black (5 YR 2/1); silty clay; oyster shell fragments (some whole)

— gradational contact —

3.62 - 4.10 : Pale yel. orange (10 YR 6/6); clayey very fine sd, disturbed mottled texture

4.10 - 4.20' : Mod. yel. br. (10 YR 5/4); clayey v.f. sd; massive

— sharp contact —

4.20 - 4.30' : Lt. gr. g (5 GY 8/1); slighty clayey v.f. sd w/ cl. lamina; mottled texture

— sharp contact —

4.30 - 6.05 : Black (N1); clay; root mottling (?) filled w/ lt g (N7) cla preserved organic matter (roots) near top

— contact uncertain —

* 6.05 - 6.32 : Dark gray (N3); clay, root mottling filled w/ lt g (N7) clay

END RECOVERY AT 6.32' TD = 9.0'

*: section in plastic bag - unclear whether continuous w/ part of section 2 in tube

COASTAL EROSION PROJECT

Location: CE-3

Remarks: Along Hwy 124 - High Island area

Vibra Core ☐ _____
Piston Core ☐ _____
Rotary Core ☒ _____
Elevation: _____

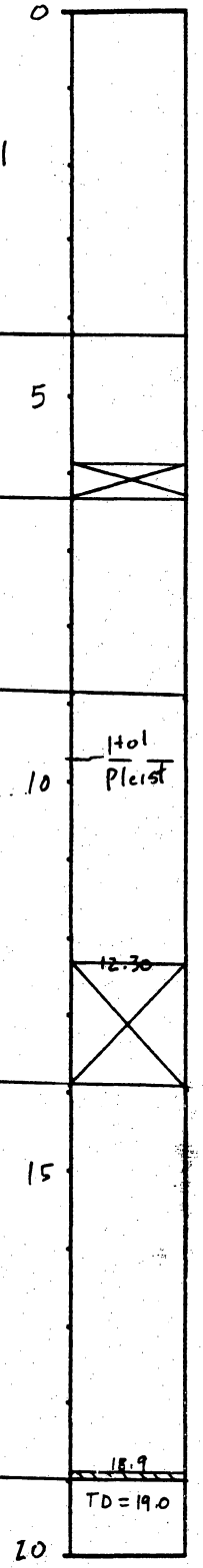

Description

0 - .46': Mod yel br (10 YR 5/4); silty to sdy cl; abdt shell frags, organic matter near top (Fill material)
— sharp contact ? —
.46 - .88: Pale br (5 YR 5/2); slightly clayey v.f. sd; disturbed, mottled texture (Fill)
— sharp contact —
.88 - 2.96': Dk yel orange (10 YR 6/6); clayey fine sd; disturbed, chaotic texture, scattered oxidation spots (Fill)
— sharp contact —
2.96 - 4.17': Grayish black (N2); slightly silty clay; sand-filled burrows concentrated near top, root mottling
— break from section 1 to 2 —
4.17 - 5.38: Grayish black (N2); clay; root mottling, lt gray (N7) mottling of uncertain origin, scattered organic matter (small)
— gradational contact —
5.38 - 5.84: Dk yel br (10 YR 4/2); clay; oxidized root mottling, grayish black (N2) mottling of uncertain origin, minor small sd-filled burrows
5.84 - 6.3': NO RECOVERY
6.3 - 8.82': Med dk grey (N4); slightly silty stiff clay; heavily mottled - oxidized root mottling, grayish black (N2) mottling; small sd-filled burrows; organic matter in lower half
— contact uncertain, break between sections 3 & 4 —
8.82 - 9.70': Dk gray (N3); slightly silty clay; mottled appearance including lt. gray bioturbation (root?) mottling, sd-filled burrows, small bits of org. matter
— sharp contact — (Hol / Pleist)
9.70 - 11.52: Md. lt. gray (N6) w/ dk yel or. (10 YR 6/6) oxidation mottling; clayey v.f. sd, fine-scale mottling filled w/ cleaner sd, oxidation mottling, oxidized organ matter
— gradational contact —
11.52 - 12.30': Lt. gray (N7) w/ dk yel or (10 YR 6/6) mottling; slightly clayey v.f. sd; fine-scale mottling, extensive non-fabric-selective oxidation, oxid. org matter (wood,
12.30 - 13.90': NO RECOVERY
13.90 - 15.36: Dk yel or (10 YR 6/6); v.f. to f. sd; 'stringy' dk gray (N3) mottlin extensive non-fabric selective oxidation
— sharp contact —
15.36 - 15.90: Yel gray (5 Y 8/1); same as above but no oxidation
— sharp contact —
15.90 - 16.52: DK gray (N3); clayey v.f. sd; irregular texture w/ some sd-ric zones + some clay-rich zones; burrows filled w/ cleaner sd
— sharp contact —
16.52 - 18.90: Yel gray (5 Y 8/1); v.f. sd; irregular zones of clayey sd, burro filled w/ clayey sd (more common near top)
END RECOVERY - 18.90'
TD = 19.0'

Location: CE-4

Remarks: Beach near Hwy 124 and High Island

Vibra Core ☐ _____
Piston Core ☐ _____
Rotary Core ☒ _____
Elevation: _____

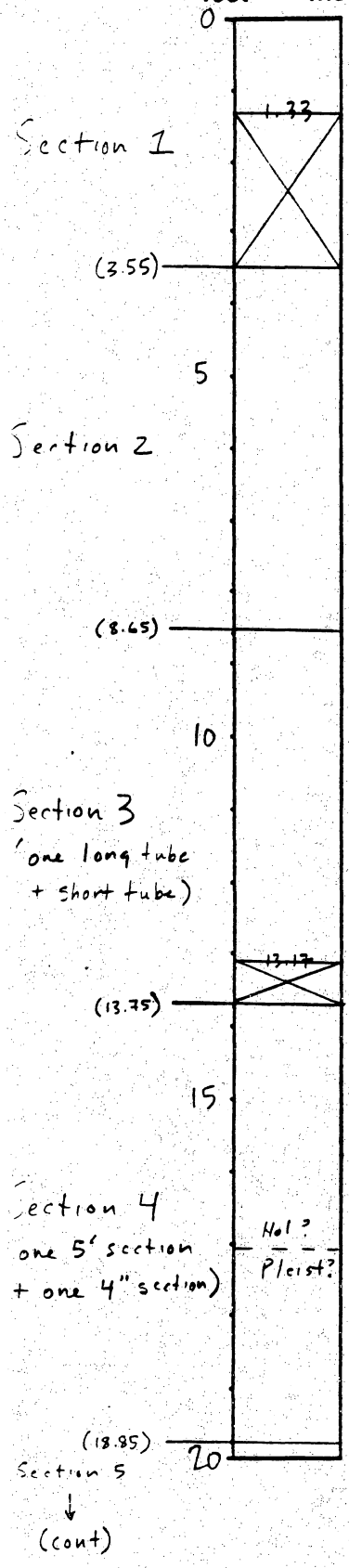

Description

0 – 0.6′: Mod. yellowish brown (10 YR 5/4); fine sand w/ coarse to granule size rock fragments (ss), outsized cobble rock fragments (ss) at base; abdt shell fragments

— sharp contact —

0.6 – 1.25′: Grayish orange (10 YR 7/4); fine to v. fine sand (fining upward) coarse to pebble size rock fragments near base; common shell fragments (decreasing upward)

— sharp contact —

1.25 – 1.33′: Grayish orange (10 YR 7/4); fine sand w/ minor shell fragments

1.33 – 3.55′: NO RECOVERY

3.55 – 3.63′: Grayish orange (10 YR 7/4); fine sand w/ minor shell fragments

— sharp contact —

3.63 – 5.13′: Grayish orange (10 YR 7/4) / Grayish black (N2); interbedded fine sand and clay, bioturbated (abdt root mottling, some burrows), sand content increases upward

0.4′ intervals → (1) thinly interbedded ripple x-laminated sand and mud (Flaser bedding) sharply overlain by mud w/ sand-filled root traces

— sharp, irregular contact —

(2) sand (~1" thick) w/ minor mud-filled root traces sharply overlain by clay w/ root traces

— sharp, highly irregular contact —

(3) sand (2½–3" thick) w/ mud-filled root traces and burrow overlain by clay w/ sand-filled root traces

— sharp, highly irregular contact —

(4) sand (~5" thick) grading upward into silty sandy clay w/ scattered root mottling

— sharp contact —

5.13 – 6.96′: Grayish black (N2); clay w/ scattered silty to fine-sand filled mottling, root traces w/ some preserved organic matter (more abundant near top)

— gradational contact —

6.96′ – 7.54′: Olive gray (5 Y 4/1); mottled silty clay w/ oxidized root traces near base

— gradational contact —

7.54′ – 8.65′: Grayish orange (10 YR 7/4) / Olive gray (5 Y 4/1); interbedded sand and silty clay; sands have mud-filled root traces, muds have scattered sand-filled mottles; contacts between sands + muds sharp but irregular (mottled); oxidized root traces in clays

— contact uncertain —

8.65 – 10.94′: Dk gr. g. (5 G 4/1); soft clay w/ one thin (~1") v.f sd bed, sd. filled burrows, lower ⅔ has oxidized mottling (root traces?)

— gradational contact —

10 ou - 12.15 : Gr black (5 GY 2/1) ; soft clay w/ thin discontinuous sand laminae ; widened small sand-filled burrows

— irrdational contact ——

12.15 - 12.94 : Dk gr g (5 GY 4/1) ; slightly silty clay, numerous burrows filled w/ clayey sd (burrows circular to wispy)

-- contact uncertain (split parts of tube)

12.94 - 13.17 : Dk gr g (5 GY 4/1) ; clayey v.f. sd ; wispy laminations ; mottling (bioturbation ?) some filled w/ clean sd, some w/ clayey sd

13.75 - 17.08' : Olive gray (5 Y 4/1) / Greenish gray (5 GY 6/1) ; clay (olive gray) w/ silty clay (greenish gray) and fine sand mottling ; mottling varies in scale from < 1/32" to 1"+ across ; nodular appearance ; mottling more extensive and larger scale towards top, sandy mottling present near top ; oxidation confined to mottled sections ; scattered oxidized root traces

— contact sharp but irregular, possible mud cracks ——

17.08 - 18.85' : Greenish gray (5 GY 6/1) / dark yellowish orange (10 YR 6/6) ; slightly muddy sand grading upward to silty clay ; fine scale mud-filled mottling (some root traces some of uncertain origin) ; faint laminations in sandy sections at base ; extensive non-selective oxidation

Location: Coastal Erosion CE-4

Remarks:

Vibra Core ☐ _____

Piston Core ☐ _____

Rotary Core ☒ _____

Elevation: _____

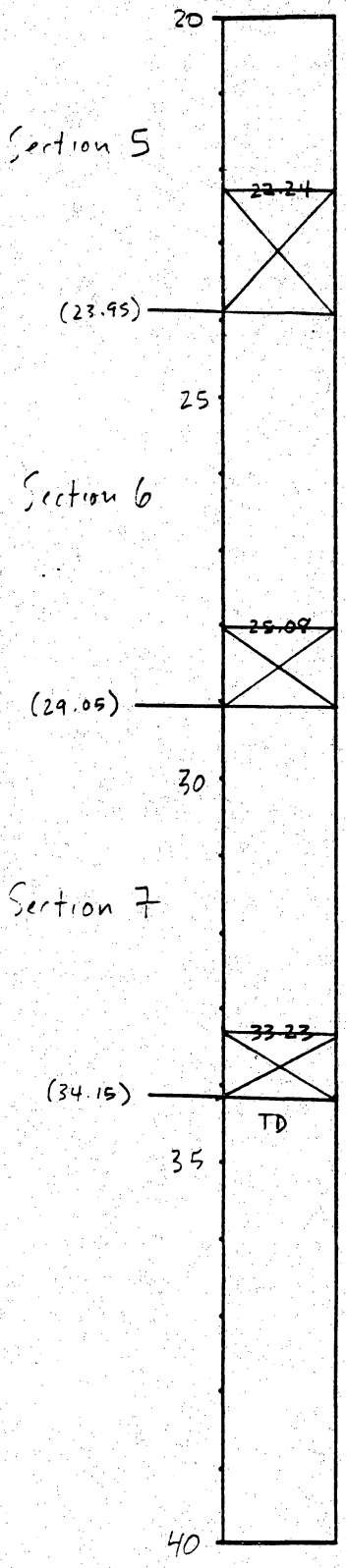

18.85 – 19.02': Dark yellowish orange (10 YR 6/6); fine sand, massive w/ small mudstone rip-up clasts; oxidized

— sharp contact —

19.02 – 19.40': Moderate yellowish brown (10 YR 5/4); sandy mud, mottled

— gradational contact —

19.40 – 20.36': Dark yellowish orange (10 YR 6/6); fine sand w/ irregular patches of clay and silty clay (interval appears to have been disturbed by coring process); extensively oxidized

— gradational contact —

20.36 – 20.74': Yellowish gray (5 Y 8/1); fine sand, indistinct horizontal laminations; scattered oxidization

— sharp, disturbed contact —

20.74 – 21.41': Yellowish gray (5 Y 8/1) / dark greenish gray (5 GY 4/1); interbedded fine sand and silty clay; sands have faint horizontal laminations, oxidized mottling; silty clay is mottled w/ wispy sand layers and oxidized root traces (?)

— sharp contact w/ possible mud cracks (or burrows) —

21.41 – 21.70': Dusky yellow (5 Y 6/4); silty to sandy clay; small oxidized mottling (probable root mottling)

— sharp, mud-draped contact; truncation suggest erosional —

21.70 – 22.24': Yellowish gray (5 Y 8/1) to dark yellowish orange (10 YR 6/6) fine sand w/ thin mudstone interbeds; interval disturbed by coring but mud/sand contacts appear sharp; scattered mud-filled root traces; irregular oxidation of sandy layers

22.24 – 23.95': NO RECOVERY

23.95 – 25.00': Med. light gray (N5); very fine sand, massive, mud rip-up clast (~½" across)

— sharp contact, possible silty mud drape —

25.00 – 25.50': Light gray (N7); very fine sand, faint irregular laminations, mudstone clasts to 1" concentrated at base

— sharp, slightly irregular contact (probably erosional) —

25.50 – 26.50': Greenish gray (5 G 6/1) / light gray (N7); slightly silty clay w/ irregular very fine sand interbeds; silty clay massive; sandy interbeds disturbed, some w/ thin muddy laminations, some sandy intervals oxidized; thickness of sand beds increases upward

— gradational contact —

26.50 – 26.96: Light greenish gray (5 GY 8/1); very fine sand w/ thin muddy laminae, sand/mud ratio decreases upward; some laminae inclined (possible ripple x-bedding)

— gradational contact —

26.96 – 27.29': Light greenish gray (5 GY 8/1); very fine sand, subhorizontal laminations (disturbed)

27.29 – 28.08': Light olive gray (5 Y 6/1); very fine sand w/ thin sandy mud laminae, high sand/mud ratio, laminae inclined (probably during coring process), fine mottling near base

28.08 – 29.05': NO RECOVERY

29.05': Dark greenish gray (5 GY 4/1); clay (only thin piece recovered)

— sharp contact —

29.05 – 30.44': Light olive gray (5 Y 6/1); very fine sand, massive, small mud rip-up clasts (concentrated near base but present throughout)

— sharp contact, possibly erosional —

30.44 – 31.82': Olive gray (5 Y 4/1); slightly silty clay, homogeneous; sand-filled burrows (~ ½" across); abundant bits of black organic debris

— gradational contact —

31.82 – 32.31': Olive gray (5 Y 4/1); slightly silty clay w/ thin very fine sand interbeds; silty clay same as above; sandy interbeds have sharp contacts, appear to have been originally horizontal

— sharp contact —

32.31 – 33.23': Light olive gray (5 Y 6/1); very fine sand w/ thin mud laminae (sand > mud); some laminations horizontal, others inclined (probable 2D ripple x-bedding)

END CORE

Location: CE-5

Remarks: Hwy 87 - ARCO facility

Vibra Core ☐ _____
Piston Core ☐ _____
Rotary Core ☒ _____
Elevation: _____

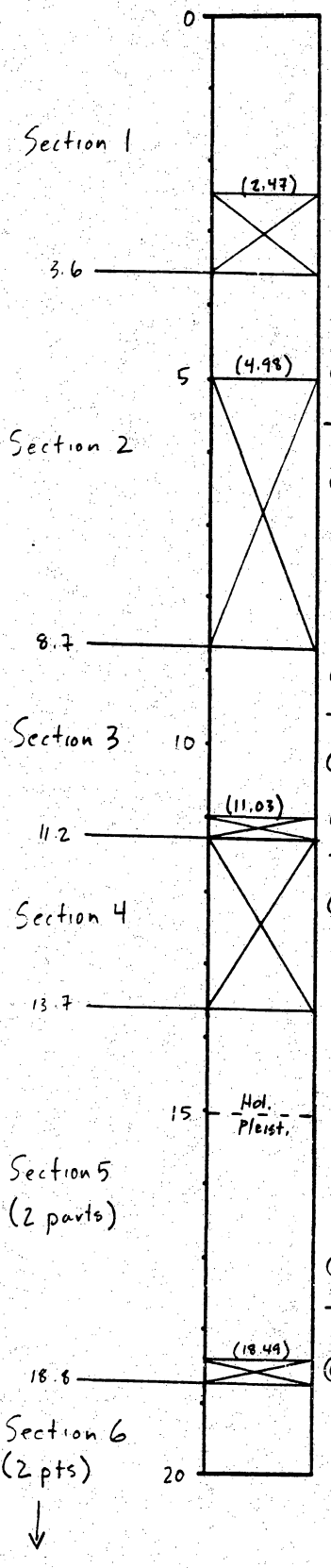

Description

0 – 1.58': Grayish orange (10 YR 7/4); f. to v.f. sd w/ scattered pebbles (ss clasts) preserved roots at top, abdt shell material (fine hash to large fragments), asphal c material (road?) at base

— sharp contact —

1.58 – 1.81: Grayish br (5 YR 3/2); clayey v.f. to f. sd; mottled w/ pockets of c x sd., preserved mud/sand laminae at base, very fine shell material

— sharp contact —

1.81 – 2.39: Grayish orange (10 YR 7/4); v.f. sd w/ thin muddy laminations; hori laminations, muddy laminae w/ bits of organic matter in lower ½, very fine shell debr

— sharp contact —

① 2.39 – 2.47: Olive gray (5 Y 4/1); sandy clay w/ v.f. sd. laminae; laminae hor

↑ 2.47 – 3.6: NO RECOVERY

↓

② 3.6 – 3.79: Grayish orange (10 YR 7/4); v.f. sd, discontinuous horiz (?) muddy lam

— sharp, erosional contact —

3.79 – 4.98': Grayish orange (10 YR 7/4) to dk gr. gray (5 GY 4/1); interbedded cla y v.f. sd and slightly sandy clay, muddier at base sandier at top, contacts between sd. & cl. sharp but irregular; clay beds have irregular pockets of clayey sd. (some bioturbation, other of uncertain origin), sands have irregular pocke

② of sandy clay (uncertain origin); small bits of organic matter

↑ 4.98 – 8.7: NO RECOVERY

↓

③ 8.7 – 11.03: Dk. gray (N3); clay; scattered pockets of v.f sd (probable burrows); small oxidized mottling (probable root mottling), oxidized vertical bioturbation

③ traces (root traces?)

↑ 11.03 – 13.7: NO RECOVERY

↓

⑤ 13.7 – 15.14: Dk gray (N3) to lt. gray (N7) at base; clay, slightly sdy at base; irre lc sdy laminae at base; fine lt. gray (N7) to black (N1) mottling, irregular lt. gray patches in lower ½, oxidized vertical bioturbation (root?) traces

— sharp, very irregular contact — (Pleistocene/Holocene contact?)

15.14 – 15.76: Med. lt. gray (N6) to dk yell. orange (10 YR 6/6); slightly sandy stiff clay; very fine mottling w/ clayey sd., pockets of dk gray clay (same as above inte l. Oxidized woody fragment, extensive oxidation

— contact uncertain —

15.76 – 18.49: Lt. gray (N7) to dk. yel. orange (10 YR 6/6); clayey silt to clayey v.f. sd; very hard; extensive fine mottling, probable vertical bioturbation traces near top filled w/ cleaner sd, elliptical clayey mottling at base (burrows?); upper ½ extensively oxidized oxidation decreasing downward

⑤ ↑ 18.49 – 18.8: NO RECOVERY

↓

⑥ 18.8 – 19.59: Lt. gray (N7), slightly sandy stiff clay; extensive light & dark mottling; chaotic, disturbed appearance; burrows filled w/ clayey sd

— contact very irregular & disturbed —

19.59 – 21.13: Very lt. gray (N8); slightly clayey sd; numerous burrows fle w/ darker gray sandy clay, upper contact extensively bioturbated; exte l clayey mottling (some root traces, others uncertain origins); very disturbe chaotic appearance

Location: CE-5

Remarks: Hwy 87 - ARCO Facility

Vibra Core ☐ _____

Piston Core ☐ _____

Rotary Core ☒ _____

Elevation: _____

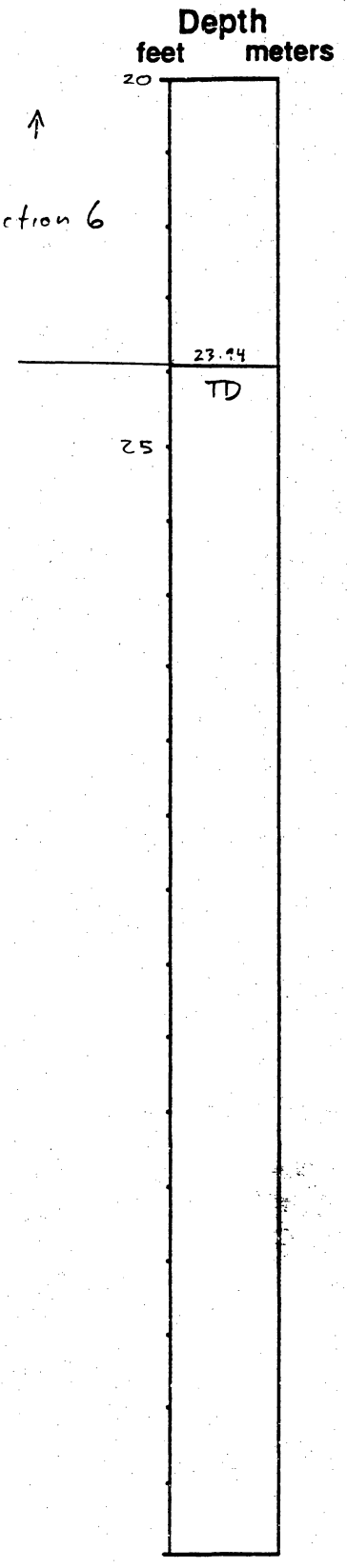

Description

— break in core section —

21.13 – 22.55 : same as above except one discreet clay interbed w/ sandy bioturbation mottling, and clay clast (?) near base

— gradational contact —

22.55 – 23.26 : very lt. gray (N8); interlaminated v.f. sd. and clay; laminae inclined (cross-bedding w/ clay drapes?); some mottling w/in clay laminae (probable bioturbation); extensive red. brn. oxidation

— sharp contact —

23.26 – 23.32 : Med gray (N5); clay; small sd-filled bioturbation traces

— gradational, bioturbated contact —

23.32 – 23.94 : very lt. gray; slightly clayey v.f. sd; mud-filled bioturbatic traces (more common at top); some preserved fine horizontal laminations; minor oxidation

TD = 23.9. END CORE

Location: CE-6

Remarks: Hwy 87 - Sea Rim State Park

Vibra Core ☐ _____
Piston Core ☐ _____
Rotary Core ☒ _____
Elevation: _____

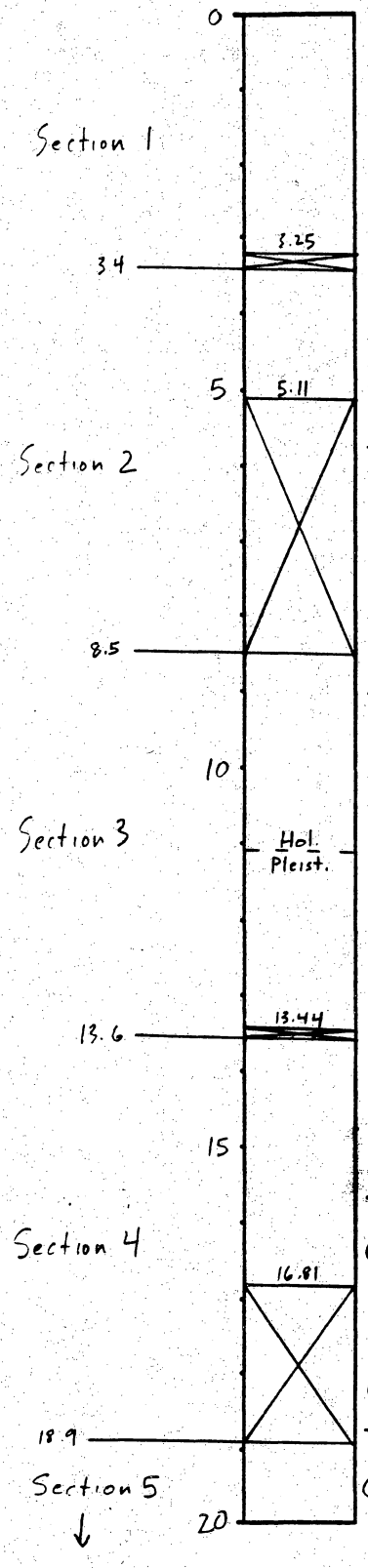

0 - 2.25 : Grayish orange (10 YR 7/4); loose v.f. sd., slightly muddy at base; th muddy laminae at base; abdt disseminated fine shell fragg., one shell hash zone towards base

— sharp contact —

2.25 - 2.60 : Dk gr gray (5 GY 4/1); clay, sandy clay at base; oxidized root trac sand-filled burrow at top; small bits of organic matter

— gradational contact —

2.60 - 3.0 : Dk yel br (10 YR 4/2); sandy clay to clayey sd w/ clay interbed; churne texture; lower contact of cl. interbed sharp, upper contact grad.; oxidized root trace fine organic debris in clayey sections

— sharp contact —

① 3.0 - 3.25 : Dk gr gray (5 GY 4/1); clay; oxidized root traces; fine organic debris

↑↓ 3.25 - 3.4 : NO RECOVERY

② 3.4 - 4.65 : Olive black (5 Y 2/1); clay; sd. filled probable bioturbation traces M. gray (N7) & grayish black (N2) mottling; small bits of black organic matter

— gradational contact —

4.65 - 5.11 : Olive black (5 Y 2/1) to grayish orange (10 YR 7/4); clay w/ v.f. sd. inter upper & lower contacts of sd sharp but irregular; abdt. sd-filled probable burrow

② oxidized root traces; fine grayish black (N2) mottling

↑↓ 5.11 - 8.5 : NO RECOVERY

③ 8.5 - 11.10 : Black (N1); soft clay; scattered sd.-filled probable burrows; mod lt. gray (N6) to lt. brn (5 YR 5/6) mottling; churned appearance; sm. to med. woody frag

— sharp, irregular contact — (probable Hol/Pleist. contact)

11.10 - 11.56 : Gr. gray (5 GY 6/1), clay; oxidized root traces; grayish black (N2) streaky mottling

— gradational contact —

11.56 - 12.18 : Med lt gray (N6); slightly sdy clay w/ v.f sd. interbed, sand content in clay decreases upward; top & bottom of sd bed irregular (bioturbated); ex fine sandy mottling (probable bioturbation)

— sharp, irregular contact —

12.18 - 13.44 : Lt gray (N7) to dk gray (N3); clayey v.f. sd w/ irregular sandy interbeds, sand content increases upward; disturbed fine laminations; extensi

③ fine mottling; oxidized vertical bioturbation traces (root traces)

↑↓ 13.44 - 13.60 : NO RECOVERY

④ 13.60 - 16.06 : Lt gray (N7); clayey sd, clay content increases upward, vertical bla streaky mottling, elliptical bioturbation (more common upward), scattered oxidatio

— gradational contact —

16.06 - 16.81 : Grayish orange (10 YR 7/4); v.f. sd, slightly clayey at top; faint

④ sub-horizontal laminations; elliptical mottling (bioturbation); extensive oxidatio

↑↓ 16.81 - 18.9 : NO RECOVERY

⑤ 18.9 - 19.15 : Grayish orange (10 YR 7/4); slightly clayey v.f. sd.; burrow (?) filled w/ sandy clay, fine-scale oxidized mottling

— sharp, irregular (loaded?) contact —

(cont)

Location: CE-6

Remarks: Hwy 87 - Sea Rim State Park

Vibra Core ☐ _____

Piston Core ☐ _____

Rotary Core ☒ _____

Elevation: _____

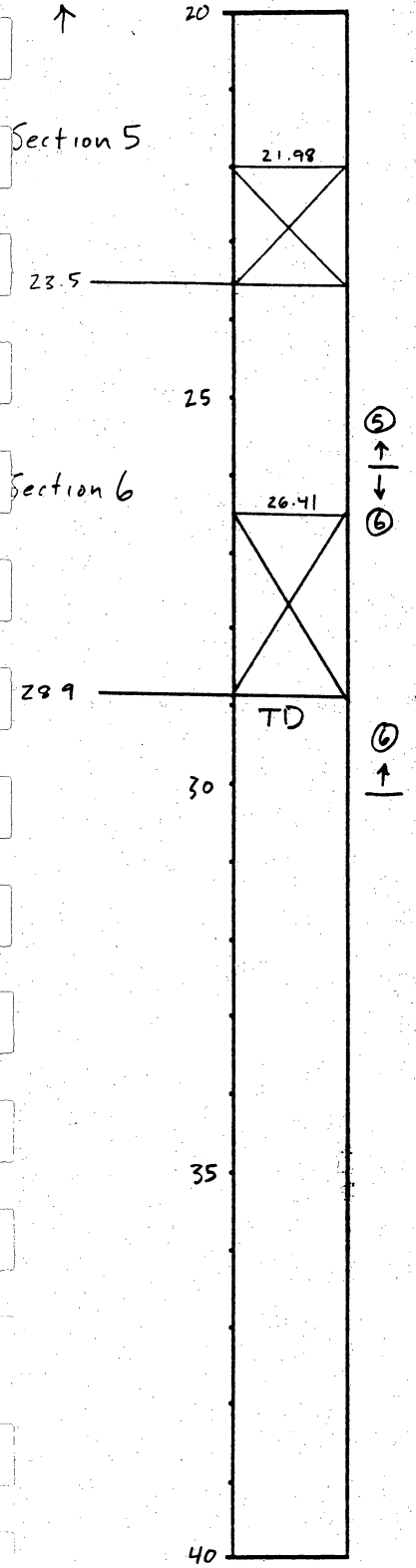

Description

19.15 – 20.15 : Greenish gray (5 GY 6/1); sandy clay; oxidized root traces (mostly upper part), burrows filled w/ clayey sd (larger in upper part, smaller in lower part)
— sharp, irregular contact —

20.15 – 20.73 : Yel. gray (5 Y 8/1); slightly clayey sd, clay content decreases upward clayey bioturbation mottling at base, discontinuous clayey laminae; scattered oxidat
— sharp, irregular contact —

20.73 – 21.50 : Yel. gray (5 Y 8/1) to dk. yel. orange (10 YR 6/6); v.f sd; horizontal laminations, tabular (?) cross-bedding; oxidation of lower ½
— gradational contact —

21.50 – 21.98 : Yel gray (5 Y 8/1); v.f. sd w/ thin clay interbeds • laminae; sand horizontally laminated; contacts w/ clay interbeds irregular (bioturbated?)

⑤ ↑ ↓ 21.98 – 23.5 : NO RECOVERY

⑥ 23.5 – 26.33 : Lt. olive gray (5 Y 5/2); stiff clay, sandy in places; upper 10" contains numerous pockets of sand – apparent soft-sediment loading & foundering of sand into underlying clay (poor recovery at top of section – details not clear); extensive reddish brown mottling of uncertain origin
— gradational contact —

⑥ ↑ 26.33 – 26.41 : Yel. gray (5 Y 8/1); v.f. sd; faint horizontal laminations, small clay clast (?)

— 26.41 – 28.9 : NO RECOVERY – END OF CORE

TD = 28.9

Location: CE 7

Remarks: Hwy 87 - Chenier Plain

Vibra Core ☐ _____
Piston Core ☐ _____
Rotary Core ☒ _____
Elevation: _____

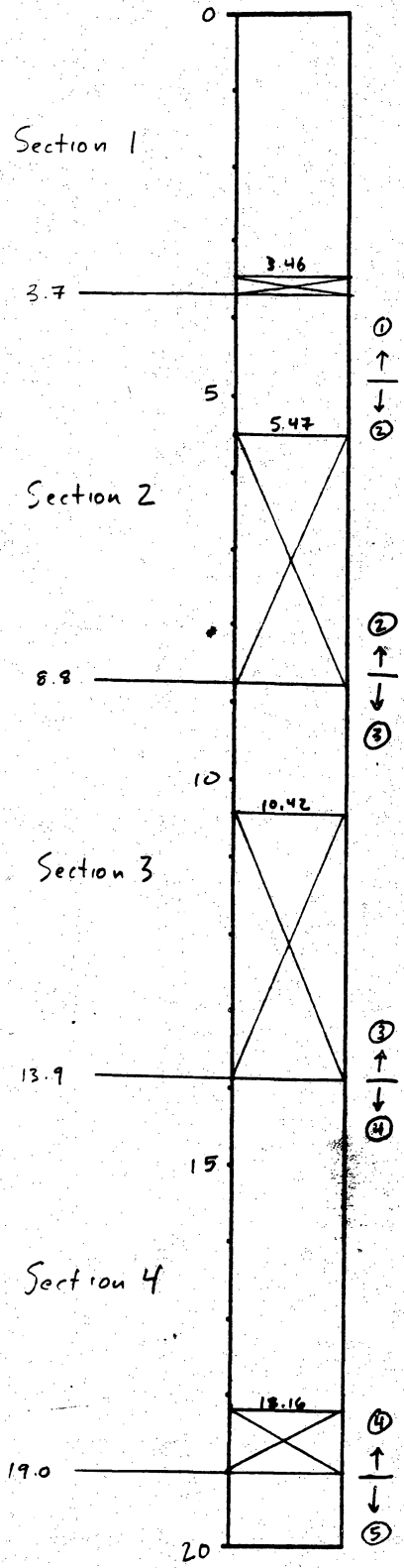

Description

0 - .875 : Dusky brn (5 YR 2/2); clayey f. to v.f. sd; roots + other organic matter, abdt. shell debris (large + small fragments)

— gradational contact —

.875 - 1.73 : Pale brn (5 YR 5/2) to dusky brn (5 YR 2/2); slightly clayey f. to vf. sd irregular pockets of very clayey sd w/ abdt organic matter, ¾" elliptical sd-f[illed] burrow w/in clayey pocket; abdt. fine shell material throughout

— sharp contact —

1.73 - 3.46 : Dk. yel. orange (10 YR 6/6); very fine sd, slightly clayey at base; heavy minerals (mostly at top); abdt. fine shell frags concentrated at top; scattered clay-rich mottling

3.46 - 3.7 : NO RECOVERY

3.7 - 5.03 : Dk yel. orange (10 YR 6/6); slightly clayey v.f. sd; fine mottling - some clayey, some cleaner sd. (probable bioturbation); large subvertical burrow near base filled w/ cleaner sd.; oxidation throughout

— sharp contact —

5.03 - 5.47 : Yel. gray (5 Y 7/2) to grayish green (10 GY 5/2); slightly clayey sd. (yel gr) w/ clay laminae (gray gr); clay laminae grouped into bundles at top + bottom of int[erval] sd. interval contains clayey mottling (probable bioturbation)

5.47 - 8.8 : NO RECOVERY

8.8 - 10.42 : Dk. yel. br (10 YR 4/2); slightly clayey v.f. sd.; color mottling (gy vs. brn) especially at base, otherwise massive in appearance; abdt. heavies

10.42 - 13.9 : NO RECOVERY

13.9 - 15.11 : Mod. yel. brn (10 YR 5/4); v.f. sd.; scattered clay rip-up clasts (possibly clay-filled burrows, can't be sure); indistinct mottling; scattered very fine shell d[ebris]

— sharp contact —

15.11 - 17.47 : Grayish br (5 YR 3/2); clayey v.f. sd - possible 1" thick clay layer at top (disrupted - can't be sure if bed or large clay-filled burrow); abdt clay-filled burrows ¼"-1" across; scattered shell frags w/in sd.

— sharp contact —

17.47 - 18.16 : Mod. yel br. (10 YR 5/4); v.f. sd w/ clay interbeds? (a[ttempt] to distinguish clay bed from coalesced mud-filled burrows); clay-filled burrows; minor shell debris

18.16 - 19.0 : NO RECOVERY

19 - 20.62 : Olive gray (5 Y 3/2); clay w/ scattered thin sand laminae; upper ⅓ contains several large v.f. sd-filled burrows - appear to have been several ~½" thick sand interbeds but original bedding disturbed by bioturbation; lower ⅓ contains thin discontinuous sand laminae scattered pockets of fine shell debris; dispersed fine organic matt[er]

Location: CE-7

Remarks: Hwy 87 - Chenier Plain

Vibra Core ☐ _____
Piston Core ☐ _____
Rotary Core ☒ _____
Elevation: _____

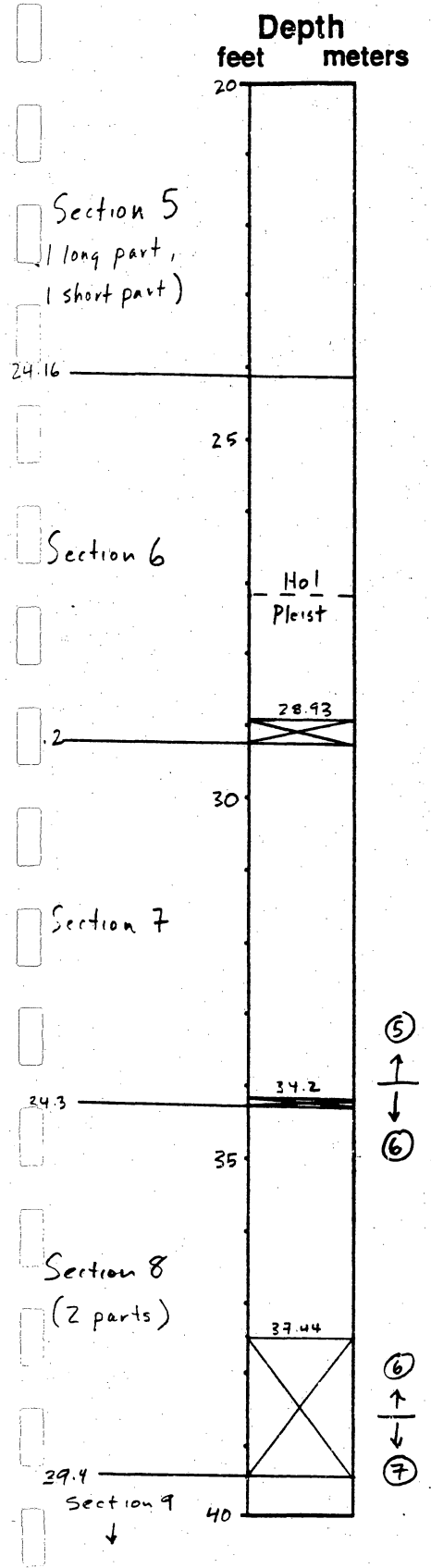

Description

20.62 – 20.79 : Yellowish gray (5 Y 7/2); v.f. sd; very abdt heavies; abdt small shell frags + one small whole shell (disarticulated)
— sharp contact, possibly erosional —

20.79 – 21.12 : Olive gray (5 Y 3/2); clay; one thin, discontinuous sd laminae; pocket of shell hash w/in clay; upper ½ contains burrows filled w/ clayey sd; scattered bits of small organic debris
— sharp contact —

21.12 – 21.37 : Yel. gray (5 Y 7/2)/Olive gray (5 Y 3/2); interbedded v.f. sd & clay; sand beds ~ ¼" thick, clay beds ¼ – ¾" thick; flaser bedding; basal contacts of sands sharp, some erosional; top contacts sands sharp sands have ripple x-bedding; clays have minor organic matter, small sd-filled burrows
— sharp, bioturbated contact —

21.37 – 21.58 : Yel gray (5 Y 7/2); v.f. sd.; ripple cross-bedding to horizontal laminations; small clay filled burrow near top
— erosional contact —

21.58 – 22.41 : same as 21.12 – 21.37 except beds slightly thicker (sands up to ¾", clays up to 1.5"),
— sharp, possibly erosional contact —

22.41 – 23.22 : Olive gray (5 Y 3/2); clay w/ minor thin sand laminae; sand laminae show some horiz. lamination; clays have minor fine shell fragments, scattered organic matter, a few small sd-filled burrows
— sharp contact —

23.22 – 23.37 : Yel. gray (5 Y 7/2); v.f. sd. w/ clay laminae & interbeds; sands have horizontal laminations & starved ripple x-bedding; clays have organic matter, small sd-filled burrows
— sharp contact —

(5) ↑ (6)

23.37 – 24.16 : Olive gray (5 Y 7/2); clay; small fragments organic matter
— contact uncertain, break in core —

24.16 – 27.12 : Olive gray (5 Y 7/2); clay; scattered thin v.f. sd. laminae most discontinuous; possible large sd-filled burrows; organic matter in clay
— sharp, burrowed contact — (probable Hol-Pleist contact)

27.12 – 28.93 : Med lt. gray (N6) to Dk yel orange (10 YR 6/6); silty to sdy stiff clay; dk gray mottling near top; extensive oxidation; circular, hard oxidation spots (burrows? or oxidized organic matter?); sd-filled mottling (probable burrows especially at base

(6) ↑ (7)

28.93 – 29.2 : NO RECOVERY

29.2 – 29.34 : Yel. gray (5 Y 7/2); v.f. sd w/ thin clay laminae
— sharp, very irregular contact —

29.34 – 29.89 : Pale yel. br. (10 YR 6/2); silty/sdy clay; v. thin discontinuous sd. laminae near base; abdt organic matter, some larger frags oxidized
— sharp contact —

Location: CE-7

Remarks: Hwy 87 - Chenier Plain

Vibra Core ☐ _____
Piston Core ☐ _____
Rotary Core ☒ _____
Elevation: _____

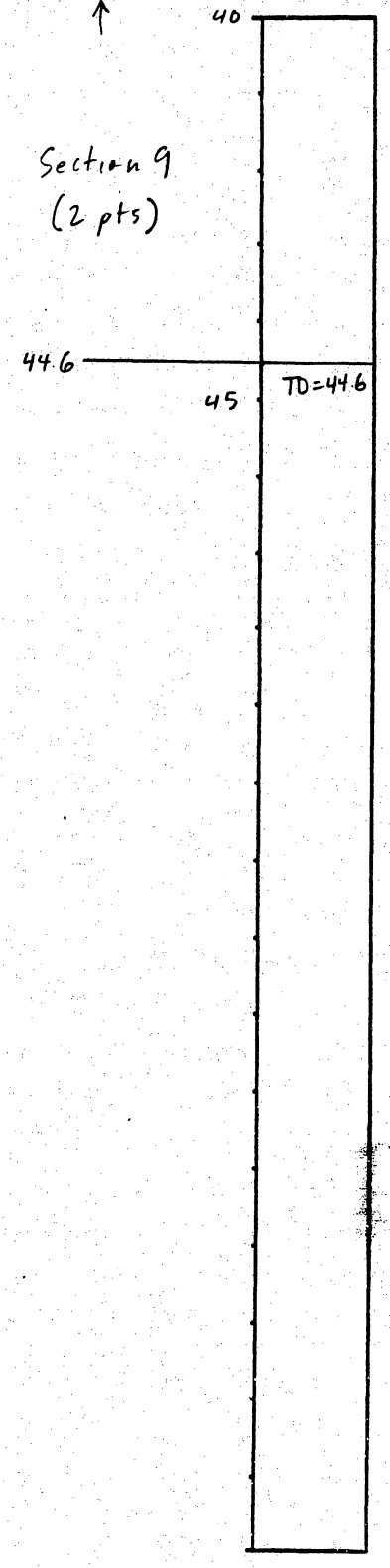

29.89 – 32.47 : Dk yel. orange (10 YR 6/6) / pale yel. br (10 YR 6/2); interbedd fine sd. and sandy clay; sd. beds ½–8" thick, sandy clay beds ½–1" sands massive to horizontal lamination, some clay rip-up clasts; sdy cla beds have concentrated areas of organics, some sd-filled mottling; b contacts of sands sharp & some erosional; lower part of interval v disrupted & chaotic (not bedded but remnants of bedding present)
— gradational contact —

32.47 – 34.14 : Greenish gray (5 GY 6/1); clay to sandy clay (sand cont increases upward), pockets of concentrated organic-rich clay; CaCO nodules, extensive oxidation; fine mottling
— sharp, irregular contact —

(7) 34.14 – 34.20 : Dk. gr. gray (5 GY 4/1); clay; mottling filled w/ light-c material (burrows filled w/ above material)

↑ 34.20 – 34.3 : NO RECOVERY

↓ (6) 34.3 – 35.18 : Grayish orange (10 YR 7/4); v.f. sd; massive appearance; ver small clay rip-up clasts (?); small clayey sd-filled burrows near base
— gradational contact —

35.18 – 35.56 : Mod. yel. br (10 YR 5/4); slightly clayey v.f. sd; sandy cl rip-up clasts? (laminated, don't look like burrows) to 1" across
— sharp contact —

35.56 – 35.75 : Grayish orange (10 YR 7/4); v.f. sd w/ minor muddy lamina near top; horizontal laminations at base
— sharp contact —

35.75 – 36.00 : Pale yel. br (10 YR 6/2); clayey v.f. sd. w/ clean sd. lamina horizontal laminations & ripple cross-lamination
— gradational contact —

36.00 – 36.44 : Pale yel br (10 YR 6/2); clayey v.f. sd.; clay mottling
— sharp contact —

36.44 – 37.44 : Pale yel br (10 YR 6/2); clayey v.f. sd. w/ clean sd & cl laminae; cleaner intervals show ripple cross-lamination; clayey intervals show horiz. lamination

↑ (8) 37.44 – 39.4 : NO RECOVERY

↓ (9) 39.4 – 40.07 : Grayish orange (10 YR 7/4); fine to v.f. sd. (fining upward) possible ripple x-lamination at base, massive at top; heavy minera
— sharp contact —

40.07 – 44.59 Dk yel br (10 YR 4/2); clay w/ abdt v.f. sd interbeds & laminae; clay has fine mottling (probable bioturbation) - scattered orga matter; sand laminae continuous & discontinuous, thicker laminae show ripple x-lamination; blob of sand near top which founder from above interval (ball & pillow); bioturbation mixes clay & sand laminae in places

TD

COASTAL EROSION PROJECT

Location: CE-8

Remarks: Hwy 87 - Chenier Plain

Vibra Core ☐ _____

Piston Core ☐ _____

Rotary Core ☒ _____

Elevation: _____

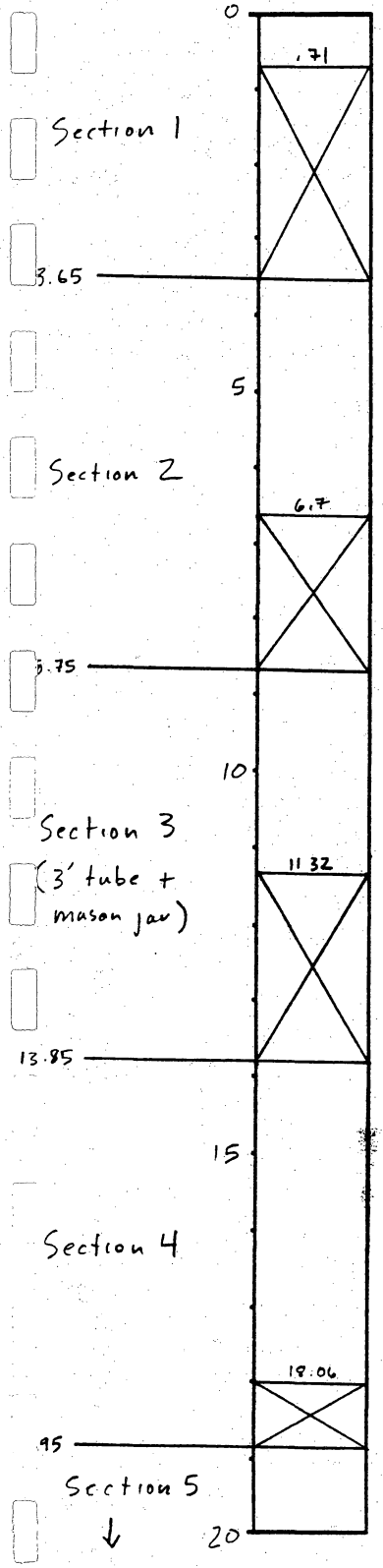

Description

0 - .71 : Grayish brown (5 YR 3/2); clayey v.f. sd.; roots + woody fragments
① shell (oyster) fragments concentrated near base

↑ .71 - 3.65 : NO RECOVERY

↓ 3.65 - 5.28 : Mod. yel. br. (10 YR 5/4); slightly clayey v.f. sd.; mottled appearance
② w/ dark organic-rich mottling in upper ½ and clayey mottling in lower ½ (probable bioturbation); heavy minerals; oxidized (esp. upper part)
— sharp contact —

5.28 - 6.70 : Mod yel br (10 YR 5/4); slightly clayey v.f. sd. (more clayey at bo
very abdt shell fragments (small frags to whole small shells) - more shelly at top; organic matter at top; discontinuous clay laminae at base; hea
② minerals

↑ 6.70 - 8.75 : NO RECOVERY

↓ 8.75 - 10.29 : Mod. yel. br (10 YR 5/4); slightly clayey v.f. sd (clay content
③ decreases upward); abdt fine shell fragments; heavy minerals; oxidized
— gradational contact —

10.29 - 10.92 : Br. gray (5 YR 4/1); slightly clayey v.f. sd.; abdt fine shell fragments; heavy minerals [same as above except color + no oxidation]
— contact uncertain —

10.92 - 11.32 : Br. gray (5 YR 4/1); v.f. sd; abdt shell fragments + small
③ whole shells [in mason jar]

↑ 11.32 - 13.85 : NO RECOVERY

↓ 13.86 - 15.31 : Grayish orange (10 YR 7/4); fine to very fine sand (fining upward),
④ shell frags at base; scattered small clay-filled burrows
— gradational contact —

15.31 - 17.23 : Dk. yel. br (10 YR 4/2); mixed very fine sd. + slightly clayey v.f. s
heavily bioturbation w/ clay-filled burrows ¼" - ½" across; bioturbation mixes clean sd + slightly clayey sd giving a churned appearance; fine shell fragments
— sharp contact —

17.23 - 18.06 : Dk yel. br (10 YR 4/2); interbedded very fine sd + clay; sd bea
¼ - 1+" thick, horizontal lamination + ripple cross-bedded; clay beds ⅛ - ½" thick, some slightly sandy; some sd-filled burrows in clay beds;
④ sand % decreases upward

↑ 18.06 - 18.95 : NO RECOVERY

↓ 18.95 - 19.82 : Pale yel. br (10 YR 6/2); very fine sd.; fine shell debris; small cl
⑤ rip-up clasts near base
— erosional contact

Location: CE-8

Remarks: Hwy 87 - Chenier Plain

Vibra Core ☐ _____
Piston Core ☐ _____
Rotary Core ☒ _____
Elevation: _____

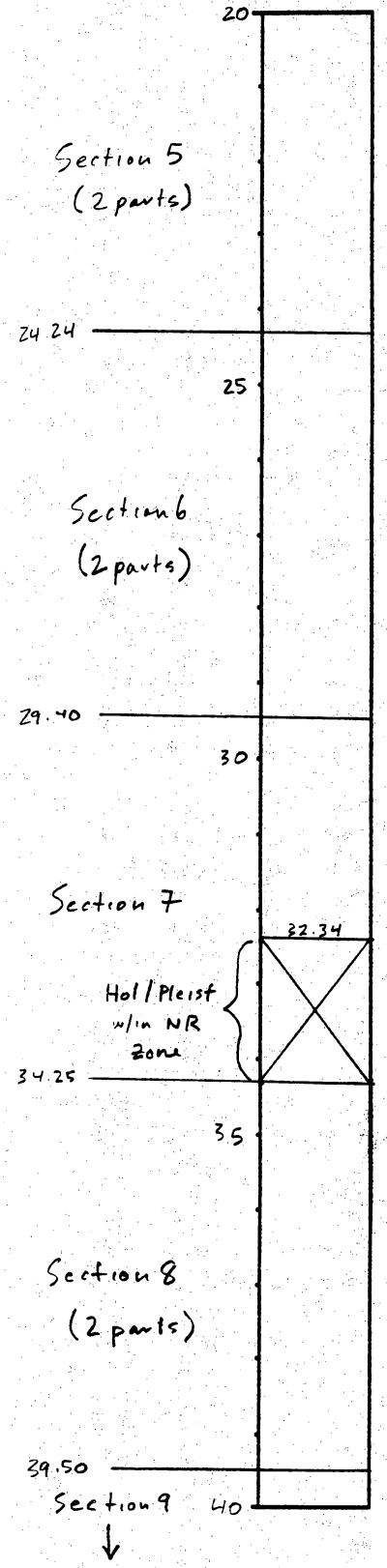

Description

— erosional contact —

19.82 – 23.08 : Olive gray (5 Y 3/2), clay - slightly sandy in places; large (2.5) burrows filled w/ fine sd and clayey sd.; faint laminations in places defin by sandy clay laminae

— sharp contact —

23.08 – 23.43 : Olive gray (5 Y 3/2); clay w/ v.f. sand & clayey sd interbed: continuous sd. beds have faint horiz. laminations + fine shell debris; discontinuous sd. beds appear to be starved ripples; upper + lower con of sd. beds sharp

— sharp contact —

23.43 – 24.08 : Olive gray (5 Y 3/2); clay; scattered sandy + clayey sd. lo scattered organic matter in clay

— gradational contact —

⑤ 24.08 – 24.24 : Dk yel br (10 YR 4/2); clayey v.f. sd; scattered fine shell

— contact uncertain (break in sections) —

⑥ 24.24 – 25.32 : Olive gray (5 Y 3/2); clay to sandy clay (sand content increa upward); sand-filled burrows; fine shell fragments, whole gastropod shell base

— gradational contact —

25.32 – 25.74 : Grayish orange (10 YR 7/4); v.f. sd; discontinuous clay lami and small clay-filled burrows; scattered fine shell fragments

— sharp, possibly erosional contact —

25.74 – 26.28 : Olive gray (5 Y 3/2); clay; sd-filled burrows - mostly small one large probable burrow near center of interval; small frags of organic mat

— sharp contact —

26.28 – 26.78 : Grayish orange (10 YR 7/4); v.f. sd w/ clay interbeds an discontinuous clay laminae; faint horiz. laminations in sd.; small cl-fille burrows; bioturbation disrupts clay beds + laminae; small shell fragments

— gradational contact —

26.78 – 28.07 : Olive gray (5 Y 3/2); sandy clay w/ discontinuous clayey sd. laminae; abdt sand + clayey sd. filled burrows; scattered fine shell fr

— gradational contact —

28.07 – 29.40 : Olive gray (5 Y 3/2); clay w/ discontinuous sd. laminae and

⑥ starved ripples; small sd-filled burrows; small bits of organic matt

— contact uncertain (break in core sections) —

⑦ 29.40 – 30.48 : Olive gray (5 Y 3/2); sandy clay; small sd-filled burrows; minor possible sd laminae (highly disrupted); abdt small shell frags near

— gradational contact —

30.48 – 32.15 : Olive gray (5 Y 3/2); slightly sdy clay; abdt fine to very fi sand laminae and interbeds, many sand layers highly disrupted; sd. layers continuous, others discontinuous (starved ripples?); few sa sd-filled burrows; small shell frags in some sd. layers

— sharp contact —

⑦ 32.15 – 32.34 : Grayish orange (5 Y 3/2); fine sand; abdt shell fragmen

32.34 – 34.25 : NO RECOVERY (Hol/Pleist contact prob w/in NR zone)

④

next page

Location: CE-8

Remarks: Hwy 87 – Chenier Plain

Vibra Core ☐ _____
Piston Core ☐ _____
Rotary Core ☒ _____
Elevation: _____

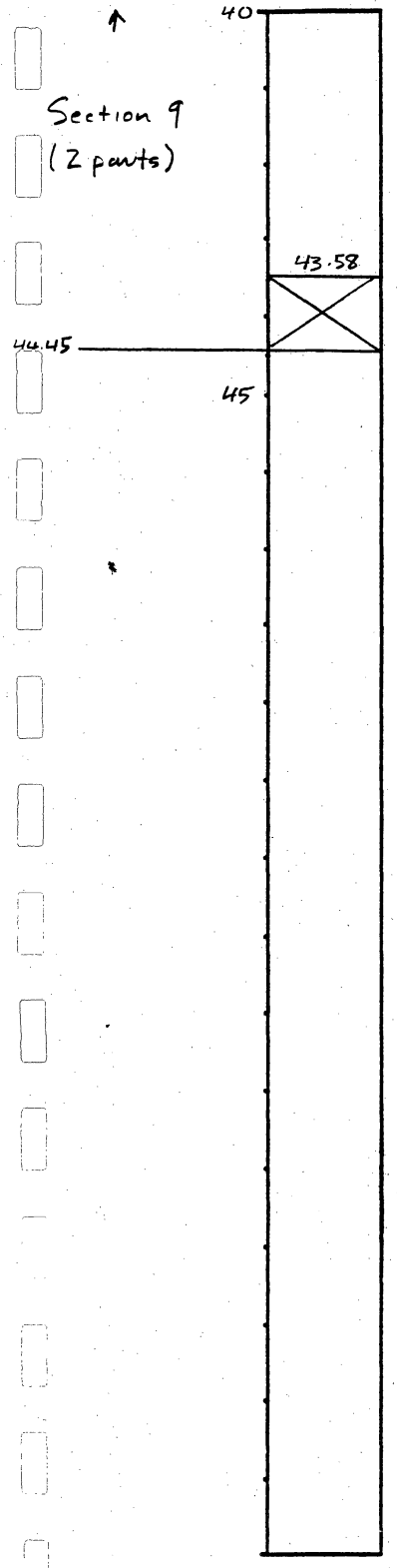

Description

34.25 – 34.92 : Lt. gray (N7); stiff silty clay; large sd-filled burrow (?); darker gray mottling (probable bioturbation), oxidized mottling
(8)
— gradational contact —

34.92 – 37.09 : Lt gray (N7); stiff silty clay; abundant 1/8 - 3/4" burrows filled w/ oxidized sandy clay; scattered burrows (?) filled w/ soft dk gray clay; streaky white mottling in lower 1/2
— gradational contact —

37.09 – 37.92 : Lt. gray (N7); stiff silty clay; abdt 1/8" burrows filled w/ oxidized sandy clay to clayey sand; fine 'stringy' white mottling
— gradational contact —

37.92 – 39.50 : Lt gray (N7); stiff silty clay; scattered burrows (< 1/8" – 1/4"), filled w/ oxidized sandy clay to clayey sand; 'stringy' white mottling; scattered black organic debris
(6)
↑
— contact uncertain (break in sections) —
↓
(9)

39.50 – 39.92 : Grayish orange (10 YR 7/4); slightly clayey v.f. sd. muddy fragments (rip-up clasts?); minor fine shell fragments
— sharp, irregular contact —

39.92 – 42.17 : Lt. gray (N7); stiff silty clay; pockets of non-silty clay; extensive "stringy" white mottling (probable bioturbation); oxidized silty to slightly sandy clay mottling (probable bioturbation); scattered black organic debris and small oxidized woody fragments
— gradational contact —

42.17 – 43.58 : Lt gray (N7); stiff clay w/ silty laminae; scattered black organic debris in clay; silt laminae mostly discontinuous and wispy; minor possible fine burrows; minor oxidation
(9)
↑

43.58 – 44.45 : NO RECOVERY

TD = 44.45'

Location: CE-9

Remarks: Sabine Pass Battleground State Park

Vibra Core ☐ _____
Piston Core ☐ _____
Rotary Core ☒ _____
Elevation: _____

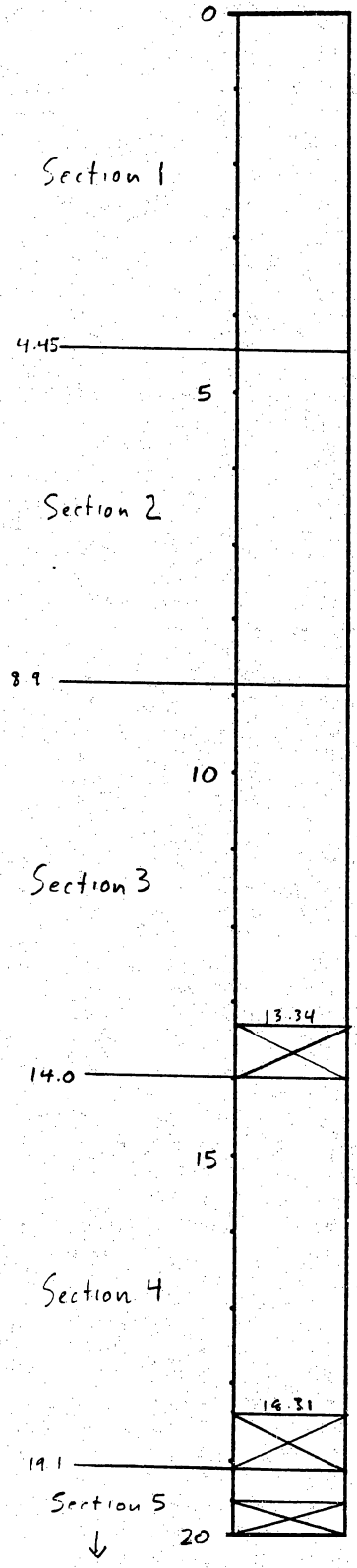

Description

[0 - 1.40] : Mod br (5 YR 3/4); clayey v.f. sd; small oyster shell fragments; roots
— gradational contact —
[1.40 - 1.0] : Dk yel orange (10 YR 6/6); v.f. sd.; unconsolidated w/ cemented nodules (concretions?); oyster shell fragments
— sharp contact —
[1.0 - 1.94] : Grayish br (5 YR 3/2); clayey sd. to sandy clay (sd. content decreases upward abdt. oyster shell frags - shell hash at top w/ one large shell, fine fragments at bas discontinuous sdy laminae near base; minor sd-filled burrows at base; organic m
— gradational contact —
[1.94 - 2.40] : Dusky yel. br (10 YR 2/2); clay; fine silt/sd filled burrows; oxidation mottling (root mottling?); fine black organic matter
— sharp contact —
[2.4 - 2.85] : Grayish orange (10 YR 7/4); v.f. sd/slt; clay + organic rich horizons; horizont laminations to ripple x-bedding
— sharp contact —
[2.85 - 3.04] : Very pale orange (10 YR 8/2); silt w/ clay interbeds; disrupted, burrowed appearance at base; horiz. laminations to ripple x-bedding (?) elsewhere
— sharp contact —
[3.04 - 3.12] : Dk yel. orange (10 YR 6/6); v.f. sd. w/ clay laminae; sd. horizontally laminated
— sharp bioturbated contact —
[3.12 - 3.87] : Dk. grn gray (5GY 4/1); clay; fine sand + silt filled burrows; dk brn oxidation mottling
— sharp contact —
[3.97 - 3.95] : Mod brn (5 YR 3/4); clay w/ v.f. sd. and clayey sd. laminae; sd. laminae have horiz. lamination
① — gradational contact —
↑ [3.95 - 5.24] : Dk grn gray (5GY 4/1); clay; small sd-filled burrows, one large (2") sand
↓ filled burrow; dk oxidation mottling; organic matter incl. small woody fragme
② — gradational contact —
[5.24 - 6.14] : Olive black (5Y 2/1); slightly sandy/silty clay; minor small sd-filled burrows; abdt black organic matter incl. small woody fragments
— gradational contact —
[6.14 - 6.47] : Olive gray (5Y 4/1); clay; small sd-filled burrows; abdt dark
② organic-rich zones
↑ [6.47 - 8.9] : NO RECOVERY
↓
③ [8.9 - 10.34] : Olive gray (5Y 3/2); clay; minor small sd-filled burrows; dark organic-rich streaks
— gradational contact —
[10.34 - 12.69] : Olive gray (5Y 3/2); clay w/ numerous v.f. sd and clayey sd interbe clay contains dk organic-rich streaks; sd interbeds 1/8 - 1/2" thick, cleaner san have horiz. laminations; sd-clay contacts generally sharp
— sharp contact —
[12.69 - 13.34] : Grayish orange (10 YR 7/4); fine to very fine sd to clayey sd clay interbeds + laminae; sds horiz. laminated to ripple x-bedded w/ ab
③ heavy minerals; clay beds < 1/8 - 1/2" thick, mostly sharp upper + lower contac
↑ [13.34 - 14.0] : NO RECOVERY
↓
④

Location: CE-9

Remarks: Sabine Pass Battleground State Park

Vibra Core ☐ _____

Piston Core ☐ _____

Rotary Core ☒ _____

Elevation: _____

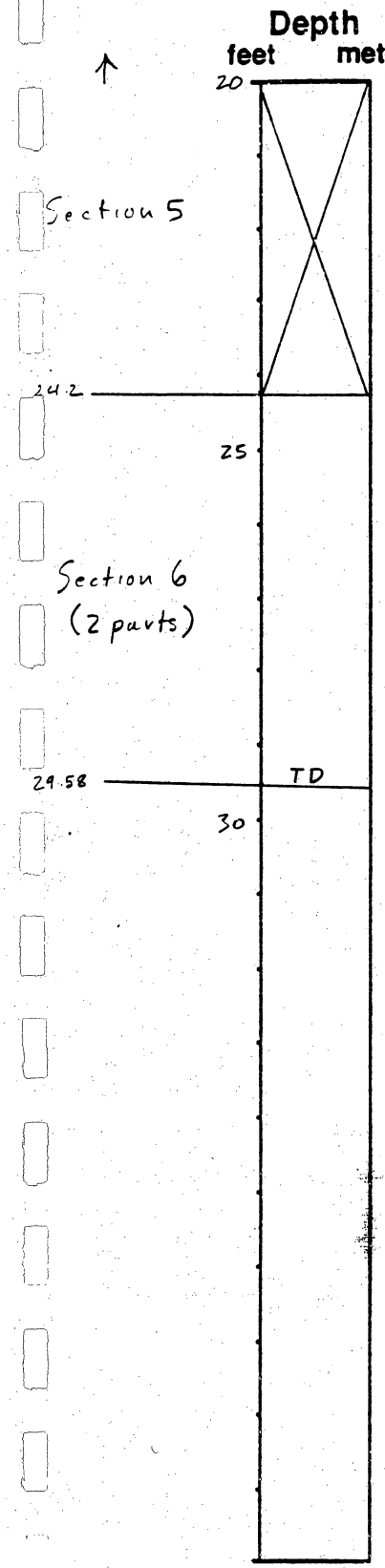

Description

④ [14.0 – 15.52] : Olive gray (5 Y 3/2); clay to sandy clay; upper ½ has convoluted sd-filled burrows, lower ½ contains one large sd-filled burrow (fills almost entire core tube); sandy clay w/ shell hash at base

— sharp contact —

[15.52 – 18.31] : Olive gray (5 Y 3/2); clay to sandy clay w/ abdt sand + clayey sd. interbeds; clay has some black organic-rich streaks; sd interbeds < ⅛-1" thick, cleaner sds have horizontal laminations and/or ripple x-bedding; sds mostly contorted but continuous, upper + lower contacts of sds mostly sharp

④↑↓ [18.31 – 19.1] : NO RECOVERY

⑤ [19.1 – 19.54] : Olive gray (5 Y 3/2); clay; zones w/ very abdt fine shell fragment (shell hash); some black organic-rich streaks

↑ [19.54 – 24.2] : NO RECOVERY

↓⑥ [24.2 – 24.45] : Olive gray (5 Y 3/2); sandy clay; very abdt fine shell fragments; sand-filled burrows or disrupted sand laminae? (can't tell which)

— sharp contact —

[24.45 – 26.45] : Olive gray (5 Y 3/2); clay (slightly sdy in places); scattered burrow filled w/ sand + clayey sand; minor very thin, discontinuous sdy laminae; scattered black organic-rich streaks; local concentrations of fine shell fragmen

— sharp contact —

[26.45 – 27.62] : Dk. yel br (10 YR 4/2); clayey v.f. sd; abdt clay-filled burrows to 1" across, areas of clean sd (possible filled burrows?); scattered fine shell fragments + whole small shells

— sharp contact —

[27.62 – 29.07] : Olive black (5 Y 2/1); clayey sand to sandy clay; chaotic, disturbed mixture - appears to have flowed/liquified during coring; scattered fine shell fragments

— gradational contact —

[29.07 – 29.30] : Olive gray (5 Y 3/2); clayey sand w/ clay laminae; one clean v.f. sd bed at top; clay laminae streaky + discontinuous; scattered fine shell fragments

— gradational contact —

⑥↑ [29.30 – 29.58] : Mod yel brn (10 YR 5/4); clayey fine sd; very abdt fine shell fragments + some larger shell fragments

TD = 29.58

NOTE: 3 attempts at drilling final interval — recovery from 1st attempt described above; very little recovery on 2nd attempt; 3rd attempt recovered 5.25' of material similar to basal part of 1st recovery (seems to me that 3rd recovery was material from below 1st recovery which may have flowed up into the hole — Bill White said they were getting "artesian" flow up the hole)

3rd recovery - Section 6 : [5.25'] : Mod yel brn (10 YR 5/4); clayey fine sd; very abdt shell material - fine fragments w/ numerous large fragment.

Location: CE-10

Remarks:

Vibra Core ☐ _____
Piston Core ☐ _____
Rotary Core ☒ _____
Elevation: _____

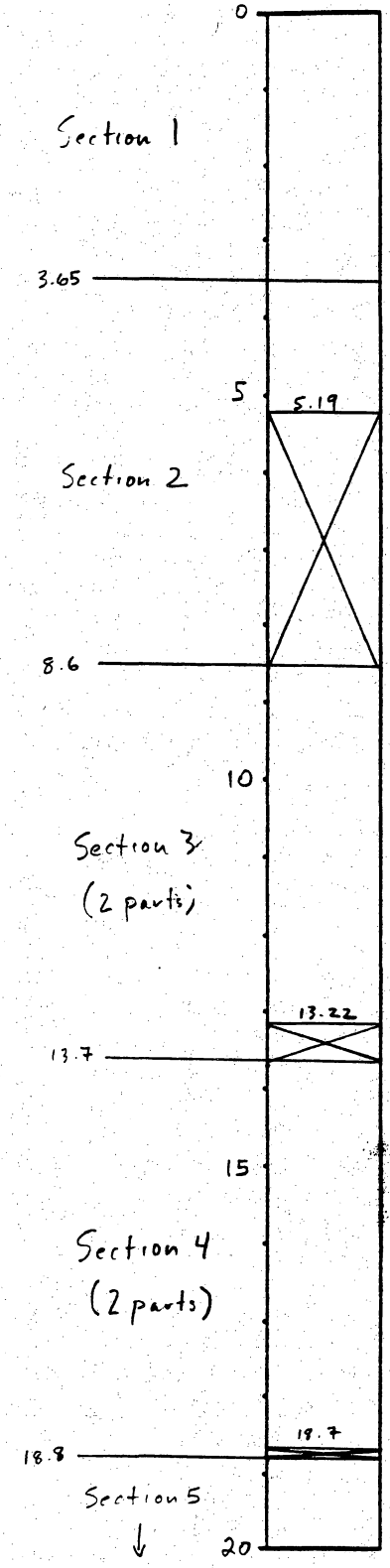

Description

0 - .62 : Dk yel br (10 YR 4/2); slightly clayey v.f. sd + silt; reeds, roots, and other organic matter; asphaltic (road) fragments; small oyster fragments

— gradational contact —

.62 - .90 : Grayish orange (10 YR 7/4); v.f. sd.; very abdt shell fragments - small to la

— gradational contact —

.90 - 1.60 : Dusky yel br (10 YR 2/2); clayey v.f. sd.; very hard; scattered small [illegible] fragments; minor oxidation mottling; scattered small frags of organic matter

— gradational contact —

1.60 - 2.12 : Dk yel br (10 YR 5/4); slightly clayey v.f. sd; black clay-rich mottling (probable bioturbation); oxidized near base

— sharp, bioturbated contact —

2.12 - 2.77 : Dk grn gray (5 G 4/1); clay; abdt dark mottling (roots); scattered preserved roots; minor burrows filled w/ clayey sd.

— sharp contact —

2.77 - 3.65 : Grayish orange (10 YR 7/4); slightly clayey fine to v.f. sd w/ possible [illegible] interbeds; abdt clay filled burrows (difficult to distinguish coalesced burrows from interbeds), fine clay-rich mottling (probable bioturbation); dark mottling associated w/ preserved organic matter

① ↑ ↓ ②

— contact uncertain, break in core sections —

3.65 - 4.65 : Dk yel orange (10 YR 6/6); fine to very fine sd, scattered clay-[illegible] burrows at top; oxidized

— sharp bioturbated contact —

4.65 - 5.07 : Dk grn gray (5 G 4/1); clay; mod. brn mottling; single sd-f[illegible] burrow; "pockets" of fine shell fragments

— gradational contact —

5.07 - 5.19 : Grayish orange (10 YR 7/4); clayey v.f. sd.; abdt fine shell f[illegible]s indistinct clay-rich mottling

② ↑ ↓ ③

5.19 - 8.6 : NO RECOVERY

8.6 - 11.27 Olive gray (5 Y 3/2); clay w/ two sd. interbeds; long sd-f[illegible]e burrow w/ 2 large 'chambers' — 'chambers' have common shell frags, scattered laminations; other small sd-filled burrows; clay has abdt black organic matter; sd interbeds < ½", disrupted by bioturbation

— sharp contact —

11.27 - 12.85 : Olive gray (5 Y 3/2); clay w/ numerous sd + cl. sd. interbeds; clay has abdt to very abdt black organic fragments, scattered small sd-filled burrows; sd. interbeds ⅛ - ½" thick, some disrupted by burrowing, faint horiz. laminations in others

— sharp contact —

12.85 - 13.22 : Grayish orange (10 YR 7/4); v.f. sd to clayey sd. w/ clay lamina sds have horiz. laminations to ripple x-beds; clay laminae < ⅛" thick

③ ↑ ↓ ④

13.22 - 13.7 : NO RECOVERY

13.7 - 14.24 : Yellowish gray (5 Y 7/2); v.f. sd; small mud rip-ups at base; minor scattered fine shell fragments; abdt heavy minerals

— sharp, irregular contact —

14.24 - 16.91 : Olive gray (5 Y 3/2); clayey v.f sd; thoroughly bioturbated — clay/silty clay-filled and sand-filled; difficult to tell what "in situ" sediment is in places - may vary from clayey sd to cleaner sd; scattered fine shell frags; one small woody fragment

Location: CE-10

Remarks: Hwy 87 - Sabine Pass

Vibra Core ☐ _____
Piston Core ☐ _____
Rotary Core ☒ _____
Elevation: _____

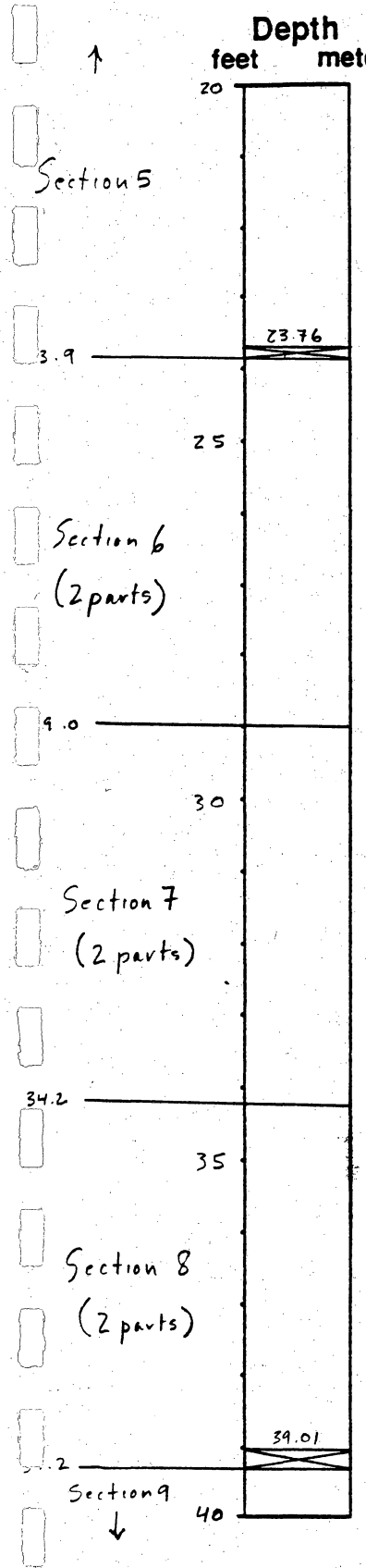

— sharp, irregular contact —

16.91 – 18.70 : Olive gray (5 Y 3/2)/Yellowish gray (5 Y 7/2); interbedded clay/silty clay and v.f. sd/clayey sd; sand/clay appox 1; clay beds 1/8 - 1½ thick, small black organic streaks, some sd-filled burrows; sd beds 1/8 - 1½" thick, mostly continuous but some lenticular, horizontal lam. t possible ripple x-beds, minor small shell frags, abdt heavy minerals

④ ↑ —

18.70 – 18.80 : NO RECOVERY

↓ ⑤

18.8 – 21.53 : Olive gray (5 Y 3/2); clay/silty clay; small black organic fragment small 'pockets' of shell fragments; long burrow filled w/ sd + shell fragments ending in sd-filled chamber w/ discontinuous laminations

21.53 – 23.57 : Olive gray (5 Y 3/2); clay/silty clay w/ v.f. sd/clayey sd interbe and laminae; clay has small black organic fragments, scattered small sd-filled burrows; sd interbeds < 1/8 - ½" thick, faint horiz. laminations, small shell fragments, mostly sharp base + top but one bed w/ gradationa top + small mud-filled burrows; sd. laminae mostly discontinuous, some inclined

— sharp contact —

23.57 – 23.76 : Yellowish gray (5 Y 7/2); clayey v.f. sd; discontinuous

⑤ ↑ mud laminae; abdt small shell fragments + one whole Polinices shell

23.76 – 23.9 : NO RECOVERY

↓ ⑥

23.9 – 24.71 : Olive gray (5 Y 3/2); clay/silty clay; numerous vertical silt, sand, an clayey sd-filled probable burrows (could be laminae deformed during coring); black organic streaks + minor fine shell fragments in clay

— sharp, irregular contact —

24.71 – 24.84 : Yellowish gray (5 Y 7/2); v.f. sd; small clay rip-up clasts (?)

— sharp, possibly erosional contact —

24.84 – 25.52 : Olive gray (5 Y 3/2); clayey v.f. sd; highly bioturbated — elliptical clay-filled burrows and vertical to near-vertical sand and silt-filled burrows; abdt fine shell fragments

— gradational contact —

25.52 – 26.40 : Yellowish gray (5 Y 7/2); v.f. sd, clayey in spots; abdt clay-filled burrows to 1" across; scattered mostly fine shell fragments

— gradational contact —

26.40 – 27.40 : Yellowish gray (5 Y 7/2); v.f. sd/clayey v.f. sd w/ scattere clay laminae; sd. has small clay/sandy clay filled burrows at base, faint horizontal laminations at top, minor fine shell fragments; clay laminae < ½" thick, disrupted + discontinuous w/ very small sd-filled burrows

— gradational contact —

27.40 – 29.05 : Olive gray (5 Y 3/2)/Yellowish gray (5 Y 7/2); interbedded v.f. sd/clayey sd and clay/silty clay; clay beds to 2½" thick, small blac organic streaks, thin discontinuous sd. laminae, scattered sd-filled burrows; sd beds to 2" thick w/ faint horizontal laminations to ripple x-beds, minor clay-filled burrows, scattered shell fragments

⑥ ↑ (concentrated in places)

— break in core sections —

Location: CE-10

Remarks: Hwy 87 – Sabine Pass

Vibra Core ☐ _____
Piston Core ☐ _____
Rotary Core ☒ _____
Elevation: _____

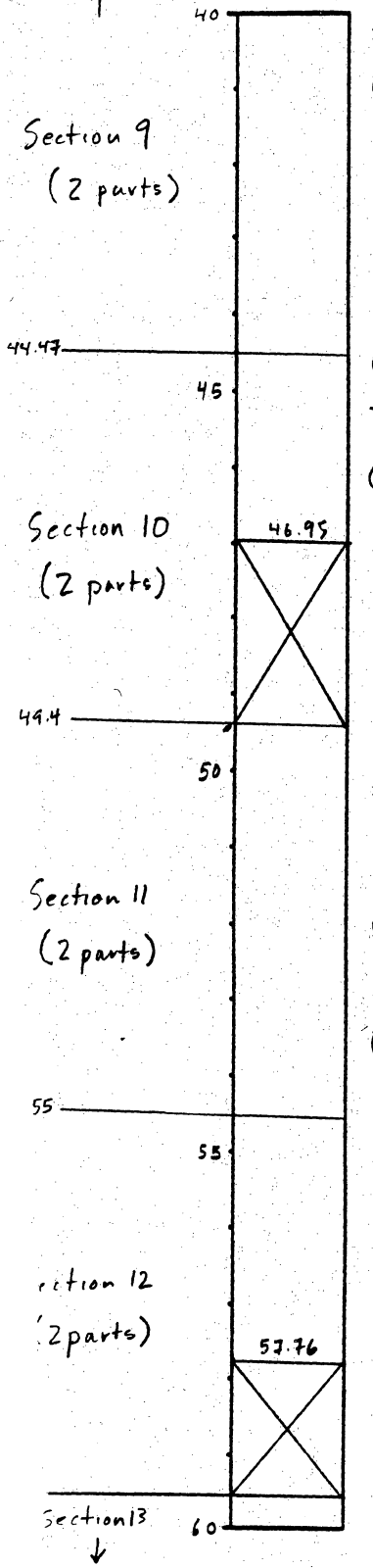

Description

29.05 – 30.18 : Olive gray (5 Y 3/2); clay to sandy clay; large sd-filled burrows, also small sd + clayey sd-filled burrows; minor discontinuous sd laminae; concentrations of fine shell fragments w/ also some larger frags
– gradational contact –

30.18 – 34.22 : Olive gray (5 Y 3/2)/ Yellowish gray (5 Y 7/2); clay/sandy clay w/ abdt v.f. sd. laminae and interbeds (clay > sand); clay has blk organic streaks, minor small sd-filled burrows; sd laminae mostly discontinuous + wispy, some w/ horiz. laminations, some w/ ripple x-bedding, some starved ripples; one pocket of concentrated shell frags, otherwise shell frags rare
– break in core sections –

34.22 – 34.43 : same as above
– gradational contact –

34.43 – 34.93 : Dk. grn gray (5 GY 4/1); silty clay; silt laminae at top, churned texture below; pockets of abdt fine organic debris
– sharp, irregular contact –

34.93 – 36.97 : Lt. olive gray (5 Y 6/1); silt/clayey silt; discontinuous clay laminae + small silty clay-filled burrows at top; churned + very chaotic texture below (coring process or bioturbation?); abdt fine micaceous material
– sharp contact –

36.97 – 39.01 : Olive gray (5 Y 3/2); clay/silty clay w/ abdt v.f sd/silt laminae, clay has small black organic fragments, micaceous in places; most sd laminae very thin (< 1/16") but some to 1/4", most laminae discontinuous and wispy, some probable starved ripples; scattered small sd-filled burrows

39.01 – 39.2 : NO RECOVERY

39.2 – 40.32 : Olive gray (5 Y 3/2); silty clay; irregularly shaped (wispy) sd-filled burrows; blotchy lt. olive gray (5 Y 5/2) mottling; black organic fragments – some dispersed, others concentrated in 'pockets' or wispy laminae
– gradational contact –

40.32 – 42.07 : Olive gray (5 Y 3/2); clay/silty clay w/ contorted v.f sd/silt laminae clay has scattered black organic fragments, one 1" thick bed w/ concentrated organic debris, scattered small sd-filled burrows; sd/slt laminae thin, wispy & contorted, one disturbed 1½" thick sd bed w/ clay-filled burrows
– sharp, irregular contact –

42.07 – 42.20 : Olive gray (5 Y 3/2); sandy clay; large pelecypod shell frags
– sharp, irregular contact –

42.20 – 42.43 : Olive gray (5 Y 3/2); silty clay; small sd-filled burrows; large pelecypod shell fragment + small shell frags
– sharp, irregular contact –

42.43 – 42.64 : Grayish orange (10 YR 7/4); v.f. sd; abdt small sdy clay filled burrows, one larger silty clay filled burrows; med to large shell frags
– sharp, irregular contact –

42.64 – 44.47 : Olive gray (5 Y 3/2); silty to sandy clay; scattered sd burrows (mostly small but one cluster of larger burrows); organic ma abdt med to large pelecypod shell fragments

Location: CE-10

Remarks: Hwy 87 - Sabine Pass

Vibra Core ☐ _____
Piston Core ☐ _____
Rotary Core ☒ _____
Elevation: _____

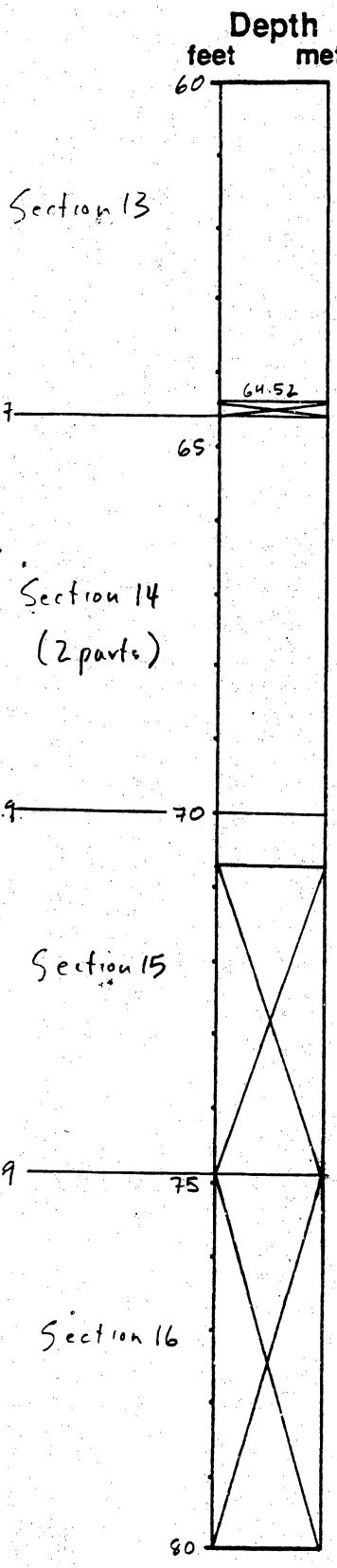

Description

— break in core sections —

10 — 44.47 – 46.99 : Olive gray (5 Y 3/2); sandy clay (possible clayey v.f. sd b at top but very little recovery); very abdt large pelecypod shell frags, al abdt fine shell frags; disturbed texture; one possible clayey sd-filled burrow near top

10 — 46.95 – 49.4 : NO RECOVERY

11 — 49.4 – 54.55 : Olive gray (5 Y 3/2); clay; abdt black organic matter-bo dispersed and concentrated in streaky laminae; minor small sd-filled burr single large shell frag at top; ¼" thick lt. brown (5 YR 5/6) bed near ba

— contact uncertain, break in sections —

12 — 54.55 – 57.76 : Greenish black (5 GY 2/1); clay; mod red br (10 R 4/6) oxidiz mottling (probable bioturbation), also irregular mod red br beds (?); irregula ¼" thick v.f. sd. bed near base; abdt small black organic matter + organ rich laminae; single shell fragment near base.

13 — 57.76 – 59.6 : NO RECOVERY

13 — 59.6 – 64.52 : same as 54.55 – 57.76 plus thin, wispy, contorted silt laminae distributed throughout interval

14 — 64.52 – 64.7 : NO RECOVERY

14 — 64.7 – 65.08 : Olive gray (5 Y 4/1); clay; abdt black organic matter; minor mod red br mottling; small $CaCO_3$ nodule

— sharp, irregular contact —

15 — 65.08 – 67.62 : Olive black (5 Y 2/1); clay w/ abdt silt laminae; abdt black orga matter in clay; silt laminae very thin, many contorted; some possible silt filled burrows

— gradational contact —

15 — 67.72 – 68.51 : Olive black (5 Y 2/1); clay; abdt black organic matter; small silt-filled burrows; minor silt laminae

— gradational contact —

14 — 68.51 – 69.99 : Black (N1); clay; extremely abdt small black organic matter + woody fragments (nearly peat in places); some woody fragmen oxidized; irregular horiz. laminations

15 — 69.99 – 70.70 : same as above plus lt. olive gray (5 Y 6/1) mottling at base

15 — 70.70 – 74.90 : NO RECOVERY

16 — 74.90 – 80.0 : NO RECOVERY

note: 3.25' of v.f. sd. w/ abdt heavy minerals + several large wood fragments recovered from ~60' after section 16 — origin unknown

Location: CE-11

Remarks: Hwy 87 - Sabine Pass

Vibra Core ☐ _____
Piston Core ☐ _____
Rotary Core ☒ _____
Elevation: _____

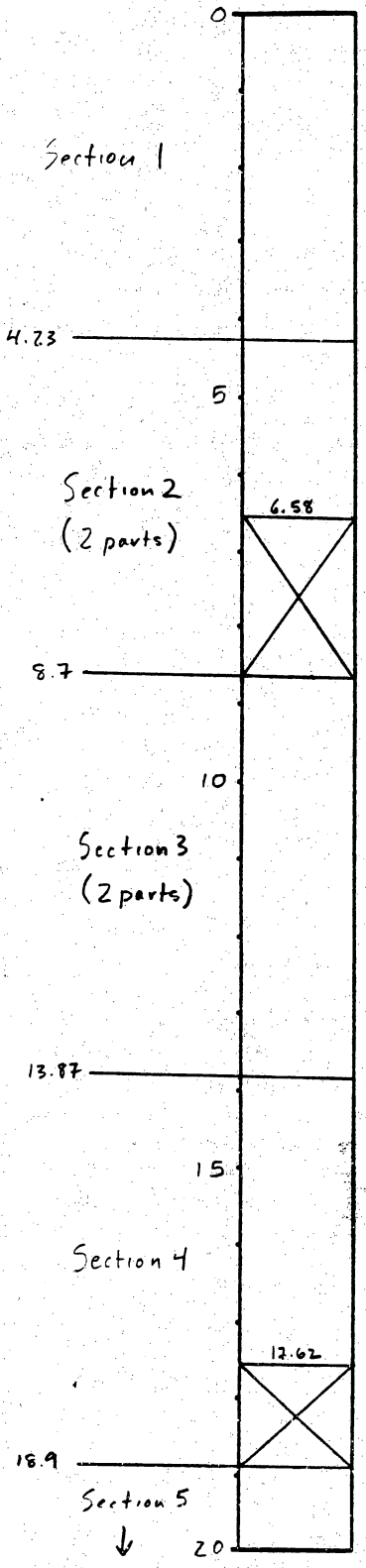

Description

0 - .5 : Grayish orange (10 YR 7/4); very fine to fine sd; v. abdt fine shell frs plus some larger oyster & other Pelecypod shell frasments; needs a sm. roc
— gradational contact —

.5 - 1.06 : Pale yel br (10 YR 6/2); clayey v f. to f. sd; abdt small to med. shell frags (mostly oysters); irregular clayey mottling
— gradational contact —

1.06 - 2.12 : Dk gray (N3); silty to sdy clay; fine sd filled burrows (?), irregul lt. gray (N7) mottling; abdt fine to med oyster shell frags
— sharp contact —

2.12 - 4.23 : Grayish black (N2); silty clay; small black organic fragments; scattered fine shell fragments; minor irregular med lt gray (N5) mottling; irre l zones of concentrated slt/sd + fine shell frags
— break in core sections —

4.23 - 4.40 : Same as above

4.40 - 6.10 : Dark gray (N3); clay; cluster of small sd-filled burrows minor scattered small sd-filled burrows; abdt greenish gray (5 GY 6/1) mottling + fine black root mottling; abdt fine black organic streaks; one of dk. yel orange (10 YR 6/6) oxidation mottling
— sharp contact —

6.10 - 6.31 : Dark gray (N3); clay w/ fine sd. interbeds; clay has black org streaks; 2 1/4 - 1/2" sd interbeds + discontinuous sd. laminae (?)
— contact uncertain —

6.31 - 6.58 : Dk. yel. br (10 YR 4/2); clayey v.f. to f. sd. w/ discontinuous cla laminae; abdt fine shell debris [this interval seems out of place]

6.58 - 8.7 : NO RECOVERY

8.7 - 9.37 : Grayish orange (10 YR 7/4); v.f. to f. sd; massive appearance; very sm mud-filled burrows near base; minor fine shell fragments
— gradational contact —

9.37 - 10.37 : Grayish orange (10 YR 7/4); v.f. to f. sd; abdt silty-clay-filled burr of 2 types - (1) small (< 1/8" across), (2) large (to 1.5" across), some larger burr have small sd-filled burrows; minor fine shell fragments
— gradational contact —

10.37 - 10.91 : Yellowish gray (5 Y 7/2); same as above except sd. different co
— sharp contact —

10.91 - 13.87 : Greenish black (5 G 2/1); clay to silty clay w/ clayey silt to v.f sd interbeds; clay has black organic streaks, abdt mica; silt interbeds continuous w/ gradational contacts; sd. interbeds mostly discontinuous + u
— break in core sections —

13.87 - 14.74 : Dk grn gray (5 GY 4/1); clay to silty clay; irregular 'blocks' laminated muddy silt (appears to be soft-sediment foundering but could be deformation due to coring process); possible sd-filled burrows (may also be soft-sediment 'blocks'); black organic streaks in clay
— gradational contact —

14.74 - 16.76 : Dk grn gray (5 GY 4/1); clay; abdt black organic matter - sma dispersed fragments and concentrated organic-rich laminae; very minor small sd-filled burrows
— sharp contact —

16.76 - 17.62 : Dk grn gray (5 GY 4/1); same as above plus several f. sd. laminae & interbeds to 3/4" thick

17.62 - 18.9 : NO RECOVERY

Location: CE-11

Remarks: Hwy 87 - Sabine Pass

Vibra Core ☐ _____

Piston Core ☐ _____

Rotary Core ☒ _____

Elevation: _____

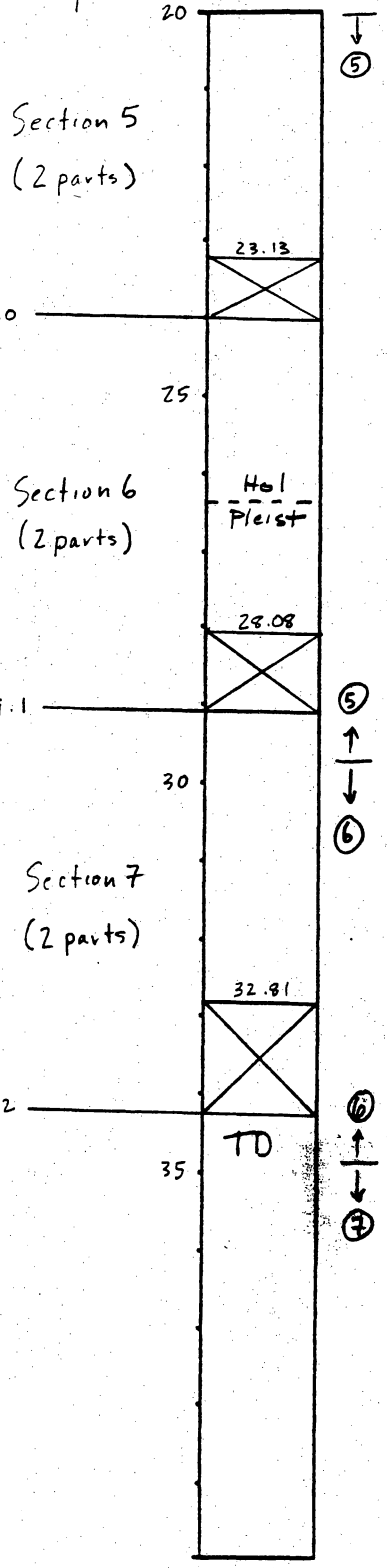

Description

18.9 – 20.15 : DK grn gray (5 GY 4/1); silty to sdy clay; several large 'blobs' of laminated fine sd to silt (appear to be more soft-sediment foundering but could be 'chambered' burrows seen in other cores); irregularly shaped sd to slt filled probable burrows; scattered fine shell frags in both clay and sdy 'blobs'

— gradational contact —

20.15 – 20.44 : Yellowish gray (5 Y 7/2); fine sd to clayey sd (clayey at base + top clean in center); abdt fine shell frags

— gradational contact —

20.44 – 21.69 : Dk grn gray (5 GY 4/1); silty to slightly sandy clay; some wispy sd. laminae in lower ½; clayey-sd-filled burrows in upper ½; abdt black organic debris - dispersed + concentrated in laminae

— sharp contact —

21.69 – 22.29 : Dk grn gray (5 GY 4/1)/ Yellowish gray (5 Y 7/2); silty clay w/ vf s to silt interbeds; clay has black organic debris; sd interbeds to ½" thick w sharp contacts, horiz. laminations to ripple x-bedding (starved ripples)

— sharp contact —

22.29 – 22.96 : Dk grn gray (5 GY 4/1); silty clay; scattered discontinuous v.f. sd/slt laminae; black organic debris in clay - dispersed + thin laminae

— contact uncertain, break in section —

22.96 – 23.13 : Dk yel br (10 YR 4/2); clayey sd; abdt small shell frags

23.13 – 24.0 : NO RECOVERY

24.0 – 26.33 : Dusky yel br (10 YR 2/2); clayey sd to sdy clay (non-homogeneou mixture), sd + clayey sd filled burrows in lower 6"; very abdt small to medium size shell fragments; small clasts of underlying material at base black organic debris in clayey parts

— sharp, probably burrowed contact (Hol/Pleist contact) —

26.33 – 28.08 : Greenish gray (5 GY 6/1) w/ dk yel orange (10 YR 6/6) mottling; stiff silty clay; highly mottled – (1) blotchy dk yel or oxidation mottling, (2) fine lt grn gray (5 GY 8/1) mottling, (3) dark brown mottling (oxidized organic matter?), (4) stringy dk gray mottling; single burrow near top filled w/ dk gray clay

28.08 – 29.1 : NO RECOVERY

29.1 – 29.31 : Grayish orange (10 YR 7/4); v.f. sd.; small clay-filled probable burr fine shell fragments

— gradadational contact —

29.31 – 30.48 : Grayish orange (10 YR 7/4); churned mixture of silt and clay (appears to have been interbedded silt + clay); intensely bioturbated - abdt large horiz. burrows, also large randomly oriented burrows; blotchy dk brn (oxidation?) mottling

— gradational contact —

30.48 – 31.56 : Grayish orange (10 YR 7/4); silt w/ thin stiff clay laminae, one ½" thick stiff clay interbed; silt horizontally laminated; very abdt large horiz burrows (x-sections + axial cuts); blotchy dk yel or oxid. mottli

— gradational contact —

31.56 – 32.81 : Greenish gray (5 GY 6/1); stiff silty clay w/ silty laminae; most laminae discontinuous; # of laminae increases upward; irregular dk red brn mottling (oxidized woody debris?); blotchy dk yel or oxid mottling

COASTAL EROSION PROJECT

Location: CE-12

Remarks: Keith Lake

Vibra Core ☐ _____
Piston Core ☐ _____
Rotary Core ☒ _____
Elevation: _____

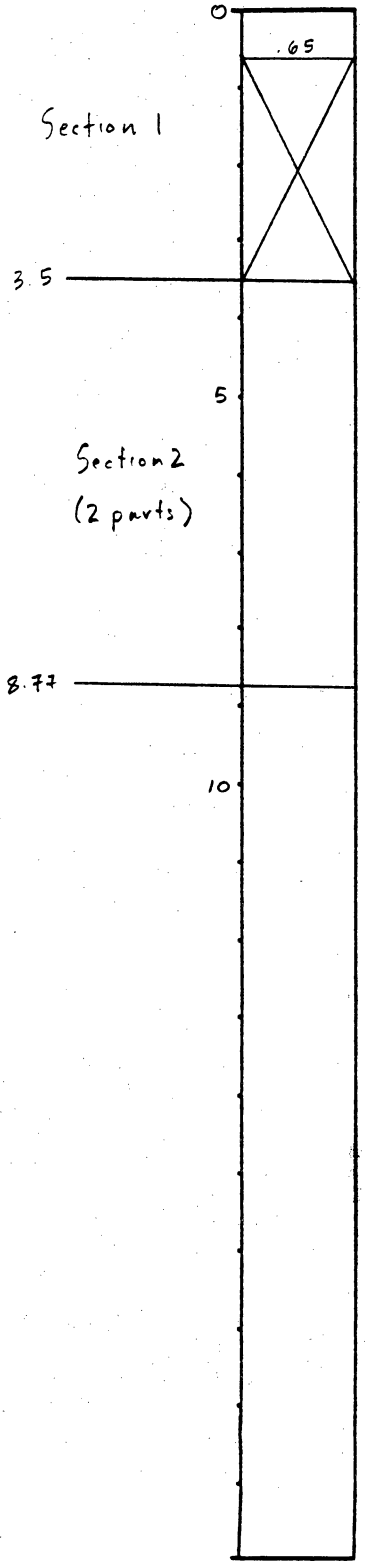

Description

0 - .40 : Dusky yel. br (10 YR 2/2); clayey v.f. sd; pelleted appearance in upper 2 abdt roots + organic matter; scattered fine shell fragments
— gradational contact —
① .40 - .65 : Grayish orange (10 YR 7/4); v.f. sd, slightly clayey at top; 2 pieces gravel at base (one ss clast, one quartzite?); small shell frags
↑ .65 - 3.5 : NO RECOVERY
↓ 3.5 - 3.79 : Lt. olive gray (5 Y 6/1); clayey v.f/f. sd; very abdt small shell frags
② — gradational contact —
3.79 - 4.75 : Yellowish gray (5 Y 7/2); v.f-f. sd; scattered fine clayey mottling; horiz. laminations in lower 1/3; very abdt fine to medium shell frags (one concentrated shell hash zone at 3.3 - 3.4')
— gradational contact —
4.75 - 4.94 : Yellowish gray (5 Y 7/2); v.f-f. sd w/ clay laminae + interbeds; one clay bed 1/4" thick, rest of laminae << 1/8"; minor fine shell frags
— sharp contact —
4.94 - 5.46 : Dk greenish gray (5 GY 4/1); silty clay w/ sd + clayey sd interbeds; clay has abdt organic matter - concentrated laminae + dispersed 'streaks'; 3 sd interbeds, each ~ 1/8" thick - clean sd to clayey sd, one w/ abdt fine shell frags
— sharp contact —
5.46 - 5.98 : Mod yel. br (10 YR 5/4); clayey to slightly clayey v.f. sd; abdt fine to med. shell frags (one concentrated shell hash layer at 5.7
— contact uncertain, break in core tube —
5.98 - 6.73 : Grayish orange (10 YR 7/4); v.f. sd; very minor fine shell frags
— gradational contact —
6.73 - 8.77 : Olive gray (5 Y 4/1); slightly clayey v.f. sd; scattered small clay-filled burrows; scattered fine to med shell frags

TD

Location: CE-12A

Remarks: Keith Lake

Vibra Core ☐ _____
Piston Core ☐ _____
Rotary Core ☒ _____
Elevation: _____

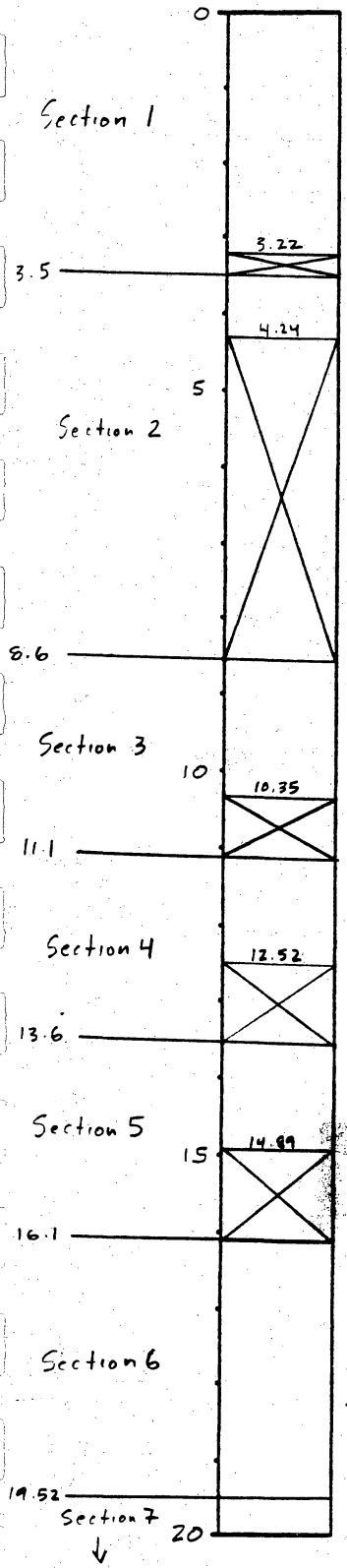

Description

0 – .33 : Mod. brown (5 YR 3/4); slightly clayey fine sd; roots + grass at top; fine shell frags

① — gradational contact —

.33 – .89 : Dk. yel orange (10 YR 6/6); slightly clayey fine sd; discontinuous clayey laminae near base; abdt fine shell frags + whole small shells; single granule-size clast; preserved roots; oxidized

— sharp contact —

.89 – 1.60 : Grayish black (N2); silty clay; sd-filled burrows at top; fine mod. red br. (10 R 4/6) mottling (root mottling); blotchy greenish gray (5 GY 6/1) mottling at bo

— gradational contact —

1.60 – 2.22 : Greenish gray (5 GY 6/1); silty to sdy clay; very abdt fine shell frags; irregular grayish black (N2) mottling

— gradational contact —

2.22 – 2.91 : Dk yel orange (10 YR 6/6); clayey fine to med. sd; irregular zones of sdy clay (possible burrows); abdt fine shell frags; sdy areas oxidized

— sharp contact —

2.91 – 3.22 : Dk. yel. orange (10 YR 6/6); fine sd; extremely abdt fine shell frags, concentrated shell hash at top; oxidized

① ↑ ↓

3.22 – 3.5 : NO RECOVERY

3.5 – 3.62 : Dk yel. br (10 YR 4/2); clayey fine sd; fine shell frags

— sharp contact —

② 3.62 – 4.12 : Lt. br (5 YR 5/6); slightly clayey v.f. to f. sd; extremely abdt fine shell frags

— sharp contact —

4.12 – 4.24 : Grayish green (5 G 6/2); fine sd w/ single clayey sd. lamina; faint horiz laminations; very minor fine shell frags

↑ ↓

4.24 – 8.6 : NO RECOVERY

8.6 – 9.93 : Lt olive gray (5 Y 5/2); v.f. to f. sd; single clay-filled burrow at top; minor fine shell frags; abdt. heavy minerals

— gradational contact —

③ 9.93 – 10.20 : Lt. olive gray (5 Y 5/2), v.f. to f. sd; extremely abdt small to medium shell frags

— sharp contact —

10.20 – 10.35 : Lt. olive gray (5 Y 3/2); v.f. to f. sd.; fine shell frags; abdt heavy minerals

↑ ↓

10.35 – 11.1 : NO RECOVERY

11.1 – 12.37 : Mod. yel. br (10 YR 5/4); fine sd; ~ ⅛" mod red br (10 R 4/6) oxidized probable burrows; preserved roots; scattered fine shell frags (more abdt downward); abdt heavy minerals

④

— gradational contact —

12.37 – 12.52 : Mod yel br (10 YR 5/4); slightly clayey f. sd; abdt fine to med. shell frags; abdt heavy minerals

↑ ↓

12.52 – 13.6 : NO RECOVERY

13.6 – 14.66 : Mod yel br (10 YR 5/4); v.f. to f. sd; faint probable burrows marked by mod. red br (10 R 4/6) oxidation; minor very small clay-filled burrows; minor scattered fine shell frags; abdt heavy minerals

⑤

— gradational contact —

14.66 – 14.89 : Mod yel br (10 YR 5/4); v.f. to f. sd; clay-filled burrows to ½" across; minor scattered fine shell frags; abdt heavy minerals

↑

14.89 – 16.1 : NO RECOVERY

Location: CE-12A

Remarks: Keith Lake

Vibra Core ☐ _____
Piston Core ☐ _____
Rotary Core ☐ _____
Elevation: _____

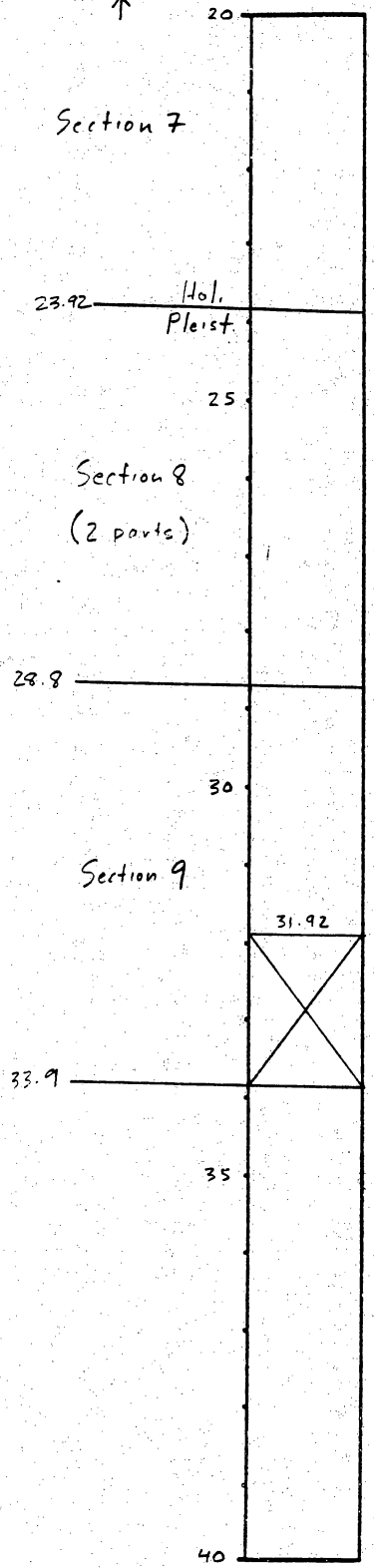

Description

16.1 – 16.27 : Grayish orange (10 YR 7/4); clayey f. to v f. sd (fragmentary recovery, tough to say much)

— sharp contact —

16.27 – 19.19 : Olive gray (5 Y 3/2); clay to silty clay w/ scattered fine sd. interbeds; sd interbeds ¼–1" thick, some w/ small clay-filled burrows; clo has large sd-filled 'chamber' burrow at top, other scattered small sd-filled burrows; dispersed fine black organic debris

(6)

— sharp contact —

18.19 – 19.52 : Olive gray (5 Y 5/2); clay to silty clay : dispersed fine black organic debris, some organic-rich laminae

— break in section —

19.52 – 20.94 : Olive gray (5 Y 5/2); clay, slightly sdy in places; small, indistinct clayey-sd-filled burrows; abdt fine black organic-rich laminae

— gradational contact —

20.94 – 23.48 : Olive gray (5 Y 5/2); silty clay w/ abdt silt, v.f. sd., and claye laminae; clay has abdt fine black organic-rich laminae; silt/sd laminae most discontinuous, wispy, more clayey at top of interval, cleaner silt/sd in lowe laminae abundance increases upward for lower ⅔ of interval then slowly de upward for upper ⅓

(7)

— gradational contact —

23.48 – 23.92 : Olive gray (5 Y 5/2); clay to silty clay; single thin sd laminae abdt fine black organic debris, mostly in streaky laminae

— break in sections — (Hol/Pleist contact w/in break)

23.92 – 26.21 : Greenish grey (5 GY 6/1); stiff silty clay; extensive mod br. (10 R 4/6) mottling (probable oxidized burrows), small stringy burrows filled w/ grayish black (N2) clay; cluster of med. shell frags at top scattered small oxidized woody fragments

— gradational, highly burrowed contact —

26.21 – 28.38 : Grayish orange (10 YR 7/4); v.f. to med. sd. (generally f upward – lower .38' med sd, rest fines up from fine to very fine); heav bioturbated – large sand + mud-filled burrows in upper ½, fine mod. red. br (10 R 4/6) mottling (probable bioturbation) throughout, small clay-filled burrows in lower ½

(8)

— sharp contact —

28.38 – 28.8 : Greenish gray (5 GY 6/1); stiff sdy clay; fine mod red br (10 R 4/6) oxidized mottling, fine yellowish gray (5 Y 3/2) mottling – bo probable bioturbation

— break between sections —

28.8 – 29.47 : Yellowish gray (5 Y 7/2); interbedded v.f sd + silty clay (sand clay); abdt small stringy burrows; abdt dk yel or (10 YR 6/6) + mod red br (10 R 4/6) mottling; small oxidized organic frogments

— gradational contact —

29.47 – 31.42 : Yellowish gray (5 Y 7/2); interbedded v.f. sd/slt + silty clay (sand clay); beds ⅛–½" thick; some sds have ripple x-bedding, others horiz lam Scattered small burrows; small organic fragments, mostly oxidized

9

— gradational contact —

31.42 – 31.92 : Pale yel. br (10 YR 6/2); stiff silty clay w/ wispy v.f. sd/s beds; sdy clay-filled burrows, very fine burrows filled w/ black clay

31.92 – 33.9 : NO RECOVERY TD = 33.9

Location: CE-12A

Remarks: Keith Lake

Vibra Core ☐ _____

Piston Core ☐ _____

Rotary Core ☒ _____

Elevation: _____

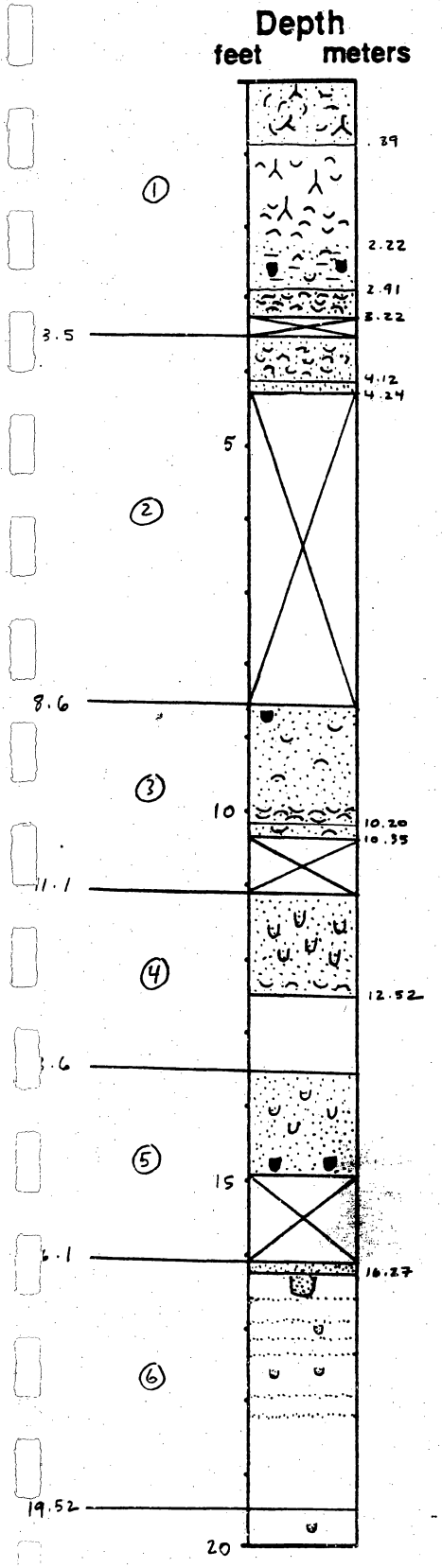

Location: CE-12A

Remarks: Keith Lake

Vibra Core ☐
Piston Core ☐
Rotary Core ☒
Elevation:

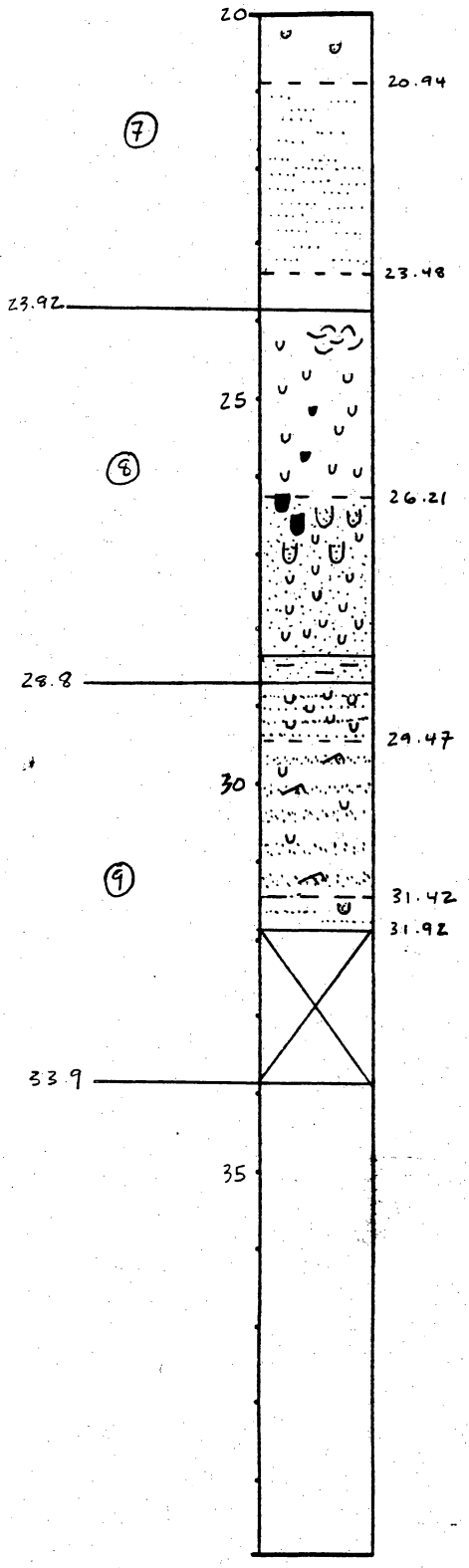

Location: CE-13

Remarks: Keith Lake

Vibra Core ☐ _____

Piston Core ☐ _____

Rotary Core ☒ _____

Elevation: _____

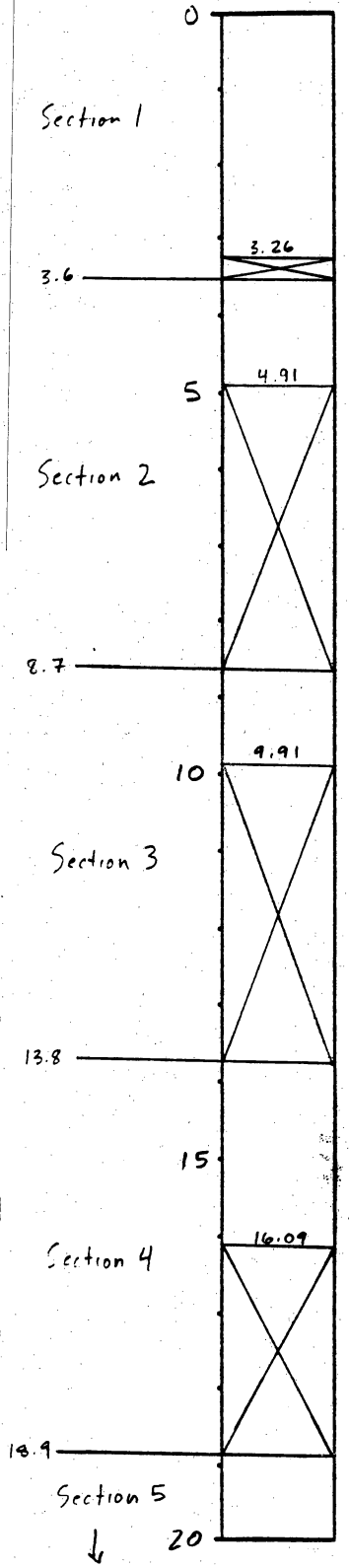

Description

0 – .5 : Dk. yel br (10 YR 4/2); clayey fine sd; chaotic texture; abdt shell frag

— sharp contact —

.5 – .94 : Grayish orange (10 YR 7/4); v.f. sd; faint horiz. laminations; abdt heavy minerals; very minor fine shell frags; patchy oxidation

— sharp contact —

.94 – 1.27 : Ducky yel. br (10 YR 2/2); clayey v.f. sd; chaotic texture - possibly bioturbated; abdt fine shell frags

— sharp contact —

1.27 – 1.60 : Dk. yel. orange (10 YR 6/6); fine sd; faint horiz. laminations at top; very abdt small to med shell frags w/ some small whole shells

(1) — sharp contact —

1.60 – 2.83 : Dusky yel. br (10 YR 2/2); sandy clay, one ½" thick v.f. sd bed at 2. chaotic texture; small sd-filled burrows at top; dk yel. br (10 YR 4/2) and grn gray (5 GY 6/1) mottling; abdt fine shell frags

— sharp contact —

2.83 – 2.97 : Yellowish gray (5 Y 7/2); sdy shell hash; shell frags small

— gradational contact —

2.97 – 3.26 : Yellowish gray (5 Y 7/2); slightly clayey v.f. sd w/ discontinuous clay laminae; abdt fine mod. red br (10 R 4/6) mottling - probable bioturbation

3.26 – 3.6 : NO RECOVERY

3.6 – 4.14 : Greenish gray (5 G 6/1); v.f. to f. sd; faint fine mottling; blotchy areas of mod. red br. (10 R 4/6) oxidation; common heavy minerals; single small

(2) black organic fragment; strong odor

— gradational contact —

4.14 – 4.91 : Yellowish gray (5 Y 7/2); fine sd; abdt small to med shell frags common heavy minerals; 2" thick zone of dk yel orange (10 YR 6/6) oxidation

4.91 – 8.7 : NO RECOVERY

8.7 – 9.67 : Mod. yel. br (10 YR 5/4); fine sd; single clay lamina at 9'; abdt fine shell frags (decreasing upward); abdt heavy minerals

(3) — sharp contact —

9.67 – 9.91 : Dk yel br (10 YR 4/2); slightly clayey fine sd.; abdt small to med shell frags; single small clay-filled burrow

9.91 – 13.8 : NO RECOVERY

(4) 13.8 – 16.09 : Mod yel. br (10 YR 5/4); v.f. to f. sd.; scattered small clay-filled burrows; minor fine shell frags; abdt heavy minerals

16.09 – 18.9 : NO RECOVERY

18.9 – 19.80 : Grayish orange (10 YR 7/4); v.f. to f. sd.; clay-filled burrows at base; minor fine shell frags; abdt heavy minerals

— sharp contact —

19.80 – 21.13 : Olive gray (5 Y 4/1); sandy clay to clayey sd (sand % increases upward

(5) abdt small to med shell frags

— gradational contact —

21.13 – 24.15 : Olive gray (5 Y 3/2); clay to silty clay (silt % increases upward); large sd-filled 'chamber' burrow at top, small to med clayey sd-filled burrows throughout; abdt 'streaks' of black organic (?) matter; scattered fine shell frags at top

— break in core sections —

Location: CE-13

Remarks: Keith Lake

Vibra Core ☐ _____
Piston Core ☐ _____
Rotary Core ☒ _____
Elevation: _____

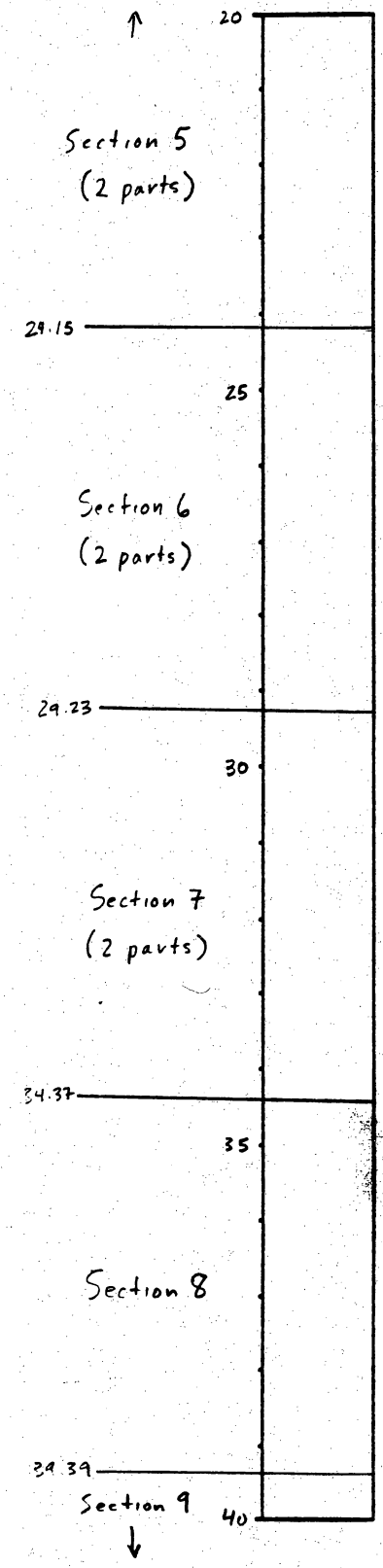

24.15 – 25.23 : Dk. grn gray (5 GY 4/1); clay to sdy clay (sand % decreases upward small sd-filled burrows; abdt fine black organic fragments

— gradational contact —

25.23 – 29.06 : Brownish gray (5 YR 4/1); clayey v.f. sd/silt w/ discontinuous clay laminae; disturbed texture - probably thoroughly bioturbated; scattered sma[ll] to med sd-filled burrows, scattered small to med clay-filled burrows; very min[or] shell frags

⑥

— sharp contact —

29.06 – 29.23 : Olive gray (5 Y 3/2); slightly sdy clay; very small sd-fille[d] burrows; abdt small black organic (?) fragments

— break in core sections —

29.23 – 30.50 : Olive gray (5 Y 3/2); slightly sdy clay; small to med sd-filled bu[rrows]; abdt small black organic (?) fragments

— gradational contact —

30.50 – 32.81 : Olive gray (5 Y 4/1); clayey v.f. sd/silt w/ irregular clay laminae

⑦

disturbed texture - probably thoroughly bioturbated; scattered sd-filled burr[ows]; irregular clay-filled burrows (coalesced burrows difficult to distinguish f[rom] laminae); abdt black organic (?) fragments in clayey sections; minor shell f[rags]

— gradational contact —

32.81 – 34.37 : Olive gray (5 Y 3/2); sandy clay w/ clayey sd interbeds; cla[y] sd interbeds 1/8 – 1/2" thick w/ small clay-filled burrows; clay has small sd/silt-filled burrows, abdt small black organic (?) fragments, minor shell fr[ags]

— break in core sections —

34.37 – 37.12 : Olive gray (5 Y 3/2); silty clay; small silt-filled burrows, medium-size clayey sd-filled burrows; scattered small to medium oyster shell frags; abdt small black organic fragments

— gradational contact —

⑧

37.12 – 38.54 : Olive gray (5 Y 3/2); silty to sdy clay; very abdt med [to] large oyster frags

— gradational contact —

38.54 – 39.39 : Olive gray (5 Y 3/2); silty clay; abdt fine black orga[nic] matter; minor very small silt-filled burrows

— break in core sections —

continued next page

COASTAL EROSION PROJECT

Location: CE-13

Remarks: Keith Lake

Vibra Core ☐ _____
Piston Core ☐ _____
Rotary Core ☐ _____
Elevation: _____

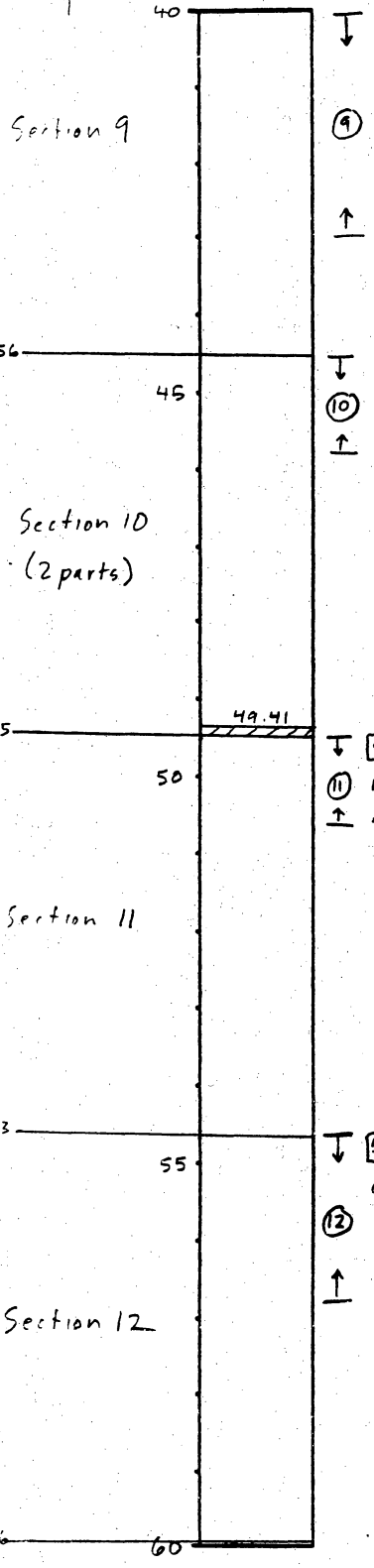

↓ 39.39 – 42.56 : Olive gray (5 Y 3/2); silty clay w/ 1" thick clayey sd bed at 39.6'; scattered small to med sd + clayey sd-filled burrows; cluster of oyster shell frags at top; very abdt fine black organic (?) matter

(9) – gradational contact –

42.56 – 44.56 : Olive gray (5 Y 3/2); clay to silty clay; single small sd-filled burrow; minor fine black organic matter

↑ – break in core sections –

↓ 44.56 – 49.41 : Olive gray (5 Y 3/2); clay to silty clay; scattered fine black organic

(10) matter; very minor fine shell frags

↑ 49.41 – 49.5 : NO RECOVERY

↓ 49.5 – 54.73 : Olive gray (5 Y 3/2); clay to silty clay; abdt fine black organic (?)

(11) matter, some in concentrated laminae; blotchy mod red br (10 R 4/6) mottling

↑ – break in core sections –

↓ 54.73 – 59.96 : Dk grn gry (5 GY 4/1); clay to silty clay w/ several 1/8 – 1/2" thick clayey sd interbeds; scattered small sd + clayey sd filled burrows; very abdt

(12) fine black organic (?) matter – dispersed and in concentrated in thin laminae

blotchy mod red br (10 R 4/6) mottling

↑ – break in core sections –

Location: C.E-13

Remarks: Keith Lake

Vibra Core ☐ _____
Piston Core ☐ _____
Rotary Core ☒ _____
Elevation: _____

Depth feet	Depth meters		Description
60			
		↓	59.96 – 60.40 : Dk grn gray (5 GY 4/1); clay to silty clay; scattered fine black organic matter
			– gradational contact –
			60.40 – 62.48 : Dk grn gray (5 GY 4/1); clay to silty clay w/ sd + clayey sd laminae; scattered small sd + clayey sd-filled burrows; abdt fine black organic matter
Section 13		(13)	dispersed + concentrated laminae
			– gradational contact –
			62.48 – 64.98 : Dk grn gray (5 GY 4/1); clay to silty clay; minor very small sd-filled burrows; abdt fine black organic matter – dispersed + concentrated laminae; blotchy mod red br (10 R 4/6) mottling, one 1" thick mod red br "bed" w/ sharp top + gradational base
64.98	65	↑↓	– break in core sections –
			64.98 – 70.19 : Olive gray (5 Y 4/1); clay; irregular mod yel br (10 YR 5/4) "beds" – ½ – 1½" thick, sharp but irregular contacts; very minor discontinuous thin sd laminae; minor very small sd-filled burrows; abdt fine black
Section 14		(14)	organic fragments – dispersed + in irregular laminae
		↑	– break in core sections –
	70		
70.19			
		↓	70.19 – 72.77 : Olive gray (5 Y 4/1); clay; irregular olive gray (5 Y 3/2) mottling; abdt fine black organic fragments – dispersed + in irregular laminae
			– gradational contact –
		(15)	72.77 – 75.16 : Olive gray (5 Y 4/1); clay w/ discontinuous silt/v.f. sd laminae; clay has darker olive gray (5 Y 3/2) horizons, scattered clayey-sd filled burrows, and very abdt fine black organic fragments; sand laminae thin (< ⅛") and irregular
Section 15		↑	– break in core sections –
75.16	75		
		↓	75.16 – 77.81 : Olive gray (5 Y 4/1); clay; minor small silt/sd-filled burrows; irregular mod yel br (10 YR 5/4) horizons (beds?); very abdt fine black organic fragments – dispersed + in irregular laminae
			– sharp contact –
Section 16		(16)	77.81 – 78.12 : Yellowish gray (5 Y 7/2)/Olive gray (5 Y 4/1); interbedded v f s and clay; 3 sd beds, each ~ ½" thick w/ internal irregular clay laminae; clay same as above interval
			– sharp contact –
			78.12 – 80.08 : Olive gray (5 Y 4/1); clay; very abdt fine black organic fragments
80.08	80	↑	– break in core sections –

Location: CE-13

Remarks: Keith Lake

Vibra Core ☐ _____
Piston Core ☐ _____
Rotary Core ☒ _____
Elevation: _____

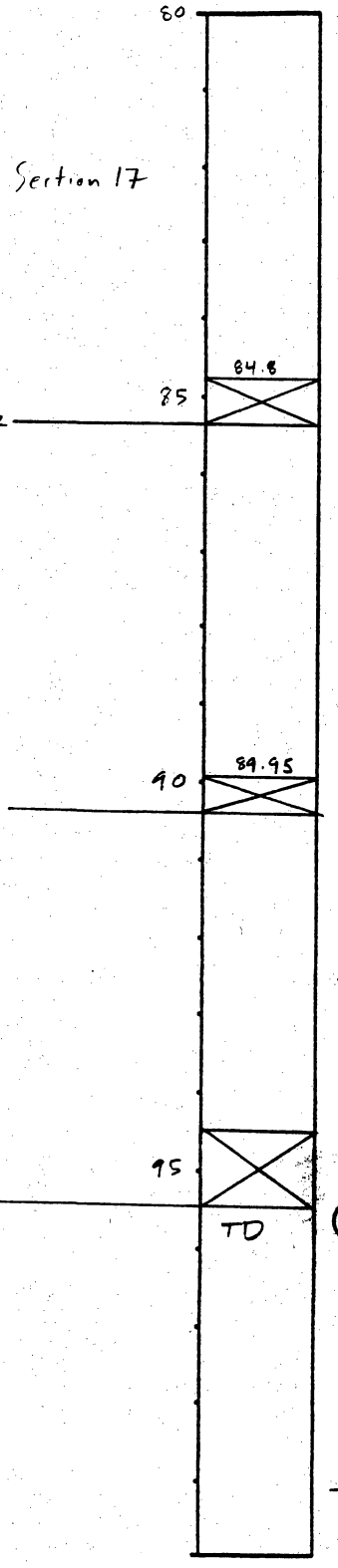

Description

80.08 – 82.37 : Olive gray (5 Y 3/2); clay; minor small silt-filled burrows; blotchy mod. yel. br. (10 YR 5/4) mottling; scattered very fine shell fragmen
— sharp, irregular contact —

82.37 – 82.54 : Yellowish gray (5 Y 7/2); fine to med. sd; fine shell frosment
— sharp, irregular contact —

82.54 – 83.12 : Olive gray (5 Y 3/2); clay w/ 2½" thick clayey sd bed; clay has blotchy mod yel. br. (10 YR 5/4) mottling, abdt fine black organic fragments, med to large oyster shell frags; clayey sd. bed has med to large oyster shell frags, fine black organic fragments (17)
— sharp contact —

83.12 – 84.35 : Yellowish gray (5 Y 7/2); silt to v.f. sd; irregular clayey laminae; small clay-filled burrows at top; irregular horiz. laminations at base; scattered fine black organic frosments
— erosional contact —

84.35 – 84.8 : Dusky yel. br (10 YR 2/2); clay to silty clay; very thin discontinuous sd. laminae; scattered very fine shell frags

84.8 – 85.2 : NO RECOVERY

85.2 – 86.2 : Olive black (5 Y 2/1); silty clay w/ irregular silt/sd laminae; abdt sm silt/sd-filled burrows; chaotic fabric - difficult to distinguish sdy laminae from sd-filled burrows (18)
— gradational contact —

86.2 – 89.95 : Greenish gray (5 GY 6/1); clayey v.f. sd/silt; very chaotic fabric - appears heavily bioturbated but difficult to identify individua burrows; irregular zones of dark gray (N3) mottling w/ stringy silty laminae (?- "laminae" present only w/in dark gray mottled zones)

89.95 – 90.3 : NO RECOVERY

90.3 – 92.24 : Greenish gray (5 GY 6/1); stiff silty/sdy clay; irregular large burrow(s) filled w/ med dk. gray (N4) clay; stringy silty laminae (?) near base irregular mod. red. br (10 R 4/6) mottling (oxidized organic matter or possibly root mottling?)
— gradational, heavily burrowed contact —

92.24 – 93.94 : Dk. yel. orange (10 YR 6/6); v.f. sd/silt; heavily bioturbate large indistinct burrows at top filled w/ overlying clayey material, rest of interval contains abdt medium sd-filled and clay-filled burrows; very minor shell frags (19)
— gradational contact —

93.94 – 94.57 : Greenish gray (5 GY 6/1); stiff silty clay; abdt sd-filled burrows; irregular silty/sdy laminae at base; abdt fine shell frags

94.57 – 95.4 : NO RECOVERY

TD = 95.4

Location: CE-13

Remarks: Keith Lake

Vibra Core ☐ _____

Piston Core ☐ _____

Rotary Core ☒ _____

Elevation: _____

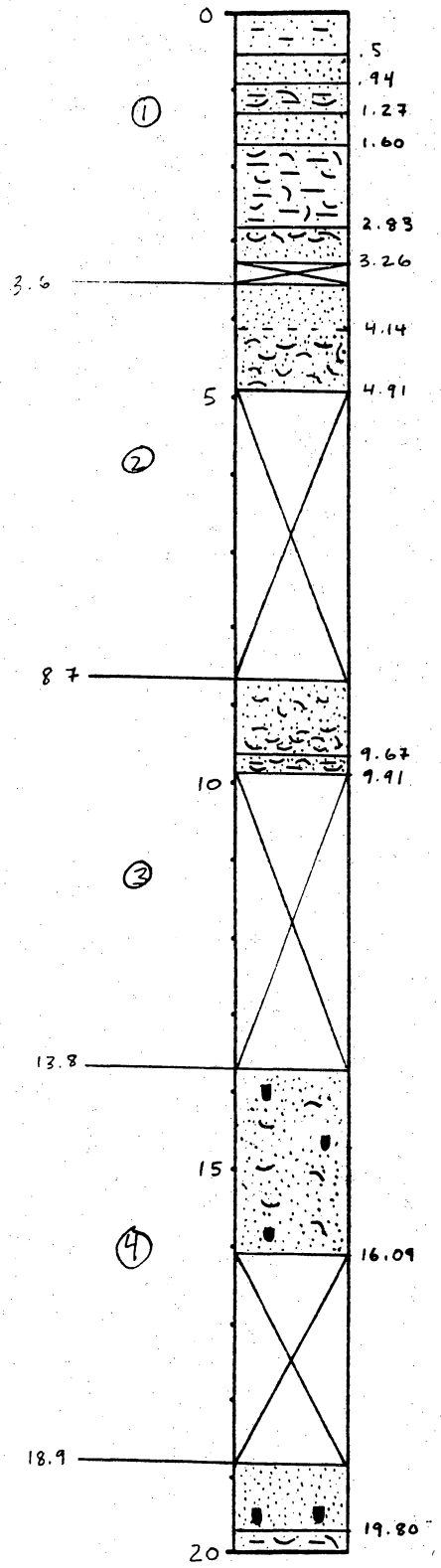

Location: CE-13

Remarks: Keith Lake

Vibra Core ☐
Piston Core ☐
Rotary Core ☒
Elevation:

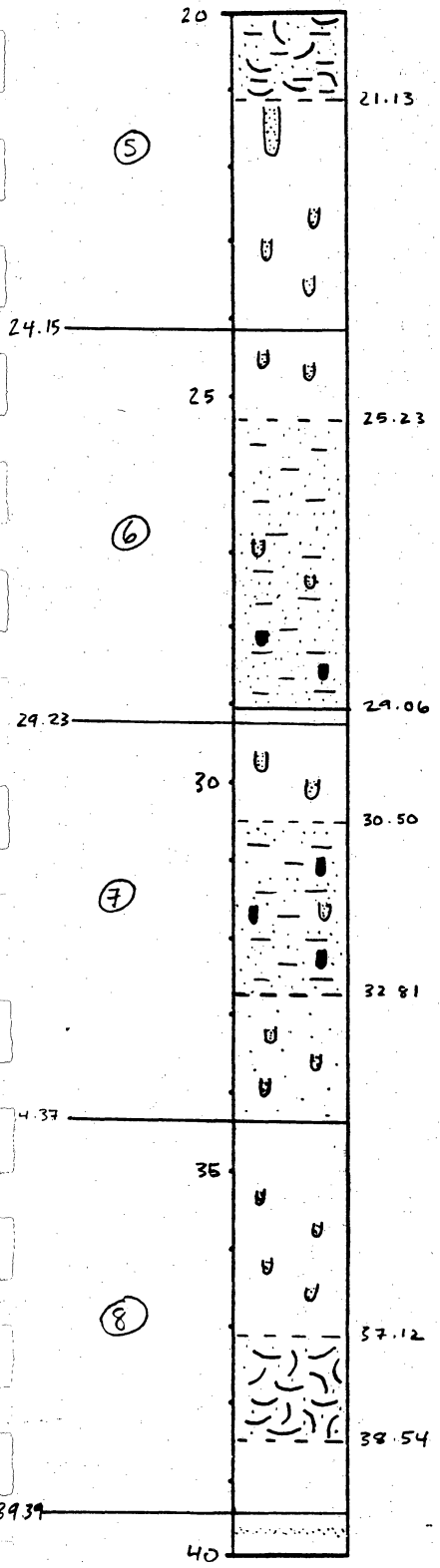

Location: CE-13

Remarks: Keith Lake

Vibra Core ☐ _____

Piston Core ☐ _____

Rotary Core ☒ _____

Elevation: _____

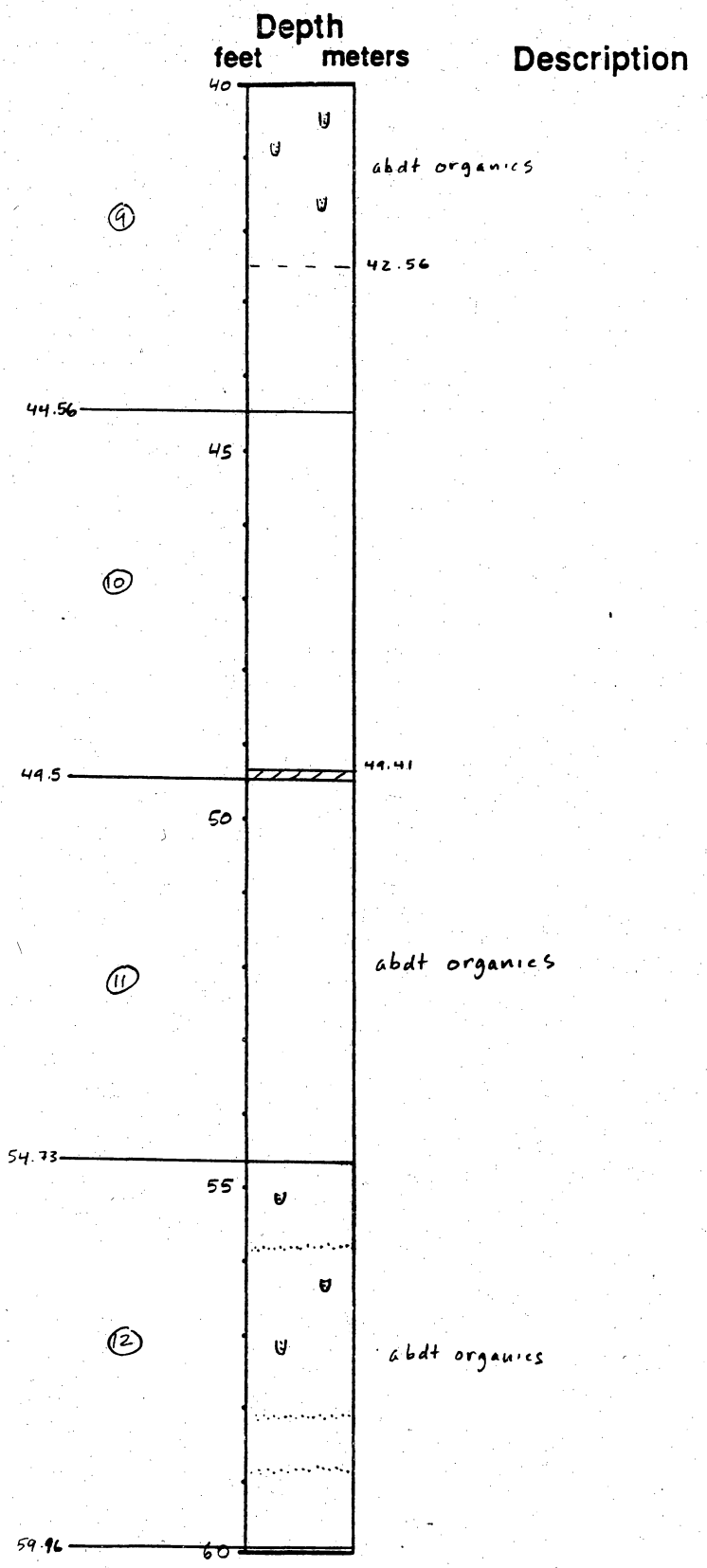

Location: CE-13

Remarks: Keith Lake

Vibra Core ☐ _____

Piston Core ☐ _____

Rotary Core ☒ _____

Elevation: _____

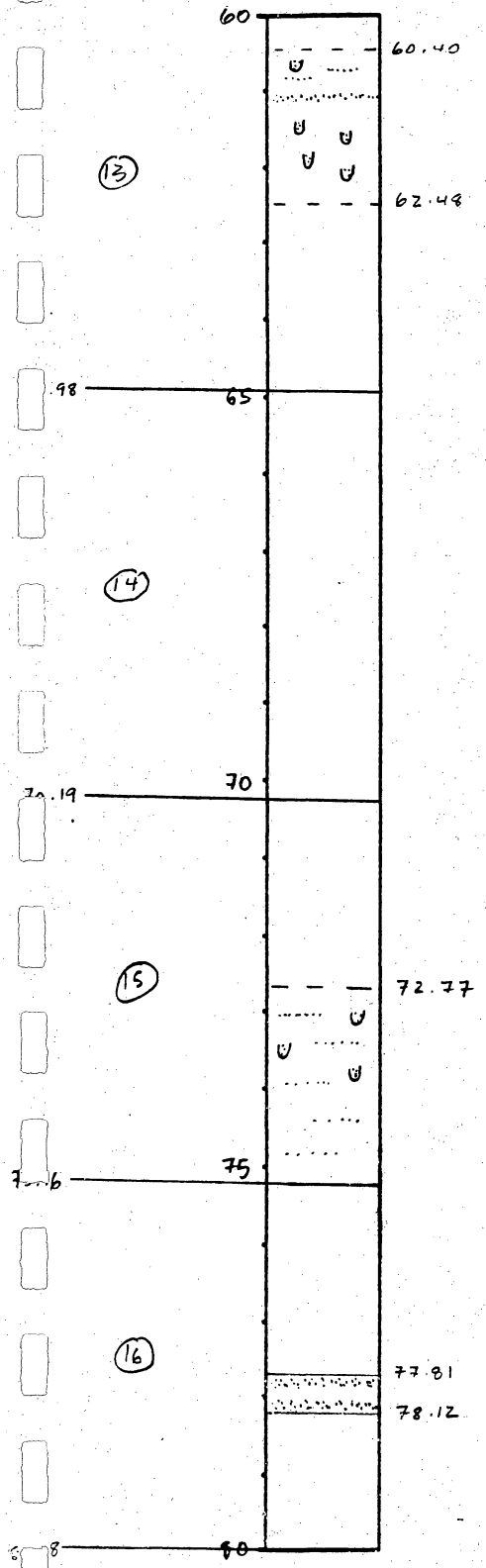

Location: CE-13

Remarks: Keith Lake

Vibra Core ☐

Piston Core ☐

Rotary Core ☒

Elevation:

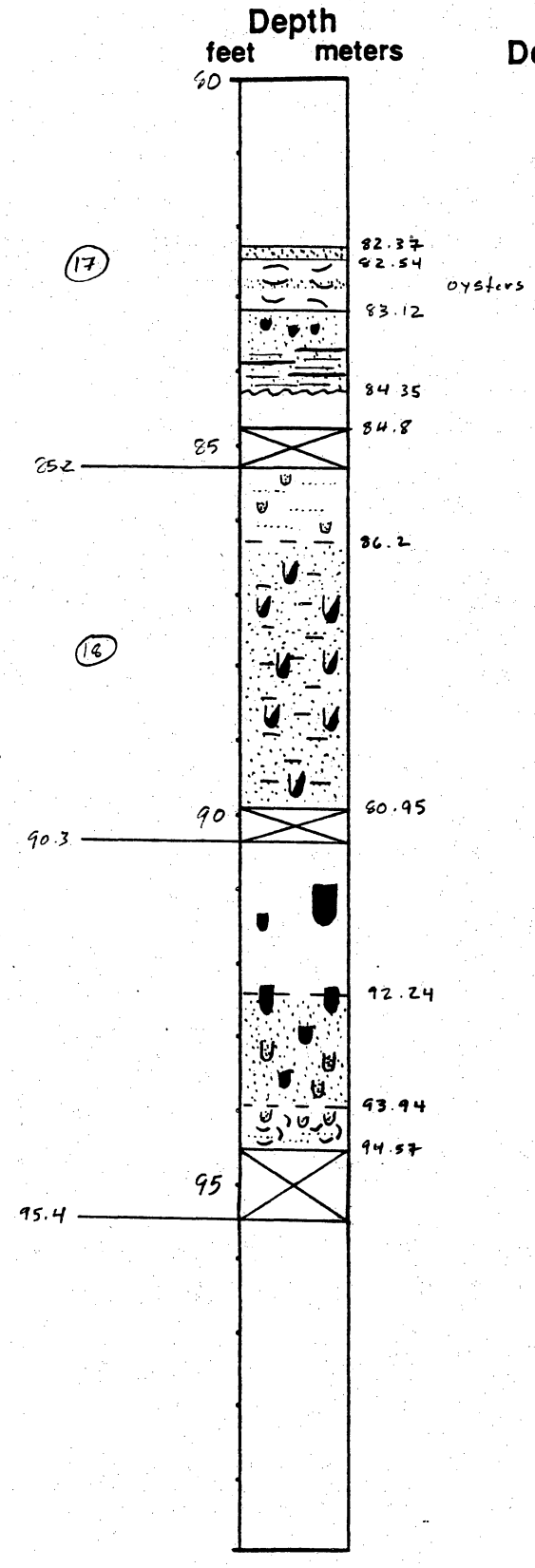

Location: CE-14

Remarks: Hwy 87 - Neches River

Vibra Core ☐ _____
Piston Core ☐ _____
Rotary Core ☒ _____
Elevation: _____

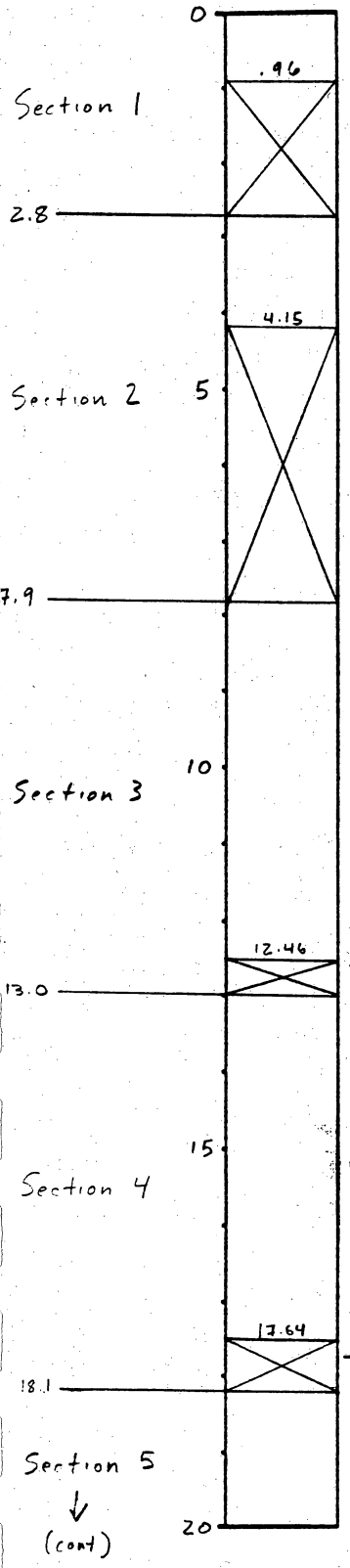

Description

0 - .65: Grayish orange (10 YR 7/4); fine sd; irregular laminations (ripple x-bedding?) at base; abdt roots + organic matter at top; asphalt (road) fragments in upper ½; oxidized iron-rich concretion

① — sharp contact —

.65 - .96: Yellowish gray (5 Y 7/2); sandy shell hash; very abdt small to medium oyster shell frags; asphalt road material at top

.96 - 2.8: NO RECOVERY

2.8 - 2.9: Yellowish gray (5 Y 7/2); fine sd; abdt med oyster shell frags

— sharp contact —

2.9 - 3.4: Dark gray (N3); clay; single ½" thick irregular fine sd. bed w/ small shell frags; clay has irregular light gray (N7) mottling; scattered organic frags

② — sharp, irregular contact —

3.4 - 3.98: Black (N1); clay; very abdt organic matter - peat-like in places; scattered small sd-filled burrows (?)

— sharp contact —

3.98 - 4.15: Dark gray (N3); clay; irregular blotchy light gray (N7) mottling

4.15 - 7.9: NO RECOVERY

7.9 - 8.48: Black (N1); clay; very abdt organic matter - peat-like in place small burrows (?) at base filled w/ light gray (N7) clay

— gradational contact —

8.48 - 10.33: Grayish black (N2)/Lt. olive gray (5 Y 6/1); clay; alternating grayish black + lt. olive gray beds; abdt burrows (?) - filled w/ grayish black clay in lt. olive gray beds and vice versa; scattered fine silt-filled burrow abdt fine black organic fragments

③ — gradational contact —

10.33 - 12.46: Dark gray (N3); clay; blotchy, irregular med lt. gray (N6) mottlin abdt fine black organic matter; minor discontinuous v.f. sd. laminae

12.46 - 13.0: NO RECOVERY

13.0 - 14.64: Grayish black (N2); clay; irregular lt. olive gray (5 Y 6/1) beds and fine mottling (probable burrows); scattered small sd-filled burrows; abdt fine black organic matter

— gradational contact —

14.64 - 15.78: Black (N1); organic-rich clay; very abdt organic matter including small woody fragments

④ — gradational contact —

15.78 - 17.64: Olive black (5 Y 2/1); clay; several irregular lt. olive gray (5 Y 6/1 'beds' w/ olive black mottling (probable bioturbation); abdt fine black organic matter including small woody fragments

17.64 - 18.1: NO RECOVERY

18.1 - 20.95: Grayish black (N2)/Lt olive gray (5 Y 6/1); clay; single thin (<¼") s bed at 20.3', minor wispy silt laminae: alternating grayish black + lt. olive gray clay beds, each w/ extensive mottling of opposite color; abdt fine black organic matter, especially grayish black beds

— gradational contact —

Location: CE-14

Remarks: Hwy 87 - Neches River

Vibra Core ☐ _____

Piston Core ☐ _____

Rotary Core ☒ _____

Elevation: _____

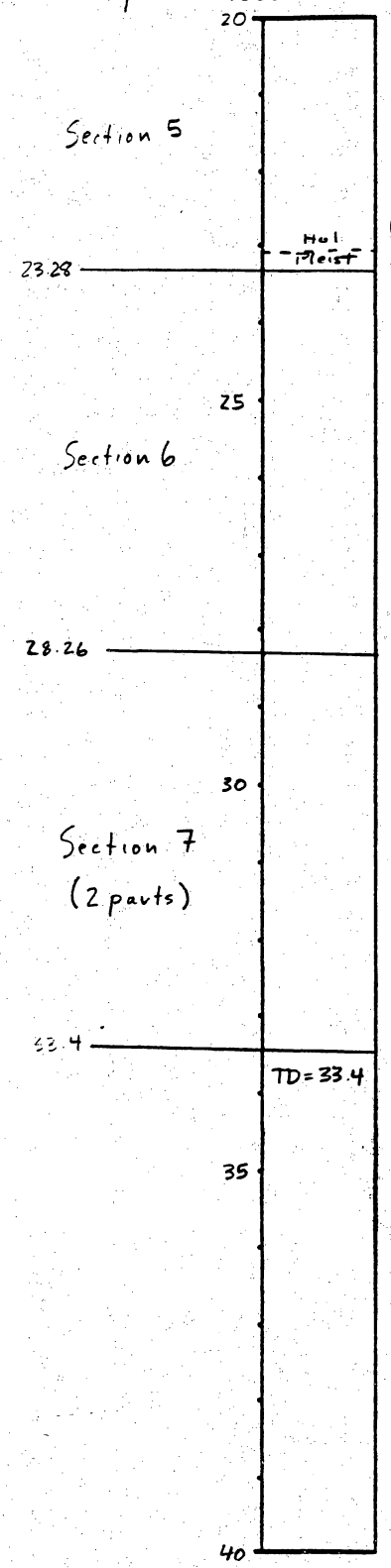

20.95 – 22.24 : Lt olive gray (5 Y 6/1); clay; minor wispy silt laminae toward base; abdt fine black organic matter including small woody fragments

— sharp contact —

22.24 – 23.07 : Olive black (5 Y 2/1) / Yellowish gray (5 Y 7/2); interbedded v.f. to f sd and clay; clay beds ⅛ – ½" thick w/ sharp bases & tops, abdt fine blac organic matter; sd beds from ⅛ – 3" thick w/ discontinuous clay laminae, abdt heavy minerals, fine black organic matter including small woody fra, yellow sulfur staining? at base

⑤

— sharp contact — (Hol / Pleist contact)

23.07 – 23.28 : Dark yel. brown (10 YR 4/2); slightly clayey fine sd; very abd small to med. oyster shell frags

— break in core sections —

25.28 – 23.51 : Same as above

— sharp contact —

23.51 – 25.61 : Greenish gray (5 G 6/1); stiff silty clay; extensive mod. brn (5 YR 4/ oxidation; indistinct mottling - probably thoroughly bioturbated but can't pick out specific burrows

⑥

— gradational contact —

25.61 – 28.26 : Dk. yel orange (10 YR 6/6) / Med. gray (N5); stiff sdy clay; variab texture - med gray stiff clay w/ irregular dk. yel orange oxidized sandy zone sandy zones probably filled burrows but can't definitively identify burrows

— break in core sections —

28.26 – 29.22 : Brownish gray (5 YR 4/1); stiff clay to silty clay; stringy silt la fine dk yel orange (10 YR 6/6) mottling (possible root mottling?); nodular dark gray (N3) to lt. olive gray (5 Y 6/1) mottling - probable burrows

— sharp, irregular contact —

29.22 – 30.07 : Yellowish gray (5 Y 7/2); silt w/ stiff clay interbeds - laminae; extensive mottling - probably heavily bioturbated; dk yel. orange (10 YR 6/6) oxidation staining of siltier zones

— sharp contact —

30.07 – 32.60 : Brownish gray (5 YR 4/1) / Yellowish gray (5 Y 7/2); stiff silty clay w/ silt interbeds - laminae, silt beds - laminae mostly discontinuous - wispy; heavily bioturbated - silty beds - laminae disrupted - mottled; dk. yel. orange (10 YR 6/6) oxidation of silty zones; oxidized organic frags

— gradational contact —

32.60 – 33.4 : Brownish gray (5 YR 4/1); stiff clay w/ wispy silt laminae; silt content increases upward; dk yel. orange (10 YR 6/6) oxidation; oxidized possible organic fragments; small burrows, visible mostly in silty lamin

TD = 33.4

Location: CE-15

Remarks: Hwy 87 - Neches River

Vibra Core ☐ _____
Piston Core ☐ _____
Rotary Core ☒ _____
Elevation: _____

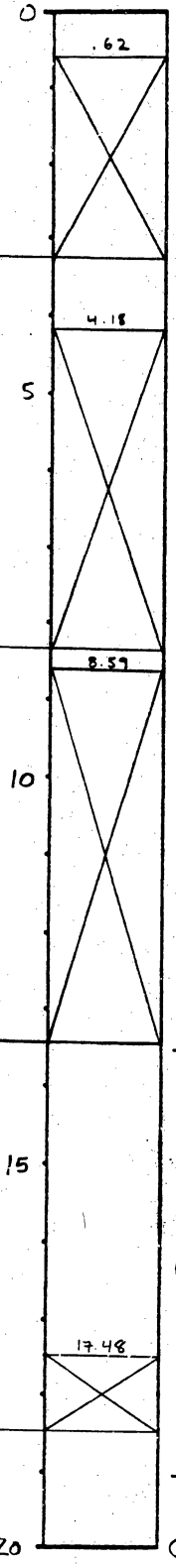

Description

[0 - .46]: Mod. yel. br (10 YR 5/4); silty v.f. to f. sd w/ scattered granule-sized carbonate? rock fragments; abdt roots, twigs, seeds & other organic matter; pieces of glass → FILL/SOIL

① – sharp contact –

[.46 - 6.2]: White (N9); granule to small pebble size carbonate rock fragments w/ small to med oyster shell frags → FILL

[.62 - 3.2]: NO RECOVERY

[3.2 - 3.45]: Yellowish gray (5 Y 7/2); slightly clayey v.f. sd/silt; mottled texture; abdt small to med. oyster shell frags

– sharp, irregular contact –

② [3.45 - 3.91]: Grayish brown (5 YR 3/2); slightly clayey v.f. sd; discontinuous clay laminae; chaotic texture; abdt small to med oyster shell frags, concentrated at top

– sharp contact –

[3.91 - 4.18]: Yellowish gray (5 Y 7/2); sdy shell hash; very abdt small to large oyster shell frags; clayey laminae at top

[4.18 - 8.3]: NO RECOVERY

[8.3 - 8.59]: Grayish black (N2); sdy clay; abdt fine shell frags; abdt organic matter ③

[8.59 - 13.4]: NO RECOVERY

[13.4 - 13.59]: Black (N1); clay; 'nodular' med. gray (N5) mottling; abdt disseminat. fine black organic matter

– sharp contact –

[13.59 - 13.78]: DK. yel br. (10 YR 4/2); clayey v.f. to f. sd.; very abdt small to large oyster shell frags

– sharp contact –

④ [13.78 - 15.96]: Black (N1); clay; very abdt organic matter including several peat-like horizons; scattered fine greenish gray (5 GY 6/1) mottling - probable bioturbation

– gradational contact –

[15.96 - 17.48]: Olive gray (5 Y 3/2); clay; irregular lt. olive gray (5 Y 6/1) 'birds' abdt fine black organic matter w/ some concentrated in discontinuous laminae

[17.48 - 18.5]: NO RECOVERY

⑤ [18.5 - 20.98]: Olive black (5 Y 2/1); clay; scattered lt. olive gray (5 Y 6/1) mottling – probable burrows; disseminated fine black organic matter

– gradational contact –

Location: CE-15

Remarks: Hwy 87 - Neches River

Vibra Core ☐ _____
Piston Core ☐ _____
Rotary Core ☒ _____
Elevation: _____

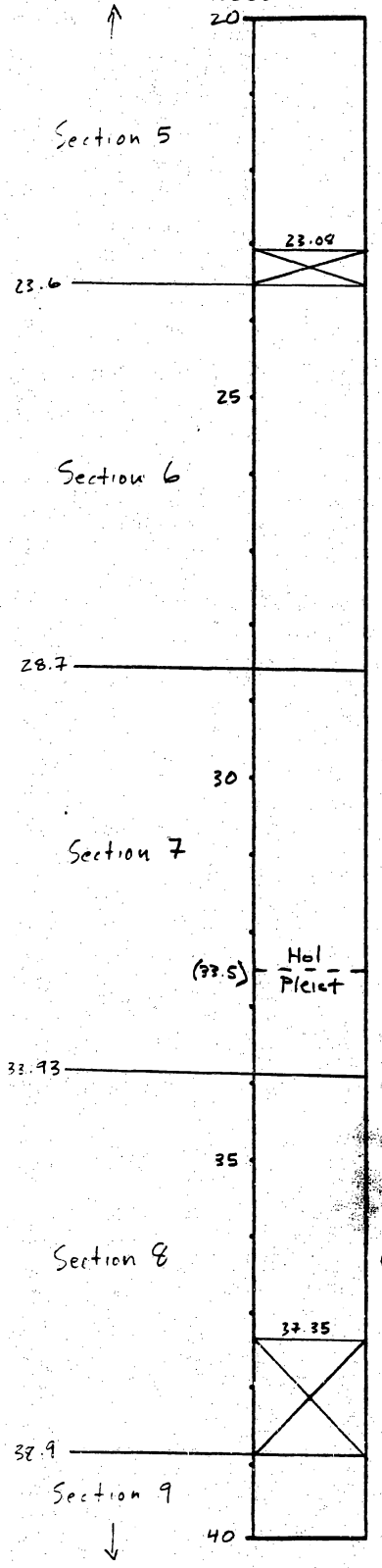

20.88 – 23.08 : Olive black (5 Y 2/1); clay; several lt. olive gray (5 Y 6/1) beds
⑤ abdt lt. olive gray mottling – probable bioturbation; very abdt fine black org matter – disseminated and abdt irregular organic-rich laminae

23.08 – 23.6 : NO RECOVERY

23.6 – 26.06 : Olive black (5 Y 2/1); clay; several lt olive gray (5 Y 6/1) beds abdt lt. olive gray mottling (probable bioturbation), especially near base abdt disseminated fine black organic matter
– gradational contact –

26.06 – 27.56 : Lt olive gray (5 Y 6/1); clay; very abdt fine black organic matter, mostly in discontinuous organic-rich laminae; scattered small woody fragments
⑥ – gradational contact –

27.56 – 28.70 : Olive gray (5 Y 4/1); clay; abdt small, wispy silt-filled burrows? at base; common disseminated fine black organic matter
– break in core sections –

28.7 – 32.28 : Olive gray (5 Y 4/1); clay; silt-filled burrows (possibly distinct laminae?) at top; 1" thick v.f. sd bed w/ faint horizontal laminations – burrowed basal contact at 31.7'; common fine black organic matter
– gradational contact –

32.28 – 32.7 : Olive gray (5 Y 4/1); clay; common fine shell frags; common fine black organic matter
⑦ – gradational contact –

32.7 – 33.49 : Dusky brown (5 YR 2/2); clayey peat; very abdt organic matter, including fibrous woody matter; crude horiz. laminations
– sharp contact – (Hol/Pleist contact)

33.49 – 33.93 : Very pale orange (10 YR 8/2); fine sd; irregular clayey/organic-rich laminae at top; abdt organic matter including fine rootlets
– break in core sections –

33.93 – 34.93 : Yellowish gray (5 Y 7/2); fine to med sd; abdt heavy minerals
– gradational contact –

34.93 – 37.35 : Pale yel. br (10 YR 6/2); fine sd; cluster of roots – very small clay-filled burrows at top; irregular yellowish gray (5 Y 7/2) mottling – possible burrows; very abdt heavy minerals
⑧

37.35 – 38.9 : NO RECOVERY

38.9 – 39.54 : Yellowish gray (5 Y 7/2); fine to med sd; abdt heavy minerals
– gradational contact –

Location: CE-15

Remarks: Hwy 87 - Neches River

Vibra Core ☐ _____
Piston Core ☐ _____
Rotary Core ☒ _____
Elevation: _____

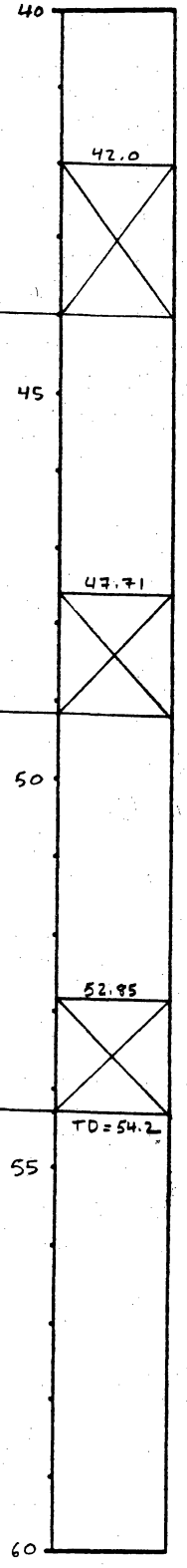

Description

39.54 – 42.0 : Mod. yel. br (10 YR 5/4); fine to med sd; mottled texture – probable burrows; scattered large clayey sd-filled burrows in lower ½; abdt heavy minerals

(9)

42.0 – 44.0 : NO RECOVERY

44.0 – 46.75 : Mod. yel. br (10 YR 5/4); fine to med. sd – generally fining up mottled texture – probably burrowed but can't identify individual burrows except for a few large clayey sd-filled burrows at base; scattered roots; abdt heavy minerals

– sharp contact –

(10)

46.75 – 47.19 : Yellowish gray (5 Y 7/2); med to coarse sd; abdt heavy minerals

– sharp contact –

47.19 – 47.33 : Light olive gray (5 Y 6/1); fine sd w/ single clay-rich lamina; horiz laminations

– sharp contact –

47.33 – 47.71 : Yellowish gray (5 Y 7/2); med to coarse sd; abdt heavy minerals

47.71 – 49.1 : NO RECOVERY

49.1 – 52.85 : Grayish orange (10 YR 7/4); med to very coarse sd; very abdt heavy minerals

(11)

52.85 – 54.2 : NO RECOVERY

TD = 54.2

NOTE: 4.9' of material was left in core barrel after last run

0 – 2.83' (54.2 – 57.03) : Yellowish gray (5 Y 7/2); med to coarse sd; single clayey laminae at base; very abdt heavy minerals

– sharp, irregular contact –

2.83 – 4.04 (57.03 – 58.24) : Yellowish gray (5 Y 7/2); fine to med sd w/ irregular 'interbeds' of med to coarse clayey sd.

– sharp contact –

4.04 – 4.94 (58.24 – 59.14) : Mod yel br (10 YR 5/4); clayey med to very coarse sd; scattered small clay-filled burrows

Addendum 3. Stages and Durations of Post-storm Beach Recovery, Southeastern Texas Coast, U.S.A.

Journal of Coastal Research	10	4	884–908	Fort Lauderdale, Florida	Fall 1994

Stages and Durations of Post-Storm Beach Recovery, Southeastern Texas Coast, U.S.A.

Robert A. Morton, Jeffrey G. Paine and James C. Gibeaut

Bureau of Economic Geology
University of Texas at Austin
Box X, University Station
Austin, TX 78713, U.S.A.

ABSTRACT

MORTON, R.A.; PAINE, J.G., and GIBEAUT, J.C., 1994. Stages and durations of post-storm beach recovery, southeastern Texas coast, U.S.A. *Journal of Coastal Research*, 10(4), 884–908. Fort Lauderdale (Florida), ISSN 0749-0208.

Severely eroded beaches of the southeastern Texas coast monitored for ten years following a category 3 hurricane reveal four time-dependent stages of recovery. The dominant processes during the four stages of recovery are as follow: (1) rapid forebeach accretion, (2) backbeach aggradation, (3) dune formation and (4) dune expansion and vegetation recolonization. Only undeveloped beaches experienced all four stages of post-storm recovery. Developed beaches reached stage 2, but additional recovery was prevented because beach widths seaward of the houses were too narrow to permit eolian transport and construction of dunes.

Post-storm recovery lasted four to five years before the beaches of Galveston Island began responding to local events that dictated subsequent changes in beach volume. Only two of seven profile sites experienced complete recovery in terms of sand volume gained, compared to the volume lost during the storm. Partial recovery at the other sites ranged from 7% to 71% of the volume eroded during the storm. After the four- to five-year period of partial recovery, several beach segments entered an erosional phase that reflects the long-term trend of beach behavior.

Post-storm beach responses at individual sites were highly variable and included the following: (1) erosion and continuous loss of beach volume, (2) partial recovery and subsequent erosion, (3) complete recovery, and (4) continuous gains in beach volume that greatly exceed the volume eroded by the storm. Some of the factors that locally controlled beach response were interactions with shoals at an adjacent tidal inlet, the adverse effects of updrift coastal structures, and along-shore migration of shoreline rhythms that alter sand supply.

The maximum cumulative recovery of sand occurred four years after the storm when approximately 67% of the eroded sand could be accounted for, as storm washover terraces deposited on the barrier flat (12%) or as beach and dune sand returned during the recovery phase (55%). Apparently the remaining volume of sand eroded from, but not returned to the beach, was transported downdrift and stored on the shoreface where it has contributed to spit accretion on Galveston Island.

ADDITIONAL INDEX WORDS: *Coastal processes, beach profiles, shoreline changes, nearshore sand transport, storm impacts.*

INTRODUCTION

The geological work of major coastal storms and the immediate impact of those storms on developed and undeveloped beaches have been topics of substantial research efforts for the past three decades. Recent interest in these high-energy events relates to assessing the physical and biological damage caused by storms (FINKL and PILKEY, 1991), as well as obtaining field data to calibrate and test models that predict beach and dune erosion induced by storms (KRIEBEL and DEAN, 1985; LARSON *et al.*, 1990). Despite the wealth of pre- and post-storm data in some geographical regions, there have been few studies of the long-term impacts of major storms and whether the beaches and dunes eventually recover to their pre-storm position. Most post-storm studies report on the instantaneous beach and dune erosion caused by elevated water levels, and some include the immediate onshore transport of sand and initial phases of beach recovery following the storm (ZEIGLER *et al.*, 1959; WARNKE *et al.*, 1966; KATUNA, 1991; SEXTON and HAYES, 1991). Usually these post-storm studies monitor the storm-eroded beaches for a period of no more than one or two years. In contrast to the short-term studies, longer-period time-series analysis of beach profiles (≥ 10 years) typically are designed to reveal trends of beach stability (ELIOT and CLARKE, 1989), the relationships among coastal processes, beach fluctuations, and sediment textures (LEE and BIRKEMEIER, 1993), or the relationship between washover deposition and dune growth (RITCHIE and PENLAND, 1988). Beach profile rec

94001 received and accepted 6 January 1994.

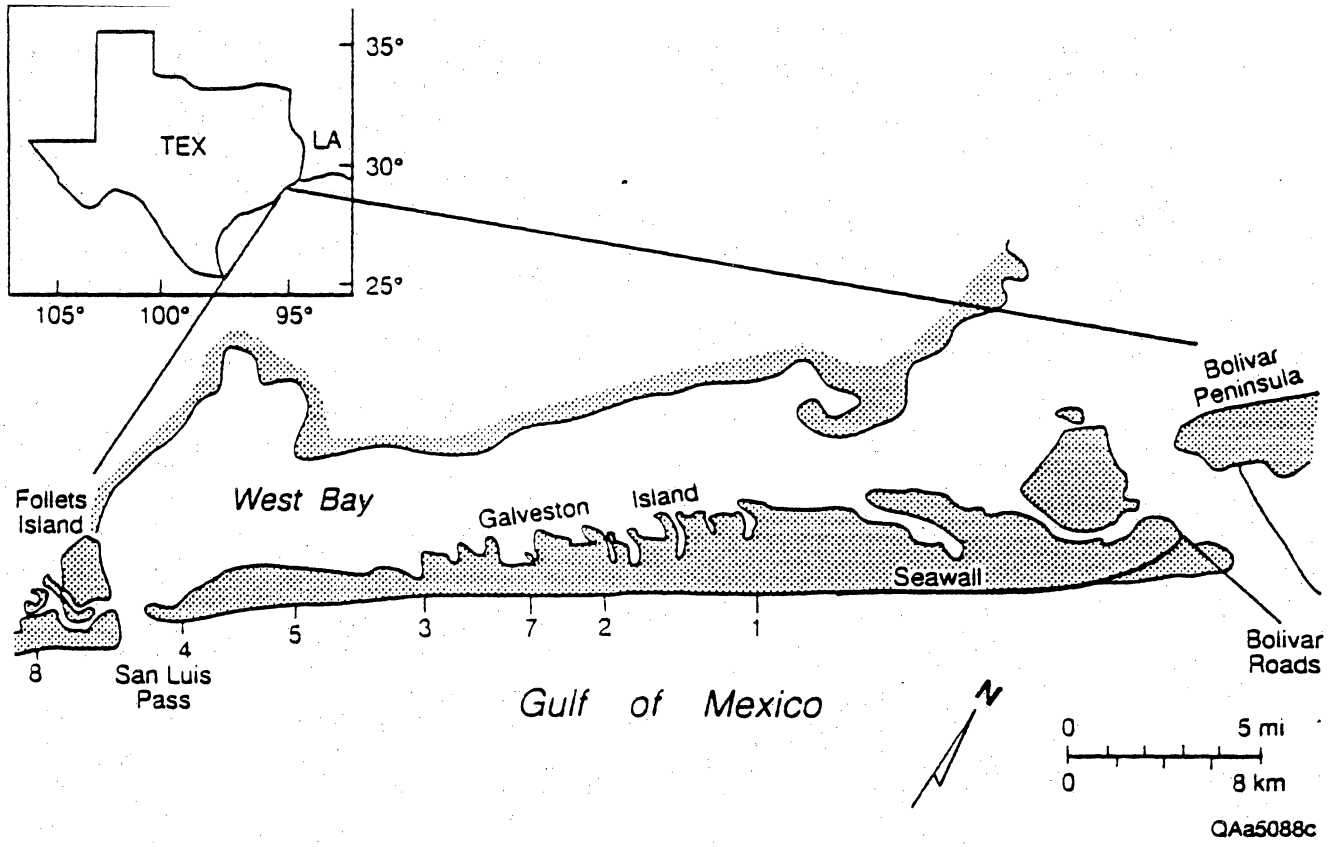

Figure 1. Location of study area and beach profile sites on Galveston Island and Follets Island, Texas.

ords of decadal duration are not used specifically to examine the variability of post-storm beach recovery or to document the systematic recovery processes and beach evolution after a severe erosional event.

The purposes of this study are to describe the stages of post-storm recovery of fine-grained sand beaches along a microtidal, storm-dominated coast and to differentiate the period of post-storm recovery from other beach responses that are recorded by changes in beach volume. Other research objectives are to document volumetric gains and losses along two barrier islands separated by a tidal inlet, to determine the sites of erosion and deposition across the beach profile, and to relate the beach responses at each profile site to the historical trends of shoreline movement and to observed changes in sand supply.

The study area, a 30 km segment of the southeastern Texas coast (Figure 1), includes the zone of maximum storm impact and the beaches upcoast and downcoast of the site where the storm center made landfall (Figure 2). Beach profiles and field conditions monitored at seven sites for ten years after Hurricane Alicia provide a unique opportunity to characterize the post-storm beach responses, to quantify the extent of beach recovery, and to evaluate the morphological controls, variations in sediment supply, and coastal processes responsible for gains and losses in beach volume.

PHYSICAL SETTING

The southeastern Texas coast is a sandy, microtidal region where wave energy is generally low and the beaches are composed of fine sand. The low backbeach elevations and fine sand composition make the beaches extremely vulnerable to erosion during storms. Consequently, storms are the primary geological agent responsible for transporting most of the sand in the littoral zone.

At Galveston, shallow water waves greater than 1 m high occur less than 1% of the time (U.S. Army Corps of Engineers, 1983). Most waves approach the coast from the southeast, but shoreline orientation and seasonal wind patterns cause the littoral drift direction to reverse periodically. Gross littoral drift from bi-directional transport is about 200,000 m^3/yr, whereas net drift is about

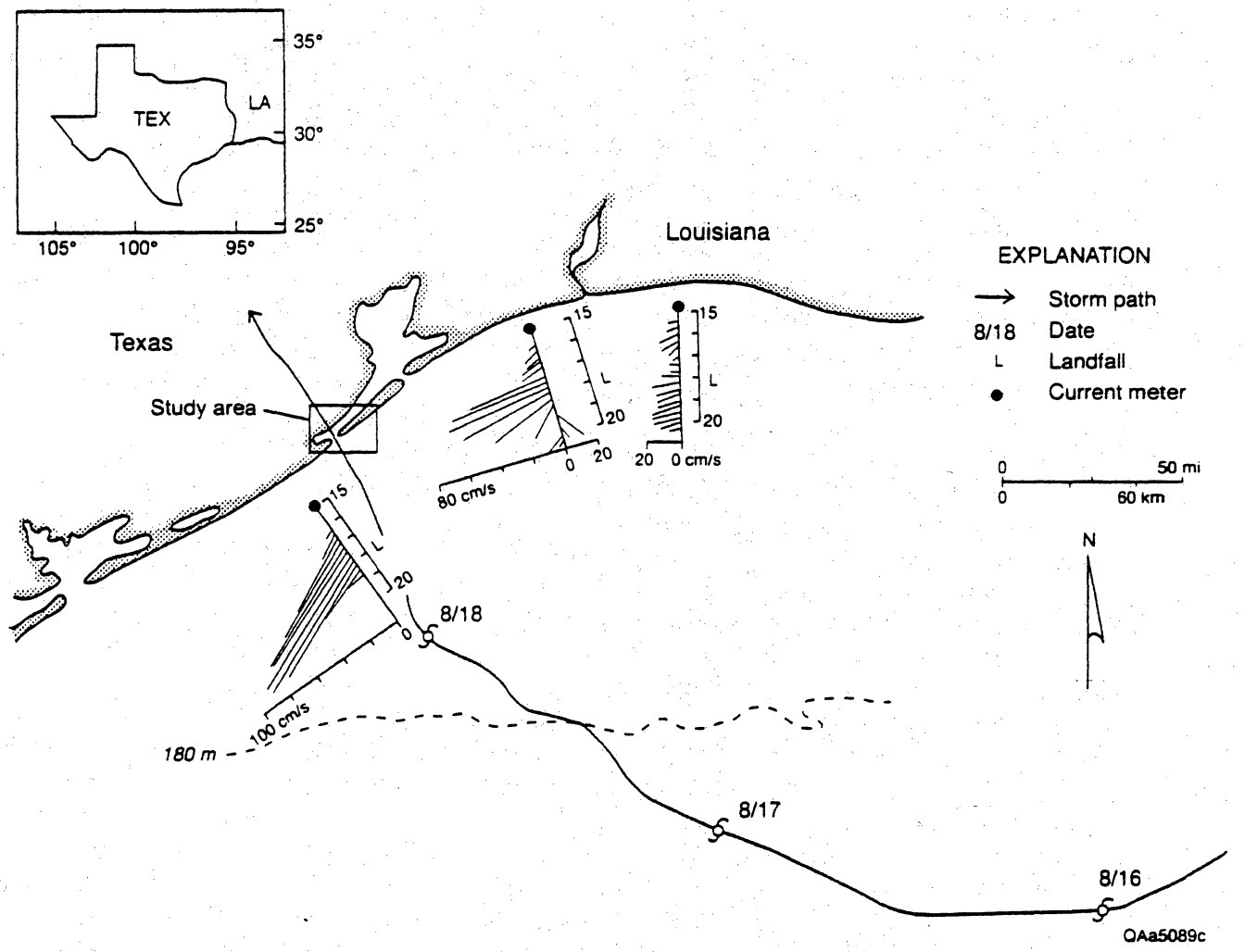

Figure 2. Path of Hurricane Alicia and nearshore current velocities during the storm with respect to the study area. From MORTON (1988).

45,000 m³/yr to the southwest (U.S. ARMY CORPS OF ENGINEERS, 1983).

In the northern Gulf of Mexico, the direction and strength of predominant winds are seasonally distributed. Light to moderate southeast winds prevail most of the year. During the winter and spring, strong winds shift to the east and northeast as Arctic frontal systems pass through the coastal zone. Highest sustained wind velocities accompany major hurricanes, which normally follow a westward path in the Gulf of Mexico. Before hurricanes cross the Texas coast, their counterclockwise wind circulation drives nearshore currents to the southwest (Figure 2).

Astronomical tides at Galveston are diurnal or mixed and typically have a mean range of only 66 cm (U.S. ARMY CORPS OF ENGINEERS, 1983). The wind-induced changes in water level are commonly larger than those caused by the astronomical tides. Wind tides coupled with changes in barometric pressure often cause water levels on Gulf beaches to be raised or lowered as much as one meter compared to the predicted astronomical tides. During the winter and early spring, dramatic changes in water level accompany the passage of Arctic air masses. Preceding the cold front, low barometric pressures and strong onshore winds combine to flood the Gulf beaches. After the front crosses the coast, wind directions reverse, and the wind blows offshore, abruptly lowering water levels and greatly reducing wave energy.

The tide gauge at Galveston, which has the longest record in Texas, shows a relative rise in sea level that averages 6 mm/yr (LYLES *et al.*, 1988). This rate of rise is about three times greater than the global eustatic sea-level rise, which averages about 1.5 to 2 mm/yr (GORNITZ and LEBEDEFF, 1987). Most of the incremental loss in coastal el-

evation is caused by subsidence of the land surface (SWANSON and THURLOW, 1973; PAINE, 1993).

The upper shoreface of Galveston Island and Follets Island is a dynamic zone where shore-parallel sand bars are constructed and disrupted or driven ashore. The first bar is commonly located at the toe of the forebeach and exposed at low tide, whereas the crest of the third bar is located in water depths of about 3 m. The landward increase in physical energy across the shoreface from deeper to shallower water is reflected in the slope, morphology, and sediment textures of the shoreface. Muddy sediments deposited below normal wave base on the inner shelf merge with muds and sandy muds of the lower shoreface (WHITE *et al.*, 1985). The muddy composition of the lower shoreface and shelf indicates that these environments are not sources of sand for post-storm beach recovery, and they appear to be sinks for sand eroded from the beach and upper shoreface. A band of sandy shoreface sediments approximately 3 km wide parallels the islands and extends from water depths of about 10 m to the intertidal zone of the beach. At the adjacent tidal inlets, relatively clean sand extends from the shoreline seaward at least 5 km and merges with the ebb-tidal deltas at Bolivar Roads and San Luis Pass (Figure 1). The large areal extent of shoreface sand suggests an abundance of sand in the littoral system that is available for transport to the northeast or to the southwest.

The distribution of nearsurface sediments on the seafloor gives an incomplete picture of the volume of sand available from subaqueous erosion as the shoreline retreats. The core of Galveston Island is composed of sand, but the southwestern end of the island and neighboring Follets Island overlie delta and estuarine muds of the ancestral Brazos River headland (BERNARD *et al.*, 1970). Therefore, less sand is released to the littoral system when barrier segments close to the headland erode.

Since the mid-1800's, the beaches of Galveston and Follets Islands have experienced variable histories of beach mobility. The difference in beach mobility from one site to another can be traced to storms and engineering projects that have disrupted the supply of beach sand. The principal factors causing long-term beach erosion along the southeastern Texas coast are a deficit in sediment, a relative rise in sea level, and frequent storms (MORTON, 1979).

In August 1983, Hurricane Alicia crossed the southwestern end of Galveston Island (Figure 2). The maximum open coast surge near landfall was 3.8 m, which lasted about 3 hours and caused substantial property damage and economic losses (U.S. ARMY CORPS OF ENGINEERS, 1983). Some of the destruction was directly related to beach and dune erosion that excavated large volumes of sand from beneath the front row of houses causing the vegetation line to retreat as much as 40 m (MORTON and PAINE, 1985). As a result of the extensive beach and dune erosion, about 200 houses on the West Beach of Galveston Island were left on the barren sand beach, although they had been built landward of the pre-storm vegetation line.

Hurricane Alicia eroded about 1.5 million m^3 of sand just from the southwestern 30 km (West Beach) of Galveston Island (MORTON and PAINE, 1985). This volume of beach and dune erosion was estimated by comparing post-storm beach profiles (1983) with February 1980 beach profiles surveyed by the U.S. Army Corps of Engineers. The actual beach morphology at each profile site immediately before Alicia is unknown; therefore, the estimated erosion volumes may be slightly high because Hurricane Allen in August 1980 had a minor impact when it briefly flooded the beaches of Galveston Island with a maximum water level of 1.5 m (U.S. ARMY CORPS OF ENGINEERS, 1980). Although they may lack precision, the estimated eroded volumes provide an alternative quantitative basis for tracking the post-storm beach responses in addition to the actual post-storm surveys. The volume of sand eroded by Alicia from the northeastern end of adjacent Follets Island was not estimated because an accurate pre-storm survey was not conducted at that site.

The volume of sand eroded by Alicia at each profile site on Galveston Island ranged from 51 m^3/m to 73 m^3/m and averaged 61 m^3/m (MORTON and PAINE, 1985). Alicia was a minimum category 3 storm (Saffir/Simpson scale), and yet the volume of beach and dune sand eroded near the storm's eye was similar to the volumes of beach sand eroded by Hurricane Hugo, which was a much more powerful storm (category 4). BIRKEMEIER *et al.* (1991) reported that Hugo eroded an average of 28 m^3/m from Myrtle Beach and 58 m^3/m from Debidue Beach. Both of these South Carolina beaches are just north of where the eye of Hugo

crossed the coast, which placed them in the position of maximum storm surge and beach erosion.

The combined erosional effects of Hurricanes Allen and Alicia obliterated the dunes along West Beach of Galveston Island and northeastern Follets Island. Therefore complete post-storm beach recovery would require reconstruction of the pre-existing dunes.

POST-STORM BEACH RESPONSES AT MONITORING SITES

Beach responses after Hurricane Alicia were determined by comparing a series of beach profiles recorded at six sites along the West Beach of Galveston Island and at one site on Follets Island, the adjacent barrier that is downdrift of Galveston Island (Figures 3–9). The profile sites are three to six kilometers apart (Figure 1), and they were intentionally located in undeveloped areas to avoid beach modifications caused by post-storm human activities.

The beach profiles were surveyed using graduated rods and chain (EMERY, 1961). Elevations for each profile were estimated from nearby benchmarks either surveyed by the Corps of Engineers or maintained by the National Ocean Service. Profiles 4 and 8 (Figure 1) are referenced to existing benchmarks, and Profile 3 was originally established at a benchmark that was later destroyed due to road construction.

Quarterly beach surveys were conducted for the first two years following the storm (1983–1985), and then annual surveys were conducted until 1993. A total of 15 profiles spanning ten years are available for comparing changes in beach shape and volume at each site. An exception is the Follets Island site where nine profiles were recorded for the same ten-year period. After Alicia, we observed filling of ocean-front lots, placement of riprap and bulkheads in the backbeach, construction of artificial dunes, and other profile manipulations in adjacent developed areas that locally altered the shape of the beach and interfered with the recovery processes (MORTON and PAINE, 1985). These physical activities and their impact on adjacent beaches were not studied in detail.

Profile 1

This profile site (Figure 1) is located near a county park about 3.5 km southwest of the Galveston seawall. The profile marker is a reinforced concrete frame that supported a tower used during World War II to search for submarines in the Gulf of Mexico. In the 1940's, the observation tower was located just landward of the foredune ridge. Now all that remains of the tower is the concrete base, which is in the ocean much of the time and serves as unequivocal field evidence that the beach is eroding at this site. Studies of shoreline stability based on aerial photographs confirm that the beach at Profile 1 is eroding at an average rate of about 3.3 m/yr (PAINE and MORTON, 1989).

Together Hurricanes Allen and Alicia destroyed the dunes and eroded a large volume of sand from the beach at Profile 1. The shoreline (zero elevation intercept), however, did not move very much as a result of either storm (Figure 3A). Beach recovery during the first year after Alicia was characterized by continuous berm reconstruction and seaward advancement of the berm crest and shoreline to its pre-storm position. Nearly all the sand transported onshore was added to the seaward end of the profile and no appreciable volume of sand accumulated in the backbeach. A small volume of wind-blown sand was deposited at the face of the erosional escarpment, but the largest volume of sand was deposited in the berm crest and forebeach. Despite the moderate volume of sand returned to the beach during the first post-storm year, backbeach elevations remained well below their pre-storm elevations (MORTON and PAINE, 1985). During the first post-storm year, onshore transport and accumulation of beach sand were recorded continuously even during the winter months when waves in the Gulf of Mexico are highly energetic and beach volumes normally decrease.

By the second post-storm winter (1984), the systematic onshore transport of sand was briefly disrupted and net sand losses were recorded (Table 1 and Figure 10). The winter flooding and erosion of the beach also redistributed the sand so that some of the sand eroded from the forebeach was transferred to the backbeach, raising backbeach elevations about 0.3 m near the erosional escarpment (Figure 3B).

During the next two years (post-storm years 3 and 4), the forebeach remained relatively stable while the backbeach elevations were lowered slightly by deflation. Sand excavated from the backbeach by eolian processes was deposited over and seaward of the erosional escarpment forming low dunes and increasing elevations at the toe of the dunes. By October 1987, the newly formed foredune was about 1.5 m high above the backbeach (Figure 3A). As measured by sand volume

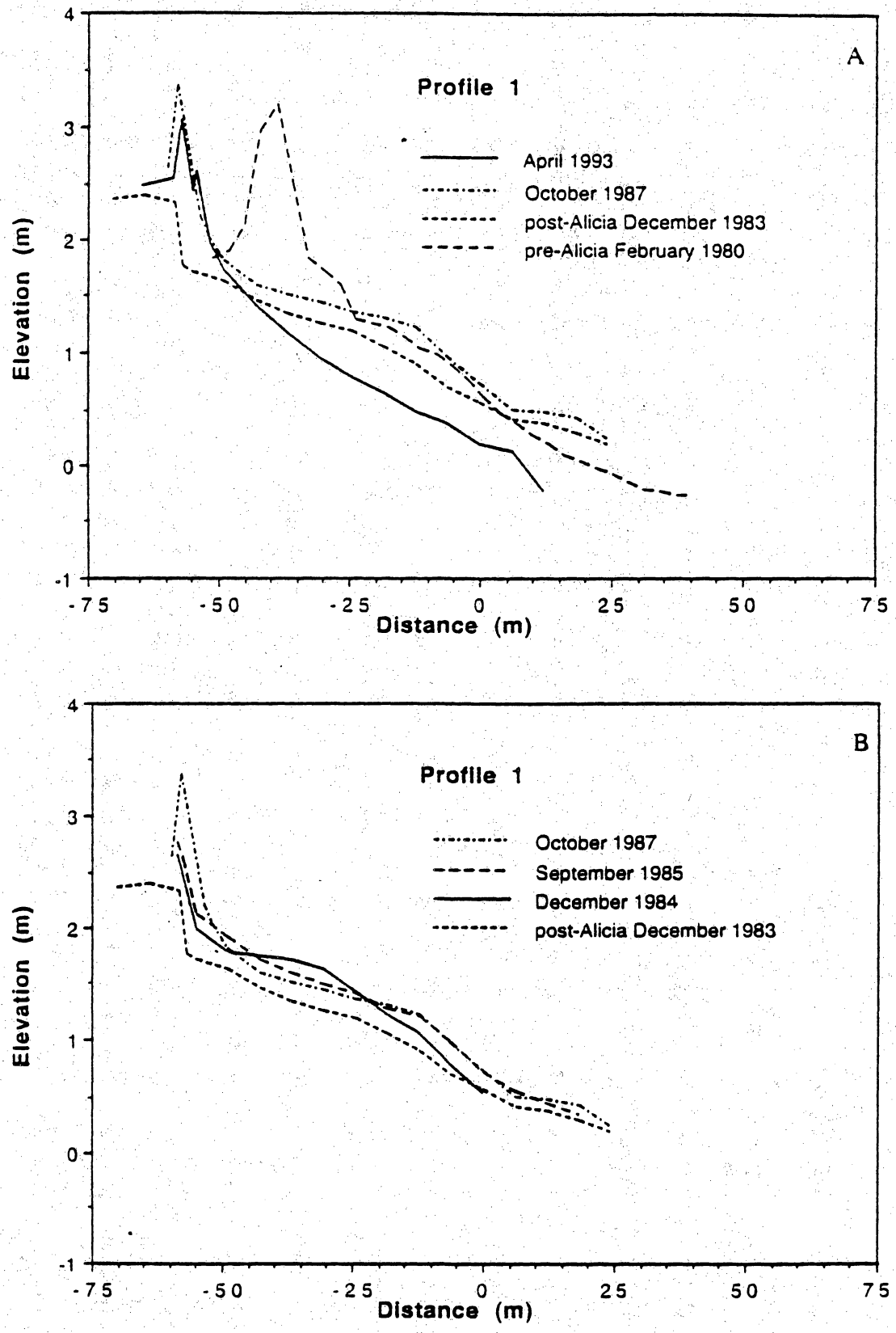

Figure 3. Summary of beach changes at Profile 1 from (A) 1980 to 1993 and (B) 1983 to 1987.

across the profile, maximum beach recovery occurred in the summer five years after the storm (1988) when about 47% of the eroded sand had been returned to the beach (Table 1).

After the fifth post-storm summer, the beach at Profile 1 entered into a phase of continuous erosion that removed much of the recovered foreshore sand and eventually lowered the beach el-

Table 1. *Beach recovery at each profile site and for the entire West Beach segment of Galveston Island expressed as a percent of sand volume eroded by Hurricane Alicia.*

Date	Profile 1	Profile 2	Profile 7	Profile 3	Profile 5	Profile 4	West Beach
Aug. 1983	0.0	0.0	0.0	0.0	0.0	0.0	0.0
Dec. 1983	7.3	18.6	16.9	24.4	30.4	1.4	18.3
Feb. 1984	11.6	26.7	25.9	36.9	18.0	5.5	22.8
May 1984	33.0	25.4	31.5	40.4	28.1	1.5	27.8
Aug. 1984	46.4	45.1	39.2	53.3	42.9	7.6*	39.5
Dec. 1984	32.9	26.8	48.6	57.7	30.4	6.5	37.3
Feb. 1985	13.1	39.0	50.2	57.9	30.9	−6.8	35.0
May 1985	36.6	35.8	55.3	68.3	37.3	−1.1	40.7
Sept. 1985	43.3	50.0	54.8	86.6	40.1*	−4.0	48.3
June 1986		59.9			23.7		
Oct. 1987	45.2	68.8*	71.2*	104.5*	24.7	−11.3	55.3*
Aug. 1988	46.6*	67.0	67.9	99.3	29.7	−39.3	54.1
Sept. 1989	37.3	47.9	69.5	67.9	34.0	−25.8	45.5
Aug. 1990	26.2	69.2	83.2	85.4	51.4	−27.9	59.1
Nov. 1991	10.6	46.5	78.2	100.0	45.4	−4.5	56.2
April 1993	−11.8	82.4	71.4	160.5	42.9	59.3	80.3

* maximum post-storm recovery

evation even below the post-Alicia level (Figure 3A). At the same time sand deposition was limited to the dunes. There was a slight decrease in dune width and dune height, but the dune morphology was essentially stable. The post-recovery erosional phase was accelerated in 1988 by abnormally high tides and waves as Hurricane Gilbert passed westward through the central Gulf of Mexico. Beach erosion at Profile 1 continued into the tenth post-storm year (1993) as beach elevations became progressively lower and the profile took on a pronounced concave shape (Figure 3A).

The history of beach responses at Profile 1 can be synthesized by comparing the pre-storm, immediate post-storm, and most recent beach profiles (Figure 3A). Both the pre-storm and most recent profiles have similar shapes indicating that the profile is once again in equilibrium with the normal erosional processes that characterize this segment of beach. However, the overall profile has retreated landward approximately 18 m, and the 1993 forebeach elevations were even lower than those immediately after Hurricane Alicia. The reversal in trend from post-storm recovery to continuous erosion resulted in an additional net loss of beach volume that, in 1993, was about 12% of the amount eroded by Alicia (Table 1).

Profile 2

Profile 2 (Figure 1) is located near the northeastern end of Galveston Island State Park between a natural beach segment and low-impact park facilities (picnic shelters and low wooden dune bridges). The beach at Profile 2 is undergoing long-term erosion at an average rate of 2.7 m/yr (PAINE and MORTON, 1989).

Initial beach recovery following Hurricane Alicia involved berm reconstruction and rapid seaward advancement of the berm crest and shoreline. Most of the sand delivered to the profile was deposited near the berm crest while backbeach elevations remained at or slightly below their post-storm position. At the same time a small amount of eolian sand was deposited at the erosional escarpment initiating the reconstruction of dunes. High waves associated with frontal passage during the second post-storm winter (1984) eroded the beach and lowered the forebeach profile to the same position it occupied immediately after Alicia. Sand stripped off the forebeach was deposited in the backbeach increasing backbeach elevations by as much as 0.5 m (Figure 4B). The profile again began to recover by rebuilding the forebeach while the backbeach remained unchanged. Later in the summer of the second post-storm year (1985), sand accumulated on the forebeach and in the dunes (Figure 4B). Recovery in the third post-storm year was characterized mainly by dune expansion and growth to an elevation of about one meter above the backbeach while a small volume of sand was deposited at the berm crest. Major dune growth occurred during the summer of the fourth post-storm year (1987), and most of the new sand added to the profile was deposited in the dunes above the erosional escarpment. The forebeach and backbeach away

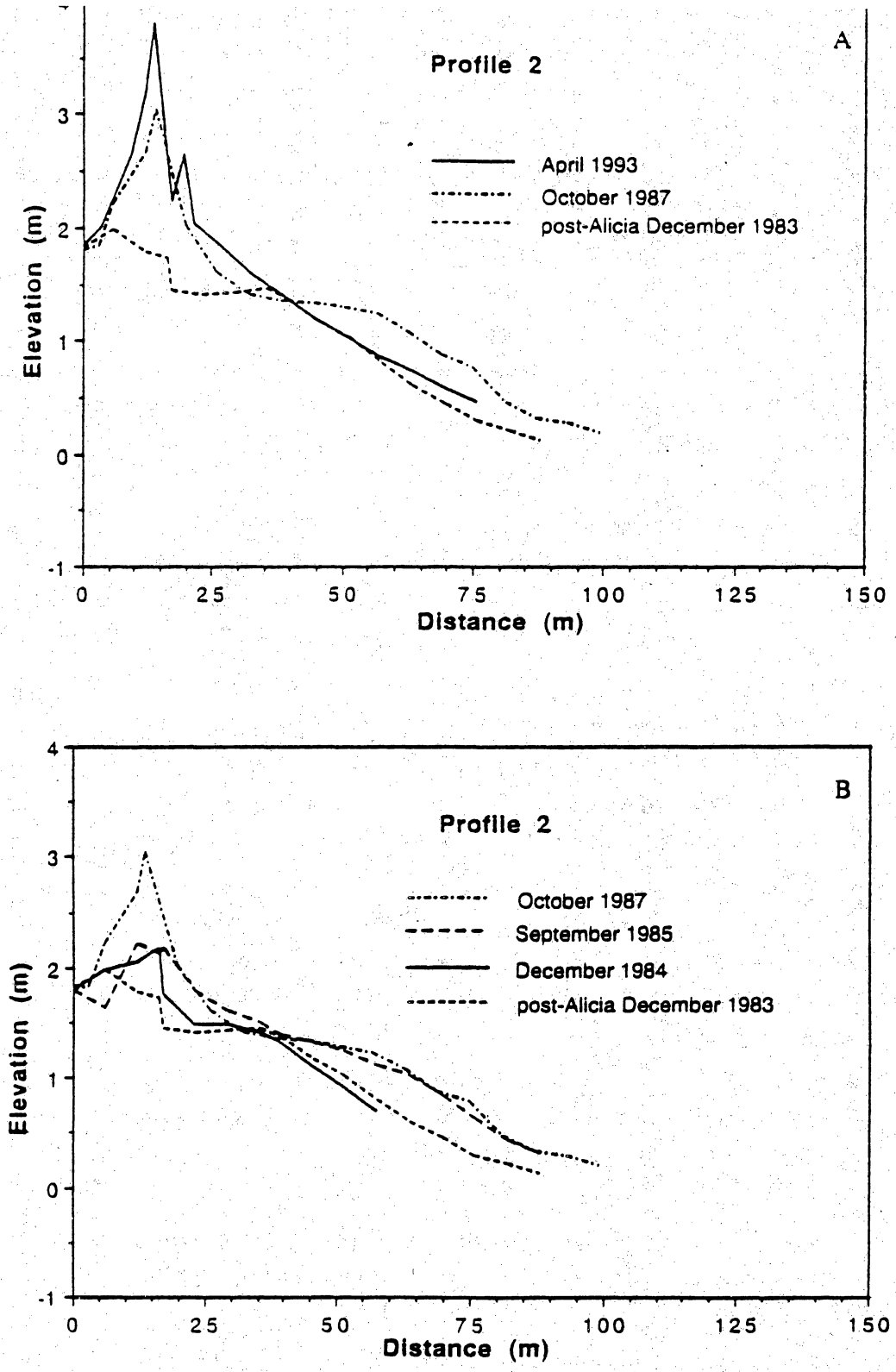

Figure 4. Summary of beach changes at Profile 2 from (A) 1983 to 1993 and (B) 1983 to 1987.

from the dunes remained stable as the beach at this site reached its maximum recovery of 69% four years after the storm (Table 1, Figure 4B).

In the fifth post-storm year (1988), the beach at Profile 2 began losing volume as a result of minor erosion of the forebeach (Table 1, Figure 10). At the same time, the higher elevations along the backbeach and dunes remained unchanged.

Beach erosion associated with Hurricane Gilbert in 1988 continued in 1989 when the forebeach was lowered to the levels recorded immediately after Hurricane Alicia. The following year the forebeach regained much of the lost volume and elevation, but there was no change in sand volume of the backbeach or dunes.

Beach changes at Profile 2 between 1991 and 1993 involved continued erosion of the forebeach and minor sand accumulation in the backbeach and dunes. The dunes attained an elevation of more than 2 m above the erosional escarpment (Figure 4A). Some broadening at the base of the dunes was artificially assisted by the dumping of beach scrapings that included organic debris and other beach litter.

A precise comparison between the 1980 pre-Alicia and 1993 post-Alicia profiles at site 2 could not be made. The 1980 profile was taken along a beach access road that artificially keeps the dunes landward of their natural position. Superimposing the 1980 and 1993 profiles would incorrectly suggest that the 1993 profile represents not only complete recovery of the beach but seaward advancement of the dunes as well. Because the 1980 profile is biased, the summary of post-Alicia changes is based on comparing the profiles immediately after the storm (1983) with those representing maximum recovery (1987) and the most recent profile (1993). This comparison (Figure 4A) shows that the flat horizontal backbeach constructed at the period of maximum recovery later eroded, and the forebeach was lowered to a position similar to its 1983 post-storm position. The backbeach and dunes gained sand volume and elevation after Alicia, but the deposited volume did not equal the sand volume eroded by the storm (Table 1). The five-year (1988–1993) post-recovery forebeach erosion (Figure 4A) is consistent with the long-term deficit in sand supply at the site.

Profile 7

Profile 7 (Figure 1) is located just southwest of the Jamaica Beach subdivision in an undeveloped area that has a long-term erosion rate of 2.8 m/yr (PAINE and MORTON, 1989). Historically, this segment of the coast has been slightly more stable compared to the eroding beaches to the northeast at profile Sites 1 and 2.

Immediately after Hurricane Alicia, Profile 7 experienced rapid seaward advancement of the berm crest and the shoreline accreted to its pre-storm position. Deposition of sand was limited to aggradation of the berm crest and storage of a large volume of sand on the forebeach that formed a broad swale between the erosional escarpment and berm crest and limited the horizontal extent of wave runup. This restricted deposition on the forebeach kept backbeach elevations low, preventing buildup of the backbeach and postponing dune reconstruction.

During the second post-storm winter (1984), the beach profile changed dramatically as sand eroded from the forebeach filled in the swale and constructed a flat backbeach (Figure 5B). The beach remained stable through the second post-storm summer (1985). During the fall, the forebeach eroded slightly and sand was transferred to the backbeach increasing elevations. Aggradation of the backbeach was accompanied by construction of low dunes above the erosional escarpment (Figure 5B). By the fourth post-storm year (1987), aggradation of the forebeach and construction of low dunes continued and the dunes gained elevation as most of the sand was deposited in the dunes. This period also coincided with the maximum volume of sand returned to the beach after Hurricane Alicia during the systematic recovery phase (Table 1, Figure 5B).

During the fifth post-storm year (1988) the forebeach began eroding, and the erosion caused by Hurricane Gilbert continued into the sixth year. This erosion lowered the forebeach to its post-Alicia elevations, and there was no appreciable change in backbeach sand volume except vertical growth of the dunes. In the seventh post-storm year (1990), the berm crest and forebeach were reconstructed and a minor volume of sand was added to the dunes. The backbeach remained essentially unchanged. Subsequent beach changes involved minor erosion of the forebeach and dune growth. The profile retained a convex shape, unlike the beaches to the northeast where erosion is greater. The profile achieved only partial recovery (83%) in terms of sand volume returned to the beach before the most recent erosional trend began in 1991 (Table 1).

In 1993 backbeach elevations and morphology of the beach were similar to pre-storm conditions, but the profile was shifted landward and the dunes occupied a position about 30 m landward of their 1980 position (Figure 5A). The rate of erosion is lower than beaches to the northeast, and conforms to the long-term trend of beach stability.

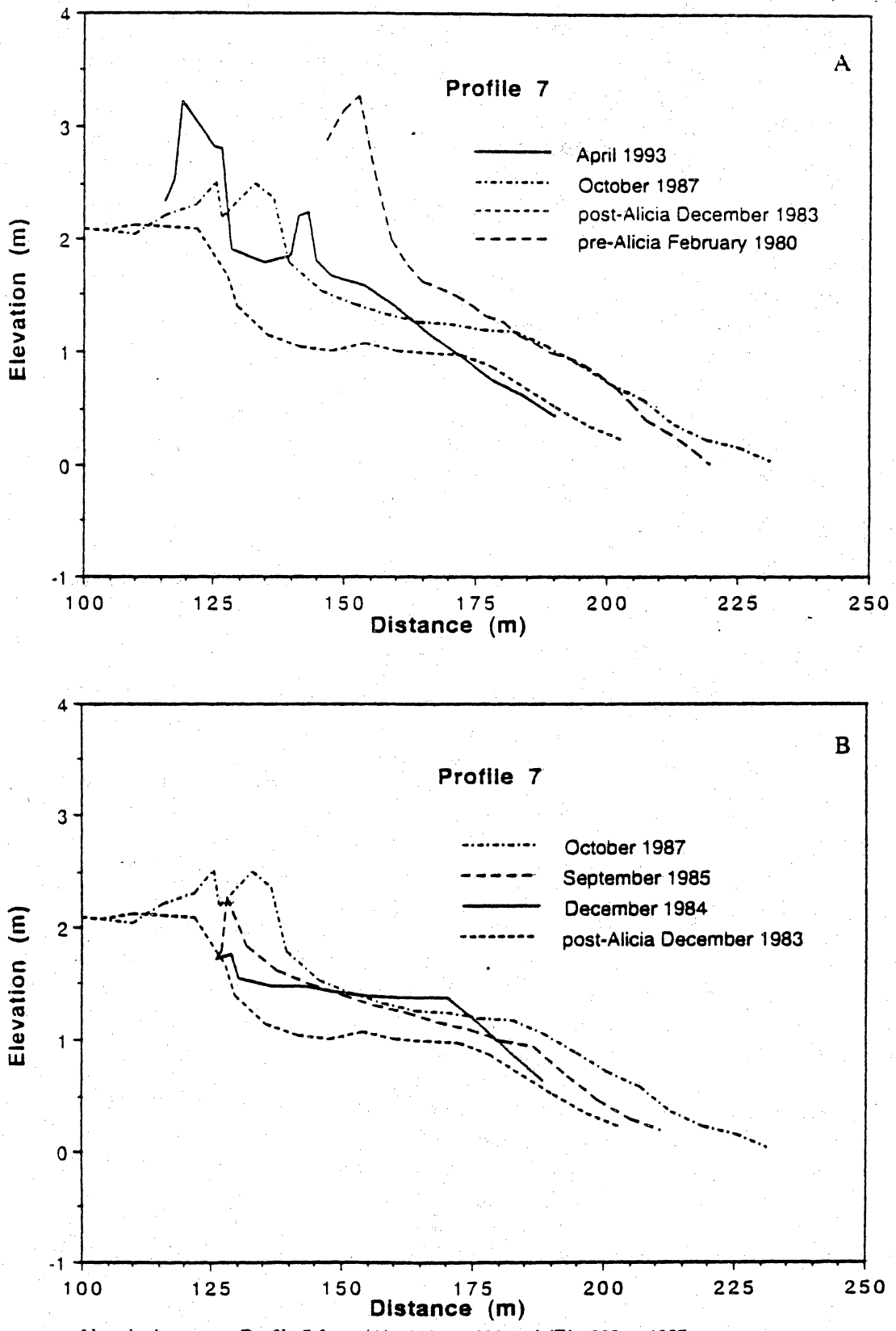

Figure 5. Summary of beach changes at Profile 7 from (A) 1980 to 1993 and (B) 1983 to 1987.

Profile 3

Profile 3 (Figure 1) represents the most stable segment of West Beach on Galveston Island. This relative stability is reflected in lower long-term erosion rates that have averaged about 1.1 m/yr (PAINE and MORTON, 1989).

During the first year after Hurricane Alicia, beach recovery at Profile 3 consisted of berm re-

construction and rapid forebeach accretion to the pre-storm position. Backbeach elevations remained unchanged from the immediate post-storm elevations until the second post-storm winter (1984) when the forebeach eroded and sand was transported landward and deposited in the backbeach. Sand deposition raised backbeach elevations approximately 40 cm, and low dunes began to form above and seaward of the erosional escarpment (Figure 6B). The beach continued to accrete, and the dunes grew vertically during the summer of the second post-storm year (1985) when large volumes of sand were added to the entire beach profile. From the second to the fourth post-storm year (1987), the berm crest continued to accrete increasing beach width. The backbeach deflated and lowered slightly in elevation. Dunes grew vertically and expanded laterally forming a continuous foredune ridge more than 2 m above the backbeach (Figure 6B).

In the fifth post-storm year (1988) the forebeach eroded slightly and there was a net loss of sand from the profile. Beach changes the next year involved slight landward migration of the dunes as sand avalanched down the dune slipface onto the vegetated barrier flat. This dune migration was also accompanied by a slight increase in dune elevation while the wide backbeach and forebeach were maintained. Dune growth continued in 1990 and 1991, and by 1993 a large volume of sand was added across the entire beach profile (Figure 6A).

There appears to be a secondary dune forming seaward of the foredune (Figure 6A). It is actually an artificial sand ridge locally created to control vehicular traffic on the beach. The artificial ridge represents an actual volume of sand deposited on the backbeach. The morphology is dictated by maintenance of the road between the artificial ridge and foredunes.

Comparing the 1980, 1983, and 1993 profiles shows that the volume of sand accumulating at Profile 3 greatly exceeds the volume eroded by the storm (Figure 6A, Table 1). The extant dunes are much higher and broader than their predecessors (Figure 6A). By 1993, 60% more sand was on the beach than before the storm (Table 1). The morphology of the dunes and backbeach before Alicia and in 1993 are similar. The break in backbeach slope is shifted landward about 15 m. Also in 1993, the dunes and backbeach elevations at Profile 3 were higher than before the storm. Dense vegetation has stabilized the foredunes, and they are no longer migrating onto the vegetated barrier flat subenvironment.

Profile 3 represents conditions where the volume of sand returned to the beach exceeds the volume eroded by the storm, and yet the positions of the morphological features are shifted landward suggesting beach erosion. This particular beach segment has experienced net retreat in terms of dune position. The volume of beach sand has actually increased as a result of sand eroded from adjacent beaches, most likely those to the northeast that were updrift during the storm. The surplus volume of beach sand is stored primarily in the dunes and backbeach.

Profile 5

Profile 5 (Figure 1) was established where beachfront houses were widely spaced. It did not appear that the development would interfere with beach processes because the houses were about 10 m landward of the post-Alicia erosional escarpment. Since the storm, the sparsely developed area has been more densely developed. The backbeach morphology has been modified locally by attempts to artificially reconstruct dunes and reestablish the vegetation line seaward of the post-Alicia escarpment. The composition and color of fill material placed on the backbeach is so different from the natural beach sand that natural changes in profile morphology are easily distinguished from human alterations to the profile. The profile has been maintained at this site because it records typical low-cost responses to beach erosion (artificial dunes, sand fences) and their interaction with normal beach processes. Profile 5 also represents a transitional beach segment between the more stable beach at Profile 3 and the unstable beach at Profile 4 (Figure 1). The long-term trend of shoreline movement at Profile 5 is erosion, which has averaged about 2.7 m/yr (PAINE and MORTON, 1989).

By the end of the first post-storm summer (1984), the berm at Profile 5 had been reestablished by minor aggradation at the berm crest. The forebeach had slowly advanced to its pre-Alicia position, but the backbeach and the erosional escarpment remained the same as immediately after the storm. A low ($\approx$1.3 m) artificial dune ridge was constructed in the middle of the backbeach about 25 m seaward of the erosional escarpment (Figure 7B). During the second post-storm winter (1984), sand was eroded from the

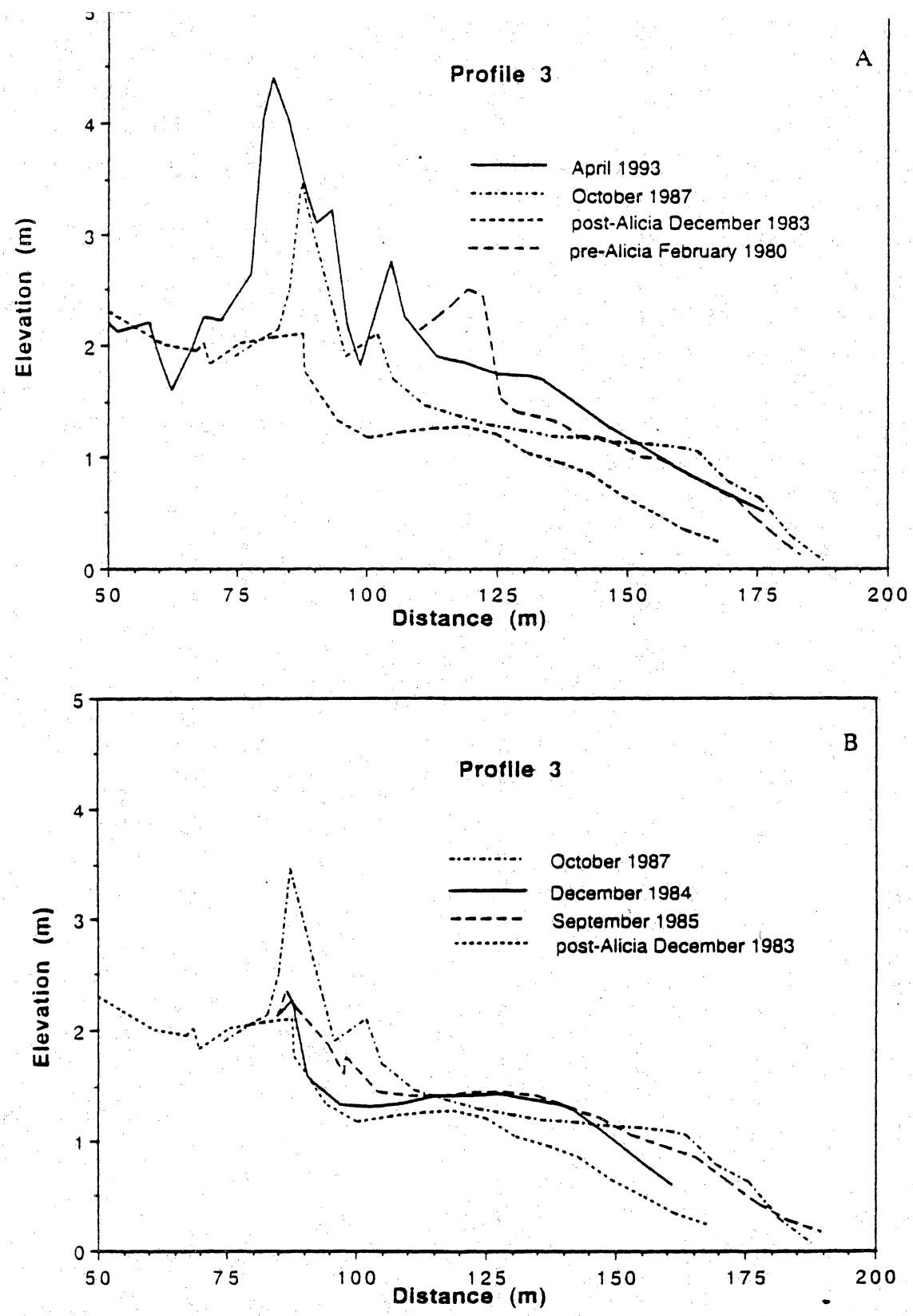

Figure 6. Summary of beach changes at Profile 3 from (A) 1980 to 1993 and (B) 1983 to 1987.

forebeach and deposited at the toe of the artificial ridge. This completely blocked the landward transport and deposition of sand in the backbeach and near the erosional escarpment. The eroded forebeach remained near its pre-Alicia position throughout the remainder of the second post-storm year and no appreciable volume of sand was added to the profile. The maximum beach recovery, which

occurred at the end of the second post-storm year (1985), amounted to only 40% of the volume eroded by the storm (Table 1).

In the third post-storm year (1986), the forebeach eroded and sand was deposited at the toe of the artificial ridge, which continued to prevent accumulation of sand in the backbeach or at the erosional escarpment. The only sand volume added to the beach during this period was minor eolian accumulation on the artificial ridge. The fourth and fifth post-storm years (1987–1988) were characterized by erosion and steepening of the forebeach while the height of the artificial ridge increased slightly as a result of minor eolian deposition (Figure 7B). During the fifth post-storm year (1988), high waters from Hurricane Gilbert flooded the beach, eroded the forebeach, destroyed the artificial ridge, and deposited the eroded material in a washover terrace above and seaward of the erosional escarpment. The washover deposit was composed mainly of resedimented artificial ridge material, but some washover sand also eroded from the forebeach. The washover material instantaneously raised the backbeach elevation as much as 0.75 m above the post-Alicia elevation, which had not aggraded because of the artificial ridge. In the sixth post-storm year (1989), another low mound of muddy fill material was placed on the backbeach in the same position as the previous artificial ridge. The next year (1990) a fall storm destroyed this second artificial ridge and added the fill to the Gilbert washover deposit above the erosional escarpment. Subsequent beach changes at Profile 5 involved continued erosion of the forebeach and transfer of sand onto the backbeach where it filled in and aggraded about 0.5 m between the remnant erosional escarpment and former artificial ridge. The most recent profile changes included erosion of the forebeach and artificial construction of another (third) ridge that caused the profile landward of the ridge to be static. Continued erosion since 1989 has lowered the forebeach to a position that is lower than the post-Alicia beach (Figure 7A).

Beach changes at Profile 5 are difficult to interpret without substantial documentation of the profile modifications. This is because the observed changes in sediment volume from the dunes landward are an artifact of profile manipulation and instantaneous construction of low ridges by the property owners. Discounting the volume of material added to the beach by human activities and redistributed by Hurricane Gilbert, it is clear that the profile has not gained any significant volume since the initial natural recovery. That recovery accounted for only about 40% of the volume eroded by the storm. No natural foredunes have formed at the site and the forebeach profile has shifted landward about 10 m indicating net erosion of the beach.

Profile 4

Profile 4 (Figure 1) is located just east of San Luis Pass and is the closest profile site to the landfall of Hurricane Alicia (Figure 2). This site experiences large fluctuations in beach volume caused by the exchange of sand with shoals of the tidal inlet; however, the long-term trend is erosion, which has averaged about 9.2 m/yr (PAINE and MORTON, 1989). Compared to other profile sites on Galveston Island, the barrier is narrower and slightly lower at Profile 4. These conditions coupled with the long-term erosion prevent the accumulation of dunes and invite repeated washover. Consequently, the barrier flat is composed of stacked washover deposits and the vegetation line either coincides with an erosional escarpment during cycles of erosion or with low, sparsely vegetated dunes during cycles of sand accumulation.

At Profile 4, the volume of sand added to the beach during the first post-storm year was minor and there was no significant recovery (Table 1). Instead, the forebeach gained and lost minor amounts of sand during each quarter, but no systematic trend in sediment flux was established. The total volume of sand added to the beach in the first post-storm year was only 7% of the volume eroded by the storm. This was also the greatest volume gain at Profile 4 during the post-storm recovery phase (Table 1).

In the second post-storm winter (1984), high waves eroded the beach and escarpment to a position below and landward of the post-Alicia beach. Erosion and loss of sand volume continued into the fifth post-storm year (1988) when large volumes of sand were removed from the beach and the profile was again lowered and shifted landward. At that time about 39% more sand was absent from the beach compared to the volume eroded by Hurricane Alicia (Table 1). During the next two years (1989 and 1990), the escarpment continued to erode but the forebeach aggraded. A net gain in beach volume resulted that reversed the erosional trend and marked the beginning of an accretionary trend. By 1991 the berm crest was

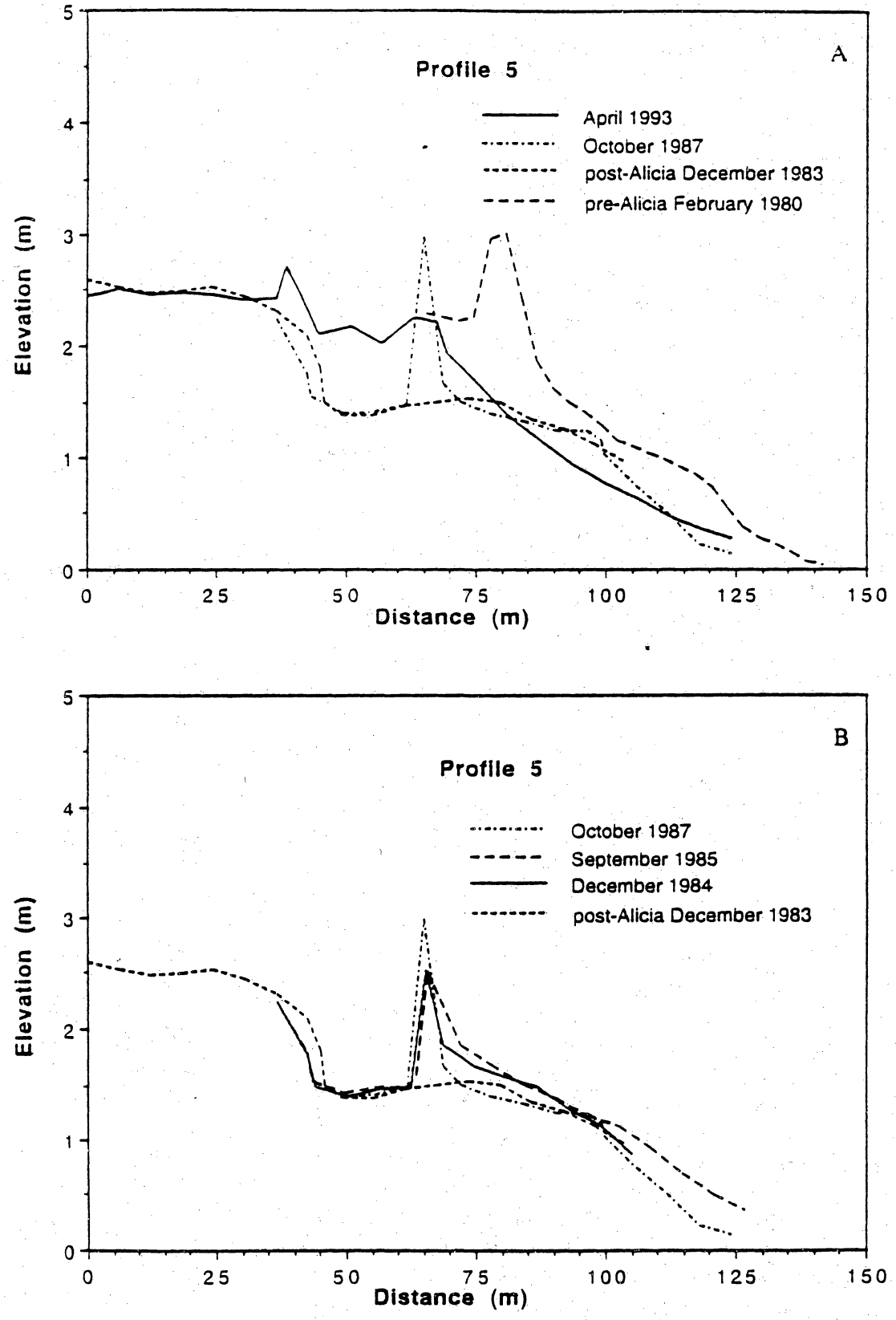

Figure 7. Summary of beach changes at Profile 5 from (A) 1980 to 1993 and (B) 1983 to 1987.

reconstructed and the forebeach accreted to a position slightly seaward of the post-Alicia position.

The most recent beach changes at Profile 4 involved deposition of a large volume of sand on the forebeach and construction of low discontinuous dunes in the backbeach seaward of the erosional escarpment and below the vegetated barrier flat (Figure 8A). The 1980 and immediate

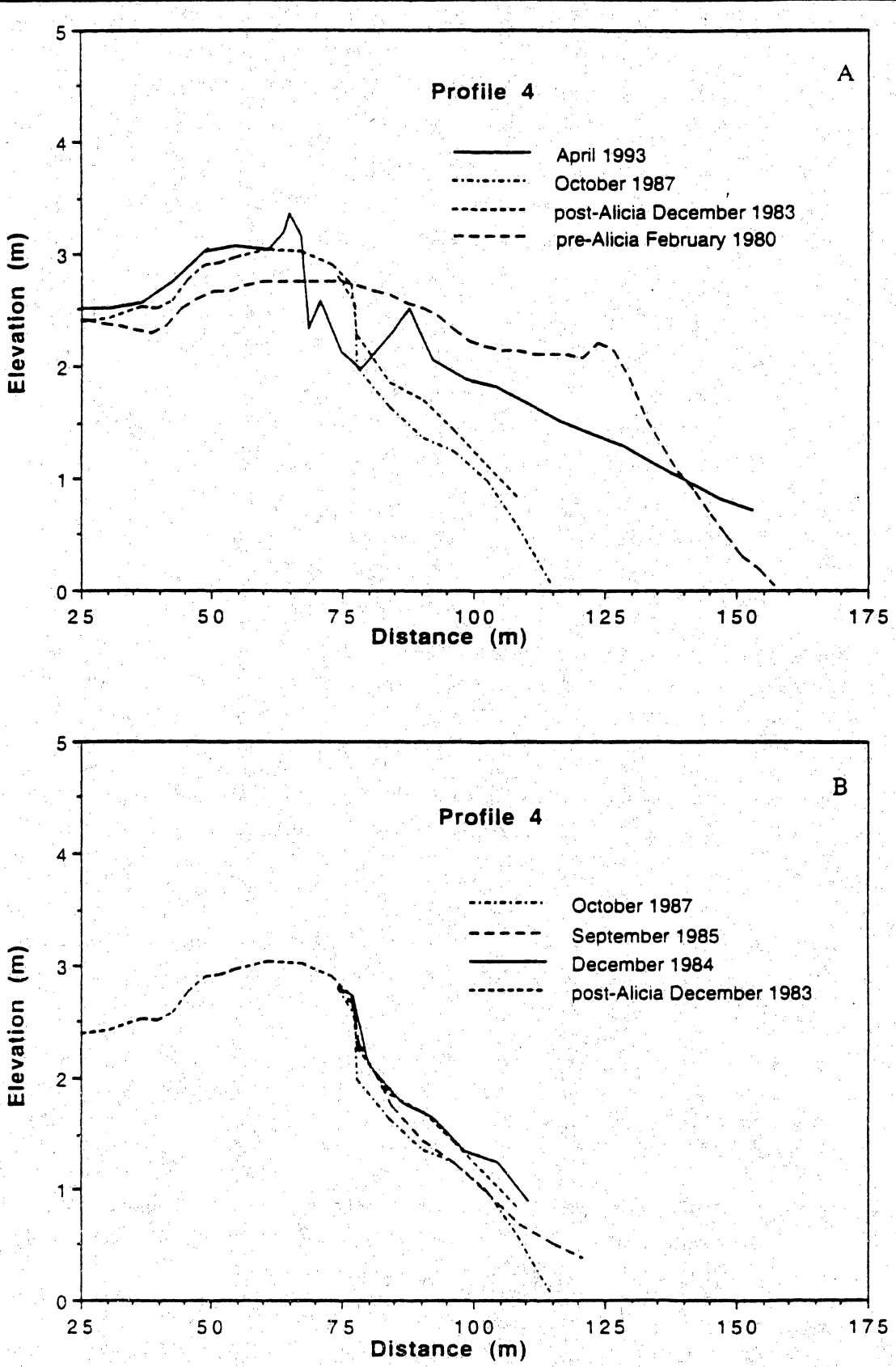

Figure 8. Summary of beach changes at Profile 4 from (A) 1980 to 1993 and (B) 1983 to 1987.

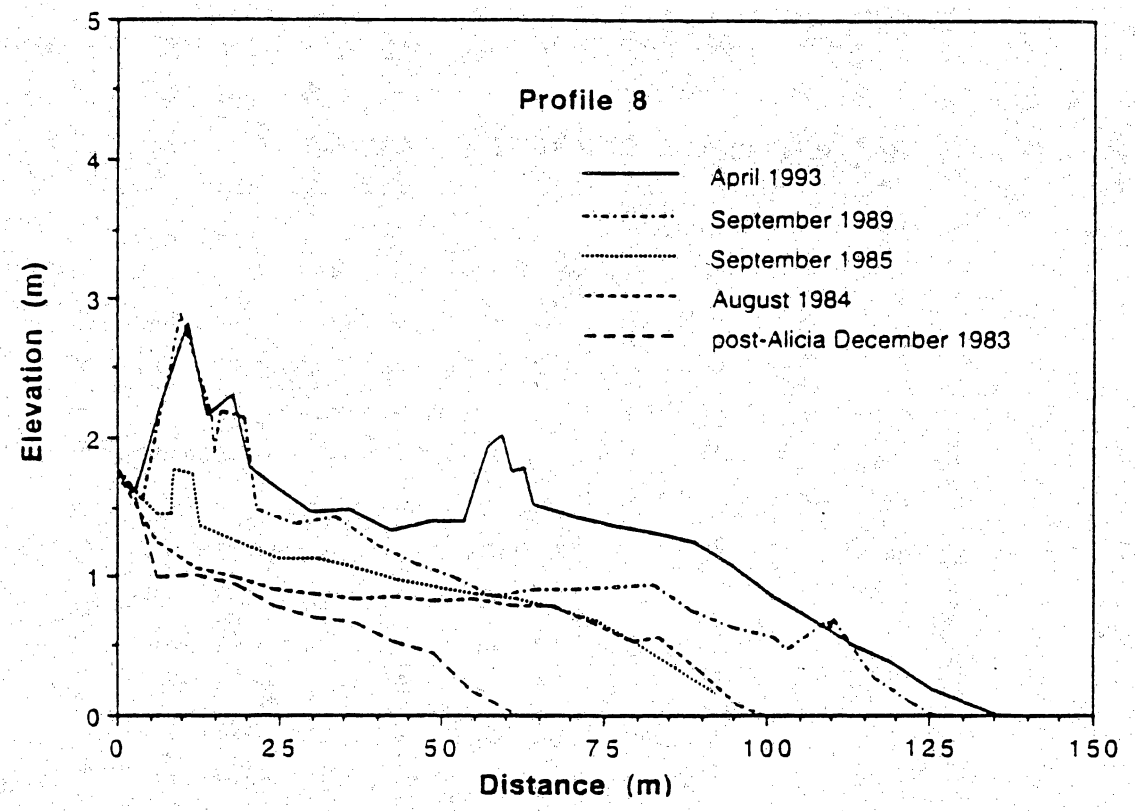

Figure 9. Summary of beach changes at Profile 8 from 1983 to 1993.

post-Alicia profiles were steep and both had similar concave shapes. Recent sand deposition has constructed a flatter beach profile (Figure 8A). Despite the recent accumulation of sand at Profile 4, there has been a net loss of sand and erosion of the beach since 1980, and the profile has not recovered even to the post-Alicia position. Approximately 40% of the volume of sand eroded by Alicia is still missing from the profile (Table 1).

Profile 8 (Follets Island)

Profile 8 represents a long undeveloped beach on the northeastern end of Follets Island (Figure 1). Before Hurricane Alicia crossed the coast, the long-term average rate of beach erosion at Profile 8 was about 4.4 m/yr. The trend immediately preceding the storm (1974–1982) was slight accretion that averaged about 2.1 m/yr (PAINE and MORTON, 1989).

During the first post-storm year the berm at Profile 8 was reconstructed and the forebeach rapidly advanced more than 30 m (Figure 9). Also a minor amount of wind-blown sand accumulated at the base of the erosional escarpment, but backbeach elevations remained at the same level as after Alicia. During the second post-storm winter (1984), sand eroded from the forebeach was deposited on the backbeach, raising backbeach elevations about 0.3 m. Later in the second post-storm year, some sand was deposited on the backbeach, as low dunes above the erosional escarpment, and on the forebeach, causing forebeach accretion.

Sand continued to accumulate on the forebeach, backbeach, and dunes. By the sixth post-storm year (1989), the dune ridge was 1.5 m high and 25 m wide at the base (Figure 9). The backbeach continued to aggrade while the berm crest and forebeach positions remained stable. The most recent (1993) volumetric changes involved a row of secondary sand dunes that formed on the backbeach about 35 m seaward of the primary foredunes (Figure 9).

An accurate pre-storm survey at Profile 8 is unavailable for determining net changes since 1980. Nevertheless, the morphology of the beach and sand volume added since Alicia indicate that much more sand has accumulated at the site than was eroded by the storm. Since 1983, more than 95 m^3/m has been deposited on the beach at Profile 8. This represents more sand deposition than at any other profile site including Profile 3 where 88 m^3/m of sand accumulated.

POST-STORM HISTORIES OF UNDEVELOPED AND DEVELOPED BEACHES

For purposes of this study, beach recovery is defined as the systematic accumulation of sand across the beach profile for at least two consecutive annual monitoring periods. Some of the many factors that influence the rate and degree of beach recovery are as follow: the degree of storm damage, subsequent storm history, long-term beach mobility, season of the storm, subsequent rainfall and extreme temperatures, and human alteration of the coastal processes. Where sand is abundant and shorelines are either stable or accreting, the beach and vegetation line will eventually return to their pre-storm positions. Conversely, where sand supply is deficient and shorelines are undergoing long-term erosion, the beach and vegetation line will not recover entirely. In fact on highly erosional coasts, the vegetation line may remain in its most landward position until the next erosional event causes further landward retreat.

Morphological Versus Volumetric Recovery

Post-storm beach recovery can be evaluated in terms of losses and gains in sand volume or in terms of pre- and post-storm positions of morphological features. Ideal complete recovery of an eroded beach would include replacing the volume of sand eroded from the beach and restoring the positions of the shoreline, berm crest, and vegetation line to their pre-storm positions. It is possible for the beach to recover the eroded volume of sand but still undergo profile retreat. It is also possible for some morphological features to return to their pre-storm positions without the beach regaining the entire volume of sand eroded by the storm.

Recovery of Undeveloped Beaches

The variability in beach responses at different sites along undeveloped beaches was analyzed by comparing profile histories for the entire period of record (Figure 10 and Table 1). This analysis reveals that beach sites only a few kilometers apart can experience completely different post-storm responses even though wave energy and tidal range at all sites are essentially uniform. The four post-storm beach responses recognized are continuous erosion, partial volumetric recovery, complete volumetric recovery, and excess morphological and volumetric recovery.

Continuous Erosion

One beach site (Profile 4) experienced nearly continuous morphological erosion and loss of sand volume for the first five years following Hurricane Alicia (Figure 10, Table 1). Recovery at Profile 4 was negligible for the first two years, and the erosional escarpment continued to retreat as the beach underwent cycles of minor deposition and erosion. This profile accumulated only a small volume of sand during the first two quarters after the storm (5.5%) when all the other profiles were making large gains. Also maximum erosion volume at this site exceeded the Alicia erosion volume by 40%, and the period of greatest erosion (1987–1988) corresponded with the period of maximum sand accumulation at most other sites (Figure 10, Table 1). Because the beach and shoreface at Profile 4 have a long history of severe erosion, it is unlikely that this beach segment will ever fully recover from Hurricane Alicia even during those periods when sand shoals become attached to the beach and the shoreline rapidly accretes.

Partial Volumetric Recovery

Most of the beach profile sites (1, 2, 7, and 5) experienced initial recovery of at least 40% before they began eroding (Figure 10, Table 1). The potential for complete morphological and volumetric recovery at any of those sites is negligible. However, Site 7 has the potential to recover additional sand volume because it is downdrift from Sites 1 and 2 and receives some of the sand released to the littoral drift system by erosion at those sites.

Complete Volumetric Recovery

Only profile Site 3 on Galveston Island recovered as much sand as was eroded by Alicia (Figure 10, Table 1). Complete volumetric recovery was achieved four years after the storm. The beach segment eroded for two years and again gained volume for three years. Considering the beach width and position of the stable dune ridge, it is unlikely that this beach segment will achieve morphological recovery before another storm causes

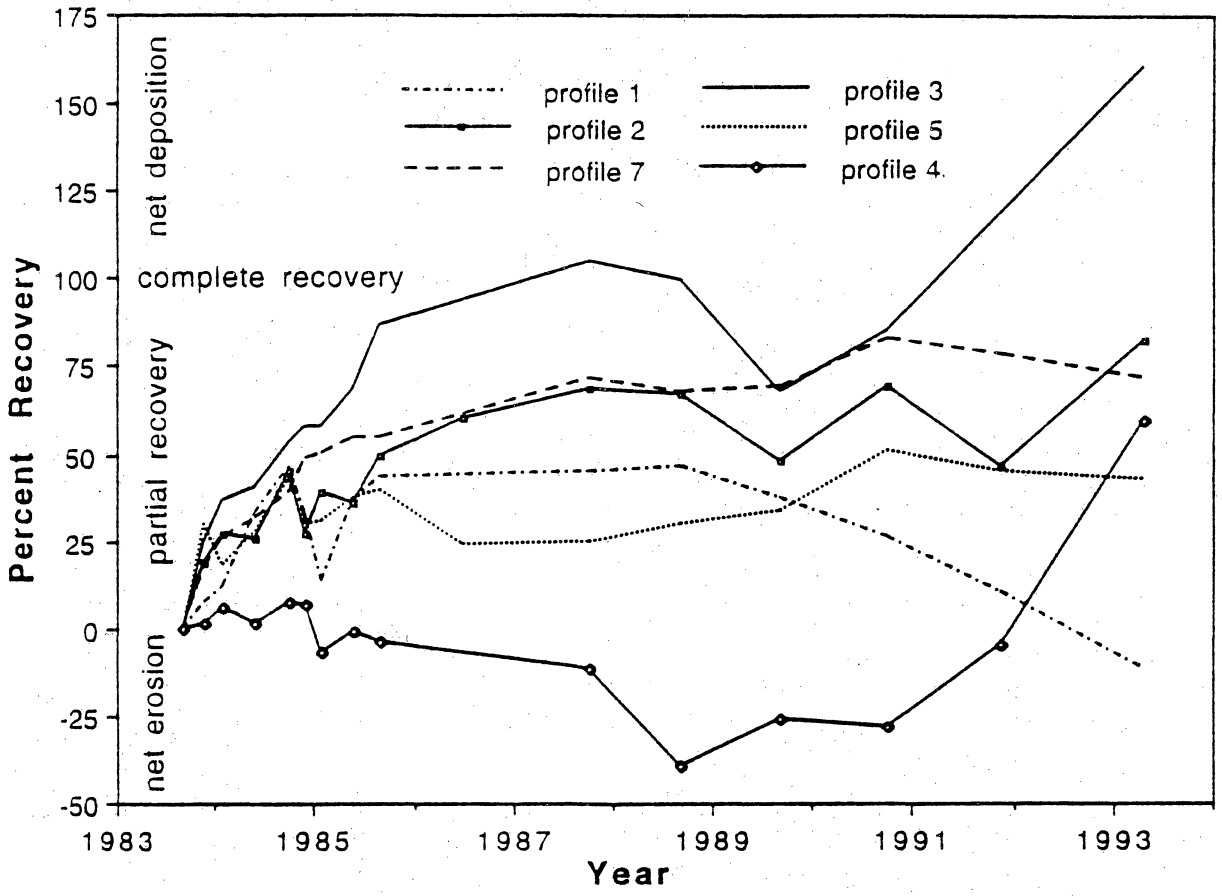

Figure 10. Cumulative beach recovery at each profile site expressed as a percent of total sand eroded by Hurricane Alicia.

significant erosion and resets the schedule of recovery.

Excess Morphological and Volumetric Recovery

The Follets Island profile site (Profile 8) has experienced nearly continuous accretion and seaward advancement of morphological features since Hurricane Alicia (Figure 9). Although the degree of storm erosion at this site is unknown, it is clear that both morphological and volumetric beach recovery have exceeded the losses caused by Alicia.

The gains in sand volume at Profile 8 have alternated among the forebeach, backbeach, and dunes. Initial deposition was almost entirely on the forebeach (Figure 9, 1983 to 1984). Then the forebeach became stable while sand was deposited in the backbeach and low dunes began to form (1984 to 1985). The next period of deposition involved accretion of the forebeach and berm crest as well as formation of a dune ridge (1985 to 1989). Most recently the dune ridge and forebeach have remained stable while the backbeach has aggraded (1989 to 1993).

Recovery of Developed Beaches

Monitoring developed beaches was intentionally avoided to eliminate the bias created by artificial manipulations of the beach profile that both hinder and promote beach recovery. Despite the absence of profile sites in developed areas, field observations and air photo interpretations confirm the striking differences in beach recovery between developed and undeveloped segments of West Beach, Galveston Island.

Forebeach recovery in both developed and undeveloped areas was similar because filled lots located in the backbeach did not interfere with post-storm deposition of the berm. Recovery of the backbeach and dunes, however, was impeded by the houses and filled lots. Measuring beach widths at unaltered lots within subdivisions showed that artificial dunes, sand fences, and other obstructions were placed 25 to 40 m seaward of the natural post-storm vegetation line (MORTON and PAINE, 1985). In some areas these distances constitued nearly half of the natural beach width. At most of the developed beach sites, the first row of houses is located where natural sand dunes

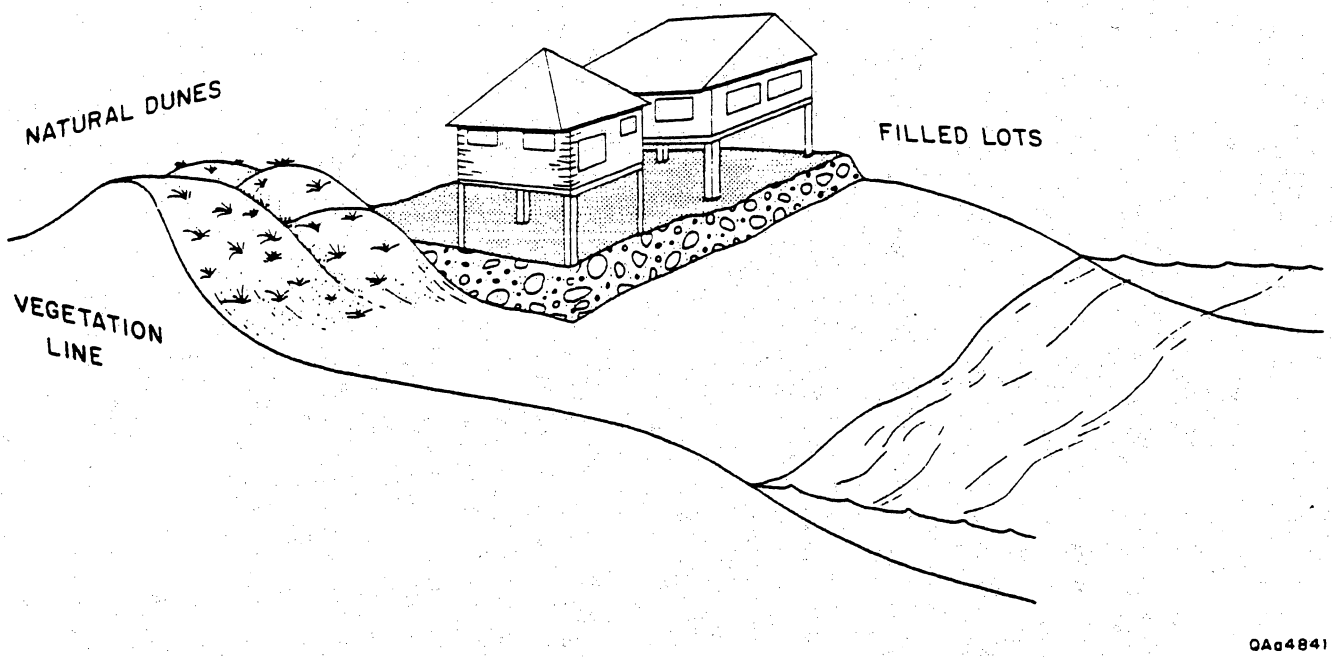

Figure 11. A sketch illustrating post-storm beach morphology in developed and undeveloped areas. Note the position of beach houses seaward of the post-storm dunes and natural vegetation line.

formed on adjacent undeveloped beaches (Figure 11). Nearly ten years after Hurricane Alicia, natural dunes have not formed where the beach is artificially narrowed. Houses and filled lots occupy much of the backbeach, which is the source of sand for dune construction. The developed lots reduced the effective fetch of wind blowing across dry sand and prevented eolian transport that is necessary for dune accumulation.

Cumulative West Beach Recovery

The phases and magnitude of beach recovery since Hurricane Alicia along the West Beach of Galveston Island are revealed by integrating profile data along the shoreline (Figure 12, Table 1). The most significant period of recovery was the first post-storm year when about 40% of the eroded sand returned to the entire beach. Recovery during the next three years was much slower, and only added another 10%, bringing the total recovery to about half the volume lost during the storm. This period of slow recovery was followed by two years of net erosion (1988 and 1989) when the net recovery was reduced to about 45% (Figure 12, Table 1). The last four years of beach monitoring recorded cycles of deposition and erosion with greater deposition resulting in a net accumulation of sand.

After a post-storm period of nearly ten years, the volume of sand on West Beach was about 80% of the volume before Hurricane Alicia. This beach recovery plus the washover sand stored on the barrier flat, accounts for about 92% of the sand eroded from West Beach. The most recent net gains in sand volume along West Beach (Figure 12) are attributed largely to the sand deposited on the forebeach at profile site 4 near San Luis Pass and in the dune ridge at profile site 3 (Table 1).

STAGES OF BEACH RECOVERY—UNDEVELOPED BEACHES

The individual histories of beach response at each profile site provide a basis for recognizing the sequential stages of beach recovery (Figure 13). Profile histories also reveal the duration of beach recovery at each site and the times when the beach was reacting to forces that disrupted the cycle of recovery. By analyzing both synoptic and sequential beach behavior at each profile site, we were able to synthesize the temporal variations in beach morphology and sand volume along a microtidal, moderate wave energy coast.

Stage 1: Berm Reconstruction and Forebeach Accretion

The first stage of beach recovery (Figure 13) begins immediately after the storm-wave energy

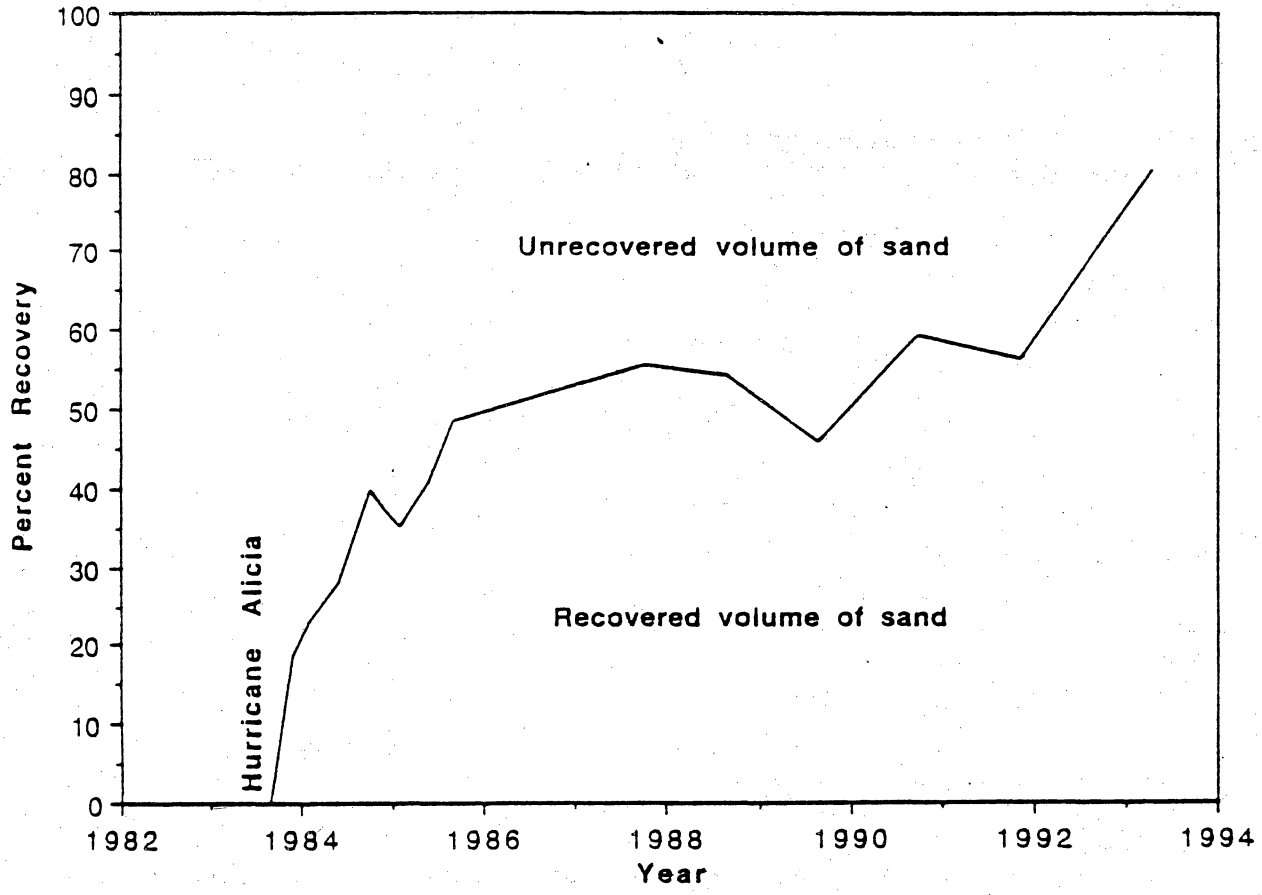

Figure 12. Cumulative recovery of West Beach, Galveston Island, expressed as a percent of total sand eroded by Hurricane Alicia.

wanes and sand from the bar system begins moving ashore (SALLENGER *et al.*, 1985). It lasts from a few months to as much as a year and is characterized by berm reconstruction and steepening of the forebeach (Figures 3, 5, 6, and 9). Stage 1 recovery primarily involves onshore transport of sand that was stored directly offshore in the bars and on the upper shoreface. The sand is redeposited by wave runup on the frequently wetted part of the forebeach and by landward bar migration on the subaqueous part of the profile. Stage 1 recovery progresses relatively rapidly as the equilibrium forebeach configuration is reestablished with the return of a large volume of sand. This earliest phase of recovery is reported frequently in the literature regardless of how severe the beach is eroded: the long-term mobility of the beach, its profile shape, or the eventual degree of recovery. Stage 1 recovery is common for most sand beaches because all the sand eroded from the forebeach, backbeach, and dunes is available just for forebeach reconstruction.

Following the initial recovery phase, morphologies of the backbeach, berm crest, and forebeach are generally similar to those of pre-storm conditions. It is for this reason that observers of post-storm conditions commonly report rapid recovery of the beach because the shoreline quickly returns to its pre-storm position. Rapid accretion of the shoreline can be a misleading indicator of beach recovery because backbeach elevations are commonly lower than those before the storm. This failure to attain pre-storm backbeach elevations is attributed to the height of subaqueous deposition, which is controlled by the limit of wave runup and spring high-tide water levels.

Stage 2: Backbeach Aggradation

The second stage of beach recovery mostly involves subaerial deposition. The predominant nearshore processes operating at this stage are minor flooding of the backbeach and eolian transport that promote accumulation of sand at and just seaward of the erosional escarpment (Figure 13). In the northern Gulf of Mexico, moderately high winter waves associated with the passage of

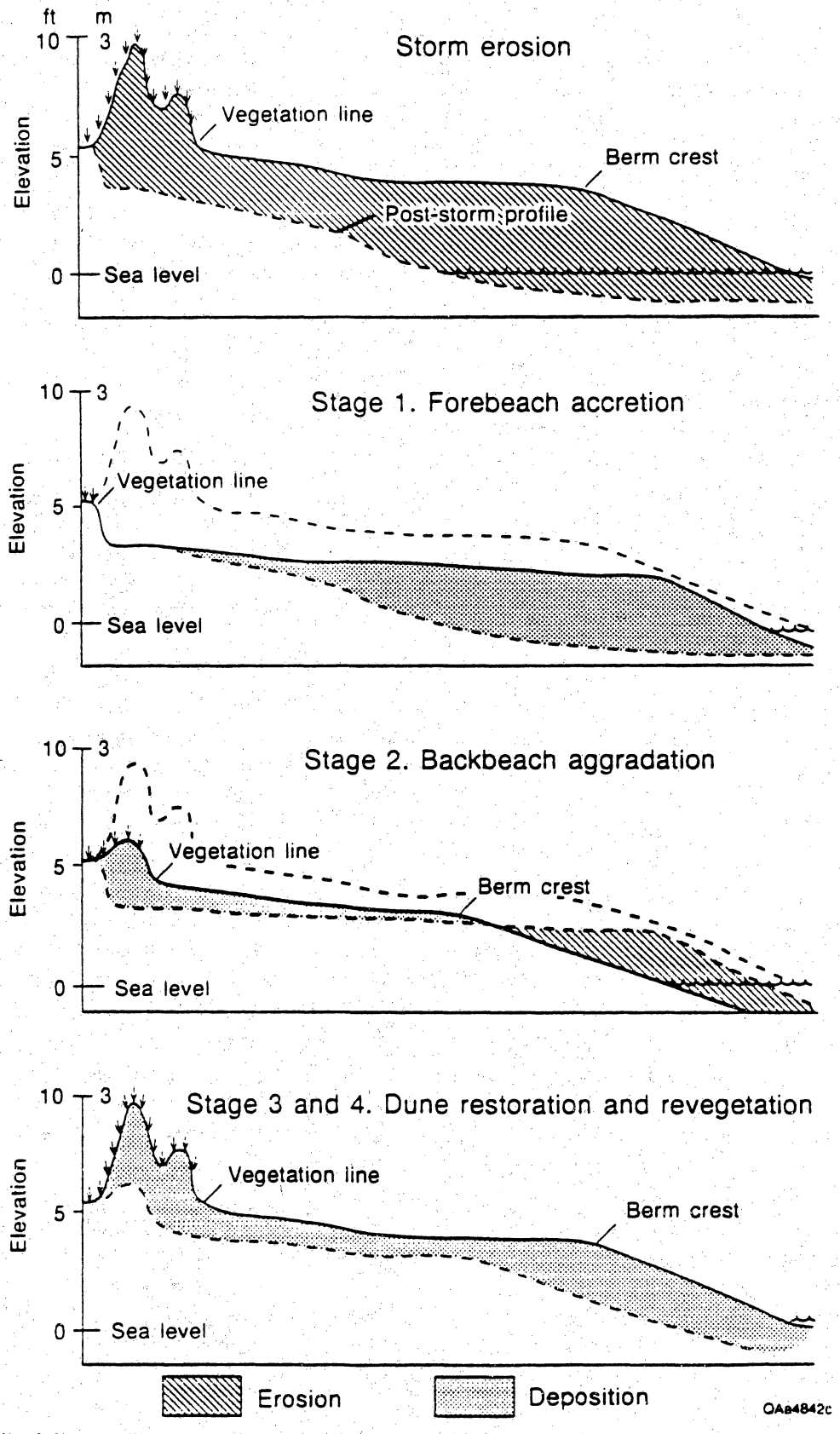

Figure 13. Generalized diagram illustrating the stages of post-storm beach recovery.

landward and seaward. Sand removed from the forebeach and deposited in the backbeach creates a high storm berm crest and increases the backbeach elevation. After these moderate-energy events, low-energy waves drive bars ashore forming a lower berm crest and reestablishing the forebeach. The raised backbeach elevations and reduced frequency of saltwater flooding of the backbeach encourage the formation of incipient dunes.

Stage 2 recovery normally begins during the second post-storm summer along coasts that have limited eolian transport and severe storm damage. This is because eolian accumulation is a function of beach width and elevation, and backbeach elevations must exceed the limits of flooding produced by normal spring high tide before significant eolian accumulation will begin. The quarterly beach profiles indicate that minimum beach widths and elevations of 50 m and 1.5 m, respectively, are necessary before eolian sand accumulation is significant and before the beach recovery progresses from Stage 2 to Stage 3.

Stage 3: Dune Formation

The second and third phases of beach recovery are gradational since they both involve subaerial deposition in the backbeach. The difference is that Stage 2 recovery processes involve sand transported by a combination of water and wind, whereas, Stage 3 emphasizes the accumulation of wind-blown sand that obscures the former erosional escarpment and wave cut dunes (Figure 13). Isolated clumps of opportunistic vegetation and debris stranded by abnormally high tides create wind shadows that promote the accumulation of low sand mounds on the backbeach. Reestablishing backbeach vegetation is critical to dune growth because the plants accelerate eolian accumulation by trapping sand, which in turn stimulates new plant growth (DAHL and GOEN, 1977). The low discontinuous hummocky mounds of sand scattered along the backbeach eventually coalesce and form low, sparsely vegetated incipient dunes. These incipient dunes grow and merge to become a more continuous foredune ridge.

The rate at which dune and backbeach vegetation is reestablished depends on the extent of ground cover before the storm and the depth of scour, which determines the survival of grass roots

minor, but roots are preserved below the depth of scour. Under these conditions, vegetation is quickly reestablished as new plant leaves emerge from old plant roots on the backbeach at the beginning of the first post-storm spring. But on severely eroded beaches such as West Beach after Alicia, where ground cover is sparse and scour is great, the grass roots and rhizomes are destroyed and vegetation recovery is slow. When dune and backbeach root systems are eliminated, recolonization by perennial vegetation is necessary to advance the vegetation line. Under these extreme conditions, vegetation recolonization takes several years and extends from the upland areas and dunes onto the backbeach.

Stage 4: Dune Expansion and Vegetation Recolonization

The transition between beach recovery Stages 3 and 4 is also gradational, and the respective stages are distinguished by the extent of vegetative ground cover and the sizes of newly created dunes. Stage 3 dunes are small, isolated, and barren, and the backbeach is sparsely vegetated. Stage 4 dunes are taller, wider, continuous, and more densely vegetated. On wide post-storm beaches, such as West Beach after Hurricane Alicia, the area of optimum dune growth may be slightly seaward of the erosional escarpment. Topographic lows between the erosional escarpment and new dunes may be partly filled with eolian and washover deposits, or they may be preserved as freshwater swales. In either case, increases in vegetative cover accompany dune growth as salt-tolerant plants stabilize the barren sand and cause sparsely vegetated areas to become overgrown with dense continuous vegetation. Plant colonization and infilling eventually advance the line of continuous vegetation seaward. This period of dune expansion and vegetation recolonization constitutes the fourth stage of recovery.

Whether or not the pre-storm vegetation line is reestablished depends on both the volumetric and morphological recovery of the beach (Figure 13). If the pre-storm profile and positions of morphological features are not reoccupied, then the vegetation line will not return to its pre-storm position. On West Beach of Galveston Island ten years after Hurricane Alicia, the natural vegetation line at the site where the most dune sand has

accumulated (Profile 3) has migrated only about 25 m seaward of the Alicia escarpment. This advanced position of the vegetation line is still about 15 m landward of its pre-Alicia position resulting in a net landward retreat of the vegetation line (Figure 6).

Forebeach Morphology and Beach Recovery

The shape of the forebeach is a leading indicator of the stage and completeness of beach recovery. During Stage 1, the forebeach and backbeach are separated by a well defined berm crest that gives the beach a pronounced convex morphology (Figures 3B, 4B, 5B, 6B, and 8). This profile configuration may last for several years until the beach begins to adjust to long-term sand deprivation and again experiences the effects of long-term erosion. At that time, the berm crest is eliminated and the beach assumes an overall concave morphology. Each of the profiles that did not recover completely from Hurricane Alicia have changed shapes from convex to concave (Figures 3, 4, 5, and 7). An exception to this general observation is Profile 4, which continued to erode during the post-storm recovery period and has never developed a convex profile (Figure 8). Only the beaches that have completely recovered or surpassed the losses of Alicia (Profiles 3 and 8) have maintained a convex forebeach morphology for the entire post-storm monitoring period (Figures 6 and 9).

CONCLUSIONS

Microtidal wave-dominated sand beaches generally recover from storm erosion in four time-dependent stages (Figure 13). Whether or not the beach completely returns to its pre-storm shape partly depends on completion of each preceding stage. The first stage of recovery involves onshore transport of sand, berm reconstruction, and forebeach accretion. Even severely eroded beaches commonly experience rapid forebeach accretion during this recovery phase. A large volume of sand rapidly returns to the forebeach because the great volume of sand temporarily stored on the upper shoreface is out of equilibrium with the normal beach and upper shoreface profile. Advancement of the shoreline within weeks or months gives the appearance that the beach has recovered when actually less than half the eroded sand may have returned. Beach recovery is incomplete at this stage, although it is commonly inferred to be complete because the shoreline typically returns to its pre-storm position. At the end of stage one, beach shape is commonly similar to that before the storm, but backbeach elevations may be lower than those before the storm. For this reason, anecdotal reports of rapid post-storm beach recovery should be questioned unless confirmed by comparison of backbeach and dune elevations surveyed before and after the storm.

The second stage of recovery is characterized by eolian processes and minor flooding of the backbeach that promote accumulation of sand seaward of the vegetation line. This onshore transfer of sand is accomplished by abnormally high waves that erode the forebeach and deposit sand in the backbeach. Transfer of sand from the forebeach to the backbeach during winter storms was also reported by SONU and VAN BEEK (1971) for a beach in North Carolina.

The second and third stages of recovery are transitional as low dunes form in the backbeach or the foredune ridge is reestablished. Eventually the backbeach becomes a zone of minor deflation or aggradation, but it also becomes a surface of sand bypass to the dunes. A minimum width of dry beach is necessary for dunes to form and this prerequisite prevented dunes from reforming on developed beaches of Galveston Island. There beach houses occupy the backbeach and block the eolian transport of sand.

Plant colonization of the dunes and seaward advancement of the vegetation line constitute the fourth and final stage of post-storm beach recovery (Figure 13). This last stage of recovery occurred only at undeveloped beaches in the study area.

On Galveston and Follets Island the post-Hurricane Alicia recovery phase lasted about four years before the beach at several profile sites began behaving differently. Post-storm beach responses ranged from no recovery to nearly continuous erosion or accretion depending on local sediment flux. Considering both volumetric and morphologic criteria, only the Follets Island site (Profile 8) recovered completely after Hurricane Alicia. Volumetric and morphologic beach recovery was incomplete at five of the seven profile sites even ten years after the storm. At the two sites where post-storm deposition surpassed storm erosion, the excess sand was stored primarily in the foredunes. Greatest losses and gains in beach volume occurred at sites adjacent to a tidal inlet sug-

ble for those large beach changes.

ACKNOWLEDGEMENTS

This work was partly supported by grants from the U.S. Geological Survey Coastal Geology Program and the State of Texas Office of the Attorney General. We thank David Adilman, Jim DiGiulio, and Cynthia Jennings, who assisted in collecting and formatting the profile data.

LITERATURE CITED

BERNARD, H.A.; MAJOR, C.F., JR.; PARROTT, B.S., and LEBLANC, R.J., SR., 1970. Recent sediments of Southeast Texas, A field guide to the Brazos alluvial and deltic plains and the Galveston Barrier island complex. *Geology Guidebook 11.* The University of Texas at Austin: Bureau of Economic Geology, 132p.

BIRKEMEIER, W.A.; BICHNER, E.W.; SCARBOROUGH, B.L.; MCCONATHY, M.A., and EISER, W.C., 1991. Nearshore profile response caused by Hurricane Hugo. *In:* FINKL, C.W., Jr. and PILKEY, O.H., Jr. (eds.), Impacts of Hurricane Hugo, September 10–22, 1989. *Journal of Coastal Research,* Special Issue 8, 113–127.

DAHL, B.E. and GOEN, J.P., 1977. Monitoring foredunes on Padre Island, Texas. *Miscellaneous Report No. 77-8.* U.S. Army Corps of Engineers, Coastal Engineering Research Center, Fort Belvoir, Virginia, 69p.

ELIOT, I.G. and CLARKE, D.J., 1989. Temporal and spatial bias in the estimation of shoreline rate-of-change statistics from beach survey information. *Coastal Management,* 17, 129–156.

EMERY, K.O., 1961. A simple method of measuring beach profiles. *Limnology and Oceanography,* 6, 90–93.

FINKL, C.W., JR. and PILKEY, O.H., JR., 1991. Impacts of Hurricane Hugo, September 10–22, 1989. *Journal of Coastal Research* Special Issue 8, 356p.

GORNITZ, V. and LEBEDEFF, S., 1987. Global sea level changes during the last century. *In:* NUMMEDAL, D.; PILKEY, O.H., JR., and HOWARD, J.D. (eds.), Sea-level fluctuation and coastal evolution. *Society of Economic Paleontologists and Mineralogists Special Publication 41,* 3–16.

KATUNA, M.P., 1991. The effects of Hurricane Hugo on the Isle of Palms, South Carolina: From destruction to recovery. *In:* FINKL, C.W., JR. and PILKEY, O.H., JR. (eds.), Impacts of Hurricane Hugo, September 10–22, 1989. *Journal of Coastal Research,* Special Issue 8, 263–273.

KRIEBEL, D.L. and DEAN, R.G., 1985. Numerical simulation of time-dependent beach and dune erosion. *Coastal Engineering,* 9, 221–245.

LARSON, M.; KRAUS, N.C., and BYRNES, M.R., 1990. SBEACH: Numerical model for simulating storm-induced beach change, Report 2, Numerical formulation and model tests. *Technical Report CERC 89-9.* U.S. Army Engineer Waterways Experiment Station, Vicksburg, Mississippi.

LEE, G. and BIRKEMEIER, W.A., 1993. Beach and nearshore survey data: 1985–1991 CERC Field Research Facility. *Technical Report 93-3.* U.S. Army Engineer Waterways Experiment Station, Vicksburg, Mississippi.

LYLES, S.D.; HICKMAN, L.E., JR., and DEBAUGH, H.A., JR., 1988. *Sea Level Variations for the United States 1855–1986.* Rockville, Maryland: U.S. Department of Commerce, National Ocean Service, 182p.

MORTON, R.A., 1979. Temporal and spatial variations in shoreline changes and their implications, examples from the Texas Gulf Coast. *Journal of Sedimentary Petrology,* 49, 1101–1112.

MORTON, R.A., 1988. Nearshore responses to great storms. *In:* CLIFTON, H.E. (ed.), Sedimentologic consequences of convulsive geologic events. *Geological Society of America Special Paper 229,* 7–22.

MORTON, R.A. and PAINE, J.G., 1985. Beach and vegetation-line changes at Galveston Island, Texas—Erosion, deposition, and recovery from Hurricane Alicia. *Geological Circular 85-5.* The University of Texas at Austin: Bureau of Economic Geology, 39p.

PAINE, J.G., 1993. Subsidence of the Texas coast: Inference from historical and late Pleistocene sea levels. *Tectonophysics,* 222, 445–458.

PAINE, J.G. and MORTON, R.A., 1989. Shoreline and vegetation-line movement, Texas Gulf Coast, 1974 to 1982. *Geological Circular 89-1.* The University of Texas at Austin: Bureau of Economic Geology, 50p.

RITCHIE, W. and PENLAND, S., 1988. Rapid dune changes associated with overwash processes on the deltaic coast of south Louisiana. *Marine Geology,* 81, 97–122.

SALLENGER, A.H.; HOLMAN, R.A., and BIRKEMEIER, W.A., 1985. Storm-induced response of a nearshore-bar system. *Marine Geology,* 64, 237–257.

SEXTON, W.J. and HAYES, M.O., 1991. The geologic impact of Hurricane Hugo and post-storm shoreline recovery along the undeveloped coastline of South Carolina, Dewees Island to the Santee Delta. *In:* FINKL, C.W., JR. and PILKEY, O.H., JR. (eds.), Impacts of Hurricane Hugo, September 10–22, 1989. *Journal of Coastal Research,* Special Issue 8, 275–290.

SONU, C.J. and VAN BEEK, J.L., 1971. Systematic beach changes on the Outer Banks, North Carolina. *Journal of Geology,* 79, 416–425.

SWANSON, R.L. and THURLOW, C.L., 1973. Recent subsidence rates along the Texas and Louisiana coasts as determined from tide measurements. *Journal of Geophysical Research,* 78, 2665–2671.

U.S. ARMY CORPS OF ENGINEERS, 1980. *Report on Hurricane Allen, 3–10 August 1980.* Galveston District Corps of Engineers, 62p.

U.S. ARMY CORPS OF ENGINEERS, 1983. *Report on Hurricane Alicia, August 15–18, 1983.* Galveston District Corps of Engineers, 185p.

WARNKE, D.A.; GOLDSMITH, V.; GROSE, P., and HOLT, J.J., 1966. Drastic beach changes in a low-energy environment caused by Hurricane Betsy. *Journal of Geophysical Research,* 71, 2013–2016.

WHITE, W.A.; CALNAN, T.R.; MORTON, R.A.; KIMBLE, R.S.; LITTLETON, T.G.; MCGOWEN, J.H.; NANCE, H.S., and SCHMEDES, K.E., 1985. *Submerged Lands of Texas, Galveston-Houston Area: Sediments, Geochemistry, Benthic Macroinvertebrates, and Associated Wetlands.* The University of Texas at Austin: Bureau of Economic Geology, 145p.

ZEIGLER, J.M.; HAYES, C.R., and TUTTLE, S.D., 1959. Beach changes during storms on outer Cape Cod, Massachusetts. *Journal of Geology*, 67, 318–336.

Addendum 4. Meso-Scale Transfer of Sand during and after Storms: Implications for Prediction of Shoreline Movement

MESO-SCALE TRANSFER OF SAND DURING AND AFTER STORMS: IMPLICATIONS FOR PREDICTION OF SHORELINE MOVEMENT

Robert A. Morton, James C. Gibeaut, and Jeffrey G. Paine

Bureau of Economic Geology

The University of Texas at Austin

Box X, University Station

Austin,Texas 78713

ABSTRACT

Monitoring beach volume changes of the Texas Coast following a major hurricane reveals the impact of storms on sand dispersal and shoreline movement at spatial and temporal scales encompassing tens of kilometers and decades. Beach volume histories at profile sites show the interdependence of sand exchange among adjacent sites and the spatial autocorrelation of sand movement. Beach volume histories also indicate periods when either longshore or cross-shore transport predominate and illustrate the long-term effects of coastal structures on beach mobility.

This study confirms that net losses of sand from updrift barriers may not be directly linked with net gains of sand on adjacent downdrift barriers. Instead, sand dispersal within a coastal compartment may depend partly on the dynamics of shoals and temporary sand storage at the intervening tidal inlet. In our study, sand eroded from the updrift barrier (Galveston Island) is deposited in a terminal sand flat of the barrier, whereas sand accreted to the downdrift barrier (Follets Island) is derived from the intermediate ebb-tidal delta (San Luis Pass). Unlike continuous sand bypassing on some microtidal, wave-dominated coasts, sand bypassing at San Luis Pass is episodic, event driven, and inefficient, and sand is not transferred directly from one barrier to the next.

Because storms rapidly redistribute beach sediment, they can be the most important factor controlling short-term (< 10 yr) shoreline movement where natural replenishment of beach sand depends entirely on updrift erosion. Large-volume, nearly instantaneous sand transport during storms can locally accelerate rates of shoreline change or reverse the trend of beach movement, thereby significantly altering projected shoreline positions even ten years into the future. Future storms will probably have even greater impact on coastal sand budgets and beach mobility as natural sources of beach sand are eliminated or become unavailable to replenish beaches.

INTRODUCTION

Erosion of beaches, dunes, and bluffs is becoming the most important source of sand to many downdrift beaches as primary sand sources such as rivers, offshore bars, and tidal deltas are depleted or their contributions to local sediment budgets are artificially reduced. Large-scale, long-term mobility of sandy shores is also partly controlled by intense storms that transport large volumes of sand moderate distances in brief periods. During these high-energy events, the balance of sand supply to nearby beaches is altered dramatically, and it is difficult to predict the sites of post-storm erosion or deposition or to anticipate sand redistribution across the beach and shoreface profile. Consequently, the ability to model and predict future shoreline positions based on short-term data (< 10 yr) may be seriously impaired (Morton, 1991; Fenster et al., 1993).

This study evaluates the impacts of storms on subaerial sand distribution and subsequent shoreline movement at spatial and temporal scales encompassing tens of kilometers and decades. We document volumetric gains and losses along two barrier islands of the Texas Gulf Coast that are separated by a tidal inlet, interpret the longshore patterns of post-storm erosion and deposition, evaluate the efficiency of sand bypassing at a tidal inlet, and relate post-storm beach responses to the historical trends of shoreline movement and to observed changes in sand supply.

Beach and shoreface volumes are difficult to quantify because much of the dynamic profile is subaqueous and seldom is the subaqueous zone of negligible sediment flux measured by repeated beach surveys. Subaerial beach changes represent only a small fraction of the total volumetric changes across the beach and shoreface. Nevertheless, as demonstrated by Aubrey (1979) and many others, storage and release of sand from the subaerial beach should be a primary indicator of shoreface processes and the availability of sand in the littoral drift system. This condition applies to the study area, which is a partly confined coastal compartment where the regional littoral drift system is blocked by large impermeable structures and where the downdrift transport of sand supplied by beach and shoreface erosion is the only source of sediment for natural beach maintenance. This physical setting constrains the sediment dispersal analysis by eliminating external sources of sand, and focuses on the longshore and cross-shore redistribution of sand that was available in the beach/shoreface system prior to the storm.

STUDY AREA

The study area encompasses a 40 km stretch of sandy barrier-island beach extending from the southwestern end of the Galveston Island seawall to northeastern Follets Island, Texas Gulf Coast (Fig. 1). These barriers have elongate, linear morphologies that characterize micro-tidal, wave-dominated coasts in temperate climates (Hayes, 1979). Ebb-tidal deltas are minor features of these coasts and because the ebb deltas are volumetically much smaller than the barriers, their dynamics have only local effects on adjacent barrier shores (FitzGerald, 1988).

In the following discussion, West Beach refers to the continuous sand beach extending from the Galveston seawall to San Luis Pass (Fig. 1). West Beach encompasses about two-thirds of the Galveston Island coastal compartment that extends from the jetties at Bolivar Roads to San Luis Pass. Littoral sand movement northeast of West Beach is restricted by the jetties, a groin field, and absence of a beach seaward of the seawall (Morton and Paine, 1985).

Gulf of Mexico

Long-term meteorological and oceanographic records at Galveston provide an exceptional data base for analyzing sediment transport in the region. Wave energy in the northwestern Gulf of Mexico is generally low to moderate, with most significant wave heights being less than 66 cm. Wave gauge measurements at Galveston show that shallow water waves greater than 1 m high occur less than one percent of the time and storm waves are typically less than 2 m high (U.S. Army Corps of Engineers, 1983). Most waves approach the coast from the southeast resulting in littoral drift to the southwest, but shoreline orientation and seasonal wind patterns cause the littoral drift direction to reverse periodically. Gross littoral drift resulting from bidirectional transport is estimated to be about 200,000 m^3/yr, whereas net drift to the southwest is estimated to be about 45,000 m^3/yr based on wave-energy flux and wind drift calculations (U.S. Army Corps of Engineers, 1983).

Mean diurnal tide range of the Gulf of Mexico at Galveston is 66 cm. Backbeaches are about one meter above sea level and are frequently flooded by abnormally high tides in the spring and late summer as a result of low pressure systems and tropical cyclones in the Gulf of Mexico. The average annual frequency of tropical cyclones crossing the Texas coast is 0.67, or about two storms every three years (Hayes, 1967). Storms that rapidly elevate Gulf water along Galveston and Follets Island and cause at least some beach erosion occur about once every 6 yrs (Morton and Paine, 1985).

Shelf, Shoreface, and Beach Sediments

Modern shelf sediments off Galveston and Follets Island are relatively thin and composed mostly of mud containing some thin, rarely graded layers of sand (Williams et al., 1979; White et al., 1985). Because the inner shelf is covered predominantly with mud, cross-shore fluxes to and from the shelf can be eliminated as important sources of sand for natural maintenance of beaches in the study area. The inner shelf is an important sink for eroded beach sand deposited principally as storm beds that are slowly accumulating in water depths of 10 m or more.

Muddy sediments of the inner shelf merge landward with sandy muds and muddy sands of the lower shoreface (White et al., 1985). A band of shoreface sand approximately 3 km wide parallels the islands and extends from water depths of about 10 m to the intertidal zone. Exceptions to this general sand trend occur at the northeastern end of each island where relatively clean sand extends seaward at least 5 km and merges with the ebb-tidal deltas. Surficial sediments within this band are composed of at least 80 percent fine sand (White et al., 1985). The broad expanse of subtidal sand along the seaward margin of the barriers reflects a sand transport system and nearshore processes that existed before the littoral drift system was altered by construction of long jetties and the Galveston seawall.

The upper shoreface is a dynamic zone of sediment transport and temporary sediment storage where three long and continuous break-point bars are maintained or driven ashore. The first bar forms at the toe of the low tide beach, whereas the third bar is located in water depths of about 3

m. The bars, which are normally about 75 to 100 m apart, migrate onshore and offshore in response to changing wave conditions (Morton 1988a).

Low-tide beaches of Galveston and Follets Island are about 50 to 60 m wide and slope gently toward the Gulf. A low, sometimes indistinct berm separates the broader and flatter backbeach from the narrower and slightly steeper forebeach. As much as 25 m of forebeach is exposed at low tide. The beaches are composed of fine sand except near San Luis Pass where migrating shell lenses can locally alter beach composition and morphology. Beach cusps and other low-amplitude shoreline rhythms are subtle because of the gentle forebeach slope, fine grain size, and low waves. The multiple breaker zones, fine sediment textures, and lack of significant shoreline rhythms produce gently sloping beaches that effectively dissipate wave energy (Wright and Short, 1984).

San Luis Pass

San Luis Pass (Fig. 1) is a stable tidal inlet that carries maximum current velocities of 0.6 to 1.0 m/s during a typical diurnal tidal cycle (Mason, 1981). The inlet margin and channels are delineated by submerged sand shoals that are modified periodically in conjunction with minor fluctuations in relative sea level (Fig. 2). During prolonged droughts, such as in the 1930s and 1950s, lower water levels expose a broad sand platform and inlet-margin shoals at the western tip of Galveston Island and a large ebb shield on the northeastern end of Follets Island. Lower water levels also concentrate tidal flow in the inlet throat, which impinges on the northeastern end of Follets Island. Since the 1960s, slightly higher water levels have submerged the ebb-delta shoals and subjected the beach to wave attack causing substantial beach erosion on the southwestern end of Galveston Island.

High-energy waves and currents periodically obliterate any well-defined shoals outlining the terminal lobes of the ebb delta and these processes construct washover fans and small channels across the broad terminal sand flat of Galveston Island (Fig. 3). The storm-constructed features are eventually modified by normal bay processes and become less distinct with time.

METHODS

Our study integrates repeated beach surveys and airphoto analyses of shoreline changes. The techniques used to investigate shoreline movement from aerial photographs are described by Morton and Paine (1985) and Morton (1991). Beach profiles were measured at seven sites (Fig. 1) using Emery poles (Emery, 1961) or a theodolite and stadia rod, and the profiles were referenced to existing features such as benchmarks and building foundations. The elevation of each reference station was estimated from nearby benchmarks either surveyed by the Corps of Engineers or maintained by the National Ocean Service.

Beach profiles at most of the sites were obtained quarterly for the first two years after Hurricane Alicia (1983) and then about once a year since 1985. Approximately 15 profiles at each site, representing a ten-year period, were used to investigate how storms impact sediment dispersion and subsequent beach recovery. Profile data were transferred to the Interactive Survey Reduction Program (ISRP), which is capable of managing data, checking for errors, adjusting profiles to common datums, and computing profile volumes (Birkemeier and Holme, 1992).

HURRICANE ALICIA

Hurricane Alicia (August 1983) was a minimal category 3 storm (Saffir-Simpson scale) that rapidly crossed the Texas shelf. Its rapid forward progress minimized beach erosion and washover by limiting the duration of beach flooding to a few hours at the peak of the tidal cycle. Beaches of the study area were inundated for only about 10 hrs during Alicia compared to flood durations of about 60 hrs during Hurricane Carla in 1961 and 8 hrs during Hurricane Allen in 1980 (Morton and Paine, 1985). Maximum open-coast surge elevation associated with Alicia was 3.9 m measured at San Luis Pass.

Alicia eroded more than 1.5 million m^3 of sand from the 30 km of West Beach (Morton and Paine, 1985). Beach erosion at profile sites ranged from 51 m^3/m to 73 m^3/m (Table 1) and erosion increased to the southwest toward the site of storm landfall (Fig. 4). Washover deposits on the barrier represented only about 12 percent (186,000 m^3) of the sand eroded from adjacent beaches, and the remaining sand volume (1.32 million m^3) was either transferred to the inner shelf and lost from the littoral drift system or transported along the shoreface to the southwest by strong currents. Sediment samples of the inner shelf collected immediately before and after the storm suggested that most of the sand eroded from Galveston Island was still on the shoreface and had not been deposited farther offshore (Morton, 1988b). Beyond this inference, no data were available to locate the former beach sand or to map its longshore distribution.

Alicia caused the greatest morphological changes at San Luis Pass where the storm crossed over shoals and barren sand flats near sea level. Storm waves and strong onshore winds (maximum wind speed 184 km/hr) constructed a washover fan on the northeast side of the inlet, while a large subaqueous and subaerial sand flat on the southwest side of the inlet was eroded (Fig. 3).

The volume of beach sand eroded from Follets Island during Alicia is unknown because a pre-storm survey was not conducted. Post-storm field observations showed that beach erosion was minor on Follets Island because it was on the side of the storm where ocean surge elevations were reduced and wave energy was dampened by offshore wind. The beach erosion estimate of 35 m^3/m (Table 1) assumes that erosion on Follets Island was less than erosion anywhere on Galveston Island and about half the maximum erosion measured at profiles 4 and 5. Post-storm sand deposition on Follets Island (Table 2) greatly exceeds the maximum storm erosion at any site on Galveston (Table 1); therefore, underestimating the initial beach erosion on Follets Island would not invalidate the conclusions of the study.

LONGSHORE SAND REDISTRIBUTION

Post-Alicia Beach Responses

Post-storm profile adjustments and partial recovery of West Beach after Hurricane Alicia lasted about four years as the onshore transport and storage of sand occurred in four time-dependent stages (Morton et al., 1994). The first stage of recovery, which lasted about one year, involved onshore sand migration, forebeach deposition, and rapid advancement of the berm crest. Sand deposition during this stage ranged from about 5 m^3/m to nearly 30 m^3/m, and increased to the southwest (Fig. 5a). The lack of significant sand deposition at site 4 probably indicates shoreface bypassing because there should have been a surplus of storm-eroded sand on the shoreface offshore from this site.

During the second phase of beach recovery, berm crests aggraded and continued to advance seaward until the second post-storm winter when high waves eroded the berms and transferred sand landward, filling in low runnels, and aggrading the backbeach near the post-storm erosional escarpment. Sand accumulation in the backbeach equaled or exceeded forebeach erosion at three sites on Galveston Island while the other beach sites experienced net erosion of as much as 10 m^3/m (Table 2, Fig. 5b). Profile evolution from a berm with low backbeach elevations (stage 1) to a broader and higher backbeach (stage 2) was important for the recovery of these beaches because foredunes could not reform until the berms reached a minimum width and elevation (Morton et al., 1994).

The third and fourth stages of beach recovery lasted two to three years, and involved foredune construction over the post-Alicia erosional escarpment and dune stabilization by vegetation. Backbeach elevations continued to increase through eolian deposition but the rate of sand accumulation slowed. In 1985, sand accumulated on the backbeach, and dunes began to form at all sites except 4 and 5 where the beach remained relatively stable. The lack of net sand accumulation at site 5 is partly attributed to construction of an artificial dune ridge in the middle of the beach that blocked both high water and eolian onshore movement of sand preventing aggradation of the backbeach and dune construction (Morton and Paine, 1985). Cumulative volumetric changes for the third and fourth years after Alicia consisted of large-scale alternating

patterns of beach erosion and deposition (Fig. 5c). Most sites accumulated from 10 to 17 m^3/m of sand (Table 2), which was deposited in the dunes and on the backbeach.

After the post-storm recovery period, beaches began responding to external forces and local changes in sand supply. Nearly all beach segments on Galveston Island experienced declines in sand volume around 1988/89 (Table 2 and Fig. 6). Systematic erosion of the forebeach persisted to the southwest except for minor sand accumulation on the forebeach at site 5 and deposition in the dunes and forebeach at site 8 (Fig. 5c). The minor but widespread erosion was caused by Hurricanes Gilbert (1988) and Chantal (1989). Gilbert was an intense storm that tracked due west through the Caribbean flooding all beaches of the Texas coast, whereas Chantal was a minimal category 1 storm that locally flooded the backbeaches of Galveston and Follets Islands.

After losing sand in 1988/89, Galveston beaches evolved in several ways. The eastern section near the seawall continued to erode, and by 1993 it had 6 m^3/m less sand than after Alicia (Table 2, Figs. 6 and 7). Beaches west of site 1 alternated between accretion and stability beginning with site 2, which accreted, site 7, which remained stable, site 3, which accreted, site 5, which remained stable, and site 4 near San Luis Pass, which showed the greatest amount of accretion (Fig. 6).

Alongshore patterns of alternating deposition and erosion were pronounced in 1991 with deposition increasing and erosion decreasing to the southwest (Fig. 5c). Sand was eroded from the forebeach at sites that lost beach volume, whereas sand accumulated on the forebeach and in the dunes at sites gaining beach volume. Sand accumulation was greatest at site 4, which previously had either eroded more or accumulated less sand than any other site. This change in sand distribution pattern apparently signaled a change in sand storage and release from the shoreface and ebb delta. Longshore alternating patterns of net deposition and erosion were greatly magnified between 1991 and 1993 (Fig. 5c). Net sand losses were caused by forebeach erosion, whereas forebeach and dune deposition resulted in net volume gains. Net accumulation of 46 m^3/m at site 4 was the greatest for any time period including those immediately following Alicia.

Beach observations and field measurements indicate that the post-Alicia surplus of shoreface sand is restricted to the northeastern end of Follets Island. Evidence for this statement is the fact that no sand accumulated at a rock revetment about 2 km southwest of site 8, and the beach about 19 km southwest of site 8 gradually eroded (Fig. 8) while sand was returning to updrift beaches. Thus the large mass of sand eroded from the flats and shoals at San Luis Pass was transported southwest only about 4 km.

Net Volume Change

The ten-year record of volumetric changes (Table 1, Figs. 6 and 7) reveals a wide range of beach responses within a single coastal compartment even though wave climate and tide range are invariant. Post-storm beach responses for the 40 km segment include (1) continuous erosion, (2) partial recovery and subsequent erosion, (3) partial recovery and subsequent stability, and (4) continuous accretion (Fig. 6).

Beach volume history at site 1 is typical of beach segments immediately downdrift of the Galveston seawall. Maximum recovery of sand, which represented only about half the volume eroded by Alicia, occurred in the first post-storm year and then remained relatively constant until sand volume steadily declined beginning in 1989. The persistent erosion resulted in a loss of 57.2 m^3/m by the end of the monitoring period, which represents a net loss of 6 m^3/m more than immediately after Alicia (Table 1, Fig. 4). In contrast, the beach at site 3 steadily gained sand and achieved volumetric recovery during the first two years after the storm (Table 1, Fig. 6). Subsequent volumetric changes at site 3 involved a period of stability and decline (1988-1989) followed by more recent gains in sand volume that resulted in a net surplus of about 33 m^3/m (Table 1, Fig. 4). Volumetric changes at site 4 are the least consistent compared to the other beach volume histories (Table 1, Fig. 6). Beach volume changed very little for the first two years after the storm and then the beach began to lose sand until 1988 when there was 29 m^3/m less sand than after Alicia. Since then, about 72 m^3/m has rapidly accumulated as a result of bar attachment from the ebb delta at San Luis Pass.

Since Hurricane Alicia, the beach at site 8 has undergone the same general stages of recovery as the beaches on Galveston, except the Follets Island site has continued to accumulate sand causing beach accretion, beach aggradation, and dune construction. This is the only beach that has systematically gained volume during each monitoring period since Alicia (Fig. 6). Annual sand accumulation at site 8 has been relatively uniform, resulting in deposition of about 98 m^3/m on the beach and dunes (Table 1, Figs. 6 and 7) at an average rate of about 10 $m^3/m/yr$.

SHORELINE MOVEMENT

Fenster and Dolan (1993) reported that long-term shoreline movement on the Outer Banks of North Carolina generally correlates with frequency and intensity of storms as well as fluctuations in local sea level. Their analyses indicate that beach erosion increased when the number of storms and length of the winter storm season increased. To evaluate the effects of specific storms or storm clusters on shoreline movement, we compared shoreline positions with the coincidence of intense hurricanes (storm surges > 2 m) during the past three decades (Figs. 9 and 10). Storm surge measurements near Galveston (Corps of Engineers, Sugg et al., 1971) indicate that 7 hurricanes caused water levels of more than 2 m since 1930. The most recent decadal trends of shoreline movement (Table 3) were also compared with beach volume changes at the nearest profile site (Table 2) to evaluate the consistency of results obtained from air photo analyses and field measurements.

General Trends

Most Texas beaches are retreating because there is a relative rise in sea level (Fig. 2), and sand volume in the littoral drift system has been both naturally and artificially reduced (Morton, 1979). Large deficits in sand supply affecting Galveston and Follets Islands are related to decreases in sand discharged by the Brazos River located to the southwest. More important to beach erosion on a historical time scale are reductions in sand delivered by longshore currents. Deep navigation channels and long jetties at harbor entrances have completely blocked the

longshore movement of sand from adjacent coastal sectors, and no additional sources of sand are available to the coastal compartment containing Galveston and Follets Islands. Littoral drift is further disrupted by the 16-km-long Galveston seawall, which prevents sand from entering the littoral system (Morton, 1988a). Periodic net losses of beach sand in this coastal compartment either by storm washover or transport onto the inner shelf are compensated for by beach erosion.

The 30-km stretch of West Beach can be divided into three segments (Fig. 1) on the basis of historical shoreline movement (Morton and Paine, 1985). Retreating segments with the highest rates of retreat are located at the extreme eastern and western ends of the beach; rates of retreat progressively decrease toward the more stable middle part of the island (Fig. 1). This pattern of extreme retreat at the ends and semi-stability in the middle of West Beach is explained by island morphology, locations of coastal structures with respect to littoral processes, and sources of beach sand. Persistent beach erosion along the eastern segment is caused by an insufficient sand supply coupled with moderately-high littoral energy that removed all subaerial sand seaward of the seawall (Morton, 1988a). Long jetties and the Galveston seawall (Fig. 1) prevent downdrift transport of sand that would otherwise replenish and help maintain West Beach. As a result of the disrupted littoral system, the beach immediately southwest of the seawall is the first available source of sand to satisfy the erosional capacity of waves and longshore currents.

Powerful tidal currents, complex wave refraction patterns, and a thin cover of mobile sand all contribute to rapid shoreline retreat at San Luis Pass. In contrast, mid-island beaches are retreating at much lower rates because they overlie a thick core of barrier sand (Bernard et al., 1970) and form a slightly concave arc (near site 3, Fig. 1). The shoreline arc captures much of the sand eroded from the eastern segment (sites 1, 2, and 7) and some eroded from the western tip (site 4) when littoral currents reverse.

Effects of Recent Storms

The potential influence of storms on beach mobility and on predictions of future shoreline positions are revealed by comparing trends and rates of shoreline movement before and after

recent storms. In the past three decades, three major hurricanes have affected the beaches of Follets and Galveston Islands. Hurricane Carla in 1961 was an intense category 4 storm that came ashore about 160 km southwest of the study area. Extremely high waves and prolonged beach flooding during Carla caused severe erosion all along the southeastern Texas coast. We are unable to quantify precisely the effects of Carla on shoreline movement, because none of the mapped shorelines immediately preceded the storm (Figs. 9 and 10). Although other factors before and after Carla influenced shoreline movement, it is clear that Carla was a dominant force causing a change from stability to retreat at site 1 (Fig. 9), reversing the trend from advancement to retreat at sites 3 and 4 (Figs. 9 and 10), and accelerating retreat at site 8 (Fig. 10).

Beach surveys by Don Harper of Texas A&M University and anecdotal accounts by local residents confirm that the beaches and dunes of Galveston Island experienced moderate erosion from Hurricane Allen (1980). By itself, Allen would have caused only moderate erosion, but the beaches had not completely recovered from Allen when Alicia struck, so the combined erosion of both storms was greater than the expected sum of average erosion for each storm. Thus, antecedent beach conditions and incomplete recovery after Allen contributed to greater beach erosion than would have been predicted by Alicia alone. Lower backbeach elevations and diminished dune volume after Allen allowed deeper wave penetration and greater sand excavation by the Alicia storm surge.

Comparing short-term (< 10 year) rates of shoreline movement immediately preceding and following Alicia (Table 3) illustrates the systematic longshore effects of cumulative storm erosion on beach mobility. After Alicia, shoreline retreat along West Beach accelerated (sites 1, 2, and 7), and rates of retreat increased to the southwest toward the storm center. At some sites, the trend of shoreline movement reversed as formerly stable segments began retreating (sites 3 and 5), and a formerly retreating beach began advancing (site 4). Immediately before Alicia, the beach of Follets Island (site 8) was slowly advancing but since Alicia, beach advancement has also accelerated. At site 8 the shoreline advanced more than 60 m, the backbeach aggraded as much as 1.4 m, and a surplus of about 60 m^3/m of sand is stored in the backbeach and dunes.

Considering the absolute rates of shoreline movement, regardless of trend, Alicia caused accelerated changes at all profile sites and reversed the trend at three of the sites (Table 3).

There is good agreement between post-storm decadal shoreline movement derived from aerial photographs and movement inferred from field measurements of beach volume (Table 1, Fig. 6). Considering the same period used for the air photo analysis (1982-1990), net losses of beach volume persisted at all profile sites on West Beach and net gains were recorded on Follets Island. The discrepancy between shoreline movement and beach volume history at site 4 documents unusual conditions whereby sand eroded from an escarpment was added to the forebeach causing advancement of the berm crest (shoreline) while the beach volume declined. Later, the beach volume at site 4 increased (Table 1, Fig. 6), which agrees with the most recent trend of shoreline advancement.

DISCUSSION

Tidal Inlet Processes

Tidal inlets can disrupt or maintain continuity of the littoral drift system between barrier islands by storing or bypassing available sand. Longshore transport may be temporarily or permanently disrupted if sand is transferred landward of the beach by spit accretion or washover deposition on barrier islands, or accumulates on flood- or ebb-tidal deltas. Seaward displacement of sand by storm-surge ebb can also temporarily or permanently remove sand from the system. Mechanisms of sand bypassing at tidal inlets that maintain the downdrift flow of sand include (1) wave-induced transport around the ebb shoals, (2) periodic exchange of sand transported into and out of inlets by tidal flow, and (3) migration of tidal channels and associated bars (Bruun and Gerritsen, 1959; FitzGerald, 1988).

Wave refraction around ebb-tidal deltas can cause littoral currents to reverse locally and deposit sand on the updrift ends of adjacent barrier islands, resulting in local shoreline advancement near the inlets (Hayes, 1979; 1991). This mechanism could explain the sand

accumulation on Follets Island; however, site 8 is about 4 km southwest of the seaward curvature of the shoreline at San Luis Pass and thus outside the zone of local reversing currents.

The large volume of sand added to the terminal flat at San Luis Pass (Fig. 3) accounts for most of the littoral drift transported along Galveston Island since Alicia. Lateral accretion on the updrift side of the inlet is caused by waves refracting into the inlet and by currents flooding across the broad sand flat into West Bay. Additional evidence for disruption of sand transport is provided by inlet morphology and water depths over the ebb-delta shoals, which are asymmetrical and separated by the main inlet channel (Fig. 3). The large updrift shoal normally is below the depth of breaking waves, whereas the downdrift shoal is covered by a field of low sand ridges constructed by breaking waves. Thus, on the updrift side of the inlet, refracting waves impinge on the beach but not on the ebb-delta shoals.

The largest and least predictable shoreline changes occur next to the tidal inlet (Fig. 10), and are controlled by complex wave and current patterns that interact with the beach as well as with shoals and tidal channels of the ebb-tidal delta. The cycles of rapid, large-scale beach erosion and deposition typically are related to attachment and separation of spits and shoals of the ebb-tidal delta as well as changes in inlet morphology and position (Oertel, 1977; FitzGerald, 1988). Galveston beaches near San Luis Pass are probably interacting with marginal flood channels that change position along the southwestern tip of the island. The continuous sand accummulation on Follets Island within a few kilometers of the inlet may be caused by (1) episodic ebb-channel switching that releases sand downdrift, (2) landward movement of ebb-delta sand displaced during Alicia, (3) landward movement of Alicia emplaced shoreface sand eroded from Galveston beaches, or (4) various combinations of these sand sources. Judging from the available data, it appears that the most likely source of sand is ebb-delta sand eroded and transported to the southwest by Alicia. This implies that shoreline accretion at site 8 will likely cease and the beach will begin eroding when the locally derived sand supply is exhausted.

Patterns of Erosion and Deposition

Longshore variations in beach volume changes (Table 2, Figs. 5-7) are caused by fluxes in the rates of sediment transport as well as temporary release and storage of sand on the beach and shoreface. The changes in beach volume may be, but are not necessarily, a response to the propagation of rhythmic beach topography. Shoreline rhythms, such as those described by Inman (1987), Dolan and Hayden (1983), and Morton (1991), are morphological features defined by shoreline position, whereas changes in sand volume may occur anywhere on the beach profile, not just at the high water line. Furthermore, the observed magnitudes and periodicities of beach volume flux (Figs. 5-7) are much greater than those caused by the short-wavelength beach cusps that are typical shoreline rhythms of the Texas coast. Thus, lateral variability of beach volume changes probably reflects local variations in sand transport mechanisms. Morton (1979) and Dolan et al. (1992) demonstrated that shoreline changes and rates of change at adjacent sampling transects on sandy coasts are highly correlated, and correlation coefficients are inversely related to the distances between transects. As expected, spatial autocorrelation of beach volume changes within the same compartment is also high (Table 2, Figs. 5 and 7), even where monitoring sites are spaced about 5 km apart.

Clarke and Eliot (1988) analyzed a ten-year record of monthly profiles from a 2 km pocket beach in Australia, and observed that beaches were more stable where bars formed, and were less stable where rip currents formed. They also concluded that short-term, small-scale fluctuations in beach volume were controlled by longshore sediment movement, whereas long-term volumetric changes were related to onshore-offshore sediment motion. These conclusions seem reasonable for a small pocket beach where nearshore circulation influenced by deep-ocean swell is confined to a single cell and substantial longshore transport is effectively blocked by promontories, but the conclusions may not be applicable to continuous sand beaches tens of kilometers long where longshore transport is unimpeded and offshore sand sources are absent. Long-term volumetric changes of these long continuous beaches should be related to longshore

sediment transport flux and either systematic or cyclical exchange of sand among adjacent beach sites and the shoreface.

The temporal and spatial changes in sand volume (Table 2, Fig. 5) provide clues to the dominant mechanism of sand transport and permit qualitative distinction between longshore and cross-shore sediment motion. The southeast Texas coast is a good candidate for this type of analysis because nearshore bathymetry is smooth and uncomplicated and bars are continuous and not disrupted by rip currents. Systematic increases or systematic decreases in sand volume at several adjacent beach sites are probably evidence of current-driven longshore transport. This pattern persisted for the first two quarters immediately after Hurricane Alicia (Fig. 5A) when surplus sand was locally available from the upper shoreface. In contrast, patterns of alternating increases and decreases in sand volume at adjacent sites (Fig. 5C) suggest wave-driven cross-shore transport whereby sand is exchanged directly between the shoreface and beach without appreciable longshore movement. Longshore differences in sand stored in or released from the beach is greatest in the summer (Fig. 5), which suggests that wave-driven cross-shore transport is the predominant mechanism. Longshore patterns of sand volume changes in the winter are irregular, suggesting a combination of both longshore and cross-shore transport. For most of the monitoring periods, the predominant sand transport directions inferred from beach volume changes agree well with the net direction of water motion derived from wind vectors and shoreline orientation (Fig. 11). The wind vectors also show that net direction of water motion is seasonal and similar from one year to the next.

Annual fluctuations in subaerial beach volume were generally less than 15 m^3/m and none were greater than 46 $m^3/m/yr$ (Table 2, Figs. 5-7). These fluxes are substantially less than seasonal beach volume changes on high-energy coasts. Minor volume flux and low seasonal mobility of Texas beaches are consistent with fine sediment textures, low wave energy, and dissipative beach morphologies as predicted by the conceptual model of Wright and Short (1984). The morphodynamics of Australian beaches studied by Wright and Short are influenced primarily by high-energy breakers and nearshore processes responding to deep ocean swell. In

contrast to their model beaches, Texas beaches respond to low-energy, locally wind-generated waves and the beaches maintain dissipative modal states regardless of whether they are fully eroded (site 1) or fully accreted (site 8). The low tide range, fine sand size, and abundant sand storage on the shoreface of Texas beaches produces broad surf zones and dissipative beach morphologies during all wave states. Morphodynamics of these beaches are clearly related to changing wave conditions, but the range of morphodynamic alterations are limited to one state of the Wright and Short model.

CONCLUSIONS

Large-scale behavior of a microtidal storm-dominated sandy coast is revealed by examining the historical record of volumetric and geomorphic beach changes. Results of the analysis show that sand bypassing at a major tidal inlet (San Luis Pass) is episodic, event-driven, and inefficient because wave refraction patterns and flood-dominated currents transport beach sand landward of the ebb delta, disrupting its downdrift migration. The terminal flat at the inlet is a sink for sand eroded from updrift beaches and subaqueous shoals of the ebb delta are sources of sand deposited on downdrift beaches. The beach volume data also suggest that for six years after Hurricane Alicia, southwesterly transported sand bypassing the beach immediately updrift of the inlet was deposited on the terminal sand flat, but since then, sand has accumulated on the forebeach causing net shoreline advancement. The shift in locus of sand deposition is attributed to changes in position of marginal tidal channels and ebb-delta shoals.

Beach erosion vulnerability partly depends on antecedent beach state, which in turn depends on the difference between storm frequency and beach recovery period. Beach erosion is accentuated when storm frequency exceeds beach recovery period especially where the local sand supply is minimal. The current frequency of significant storms at Galveston (6 yr) slightly exceeds the time required for both volumetric and geomorphic beach recovery from a moderate storm (4-5 yr). However, the lack of an adequate sand supply leaves Galveston beaches

vulnerable to future storm erosion because the volume of sand stored in the dunes is inadequate to offset the sand volume eroded by two closely-timed moderate storms (category 2-3) or a single intense storm (category 4).

The ten-year record of beach volume data reveal intracompartmental sharing (small-scale response) and longshore exchange of sand (large-scale response) among monitoring sites. Rapid, large-volume transport and storage of sand during storms (hours) and the prolonged, slow release and continuous onshore transfer of sand from the shoreface to the beach (decades) are poorly understood processes that involve the shoreface acting as a reservoir alternately storing and releasing sand for beach maintenance and dune construction. If numerical models of shoreline movement and predictive capabilities are to improve, then changes in beach volume at the myriameter (10 km) spatial scale and decadal temporal scale must be resolved.

Shoreline change analyses improved significantly after shoreline movement was recognized as being both nonuniform and nonlinear. Consequently, trend reversals as well as accelerations and decelerations in rates of shoreline movement need to be assessed if accurate modeling and prediction of future shoreline positions are expected. Our study shows that rates of shoreline movement were 1.5 to 8 times greater after Alicia than before the storm. Individual storms do not necessarily accelerate beach movement or cause trend reversals, but storm effects can be magnified if storm frequency exceeds the beach recovery period for individual storms.

Under present conditions of rising sea level and reduced sediment supply, storms of historical record are the most significant factor affecting short-term shoreline movement where updrift erosion is the primary source of sand to maintain beaches. This implies that in the future, storms will have greater impact and cause even more beach erosion especially where human activities have compartmentalized the coast and have reduced the natural supply of sand to ocean beaches.

ACKNOWLEDGEMENTS

This work was partly supported by the U.S. Geological Survey Coastal Geology Program and the State of Texas Office of the Attorney General. We thank Bill Birkemeier for providing

copies of the Interactive Survey Reduction Program and Volume software and George Kramig for beach height measurements near Freeport, Texas. David Adilman and Jim DiGiulio assisted in the field monitoring, and Cynthia Jennings helped format the profile data. Comments provided by two anonymous reviewers greatly improved the clarity and content of the paper. Publication was authorized by the Director, Bureau of Economic Geology, The University of Texas at Austin.

REFERENCES

Aubrey, D. G., 1979. Seasonal patterns of onshore/offshore sediment movement. Journal of Geophysical Research, 84: 6347-6354.

Bernard, H. A., Major, C. F. Jr., Parrott, B. S., and LeBlanc, R. J. Sr, 1970. Recent sediments of southeast Texas: A field guide to the Brazos alluvial and deltaic plains and the Galveston barrier island complex. Univ. Texas Austin, Bur. Econ. Geology, Guidebook 11, 132 pp.

Birkemeier, W.A. and Holme, S.J., 1992. User's Manual to ISRP 2.7, the Interactive Survey Reduction Program. U.S. Army Corps of Engineers, Waterways Experiment Station, Vicksburg, Mississippi, 56 pp.

Bruun P. and Gerritsen, F., 1959. Natural by-passing of sand at coastal inlets. Journal of Waterways and Harbors Division, Am. Soc. Civil Engineers, 85: 75-107.

Clarke, D. J., and Eliot, I. G., 1988. Low frequency changes of sediment volume on the beachface at Warilla Beach, New South Wales, 1975-1985. Marine Geology, 79: 189-211.

Dolan, R., and Hayden, B., 1983. Patterns and prediction of shoreline change. In: P. D. Komar, (Editor), Handbook of coastal processes and erosion. CRC Press, Boca Raton, Fla. p. 123-149.

Dolan, R., Fenster, M. S., and Holme, S. J., 1992. Spatial analysis of shoreline recession and accretion. Journal of Coastal Research, 8: 263-285.

Emery, K. O., 1961. A simple method of measuring beach profiles. Limnology and Oceanography, 6: 90-93.

Fenster, M. S., and Dolan R., 1993. Historical shoreline trends along the outer Banks, North Carolina: Processes and responses. Journal of Coastal Research, 9: 172-188.

Fenster, M. S., Dolan R., and Elder, J. F., 1993. A new method for predicting shoreline positions from historical data. Journal of Coastal Research, 9: 147-171.

FitzGerald D. M., 1988. Shoreline erosional-depositional processes associated with tidal inlets. In: D. G. Aubrey and L. Wishar (Editors), Hydrodynamics and sediment dynamics of tidal inlets. Springer Verlag, New York, p. 186-225.

Hayes, M. O., 1967. Hurricanes as geological agents: case studies of Hurricanes Carla, 1961, and Cindy, 1963. Univ. Texas Austin, Bur. Econ. Geol., Rept Invest 61, 54 pp.

Hayes, M. O., 1979. Barrier island morphology as a function of tidal and wave regime. In: S. P. Leatherman (Editor), Barrier islands from the Gulf of St. Lawrence to the Gulf of Mexico. Academic Press, New York, p. 1-27.

Hayes, M. O., 1991. Geomorphology and sedimentation patterns of tida inlets: A review. American Society of Civil Engineers, Coastal Sediments '91, 2: 1343-1355.

Inman, D. L., 1987. Accretion and erosion waves on beaches. Shore and Beach, 55: 61-66.

Lyles, S. D., Hickman, L. E. Jr., and Debaugh, H. A., Jr., 1988. Sea level variations for the United States. U.S. Department of Commerce, National Ocean Service, Rockville, Md., 182 p.

Mason, C., 1981. Hydraulics and stability of five Texas inlets. U.S. Army Corps of Engineers, Coastal Engineering Research Center, Misc. Rept. 81-1, Fort Belvoir, 105 pp.

Morton, R. A., 1979. Temporal and spatial variations in shoreline changes, Texas Gulf Coast. Journal of Sedimentary Petrology, 49:1101–1111.

Morton, R. A., 1988a. Interactions of storm, seawalls, and beaches of the Texas coast. In: N. C. Kraus and O. H. Pilkey (Editors), Effects of seawalls on the beach. Journal of Coastal Research Special Vol 4:113–134.

Morton, R. A., 1988b. Nearshore responses to great storms. In: H. E. Clifton (Editor), Sedimentologic consequences of convulsive geologic events. Geol. Soc. Am. Special Paper 229: 7-22.

Morton, R. A., 1991. Accurate shoreline mapping: past, present, and future. American Society of Civil Engineers, Coastal Sediments '91, 1: 997- 1010.

Morton, R. A. and Paine, J. G., 1985. Beach and vegetation-line changes at Galveston Island, Texas - Erosion, deposition, and recovery from Hurricane Alicia. Univ. Texas Austin, Bur. Econ. Geology, Geological Circular 85-5, 39 pp.

Morton, R. A., Paine, J. G., and Gibeaut, J. C., 1994. Stages and durations of post-storm recovery, southeastern Texas coast, USA. Journal of Coastal Research. 10: 214-226.

Oertel, G. F., 1977, Geomorphic cycles in ebb deltas and related patterns of shore erosion and accretion. Journal of Sedimentary Petrology, 47:1121-1131.

Sugg, A. L., Pardue, L. G., and Carrodus, R. L., 1971, Memorable hurricanes of the United States since 1873. National Oceanic and Atmospheric Administration, NOAA Technical Memorandum NWS SR-56, 52pp.

U.S. Army Corps of Engineers, 1983. Galveston County shore erosion study-feasibility Report and environmental impact statement. Gulf Shoreline Study Site Rept, vol 2. Galveston District Corps of Engineers, 185 pp.

White, W. A., Calnan, T. R., Morton, R. A., Kimble, T. G., Littleton, T. G., McGowen, J. H., Nance, H. S. and Schmedes, K. E., 1985. Submerged lands of Texas, Galveston–Houston area: sediments, geochemistry, benthic macroinvertebrates, and associated wetlands. Univ. Texas Austin, Bur. Econ. Geology, 145 pp.

Williams, S. J., Prins, D. A. and Meisburger, E. P., 1979. Sediment distribution, sand resources, and geologic character of the inner continental shelf off Galveston County, Texas. Coastal Engineering Research Center, Misc Rept 79-4, Fort Belvoir, 159 pp.

Wright, L. D., and Short, A. D., 1984. Morphodynamic variability of surf zones and beaches: a synthesis. Marine Geology, 56:93-118.

Figure Captions

Fig. 1. Locations of beach profile sites on Galveston Island and Follets Island, Texas. Long-term beach stability trends (1851-1980) from Morton and Paine (1985).

Fig. 2. Fluctuations in relative sea level at three tide gauges including the Galveston gauge on the bay side of the island. Data from Lyles et al. (1988).

Fig. 3. Morphologic changes at San Luis Pass (A) caused by Hurricane Alicia and (B) six years after Alicia. Shorelines mapped from vertical aerial photographs taken in July 1982, August 1983, and March, 1990.

Fig. 4. Volume of beach sand eroded by Hurricane Alicia at profile sites and net beach volume changes ten years after the storm. Profile locations shown on Fig. 1.

Fig. 5. Seasonal longshore patterns of deposition and erosion at profile sites (A) in 1984, (B) in 1985, and (C) from 1987 to 1993. Profile locations shown on Fig. 1.

Fig. 6. Cumulative volumetric changes at profile sites on Galveston and Follets Island from 1980 to 1993. Profile locations shown on Fig. 1.

Fig. 7. Ten-year record of temporal and spatial changes in beach volume along Galveston and Follets Island. Profile locations shown on Fig. 1.

Fig. 8. Fourteen-year record of relative beach height near Freeport, Texas about 19 km southwest of site 8.

Fig. 9. Shoreline movement since 1930 (A) near site 1 and (B) near site 3 on Galveston Island. Shoreline positions were derived from vertical aerial photographs. The short bars represent unnamed hurricanes.

Fig. 10. Shoreline movement since 1930 (A) near site 4 at San Luis Pass on Galveston Island and (B) near site 8 on Follets Island. Shoreline positions were derived from vertical aerial photographs. The short bars represent unnamed hurricanes.

Fig. 11. Resultant wind vectors calculated from hourly measurements of wind speed and direction at the Houston Intercontinental airport. The wind vectors approximate net water movement for the periods between the beach profile dates. Approximate net sediment movement for the same periods depends on direction of water movement relative to shoreline orientation.

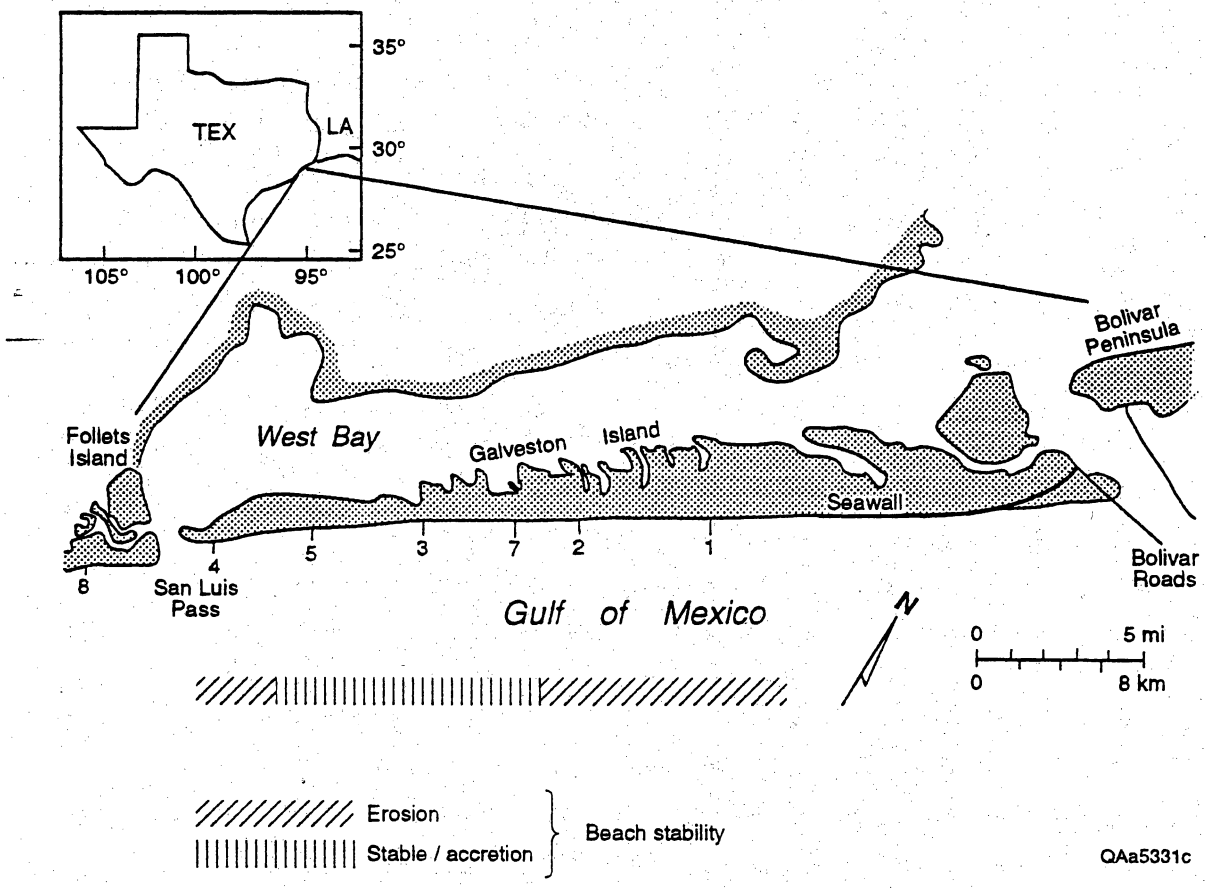
35°
30°
25°
105°
100°
95°
TEX
LA
Bolivar Peninsula
Follets Island
West Bay
Galveston
Island
Seawall
8
4
San Luis Pass
5
3
7
2
1
Bolivar Roads
Gulf of Mexico
N
0
5 mi
0
8 km
Erosion
Stable / accretion
Beach stability
QAa5331c

f.c.

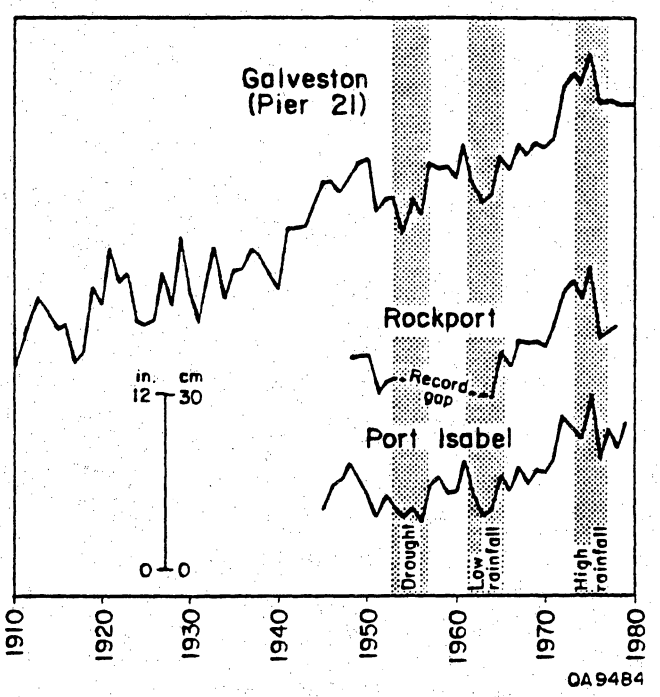
Galveston
(Pier 21)
Rockport
Record gap
Port Isabel
in. cm
12 30
0 0
Drought
Low rainfall
High rainfall
1910
1920
1930
1940
1950
1960
1970
1980
OA 9484

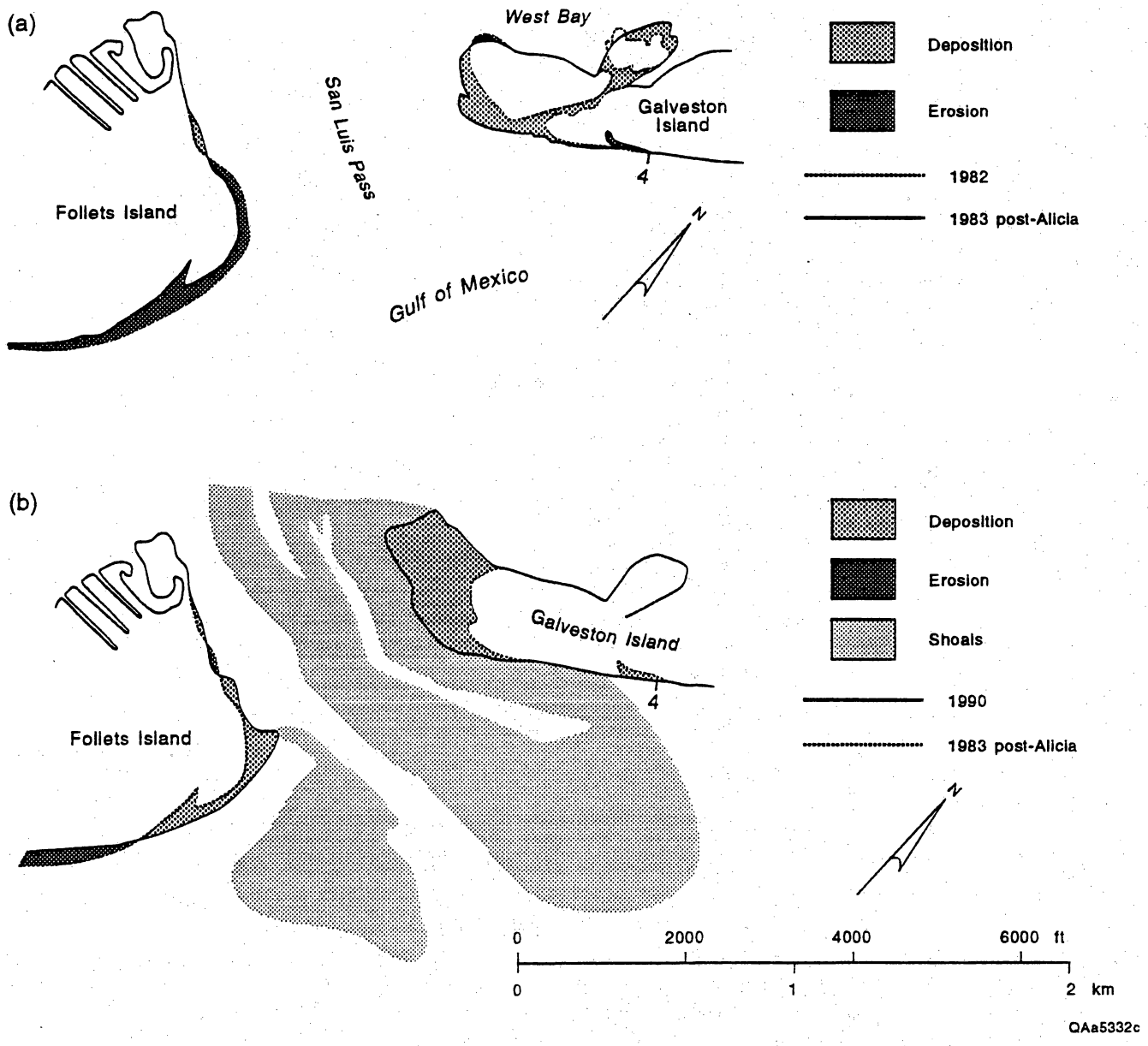
(a)
Follets Island
San Luis Pass
West Bay
Galveston Island
4
Gulf of Mexico
N
Deposition
Erosion
1982
1983 post-Alicia
(b)
Follets Island
Galveston Island
4
Deposition
Erosion
Shoals
1990
1983 post-Alicia
N
0
2000
4000
6000 ft
0
1
2 km
QAa5332c

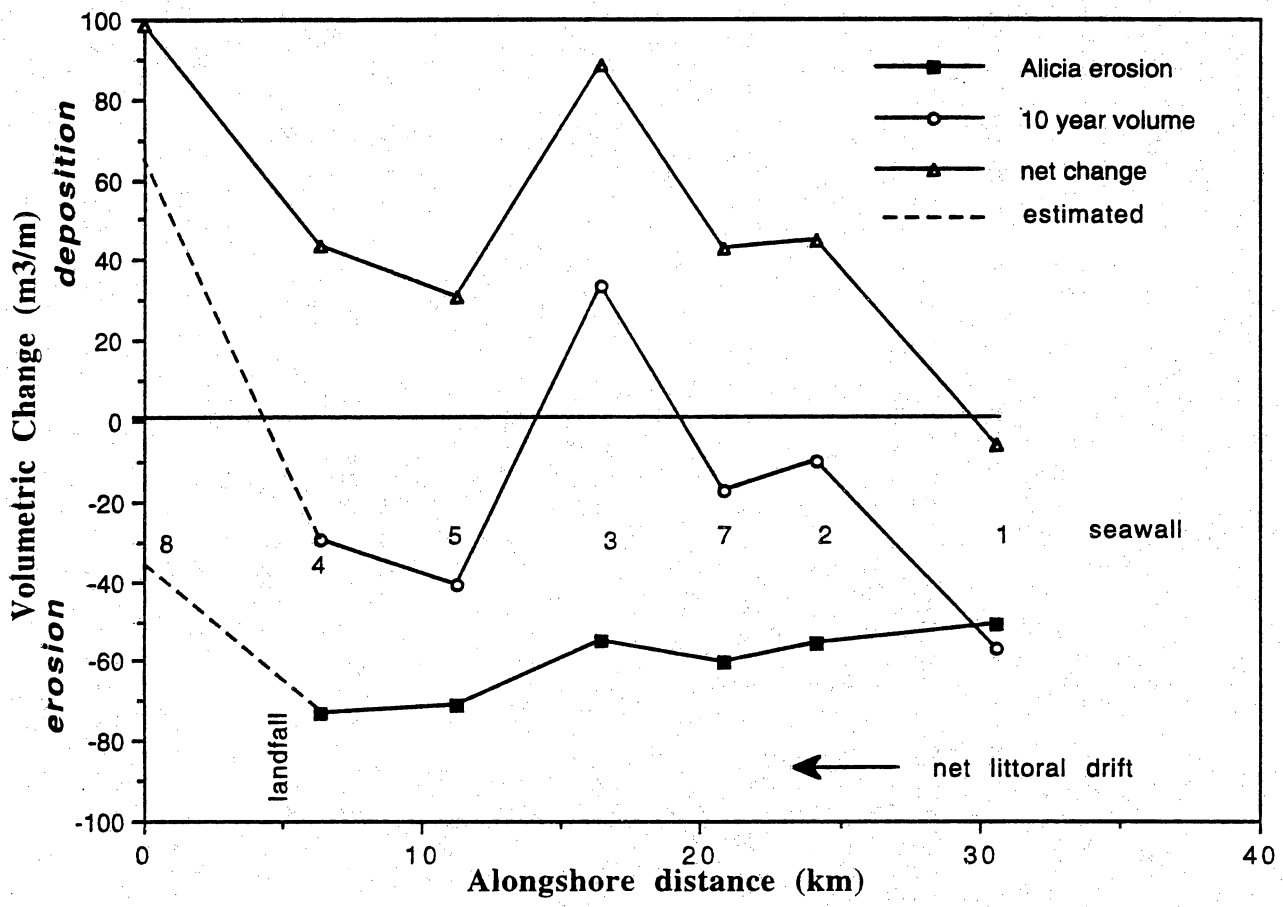
Volumetric Change (m3/m)
deposition
erosion
100
80
60
40
20
0
-20
-40
-60
-80
-100
0
10
20
30
40
Alongshore distance (km)
Alicia erosion
10 year volume
net change
estimated
8
4
5
3
7
2
1
seawall
landfall
net littoral drift

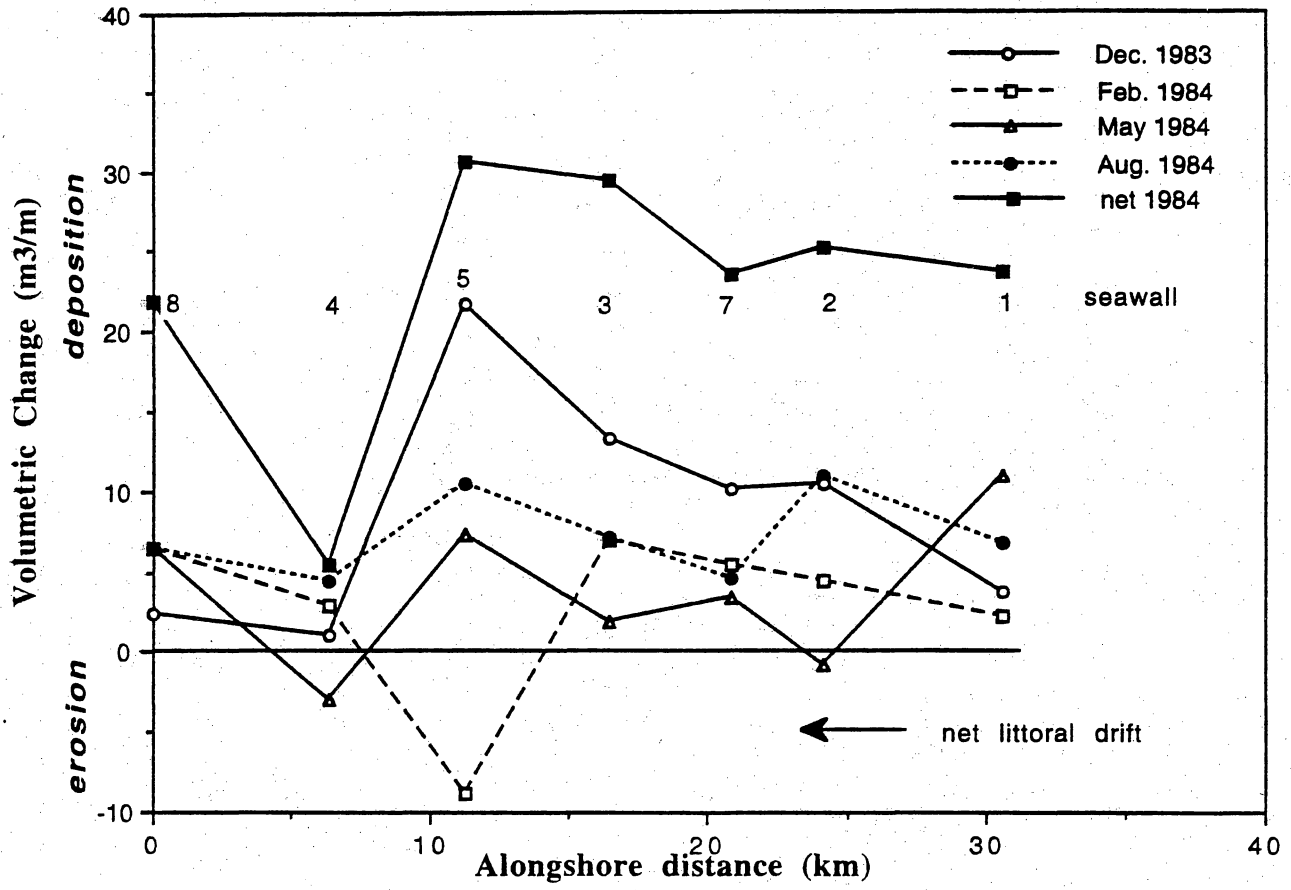
Volumetric Change (m3/m)
deposition
erosion
40
30
20
10
0
-10
0
10
20
30
40
Alongshore distance (km)
Dec. 1983
Feb. 1984
May 1984
Aug. 1984
net 1984
8
4
5
3
7
2
1
seawall
net littoral drift

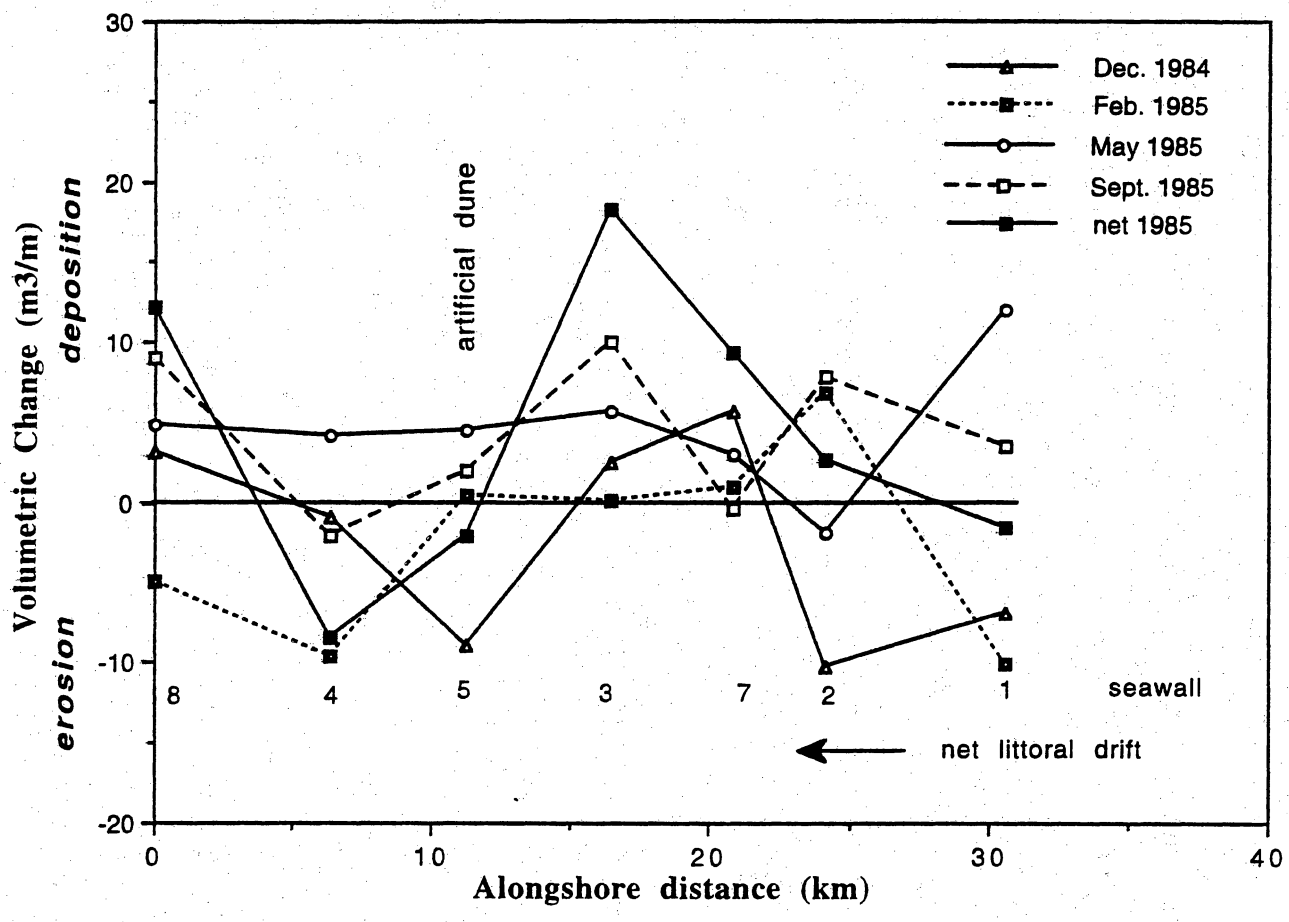
Volumetric Change (m3/m)
deposition
erosion
30
20
10
0
-10
-20
0
10
20
30
40
Alongshore distance (km)
artificial dune
Dec. 1984
Feb. 1985
May 1985
Sept. 1985
net 1985
8
4
5
3
7
2
1
seawall
net littoral drift

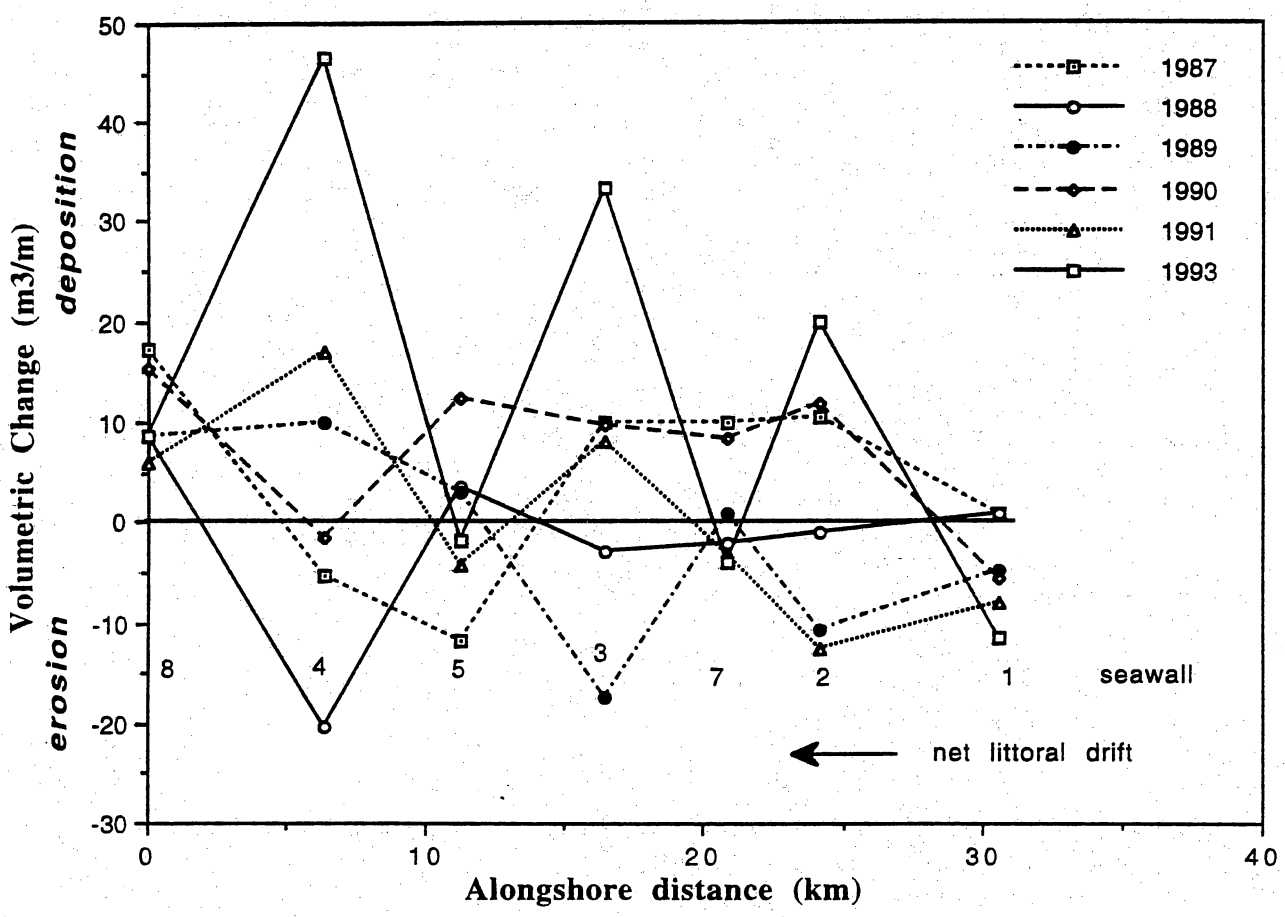
Volumetric Change (m3/m)
deposition
erosion
50
40
30
20
10
0
-10
-20
-30
0
10
20
30
40
Alongshore distance (km)
1987
1988
1989
1990
1991
1993
8
4
5
3
7
2
1
seawall
net littoral drift

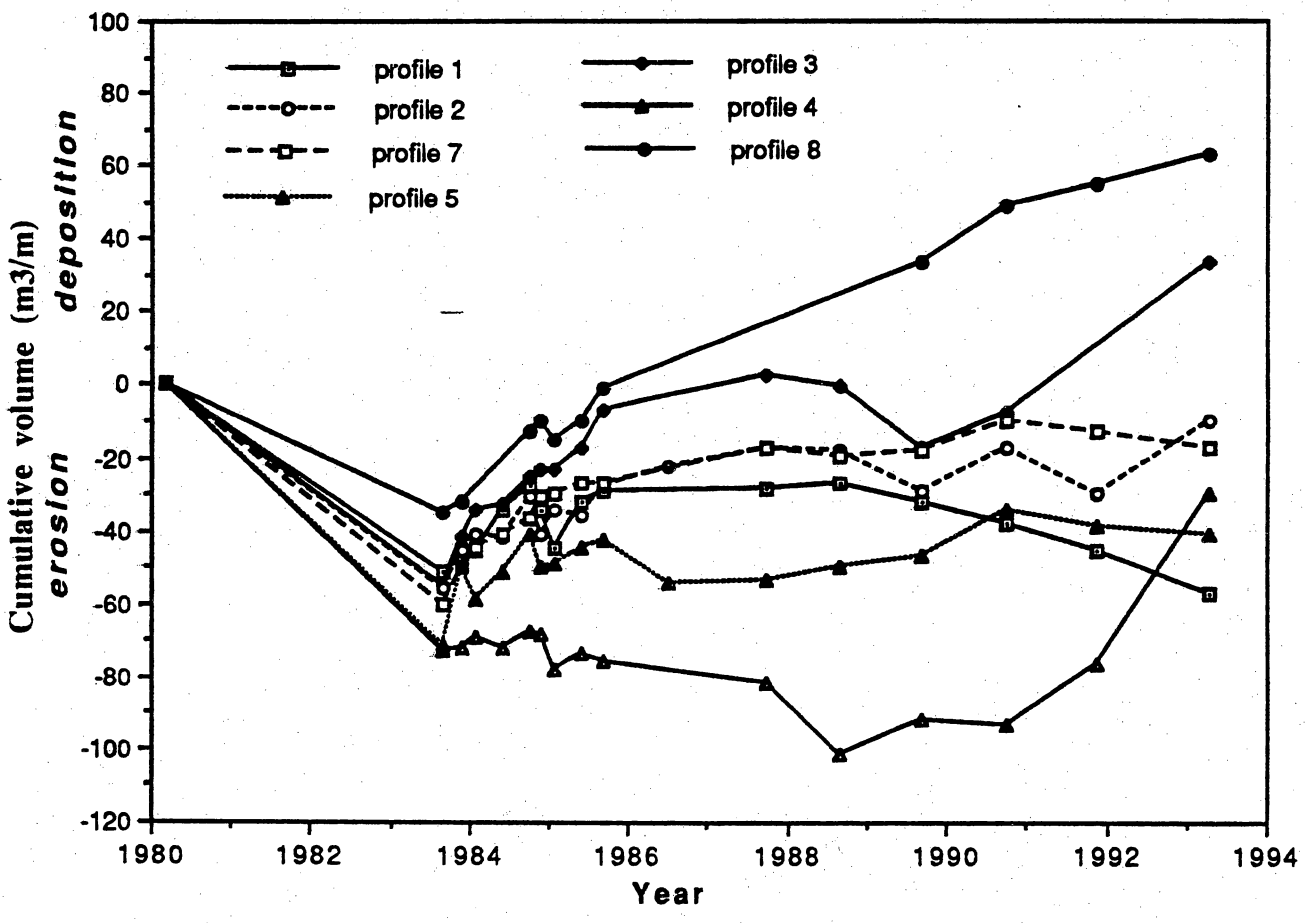
profile 1
profile 2
profile 7
profile 5
profile 3
profile 4
profile 8
Cumulative volume (m3/m)
erosion
deposition
100
80
60
40
20
0
-20
-40
-60
-80
-100
-120
1980
1982
1984
1986
1988
1990
1992
1994
Year

Beach Volume in Space and Time

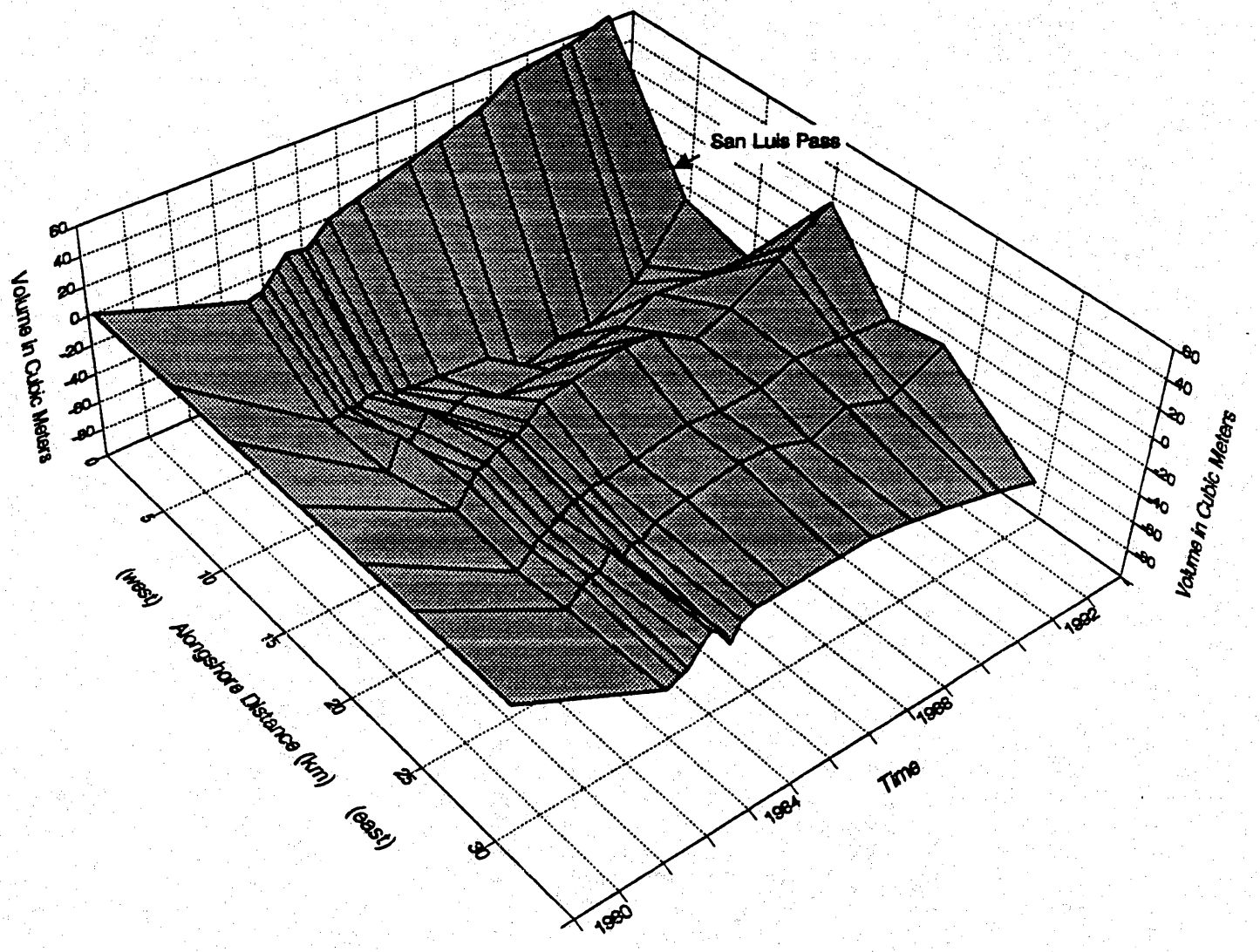

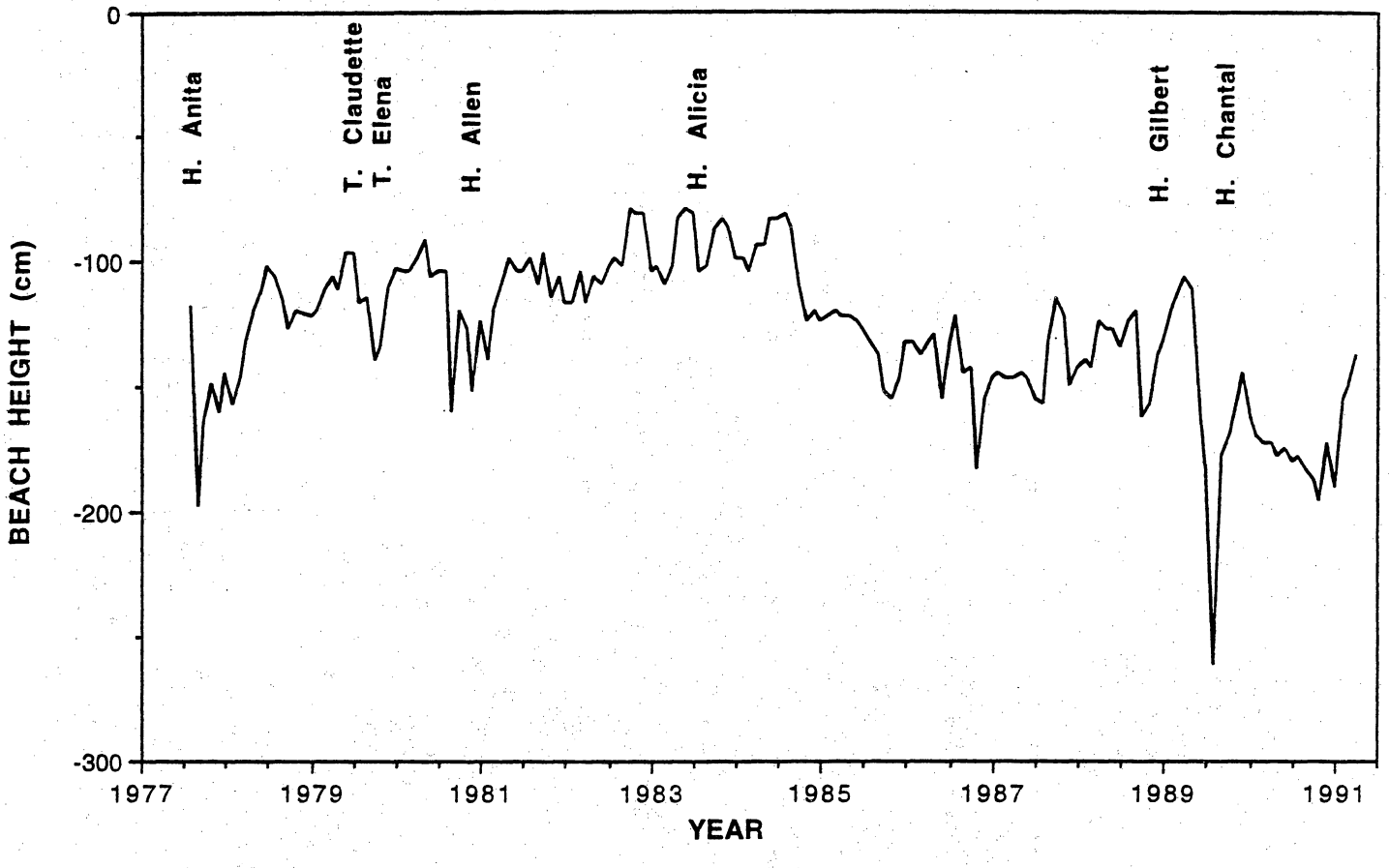
0
-100
-200
-300
BEACH HEIGHT (cm)
H. Anita
T. Claudette
T. Elena
H. Allen
H. Alicia
H. Gilbert
H. Chantal
1977
1979
1981
1983
1985
1987
1989
1991
YEAR

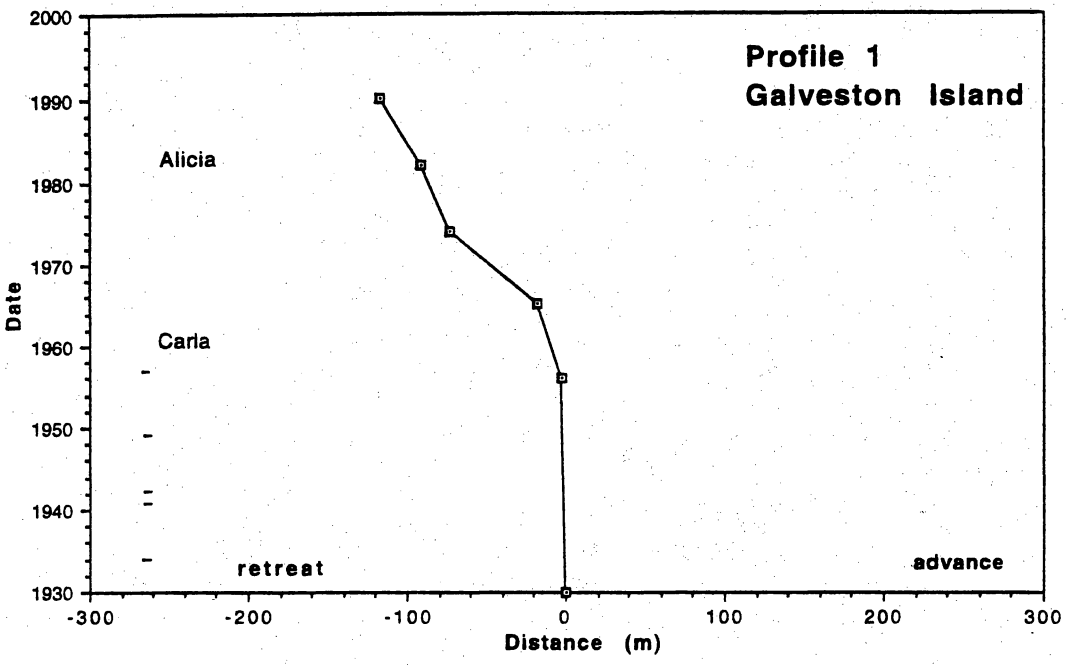
Profile 1
Galveston Island
Alicia
Carla
retreat
advance
Date
Distance (m)
2000
1990
1980
1970
1960
1950
1940
1930
-300
-200
-100
0
100
200
300

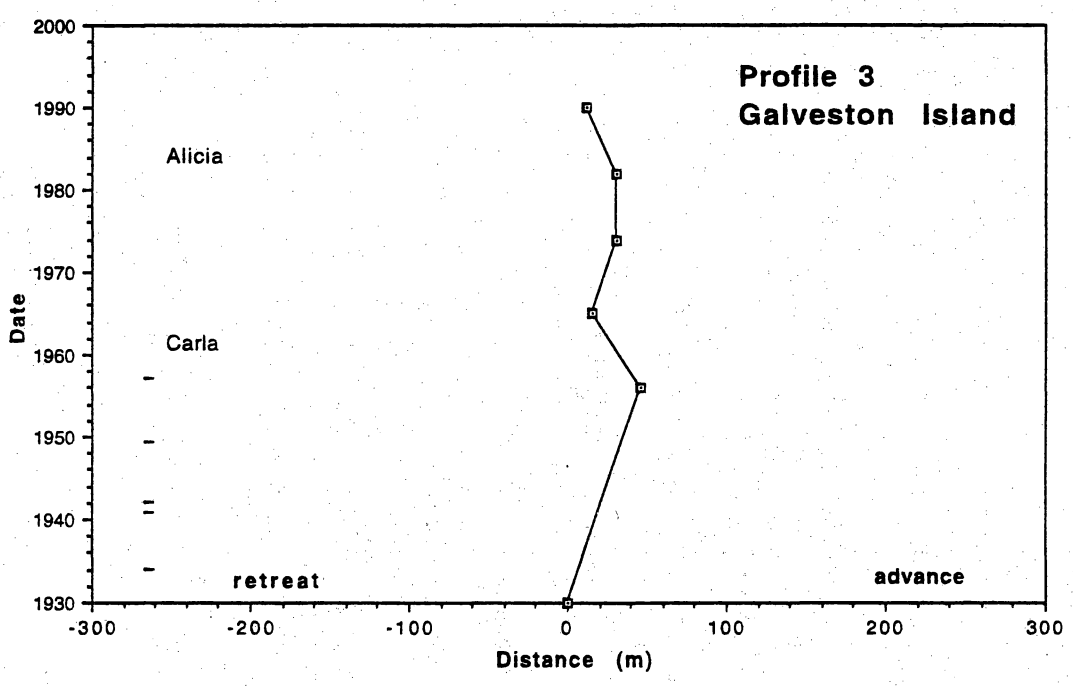
Profile 3
Galveston Island
Alicia
Carla
retreat
advance
Date
Distance (m)
2000
1990
1980
1970
1960
1950
1940
1930
-300
-200
-100
0
100
200
300

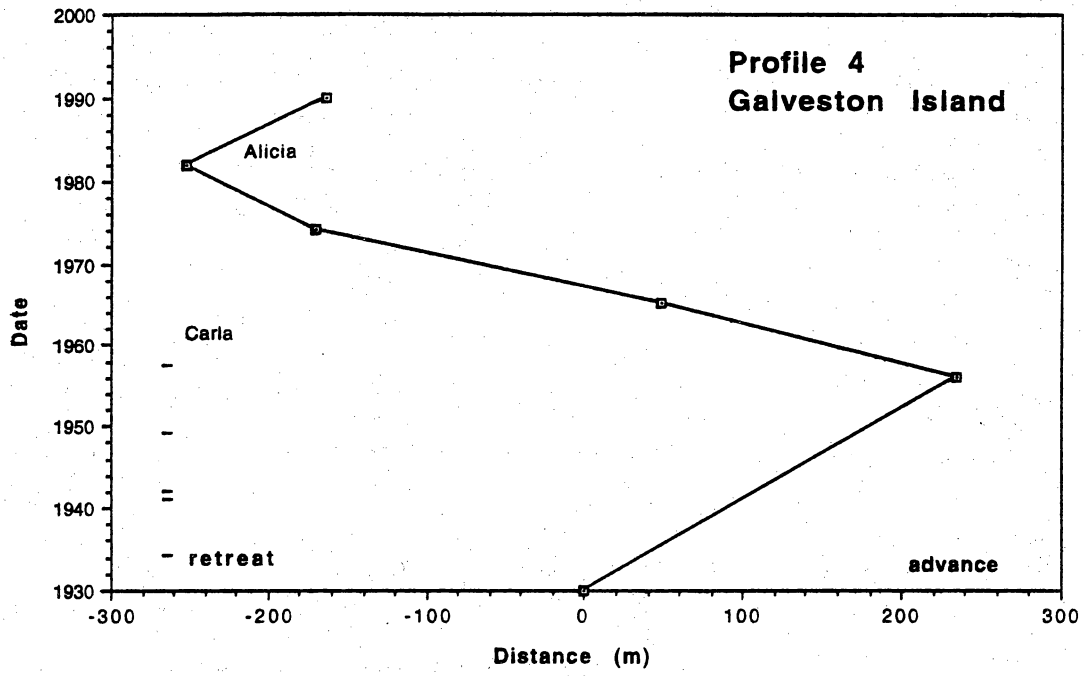
Profile 4
Galveston Island
Alicia
Carla
retreat
advance
Date
Distance (m)
2000
1990
1980
1970
1960
1950
1940
1930
-300
-200
-100
0
100
200
300

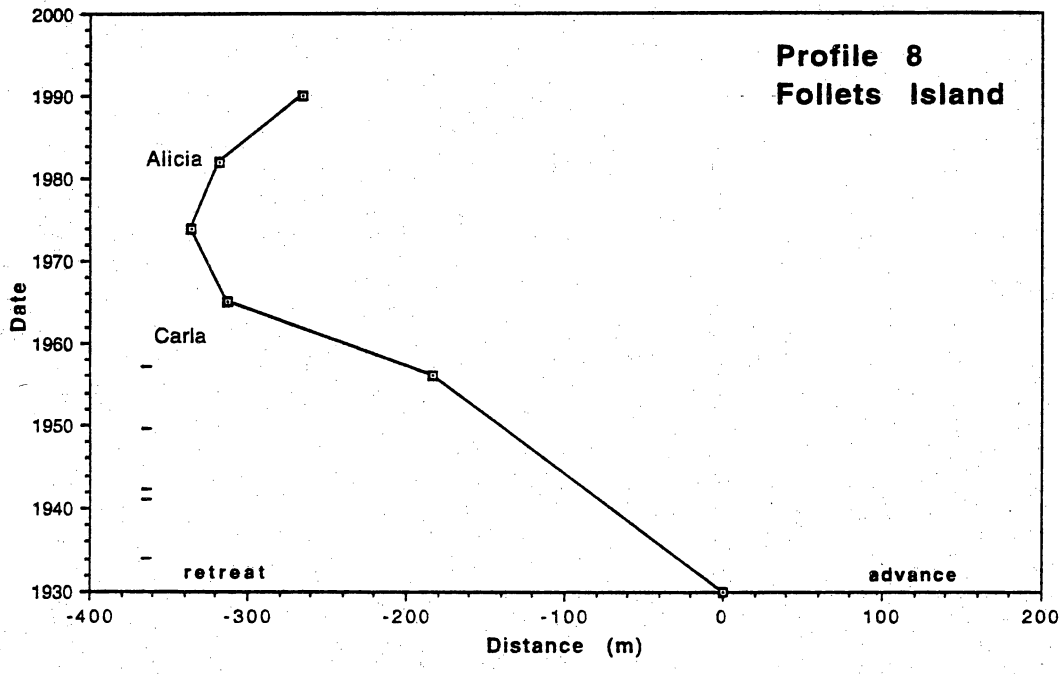
Profile 8
Follets Island
Alicia
Carla
retreat
advance
Date
Distance (m)
2000
1990
1980
1970
1960
1950
1940
1930
-400
-300
-200
-100
0
100
200

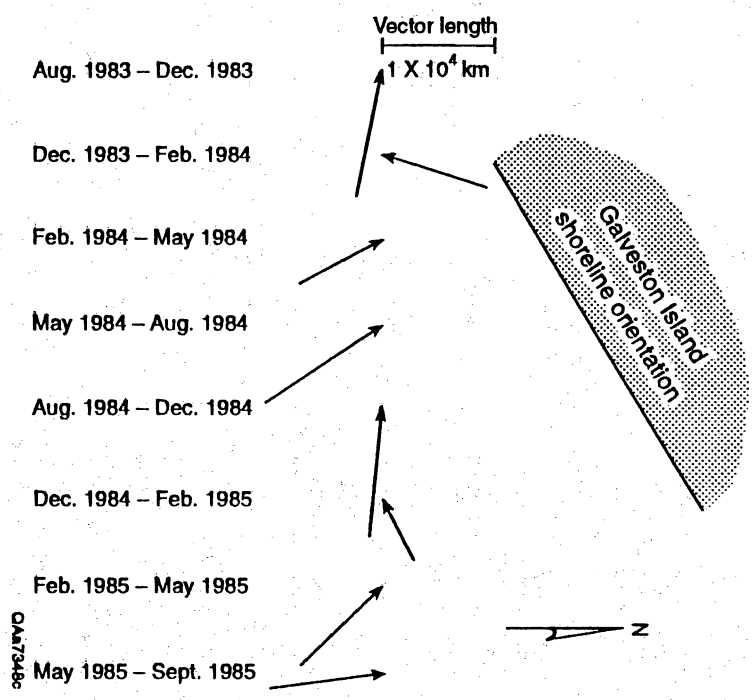
Vector length
1 X 10^4 km
Aug. 1983 – Dec. 1983
Dec. 1983 – Feb. 1984
Feb. 1984 – May 1984
May 1984 – Aug. 1984
Aug. 1984 – Dec. 1984
Dec. 1984 – Feb. 1985
Feb. 1985 – May 1985
May 1985 – Sept. 1985
Galveston Island shoreline orientation
N
OAa7348c

Table 1. Cumulative beach volume at profile sites on Galveston and Follets Islands since Hurricane Alicia. Profile locations shown on Fig. 1. NR= not recorded, * value estimated.

Date	Profile 1	Profile 2	Profile 7	Profile 3	Profile 5	Profile 4	Profile 8
Aug. 1983	-51.2	-55.8	-60.3	-55.1	-71.3	-73.0	-35.*
Dec. 1983	-47.5	-45.4	-50.1	-41.7	-49.6	-72.0	-32.5
Feb. 1984	-45.3	-40.9	-44.7	-34.7	-58.4	-69.0	NR
May 1984	-34.3	-41.6	-41.3	-32.8	-51.2	-71.9	NR
Aug. 1984	-27.5	-30.6	-36.7	-25.7	-40.7	-67.5	-13.2
Dec. 1984	-34.4	-40.9	-31.0	-23.3	-49.6	-68.3	-10.0
Feb. 1985	-44.5	-34.00	-30.0	-23.2	-49.2	-77.9	-14.9
May 1985	-32.5	-35.8	-27.0	-17.5	-44.7	-73.8	-10.1
Sept. 1985	-29.0	-27.9	-27.3	-7.4	-42.7	-75.9	-1.0
Oct. 1987	-28.1	-17.4	-17.4	2.5	-53.6	-81.3	NR
Aug. 1988	-27.3	-18.4	-19.4	-0.4	-50.1	-101.7	NR
Sept. 1989	-32.1	-29.0	-18.4	-17.7	-47.1	-91.8	33.3
Aug. 1990	-37.8	-17.2	-10.1	-8.1	-34.6	-93.4	48.8
Nov. 1991	-45.8	-29.8	-13.2	0.0	-38.9	-76.3	54.8
Apr. 1993	-57.2	-9.8	-17.2	33.3	-40.7	-29.7	63.4

Table 2. Incremental volumetric changes (m^3/m) at profile sites on Galveston and Follets Islands surveyed from August 1983 to April 1993. Stages refer to periods of post-storm recovey.

	Stage 1				
Profile	**12/83**	**2/84**	**5/84**	**8/84**	**12/84**
1	3.7	2.2	11.0	6.8	-6.9
2	10.4	4.5	-0.7	11.0	-10.3
7	10.2	5.4	3.4	4.6	5.7
3	13.4	7.0	1.9	7.1	2.4
5	21.7	-8.8	7.2	10.5	-8.9
4	1.0	3.0	-2.9	4.4	-0.8
8	2.5	6.4	6.4	6.4	3.2

	Stage 2		Stages 3 and 4		
Profile	**2/85**	**5/85**	**9/85**	**10/87**	**8/88**
1	-10.1	12.0	3.5	0.9	0.8
2	6.9	-1.8	7.9	10.5	-1.0
7	1.0	3.0	-0.3	9.9	-2.0
3	0.1	5.7	10.1	9.9	-2.9
5	0.4	4.5	2.0	-10.9	3.5
4	-9.6	4.1	-2.1	-5.4	-20.4
8	-4.9	4.8	9.1	17.2	8.6

	post-recovery changes				
Profile	**9/89**	**8/90**	**11/91**	**4/93**	**Cumulative**
1	-4.8	-5.7	-8.0	-11.4	-6.0
2	-10.6	11.8	-12.6	20 .0	45.1
7	1.0	8.3	-3.1	-4.0	43.1
3	-17.3	9.6	8.1	33.3	88.4
5	3 .0	12.5	-4.3	-1.8	30.6
4	9.9	-1.6	17.1	46.6	43.3
8	8.6	15.5	6.0	8.6	98.4

Table 3. Effects of Hurricane Alicia (1983) on shoreline movement at Galveston Island and Follets Island, Texas.

Profile Site	1974-82 m/yr	1982-90 m/yr	Observed Change
1 Tower Base	- 2.2	- 3.2	retreat accelerated
2 Gal. Is. State Park	- 1.4	- 5.8	retreat accelerated
7 Jamaica Beach	- 0.8	- 6.9	retreat accelerated
3 Sea Isle	0.0	- 3.0	trend reversed
5 Terramar	0.0	- 5.8	trend reversed
4 San Luis Pass	- 10.3	+ 11.1	trend reversed
8 Follets Island	+ 2.1	+ 6.7	advancement accelerated

Beach Stability Categories	Trend Reversed	Trend Unaltered
Rate Unchanged		
Rate Accelerated	Profiles 3, 4, 5	Profiles 1, 2, 7, 8
Rate Decelerated		

Addendum 5. Geo-Indicators of Coastline and Wetland Changes

GEO-INDICATORS OF COASTLINE AND WETLAND CHANGES

Robert A. Morton
Bureau of Economic Geology
The University of Texas at Austin, Austin, Texas U.S.A.

ABSTRACT: Coastal wetlands and shorelines worldwide are changing rapidly as a result of natural physical processes and human activities. Shoreline position and wetlands distribution are the two most reliable geo-indicators of coastal change that have global application, are relatively easy and inexpensive to monitor, and directly address the environmental problem of coastal land loss. Beach width, morphology, and composition are supplementary indicators of shoreline movement whereas fluctuations in hydroperiods, water and soil salinities, and sedimentation rates are supplementary indicators of wetland change. Monitored physical parameters that complement coastal geo-indicators include elevation and sea-level trends, frequency and intensity of storms, climate, and sediment budgets.

Shoreline position and wetlands distribution are monitored by sequentially comparing boundaries mapped from ground surveys or from aerial photographs. The geologic history and stratigraphic record establish local baseline conditions while historical conditions are determined from the oldest accurate maps. Maps depicting wetland changes and graphs illustrating cumulative shoreline movement are particularly helpful to non-scientists responsible for making decisions about future land use and resource management.

Recommended frequency for measuring coastal geo-indicators is inversely proportional to the rate of change and directly related to the availability of source materials. Systematic updating to ascertain long-term trends typically is conducted about every 5 to 10 years. More frequent analyses are subject to large errors and low signal-to-noise ratios. Event monitoring records rapid environmental changes caused by major storms or floods and provides a basis for determining how the environment responds to and recovers from high-energy events.

INTRODUCTION

Few areas of the world experience sustained environmental changes like those of coastal regions. Coastal shores and wetlands worldwide are extremely dynamic and in many areas the rates of shoreline retreat and wetland loss are accelerating. For this reason geological methods for monitoring and detecting rapid coastal change have existed for several decades primarily in response to land loss and coastal hazards issues. National assessments of extreme coastal erosion and wetlands loss were some of the first scientific data that eventually influenced coastal regulations and were incorporated into national environmental management policies in the United States, Canada, Australia, and western Europe.

Because coastal environments are some of the most dynamic on earth, it is important to continue identifying and monitoring geo-indicators of environmental change that are sensitive even though they may not be diagnostic. That is, the indicators may not identify the causal factor(s) responsible for the observed changes (fig. 1). The causes of coastal change at a particular site may never be fully understood, but this lack of explanation should not deter the establishment of long-term monitoring programs that will provide the only scientifically valid basis for future coastal planning and resource management strategies.

SHORELINE AND WETLAND CHANGES: ARE THEY REAL OR ONLY APPARENT

Predicting future shoreline positions and wetlands distribution requires an understanding of the factors that cause fluctuations in water levels, sediment volumes, and wetland habitats near the coast. Coastal shores and wetlands are constantly changing in response to a hierarchy of processes that occur as a result of daily tides, weather events, storms, and changes in climate. When reduced to their simplest terms, shoreline movement and wetlands distribution are determined largely by two independent variables: water level and sediment volume (fig. 2) that control the land-water boundary.

Fluctuations in Water Level and Sediment Volume

Changes in water level over geological time scales are controlled mainly by climate and movements in the earth's crust. Sea-level fluctuations of progressively briefer periods are related to climatic effects, cycles related to summer and winter seasons, and daily tides. Water level fluctuations cause both actual and apparent shoreline movement depending on whether or not the movement is also accompanied by changes in sediment volume (fig. 2). Temporary shoreline movement caused just by water level fluctuations are most pronounced along low-gradient coasts. These anomalous shoreline shifts can occur as a result of abnormally high water levels (abundant rainfall, floods, storms) or abnormally low water levels (droughts, offshore directed wind). Hourly readings at tide gauges are used to determine differences in water levels to prevent misinterpreting temporary water-level changes as actual beach and wetland changes.

Beach erosion and accretion are coastal responses to nearshore changes in sediment volume (fig. 2 between S_2 and S_3). Deficits and surpluses in sediment volume, also referred to as sediment budget, account for long-term beach erosion and accretion, whereas short-term shoreline fluctuations may involve only temporary removal or addition of beach material. Longshore migration of sand bars is an example of short-term shoreline fluctuations caused by temporary changes in sediment volume.

Fluctuations in sediment volume are much more irregular and difficult to predict than water-level oscillations. Also the length of shoreline effected by fluctuations in sediment volume are usually restricted whereas water level oscillations typically involve the entire shore surrounding a body of water.

Qualitative versus Quantitative Coastal Geo-indicators

Two fundamental approaches to coastal geo-indicators are possible; one that simply detects environmental change without providing a rigorous basis for prediction and one that serves as a long-term historical record and provides quantitative rates of change suitable for forecasting future conditions. Determining which approach is appropriate depends on the financial resources available, the quality of source data, and the types of applications expected from the results.

Qualitative coastal geo-indicators (discussed by Bush et al. in Chapter __) are best suited for situations where funds are extremely limited, source data are either unavailable or of poor quality, and the primary coastal management objective is to provide a quick assessment of current conditions and possible future conditions. These restrictions apply to coastal monitoring in many developing countries.

Qualitative geo-indicators are inherently limited in their application and the interpreted results can be either misleading or incorrect because observations are site specific and reflect only the most recent events that may be out of equilibrium with the long-term processes. For example, both false positive and false negative indications of beach erosion are commonly observed on beaches in diverse geological settings. There may be false indications of long-term beach erosion if field observations are made shortly after a storm causes local erosion of a stable or accreting beach. Furthermore, some beaches undergoing long-term erosion exhibit the morphologies and vegetative cover of stable or accreting beaches. Only quantitative analyses of long-term historical trends are able to avoid the potential errors associated with non-quantitative descriptors of beach stability. The remainder of this paper addresses quantitative methods of monitoring coastal change over times periods of decades to a century.

GEO-INDICATORS OF SHORELINE MOVEMENT

Shoreline Position

Each year as the world's coasts become more densely developed, the costs of property loss and structural damage near the shore dramatically increase. In response to these economic pressures, some governments have imposed strict regulations such as coastal construction setback lines and hazard zones that are designed to minimize damage and economic losses related to storms or long-term beach retreat. The construction control lines and other regulatory boundaries usually are based on long-term trends of shoreline position, which is the most reliable geo-indicator of beach stability.

For centuries shorelines have been surveyed because they represent legal boundaries separating private and public ownership of land. Shoreline position can be monitored from field observations and measurements or from historical documents such as maps and aerial photographs. The materials and methods of shoreline monitoring and their limitations are discussed in detail in later sections.

Supplementary Indicators of Shoreline Movement

Beach stability also can be determined from field measurements of beach width and from aerial photographs that permit monitoring shoreline proxies such as the vegetation line, dune line, and bluff line. These subaerial boundaries are secondary indicators of shoreline movement that can provide ancillary information about local beach dynamics or they can serve as additional ground control for mapping the high water line.

Beach Width

Measuring the width of the dry beach is a rapid, inexpensive field method of tracking shoreline movement (Wright and Pilkey 1989). This procedure involves measuring horizontal distances from a fixed reference mark to the wet-beach dry-beach boundary by pacing or with a tape measure. Conducting these measurements at several sites permits alongshore comparison of trends and rates of change. A limitation is that the measurements are subject to local variations in water level and sand storage even if the measurements are conducted during the same season (summer) when the beach achieves its maximum width. Also, it may take ten years or more of these types of measurements before the long-term trend can be separated from the annual variability (Eliot and Clarke 1989).

Morphology and Vegetation Line

Where bluffs or sea cliffs are the predominant shoreline type, position of the bluff top and bluff toe are appropriate geo-indicators of shoreline movement (Emery and Kuhn 1982). These shoreline proxies are more reliable than the wet beach-dry beach line since they are not

influenced by changes in water level. Other than this advantage, mapping the bluff top or vegetation line are subject to the same errors as mapping the shoreline since they involve scale and resolution of photography.

Although long-term movement of the vegetation line will parallel movement of the shoreline, it responds to different environmental conditions and can actually have short-term movement that is opposite to that of the shoreline. Therefore the vegetation line is less sensitive than other geo-indicators of shoreline movement. Also in some places the vegetation "line" is actually a transition zone, in other places the boundary is sharp and distinct requiring little interpretation. The problems of mapping vegetation also involve temporal changes in appearance of the vegetation line at the same site. In general, these difficulties are resolved through an understanding of coastal processes and a thorough knowledge of factors that affect appearance of the vegetation line on photographs.

Forbeach Composition

The type of material that composes the forbeach also can indicate beach stability. The clearest field evidence of long-term shoreline retreat is forebeach material with different textures, composition, and shell assemblages than the berm crest and backbeach. Anomalous beach materials often are exposed after high-energy events erode the forebeach and expose relict sediments such as bay/estuarine deposits. Along some coasts, marsh mud, peat, and indurated sediments underlie the mobile beach sediments. Concentrations of other detritus such as rock fragments or displaced brackish-water fauna from estuarine deposits also are evidence of relict sediments excavated from the shoreface as the beach retreats.

GEO-INDICATORS OF WETLAND CHANGE

Coastal wetlands are some of the most economically valuable and functionally important coastal environments because of their unique habitats, high primary productivity, and direct linkage with the food web. Therefore, future protection and management of wetlands partly

depends on developing geo-indicators of wetland change that are similar to those established for shoreline movement. Wetland distribution is a reliable geo-indicator that provides early detection of rapid changes that might threaten wetland sustenance (Dahl et al. 1991).

Wetlands Distribution

Wetland changes can follow several critical pathways depending on the causes and rates of change. Systematic transformation of coastal uplands to vegetated wetlands and vegetated wetlands to barren flats or open water generally indicate a relative rise in sea level caused by a eustatic rise and/or land subsidence (White and Tremblay 1994). Methods of monitoring the spatial distribution of wetlands are similar to those used to monitor shoreline position, which are described in later sections.

Supplementary Indicators of Wetland Change

Periodic monitoring of plant coverage, hydroperiods, sedimentation rates, and salinities provides secondary indicators of wetland change.

Vegetation Densities

Plant density is a field-based indicator of wetland status. It is monitored by identifying plant species and estimating percent coverage within a plot along transects that cross the wetland. This labor-intensive procedure has the same limitation as most field measurements in that long-period records are required before a trend is established. To maintain consistency and to avoid biased data, surveys should be conducted at the end of the growing season before annual dieback occurs.

Hydroperiod

Changes in wetland stability related to surface and ground water levels can be detected by monitoring water levels in permanently inundated wetlands and by recording the frequency and duration of flooding in wetlands that are not permanently inundated (Mitsch and Gosselink

1986). The sources of water (rivers, estuaries, upland runoff) and physical forces acting on the water (wind, tides, barometric pressure) control the hydroperiod, which can be measured using a simple and inexpensive staff gauge or with more sophisticated equipment such as automatic digital recorders.

Wetland Sedimentation Rates

Some wetlands require periodic additions of sediment in order to remain viable, whereas others are self-sustaining if plant production and accumulation of organic detritus exceed decomposition or export of detritus. Changes in the rates of organic or inorganic sediment accumulation can be detected by direct measurement or by inference from radiometric dating (Olsson 1986; Appleby and Oldfield 1992). Direct measurement involves establishing a vertical datum at a stable reference station and periodically measuring the height of the wetland surface (Cahoon and Reed 1993). Changes in wetland elevation are interpreted considering such things as plant mass, bioturbation, and in *situ* deposition or erosion of organic and inorganic sediment.

Radiometric dating is an expensive specialized geochemical technique that can yield precise rates of sedimentation. It is based on the theory that the atmosphere contains uniform concentrations of certain isotopes that are incorporated into sediments either through airfall or precipitation. Once incorporated, the isotope decreases in concentration and converts to another form (daughter product) at a rate determined by its half life. By knowing the ratio of concentrations between the parent material and the daughter product, the number of half lives can be determined and thus the age of the material can be calculated. Sediment reworking and geochemical contamination are the primary sources of error that could invalidate the dates (Olsson 1986).

To determine wetland sedimentation rates at a particular site, samples are collected from a vertical profile (core, trench) and analyzed for the isotope that is appropriate for the period of interest. Cesium 137 (^{137}Cs) is used to date sediments deposited since the 1950s, lead 210

(^{210}Pb) is used for the past 150 years, and carbon 14 (^{14}C) is used to date sediments that are 500 to 50,000 years old (Olsson 1986).

Water and Soil Salinities

Waters and soil chemistry have a profound influence on wetland structure and function (Mitsch and Gosselink 1986). Therefore, monitoring these parameters can indicate physical changes that might improve wetlands or cause their deterioration. Numerous studies have shown that encroachment of saltwater into brackish and fresh-water marshes causes plant mortality and may destroy the marsh if it is not replaced by salt-tolerant plants. A simple field procedure to detect changes in ground water and surface water involves measuring water and soil salinities.

MONITORING COMPLEMENTARY COASTAL PARAMETERS

Elevation and Sea-Level Trends

Sea-level histories, releveling surveys, and tide records can be integrated to decipher crustal deformation, elevation changes, and increased ocean volumes at a coastal site. Although historical records of relative sea level are both spotty and brief in most countries, the results show coastwide trends that demonstrate the interrelationships among vertical crustal motion, sediment compaction, and eustatic fluctuations (National Research Council 1990a; Emery and Aubrey 1991).

Several geological studies have demonstrated how unloading of thick continental ice sheets causes rebounding near former glaciers and collapse of the surrounding forebulge as evacuated crustal material returns to the uplifted regions (Clark et al. 1978; Peltier 1987). These crustal-response models also have been used to explain the variability among historical sea-level records and the current rates of vertical motion derived from those data. Long-term monitoring studies also have shown that production of subsurface fluids (oil, gas, water) can induce land subsidence and activate faults that locally cause even greater subsidence of low-lying coastal plains (Morton and Paine 1990; White and Tremblay 1994). In these areas of induced subsidence, historical

rates of relative sea-level rise are much greater than geological rates of subsidence (Morton 1979). Thus, sea level and surface elevation serve as important monitoring parameters that complement geo-indicators of shoreline movement and wetland change.

Frequency and Intensity of Storms

Storm waves and currents are capable of causing rapid shoreline retreat and wetlands destruction and for that reason storm histories are monitored to help explain observed coastal changes. Where accurate long-term meteorological records are available, shoreline movement has been correlated with the frequency and intensity of storms (Fenster and Dolan 1993). Beach retreat is greatest when storms are strong or numerous, and retreat rates are lowered when storms are infrequent or weak. Storms can be either harmful or beneficial to coastal wetlands depending on the type and amount of material removed from or added to the environment (Conner et al. 1989). Of particular interest to coastal monitoring are storm surge heights and durations because they are indicators of how deep beaches and wetlands are flooded and how long they are exposed to high energy.

Sediment Budgets

A sediment budget is an accounting method that determines the gains and losses of sediment in a coastal compartment (U.S. Army Corps of Engineers 1977). Like bank accounts, sediment budgets can be either balanced or have surpluses or deficits. A sediment surplus generally means that new land is being constructed (beach accretion, wetland aggradation) and a sediment deficit generally means that coastal land is being lost (beach or wetland erosion). The accounting procedure attempts to identify where the sediment is coming from (sources) and where it is being deposited (sinks); it also estimates the volumes of sediment gained from the sources and lost to the sinks or transferred to the adjacent downdrift coastal compartment. Common sediment sources are coastal rivers, updrift beach or bluff erosion, and the inner continental shelf.

Common sediment sinks include coastal dunes, storm washovers, tidal deltas, beach accretion, and the inner continental shelf.

Although simple in concept, accurate sediment budgets are extremely difficult to quantify because the necessary topographic and bathymetric data are generally lacking even in "data-rich" countries. Furthermore, there is a large error margin in the data analysis owing to the assumptions. For example, beach profiles are often used to estimate sediment budgets, but most of the nearshore sediment in motion is submerged, which requires detailed bathymetric surveys that seldom are available for several time periods.

Climate

At some coastal sites, weather patterns are variable enough to influence shoreline position and wetlands distribution. Therefore continuous monitoring of wind speed and direction, air temperature, and precipitation at weather stations provides a basis for interpreting the geo-indicators of coastal change. Particularly important are cycles of abundant precipitation or drought or periods of extreme temperatures. Record heat or freezes can have negative impacts on wetlands while abundant rainfall and dry periods can effect water levels, which in turn, can alter both shoreline position and wetlands distribution.

INFORMATION SOURCES AND THEIR LIMITATIONS

Basic Data

Coastal planners and resource managers need to understand past coastal changes in order to anticipate where the shoreline and wetlands will be in the future and to predict what the trends and rates of shoreline movement and wetland changes might be. These objectives are best accomplished by depicting coastal change on maps, which provide a basis for understanding the dynamics of the coast. Historical shoreline positions and wetlands distribution can be obtained

from topographic maps, aerial photographs, and ground surveys. The most common errors encountered when using maps and aerial photographs are summarized in Table 1.

Analysis of coastal change involves mapping several shorelines or wetland boundaries at the same site, comparing the boundary positions through time, and calculating rates of shoreline movement or wetland changes for several time periods (Stafford 1971; Leatherman 1983; Morton 1991, Fenster et al. 1993; Britsch and Dunbar 1993; White and Tremblay 1994). Recently, Anders and Byrnes (1991), Crowell et al. (1991), and Thieler and Danforth (1994) reviewed the types of errors typically associated with topographic maps and aerial photographs and estimated how large the errors might be if they depend on the scale of the original material.

Topographic Maps

The oldest reliable shoreline positions and wetland distributions are preserved on coastal topographic maps. In some European countries, accurate coastal charts extend back to at least the 14th century (Niemeyer 1993) but in most countries accurate maps are much more recent (Shalowitz 1964). Boundary movement is measured by comparing the oldest accurate maps with more recent surveys or maps using geographic coordinates (latitude and longitude) or fixed landmarks. Many old maps also accurately portray stable land features, such as interior ponds, tidal creeks, and hills that can be compared with the same features on more recent surveys or aerial photographs. The stable land features provide horizontal control for map comparison that does not depend on precise latitude and longitude position.

There are both advantages and disadvantages associated with using old topographic maps for shoreline and wetland change analyses. The principal advantage is that the period of record is extended as far back as possible. Furthermore, the longest reliable record of boundary change generally will provide the most reliable basis for predicting future changes (Table 1). A minor disadvantage is that documented coastal changes may be difficult to interpret because information regarding storms or other events effecting the coast is generally lacking for the earlier periods.

Aerial Photographs

Vertical aerial photographs are the most common source of shorelines and wetlands because air photos are much faster and less expensive to obtain than regional ground surveys. Both stable geomorphic features and cultural features (buildings and roads) observed on the air photos can be used to compare them with other air photos or with topographic maps. The positions of some ground features observed on air photos may be slightly inaccurate because of minor scale differences and distortions that occur across the photograph (Table 1). These minor errors are caused by movement of the plane that prevents the camera from being exactly perpendicular to the surface of the earth. Slight up and down movement of the plane causes minor changes in scale from one photograph to another, whereas slight tilting of the wings or nose of the plane causes distortions across the photograph. The distortion errors are small near the center of the photograph so, if possible, the center of the photograph should be used for mapping the shoreline. The minor errors caused by movement of the plane are inconvenient, but there are several optical and digital techniques that can be used to correct for distortions and scale differences.

The shoreline proxy most commonly mapped on aerial photographs is the high water line that separates the wet beach from the dry beach (Stafford 1971; Morton 1979; Dolan and Hayden 1983). The wet beach-dry beach line is not a tidal datum, such as the mean high water line, and it represents the highest water levels occurring immediately before the photographs were taken. Because wave runup is large on low-gradient sandy beaches, the high water line on those beaches is sensitive to changes in water level caused by strong winds or unusual tides. As a result, shoreline movement mapped for some sandy beaches may be caused by differences in water levels rather than actual changes in sediment volume (fig. 2). Shorelines mapped on aerial photographs could be reconstructed to a specific tidal datum using local correction factors for beach slope and water levels (Stafford 1971), but the dynamics of sandy beach profiles preclude making these corrections with much confidence. The potential for mislocating the shoreline on air photos due to water level fluctuations is not a problem on steep beaches or steep rocky shores.

Although a single criterion typically defines shoreline position, wetlands are defined on the combined basis of local hydrology, vegetation, and soils (Mitsch and Gosselink 1986). Frequency and duration of flooding, plant communities, and soils composition are all used to classify wetlands. The boundaries circumscribing the wetlands are identified on aerial photographs from reflectance characteristics that are related to species composition and soil wetness. Potential errors in interpreting wetlands from remotely sensed images derive from three sources: water level fluctuations, growing season of emergent aquatic vegetation, and photographic scales (Carter et al. 1979). The first two error sources cause the most serious problems because they may indicate changes in wetland distribution that are not real.

When shorelines and wetlands are mapped from aerial photographs, it is assumed that the interpreted boundary represents typical or average conditions and that subsequent changes in the boundary are caused by normal physical changes in the environment. This assumption can be verified only indirectly by examining tide gauge records, meteorological reports, and other historical documents that indicate either abnormal conditions or the lack of unusual events preceding each photographic mission.

Beach Profiles

Shoreline movement can also be documented by profiling the beach (fig. 3), a standard field method that involves making repeated measurements along a transect oriented perpendicular to the shoreline. These measurements may consist of a single observation, such as dry beach width or they may involve surveying the entire beach surface. Beach profiles require establishing a reference mark from which distances and elevations are measured along a transect. The reference mark can be a benchmark or some other stable feature such as the corner of a seawall or sign post.

The expected results determine where and how frequently beach surveys should be conducted and the type of equipment used (Table 2). Surveys that rely on a tidal datum or property boundaries should be conducted by a registered surveyor using expensive equipment. On the

other hand, simple advance and retreat of the beach can be measured with portable inexpensive equipment as long as the same profile location is reoccupied.

Beach profiles can be measured with various types of equipment ranging from simple graduated rods and chains (Emery 1961), to standard stadia rod and level, to a more accurate autotracking geodimeter with a reflecting prism (Birkemier et al. 1991). The more sophisticated techniques offer greater measuring precision, but they also require more field support and data processing equipment, such as computers and specialized software. The Emery method is a simple but accurate profiling technique that can be quickly learned by anyone.

A beach profile is obtained by adding the horizontal distances and corresponding changes in beach elevations and plotting those values on graph paper or entering the data into a computer graphics program. Changes in the beach are detected by repeating the surveys at the same site every few months or years and comparing the profiles (fig. 3). Either the sea-level datum or the berm crest can be used to indicate beach movement between consecutive surveys.

A typical shore-normal beach survey yields a one-dimensional profile that represents the relative height of the beach from a fixed reference marker. The profile also displays the position of particular beach features, such as high water line, berm crest, dunes, vegetation line, or a datum intercept such as mean sea level. Comparison of subsequent beach surveys yields a two-dimensional cross-sectional area, which represents the amount of beach erosion and deposition that occurred between surveys. A three-dimensional volumetric change in the beach can be derived from the profiles by integrating between adjacent cross-sectional areas.

Beach profiles are limited in their application because (1) they are site specific and they do not provide a continuous shoreline position along the coast, (2) it takes several days to conduct regional surveys, and (3) the "permanent" reference markers are commonly lost (covered by dense vegetation or sand) or destroyed (erosion, vandalism). A primary advantage of beach profiles is that the uncertainties of the wet beach-dry beach line are eliminated and observations of shoreline movement are based on actual field measurements rather than interpreted indirectly from aerial photographs. Another advantage is that frequent comparisons yield information

about two-dimensional beach changes that can be used to calculate the volume of sediment added to or removed from the beach. These volumetric estimates of sediment movement cannot be accurately derived from aerial photographs.

Profiling is a rapid and inexpensive field method best suited for documenting changes in beach shape and evaluating the magnitude of seasonal or short-term movement in shoreline position. Normally beach profiles are not used to establish long-term trends of shoreline movement because more than 10 years of continuous data are needed before the long-term trend can be established with confidence (Eliot and Clarke 1989).

GPS Surveys

GPS (Global Positioning System) is an advanced satellite-based electronic surveying technology that is being adapted to monitor shoreline position and wetland distribution. In the future GPS will be the field method most widely used for coastal surveys (Morton et al. 1993; Michener et al. 1993).

A potential disadvantage of GPS is the inaccuracy that is introduced by selective availability. This procedure deliberately degrades the radio signal transmitted by some satellites to prevent unauthorized users from determining precise locations, especially during war. This means that positions obtained by a single GPS receiver will only be accurate within about 100 m of its actual position. Because of selective availability, the locations provided by single GPS receivers are not accurate enough to map coastal changes.

Differential GPS techniques were developed to eliminate the uncertainty introduced by selective availability. In the differential mode of operation, two GPS receivers are used; one stays at a reference point (base station) and the other moves about (rover) conducting the survey. The reference point typically is a surveying monument or bench mark where the latitude, longitude, and elevation are known.

Beaches and wetlands are nearly ideal environments for conducting GPS surveys because the field of view with the satellites is largely unobstructed. However, some developed shores may

impede or prevent GPS surveys because of interference with the satellite signals. Isolated structures such as tall buildings may cause some minor shading, whereas dense high-rise developments may block the signal from some satellites near the horizon or cause multipath reflections severe enough to invalidate the surveys.

Techniques have been developed to accurately survey beaches by mounting a GPS antenna on a vehicle. Horizontal distances and elevations are recorded as the vehicle drives up and down the beach. An advantage of vehicle-mounted GPS surveys is that they can provide rapid, relatively inexpensive and repeatable topographic information over long distances with minimal manpower and equipment (Morton et al. 1993).

The entire beach surface between the water line and the dune line can be surveyed using GPS techniques. Shoreline positions can be frequently updated and changes in sediment volume can be determined by comparing the surfaces recorded by repeated surveys of the same beach segment. GPS surveying techniques provide positions without the need for permanent reference marks. Therefore they are particularly well suited for monitoring beaches and wetlands where the reference marks may be destroyed during a storm.

Processed Data and Compiled Databases

In the United States, national wetland changes are assessed by the National Wetlands Inventories program of the U.S. Biological Survey (Cowardin et al. 1979; Dahl et al. 1991) while shoreline movement along oceanic shores and the Great Lakes is addressed by the U.S. Geological Survey as part of their national Coastal Geology Program (Williams et al. 1991).

Distinguishing apparent coastal changes from real changes is a major challenge when using national inventories that are compiled from disparate data sets. Unqualified comparison of historical and recent data can lead to incorrect results and erroneous conclusions if knowledge of local processes and history of the surveyed area are not incorporated into the analysis along with knowledge of the mapping techniques. Potential errors in detecting shoreline movement arise from seasonal beach variability, and anomalous climatic and meteorological conditions

immediately preceding the photography used to map the shoreline. Potential sources of errors for wetlands are the same as those for shoreline movement with the addition of temporal changes in wetland classifications. A GIS is incapable of distinguishing real wetland changes from a change in classification, so some reported changes in wetlands distribution may be an artifact of evolving classification schemes.

QUANTIFYING GEO-INDICATORS OF COASTAL CHANGE

Shoreline movement and wetland changes are evaluated and summarized using similar techniques that employ visual, tabular, and graphical representations of the data.

Comparing Coastal Boundaries

Shorelines and wetland boundaries can be transferred from the original maps and aerial photographs onto large-scale topographic base maps to facilitate high-precision measurement of shoreline movement and wetland change. Linear distances and areas are measured directly from the base maps or the compiled boundaries can be digitized and entered into a geographic information system (GIS) for further data manipulation and storage (Byrnes et al. 1991; Scaflani et al. 1993). If boundaries are digitized directly from the original maps and photographs, computer algorithms are used to compare the boundaries by making statistical least-squares adjustments to correct for paper distortions as well as different projections and scales of the original materials (Leatherman 1983; Thieler and Danforth 1994).

Presenting Coastal Changes

Historical changes in shoreline position and wetlands distribution can be presented as maps, in tables, and on charts. All three forms of data presentation have advantages and disadvantages compared to the other two (Table 3). Maps of sequential boundary positions (figs. 4 and 5) illustrate coastal shorelien and wetland changes as a series of lines or patterns that are compared

to determine the magnitude and trend of change. Maps offer a visual historical representation of spatial and temporal boundary changes that are related to other geographic features and they convey where the boundary has been in the past and imply where it might be in the future.

Changes in coastal boundaries can also be presented in tables that contain the monitoring periods as well as amounts and rates of change (Table 4). The tabular data quantify what is illustrated on the map and reduce the boundary changes to an average rate of change expressed in distance or area per unit time.

Graphs depicting shoreline movement or wetland changes through time illustrate the long-term trends and short-term variability, which also can be used to predict future changes (figs. 6-9). Shoreline history plots (fig. 6) contain three fields that represent stability, advance, and retreat of the shoreline. Shoreline positions that plot around the zero axis show that the beach has fluctuated but that over the monitoring period the beach position has remained nearly unchanged. Shoreline positions that plot to the positive or negative side of the graph record long-term advance or retreat of the beach (fig. 6).

Interpreting Graphical Displays

Shoreline positions and wetland distributions derived from maps, aerial photographs, or ground surveys represent individual points in a continuum of coastal change. Most studies of coastal changes are based on a few boundary positions spanning as much as 150 yrs (figs. 4 and 7). Studies of that duration often employ two distinctly different data densities. The lowest data density is for the first 100 yrs when boundary movement is determined from two or three maps. In contrast, most coastal boundary changes have been documented during the past 50 yrs and the highest data densities are available for the past 30 yrs (figs. 7-9). The increased number of boundary positions since 1960 provides a better measure of the short-term variability and a way of distinguishing the long-term trend from the short-term fluctuations.

The shape and slope of the line connecting a series of shoreline positions can also be used to interpret the relative rate of change and to predict future shoreline positions. In the example (fig.

7) the best linear statistical fit is not a straight line through the data points, but a curved line that is flatter in recent time. This shows that the rate of erosion has increased or accelerated in recent years. If the rate of erosion had decreased, then the curve would be steeper.

Shoreline history plots commonly illustrate different rates of change or reversals in the trend (figs. 7-9). These plots also provide a basis for fitting statistically derived regression trends that can be used to predict future changes. The graphs of shoreline movement and wetlands change are useful for visualizing the long-term trends and for recognizing unusual departures from the trend (figs. 8 and 9).

Distinguishing the actual trend of shoreline movement from "noisy" data is easy when the trend is uniform and the rate of change is so large that it cannot be confused by high-frequency beach cyclicity (fig. 7). On the other hand, this task of differentiation is extremely difficult for relatively stable beaches that experience large seasonal fluctuations. This is especially true for some dynamic sandy beaches that were stable or accreting on geological time scales, but are beginning to erode as a result of both natural and human-induced decreases in sediment supply and a rise in relative sea level (Morton 1979). For some of these transitional beaches, the short-term beach fluctuations exceed the long-term movement measured on consecutive aerial photographs (see fig. 8, 1937-1974).

Analytical problems associated with nonuniform and nonlinear shoreline changes are illustrated in figure 9, which shows two trend reversals in shoreline movement near the mouth of a river. The rate of landward retreat of the shoreline between 1853 and 1930 is similar to the long-term erosion trend for this coastal compartment before navigation projects altered the littoral system. The reversal in trend at 1930 is the result of river diversion and delta construction that caused rapid outbuilding of the shoreline at the river mouth. A reduction in sediment supply after 1956 and focusing of wave energy on the delta caused renewed but more rapid retreat of the shoreline. In this example, the 1982 shoreline is still far seaward of the 1853 shoreline (net accretion), but the most recent trend is retreat and there was a decrease in the rate of retreat between 1956 and 1982. Calculated net rates of change would indicate long-term

shoreline advancement when clearly the most recent trend and predicted future trend is shoreline retreat.

Calculating Rates of Change and Predicting Future Positions

Two assumptions are made when shoreline movement is analyzed regardless of the sources of shoreline positions. First is the assumption that the state of shoreline stability does not change during each monitoring period. This assumption of uniformity requires continuous beach erosion, accretion, or stability throughout the entire monitoring period without any reversals in trend. If reversals in trend are detected in the data, then the length of record should include as much older reliable data as possible (Table 1). Extending the period of record will provide the best indicator of why the trend reversals occurred and how they should be factored into the predictions of future boundary positions. The second assumption is that the rates of change are also constant for the same period. This assumption rules out accelerations or decelerations in boundary movement. If boundary movement is nonuniform, then the most recent rates of change should be used to predict future boundary positions (Table 1). If either or both of these assumptions is incorrect then the calculated rates of change probably underestimate the actual rates of change for the period of interest (Morton 1991).

Net rates of coastal change are useful for characterizing long-term trends and for establishing average rates of change, but net changes clearly are not the best predictor of future changes. This is because the net change value is a straight-line average determined by the first and most recent boundary positions. It does not take into account fluctuations in boundary position that are typical for most coastal areas (fig. 8).

STRATEGIES FOR MONITORING COASTAL GEO-INDICATORS

Standardization of Methods

Coastal scientists and engineers are developing standard methods of detecting, quantifying, and predicting wetland changes and shoreline movement (National Research Council 1990b). Current emphasis is on standardizing data collection, data processing, and data storage so that results are accurate and can be independently reproduced. This is accomplished by examining the available technologies, assessing their reliability, ease of application, and cost. Advanced techniques commonly employee sophisticated digital recording equipment and computers to achieve high-speed data entry and management of large databases. Unfortunately these advanced monitoring techniques are unavailable in most developing countries.

In the United States, legislation has been introduced that would standardize methods used to quantify long-term shoreline movement from aerial photographs. An important coastwide application of the methodology is calculation of average annual erosion rates for purposes of establishing construction setback lines and coastal hazard insurance zones.

Regional Networks

Coastal scientists are beginning to establish regional networks of field stations similar to those used to monitor stream discharge, climate, sea level or any number of other physical parameters. Coastal monitoring networks typically include beach profile sites and reference wetland sites where geo-indicators are measured periodically to determine the magnitudes and rates of environmental change. In the United States, Canada, Australia, and the Netherlands, networks of beach profiles are surveyed for both research and coastal management objectives (Howd and Birkemeier 1987; Forbes 1987; Short and Hall 1993; Wijnberg and Terwindt 1993). Diverse wetland sites also are being monitored to develop options for their preservation and protection. The United States Biological Survey has initiated a monitoring program that includes ten coastal wetland sites where hydroperiod and rates of sedimentation are monitored systematically (Cahoon and Reed 1993).

Frequency of Monitoring Coastal Geo-indicators

Coastal planners and managers commonly want to know the optimum period for updating maps and tables of shorelines and wetlands. Considering the diversity and dynamics of open coasts, it is not possible to determine the optimum monitoring period without some knowledge of local beach and wetland dynamics. Such decisions must be based on local factors including frequency of storms, average rate of coastal change, seasonal fluctuations, and economic considerations. Data obtained from long-term monitoring should be used to establish the boundary stability for a particular coastal segment. If boundary changes have remained consistent over the entire period of record and if for geological reasons the trend can be expected to continue, then the monitoring interval is not extremely critical unless the area is being rapidly developed. If, however, long-term boundary monitoring indicates numerous reversals in trend, then the frequency of reversals might suggest an appropriate interval for future boundary monitoring.

Recommended frequency for measuring coastal geo-indicators is inversely proportional to the rate of change and directly related to the availability of source materials. Most monitoring plans incorporate two different approaches to the question of monitoring frequency. Both constant periods and specific events are guides to determining when measurements should be made. Fixed intervals of time, such as 5 or 10 years, provide a framework for planning and an estimate of when work would be needed unless there are extenuating circumstances such as a storm that would require an immediate response. Pre- and post-storm surveys of shorelines and wetlands provide a basis for assessing storm damage, evaluating the degree and rates of recovery, and recognizing the phases of post-storm recovery (Morton et al. 1994).

Digitization and Geographic Information Systems

Digital databases and geographic information systems are analytical tools that facilitate comparing historical shorelines and wetlands data and resolving differences in scales and projections of the source materials (Byrnes et al. 1991; Sclafani et al. 1993). Operational errors

associated with data conversion and manipulation within a GIS were evaluated by Walsh et al. (1987).

Although a GIS improves comparison, storage, and printing of coastal boundary information, computers do not improve the accuracy of the original boundary positions. Computers can increase the precision of mapping and statistical analyses, but the degree of accuracy depends entirely on the quality of the original data and the care taken to assure the reliability of data interpretation and entry into the GIS.

Modeling and Prediction Based on Coastal Geo-indicators

Coastal resource managers are currently focusing on how much land will be lost in the future, where the shoreline will be at some particular time, which communities will be threatened by land loss, and how much land will be flooded if sea level continues to rise. To answer these questions, several methods (models) have been developed that attempt to project shoreline positions or wetlands distribution based on assumptions regarding past changes and estimated rates of future sea level rise. Users should be aware that all long-range projections (25-50 yr) are suspect because the models are unable to anticipate significant changes in the factors that cause or control coastal changes and therefore the forecasts may not be very accurate. Despite large uncertainties, planners may want to examine model predictions because they provide at least some basis for guiding future use and development of the coast.

Models that estimate future coastal change also can be either qualitative or quantitative. Qualitative predictions of coastal evolution are based on a general understanding of how nearshore environments respond to changing oceanic conditions. Studies of modern coasts show that a rapid rise in sea level will cause narrowing of some barrier islands and accelerate the migration of other barriers while saltwater marshes or open water will replace fresh and brackish water marshes. Also during a rapid rise in sea level uplands are converted to wetlands, flood plains are enlarged, and the area that would be inundated by storms of historical record are increased. These non-quantitative

predictions of coastal change are useful for dramatizing what will happen in the future, but they are of little use when it comes to knowing where and when the changes will occur.

Quantitative predictions of future coastal change rely on either *statistical* models, *geometric* models, or *numerical (deterministic)* models. Even though all of these models can be used to predict future shoreline positions and wetland distributions, they are based on completely different assumptions (Table 5) and analytical methods. For example, statistical models do not attempt to explain the causes of coastal change. Instead, they depend on actual observations that presumably include the important conditions that cause boundary movement. Geometric models emphasize how boundary movement is controlled by shore slopes and shapes responding to increased water levels. Numerical (deterministic) models attempt to explain boundary movement as a series of equations that represent observed physical conditions and coastal processes.

Both geometric and numerical models rely on the concept of a nearshore profile that is in equilibrium with the coastal processes. Coastal engineers have suggested that offshore profiles are smooth and have a concave shape that is controlled only by the size of sand grains and the dissipation of wave energy (Dean 1991; Bodge 1992). Based on these and other assumptions, the generalized shape of the offshore profile is expressed as a mathematical equation (Bruun 1962; Dean 1991) that relates the profile shape to sediment characteristics. Recent investigations of offshore profiles, however, show that a single mathematical expression does not adequately represent all offshore profiles (Bodge 1992). Pilkey et al. (1993) discussed the assumptions of the equilibrium profile and presented strong arguments that challenge the validity of the concept. Because an equilibrium profile does not exist at most coastal sites, they also questioned the validity of shoreline change models that incorporate equilibrium profile conditions. Our incomplete understanding of complex coastal processes and the lack of an equilibrium profile are the main reasons why geometric and numerical models are unable to give reliable predictions of shoreline movement several decades into the future.

DISCUSSION

Effective coastal management plans are based on geologic frameworks and an understanding of changes in natural processes on both geological and historical time scales; otherwise, historical frames of reference used to document environmental change and to establish public policies may be out of geological context. Some environmental changes can only be understood adequately by considering natural processes over long periods. A classic example is coastal erosion. Non-specialists typically blame damming the rivers, emplacement of hard structures, or other human activities as the global causes of shoreline retreat. While these modifications aggravate the local deficit in sediment supply, many coastal areas were eroding long before human alterations interfered with the littoral system.

Natural factors such as sediment supply, wave energy, and sea level are the primary causes of coastal change, whereas human activities are catalysts that cause disequilibrium conditions that accelerate change. Human impacts on coastal shores and wetlands may be difficult to distinguish from natural environmental changes because anthropogenic effects alter existing physical processes rather than introducing a unique record of change like pollutants that act as geochemical tracers of human activities.

Although historical records of coastal change span more than a century in many countries, they are not appropriate to detect global change because they (1) represent only local conditions and (2) nearly all are incapable of accurately forecasting conditions more than a few decades into the future. Consequently, there is an ongoing need to continue monitoring coastal geo-indicators of environmental change.

ACKNOWLEDGMENTS

This work was funded partly by the U.S. Geological Survey Coastal Geology Program under cooperative agreement 14-08-0001-A0912. Publication authorized by the Director, Bureau of Economic Geology, The University of Texas at Austin.

Table 1. Principal errors associated with measurement and prediction of shoreline movement.

Method	Sources of Error	Ways of Minimizing Errors
Maps	Old topographic surveys	Use triangulation stations for geographic control
	Datum changes	Use published or annotated corrections
Photos	Radial distortion, tilt	Use spatial resection transformations
	High-water line interpretation	Acquire experiencewith coastal morphology and processes
	High-water line representation	Use large-scale format and fine-point pen
GIS	Digitizing table and cursor	Use large-scale maps and double precision digitization
	Boundary tracing	Operator experience, perform repeatability tests
	Biased geographic control	Use closely-spaced features near the shoreline
	Nonuniform beach movement	Extend the period of record to improve prediction
	Nonlinear beach movement	Use the most recent reliable period for prediction

Table 2. Important considerations and decisions to make before establishing a beach and dune monitoring program. Options are ranked from a simple comparison of beach width to complete surveys of the beach surface suitable for three-dimensional estimates of volumetric changes.

A. Type of reference markers or baseline control- Existing uncontrolled features such as seawalls and sign posts, or controlled features such as surveyed stations and geodetic benchmarks.

B. Type of beach monitoring equipment- Compass and tape measure, graduated rods and chain, theodolite, electronic total station, Global Positioning System (GPS).

C. Type of beach survey- Dry beach width, beach profiles, tidal datum (mean high water line), or entire beach surface including subaqueous as well as subaerial profiles.

D. Frequency of beach surveys- Infrequent, annual, or semi-annual depending on inferred beach stability and anticipated information requirements.

E. Training of personnel who are responsible for collecting field data.

F. Training of personnel who are responsible for analyzing and storing beach survey data (comparative profiles or surfaces), preparing shoreline change maps, tables, graphs, calculating volumetric changes, and determining sediment budgets.

G. Frequency of reporting the status of beaches and dunes- Annual , biannual, or 5-year reports on beaches (seasonal variability and storm response) and dunes (stability and extent of vegetation).

Table 3. Standard forms of presenting shoreline movement and wetland changes.

Display	Advantages	Disadvantages
Maps	1. Represent original data 2. Provide continuous shoreline coverage 3. Easy to determine geographic positions	1. May be difficult or expensive to duplicate large maps 2. Distances and rates of change are not provided 3. Interpretation is required 4. May be difficult to predict future boundary position if several boundaries are mapped
Tables	1. Easy to duplicate 2. Distances and rates of change are provided 3. Calculations or interpretations not required	1. Shoreline coverage is discontinuous 2. Locations must be determined from a map 3. Important changes in shoreline movement may not be obvious 4. May be difficult to predict future beach position if several time periods are presented
Graphs	1. Easy to duplicate 2. Illustrate the history of shoreline movement 3. Provide an empirical (visual) basis for predicting future beach position	1. Shoreline coverage is discontinuous 2. Locations must be determined from a map 3. Rates of change are not provided 4. Interpretation of plots may be required

Table 4. An example of historical shoreline movement and rates of movement for a rapidly eroding beach illustrated in figures 3 and 4.

Period	1856-1934	1934-1956	1956-1974	1974-1988	1856-1988
Distance (m)	-198	-183	-145	-134	-660
Rate (m/yr)	-2.6	-6.9	-7.2	-9.6	-5.0

Table 5. Comparison of assumptions, advantages, and disadvantages for the different types of predictive coastal change models.

Model Type	Assumptions	Advantages	Disadvantages
Statistical	Conditions that caused change in the past will not change in the future.	Easy to understand and apply. Projections are derived from average rates of coastal change or simple equations. Relies on observed boundary changes.	Predictions will be inaccurate if physical conditions at the site change significantly. Difficult to accommodate large reversals in boundary movement.
Geometric	Shoreline retreat and wetland loss are mainly caused by submergence. The beach and offshore profile are smooth and unchanging. Equilibrium conditions must be achieved before maximum recession is reached.	Easy to project shoreline and wetland positions using topographic maps and an estimate of relative sea level rise.	May greatly underestimate shoreline retreat when land loss is caused by erosion as well as submergence.
Combination	Shoreline retreat and wetland loss are mainly caused by submergence. Conditions that caused coastal change in the past will not change in the future.	Improved prediction over static geometric models	Predictions will be inaccurate if physical conditions at the site change significantly. Difficult to accommodate large reversals in boundary movement.
Numerical	Shoreline retreat and wetland loss are mainly caused by waves. Sea level is constant. The beach and offshore profile are smooth and unchanging. The equations in the model accurately simulate the physical conditions.	Mathematically sophisticated models that attempt to simulate the interactions of complex physical processes.	Requires site specific data for parameters that generally are unavailable. Requires site specific knowledge of coastal behavior. Difficult to know if results are valid.

Figure Captions

1. Common causes of coastal land loss worldwide.

2. Changes in coastal boundaries related to changes in water levels and sediment volumes. From Morton (1991).

3. Eight-year record of a rapidly retreating beach. The profiles, which were measured every two years, document persistent retreat at variable rates.

4. Map showing sequential shoreline positions of a rapidly retreating beach illustrated in fig. 3. From Pilkey et al., 1989.

5. Changes in the distribution of wetlands within a subsiding river valley near Houston, Texas. From White and Tremblay, 1994.

6. Generalized shoreline history diagram delineating the three fields of shoreline movement (advance, retreat, stable).

7. Shoreline history diagram of the rapidly retreating beach illustrated in figs. 3 and 4.

8. Shoreline history diagram of a relatively stable beach where shoreline position is temporarily altered by a period of low water (drought) and minor erosion (storm)..

9. Shoreline history diagram showing reversals in the long-term trend of shoreline movement related to local changes in sediment supply near a river mouth.

REFERENCES

Anders, F. J., and Byrnes, M. R. 1991. Accuracy of shoreline change rates as determined from maps and aerial photographs. *Shore and Beach* . 59:17-26.

Appleby, P. G., and Oldfield, F. 1992. Application of lead 210 to sedimentation studies, In M. Ivanovich & R. S. Harmon (eds) *Uranium-series disequilibrium. Applications to earth, marine and environmental sciences*:731-778. Oxford:Clarendon Press.

Birkemeier, W. A., Bichner, E. W., Scarborough, B. L., McConathy, M. A., and Eiser, W. C. 1991. Nearshore profile response caused by Hurricane Hugo, In C. W. Finkl, C. W. & O. H. Pilkey (eds) Impacts of Hurricane Hugo, September 10-22, 1989. *Journal of Coastal Research, Special Issue 8*:113-127.

Bodge, K. R. 1992. Representing equilibrium beach profiles with an exponential expression. *Journal of Coastal Research.* 8:47-55.

Britsch, L. D., and Dunbar, J. B. 1993. Land loss rates. Louisiana coastal plain. *Journal of Coastal Research.* 9:324-338.

Bruun, P. 1962. Sea level rise as a cause of erosion. *Journal of Waterways and Harbors Division.* WW1:117-133.

Byrnes, M. R., McBride, R. A., and Hiland, M. W. 1991. Accuracy standards and development of a national shoreline change data base. *Coastal Sediments '91*. 2:1027-1042.

Carter, V., Malone, D. L., and Burbank J. H., 1979. Wetland classification and mapping in western Tennessee. *Photogrammetric Engineering and Remote Sensing*. 45:273-284.

Clark, J. A., Farrell, W. E., and Peltier, W. R. 1978. Global changes in post-glacial sea level- A numerical calculation. *Quaternary Research.* 9:265-287.

Conner, W. H., Day, J. W. Jr., Baumann, R. H., and Randall, J. M. 1989. Influence of hurricanes on coastal ecosystems along the northern Gulf of Mexico. *Wetlands Ecology and Management.* 1:45-56.

Cowardin, L. M., Carter, V., Golet, F. C., and LaRoe, E. T. 1979. *Classification of wetlands and deepwater habitats of the United States*. FWS/OBS-79-31, Washington: U.S. Fish and Wildlife Services.

Crowell, M., Leatherman, S. P., and Buckley, M. K. 1991. Historical shoreline change. error analysis and mapping accuracy. *Journal of Coastal Research.* 7:839-852.

Dahl, T. E., Johnson, C. E., and Frayer, W. E. 1991. *Status and trends of wetlands in the conterminous United States, mid-1970's to mid-1980's.* Washington: U.S. Fish and Wildlife Service.

Dean, R. G. 1991. Equilibrium beach profiles: Characteristics and applications. *Journal of Coastal Research.* 7:53-84.

Dolan, R., and Hayden, B. 1983. Patterns and prediction of shoreline change. In P. D. Komar (ed) *Handbook of coastal processes and erosion*:: 123-149. Boca Raton: CRC Press.

Eliot, I. and Clarke, D. 1989. Temporal and spatial bias in the estimation of shoreline rate-of-change statistics from beach survey information. *Coastal Management.* 17:129-156.

Emery, K. O. 1961. A simple method of measuring beach profiles. *Limnology and Oceanography.* 6:90-93.

Emery, K. O., and Aubrey, D. G. 1991. *Sea levels, land levels, and tide gauges.* New York: Springer-Verlag.

Emery, K. O., and Kuhn, G. G. 1982. Sea cliffs. Their processes, profiles, and classification. *Geological Society of America Bulletin.* 93:644-654.

Fenster, M. S., Dolan, R., and Elder, J. F. 1993. A new method for predicting shoreline positions from historical data. *Journal of Coastal Research.* 9:147-171.

Fenster, M. S., and Dolan, R. 1993. Historical shoreline trends along the outer Banks, North Carolina. Processes and responses. *Journal of Coastal Research.* 9:172-188.

Forbes, D. L., 1987, Shoreface sediment distribution and sand supply at C^2S^2 sites in the southern Gulf of St. Lawrence. *Coastal Sediments '87* :694-709.

Howd, P. A., and Birkemeier, W. A. 1987. *Beach and nearshore survey data, 1981-1984, Technical Report CERC-87-9.* Fort Belvoir Va.: Coastal Engineering Research Center.

Leatherman, S. P. 1983. Historical and projected shoreline mapping. *Coastal Zone '83..* 3:1902-1909.

Michener, W. K., Jefferson, W. H., Karinshak, D. A., and Gilbert, C. 1993. Incorporating global positioning system technology into coastal mapping and research efforts. In H. S. Bolton (ed) *Coastal Wetlands:*332-346. New York: American Society of Civil Engineers.

Mitsch, W. J., and Gosselink, J. G. 1986.*Wetlands*. New York: Van Nostrand Reinhold.

Morton, R. A. 1979. Temporal and spatial variations in shoreline changes, and their implications, examples from the Texas Gulf Coast. *Journal of Sedimentary Petrology*. 49:1101–1111.

Morton, R. A. 1991. Accurate shoreline mapping-past, present and future.*Coastal Sediments '91*. 2:997-1010.

Morton, R. A., and Paine, J. G. 1990. Coastal land loss in Texas - An overview. *Transactions Gulf Coast Association of Geological Societies*. 40:625-634.

Morton, R. A., Leach, M. P., Paine, J. G., and Cardoza, M. A. 1993. Monitoring beach changes using GPS surveying techniques. *Journal of Coastal Research*. 9:702-720.

Morton, R. A., Paine, J. G., and Gibeaut, J. C. 1994. Stages and durations of post-storm beach recovery, southeastern Texas Coast. *Journal of Coastal Research*. 10:884-908.

National Research Council 1990a. *Sea-level change*. Washington: National Academy Press.

National Research Council 1990b. *Managing coastal erosion*. Washington: National Academy Press.

Niemeyer, H. D. 1993. Long-term morphodynamical behaviour of the East Frisiam Islands and coast. In J. List (ed) *Large-scale Coastal Behavior '93*. U.S. Geological Survey Open-File Report 93-381:145-148.

Olsson, I. U. 1986. Radiometric dating. In B. E. Berglund (ed), *Handbook of Holocene Palaeoecology and Palaeohydrology*: New York: John Wiley & Sons.

Peltier, W. R. 1987. Deglaciation-induced vertical motion of the North American continent and transient lower mantle rheology. *Journal of Geophysical Research*. 91:9099-9123.

Pilkey, O. H., Morton, R. A., Kelley, J. T., and Penland, S. 1989. *Coastal Land Loss. Short Course Notes, 28th International Geological Congress*. Washington: American Geophysical Union.

Pilkey, O. H., Young, R. S., Riggs, S. R., Sam Smith, A. W., Wu, H., and Pilkey, W. D. 1993. The concept of shoreface profile of equilibrium. a critical review. *Journal of Coastal Research.* 9:255-278.

Sclafani, V., Jones, B., and Carney, D. F. 1993. Using GIS to monitor wetla... loss/gain. *Coastal Zone '93.* 1:847-859.

Shalowitz, A. L. 1964. *Shore and sea boundaries..* Publication 10-1. Washington: U.S. Dept. of Commerce.

Short, A. D., and Hall, W. 1991. Long-term wave height and beach profile changes, Narrabeen Beach, Australia. In J. H. List (ed) *Large-scale Coastal Behavior '93.* U.S. Geological Survey Open-File Report 93-381:177-180.

Stafford, D. B. 1971. *An aerial photographic technique for beach erosion surveys in North Carolina, Tech. Memo. 36*: Fort Belvoir, Va: Coastal Engineering Research Center.

Thieler, E. R., and Danforth, W. W. 1994. Historical shoreline mapping(1). Improving techniques and reducing positioning errors. *Journal of Coastal Research.* 10:549-563.

U.S. Army, Corps of Engineers, 1977, *Shore Protection Manuel., Vols. I, II, and III.* Coastal Engineering Research Center: Fort Belvoir, Virginia.

Walsh, S. J., Lightfoot, D. R., and Butler, D. R. 1987. Recognition and assessment of error in geographic information systems. *Photgrammetric Engineering and Remote Sensing.* 53:1423-1430.

White, W. A., Tremblay, T. A. 1994. Submergence of wetlands as a result of human-induced subsidence and faulting along the upper Texas Gulf Coast. *Journal of Coastal Research.* 10, p.

Williams, S. J., Dodd, K., and Gohn, K. K. 1991. *Coasts in Crisis. Circular 1075.* Washington: U.S. Geological Survey.

Wijnberg, K. M., and Terwindt, J. H. J. 1993. The analysis of coastal profiles for large-scale coastal behavior. In J. H. List (ed) *Large-scale Coastal Behavior '93.* U.S. Geological Survey Open-File Report 93-381:224-227.

Wright, H. L. III, and Pilkey, O. H. Jr. 1989. *The effect of hard stabilization upon dry beach width.* Durham N.C: Duke University, Program for the Study of Developed Shorelines.

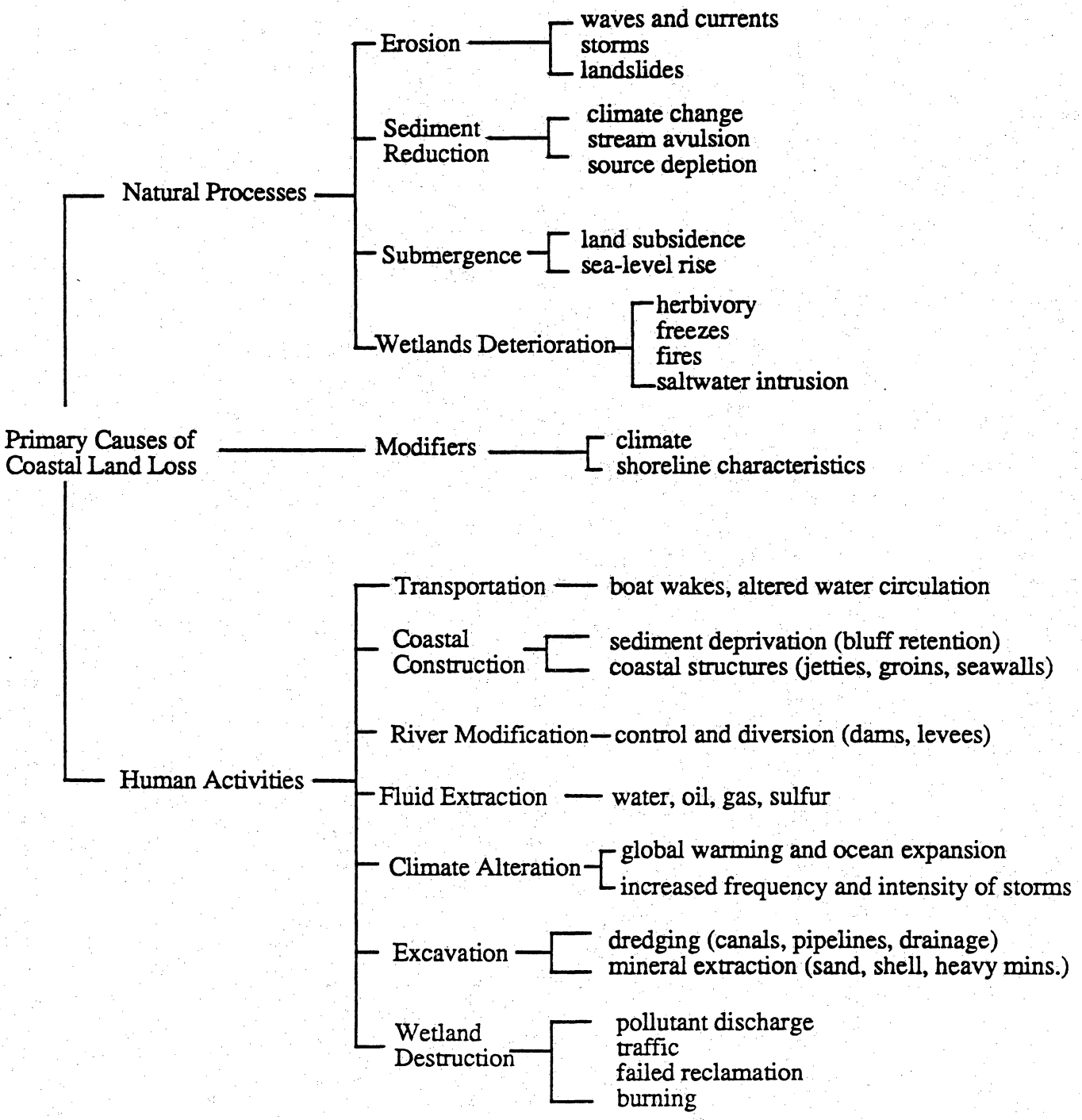
Primary Causes of Coastal Land Loss
Natural Processes
Erosion
waves and currents
storms
landslides
Sediment Reduction
climate change
stream avulsion
source depletion
Submergence
land subsidence
sea-level rise
Wetlands Deterioration
herbivory
freezes
fires
saltwater intrusion
Modifiers
climate
shoreline characteristics
Human Activities
Transportation
boat wakes, altered water circulation
Coastal Construction
sediment deprivation (bluff retention)
coastal structures (jetties, groins, seawalls)
River Modification
control and diversion (dams, levees)
Fluid Extraction
water, oil, gas, sulfur
Climate Alteration
global warming and ocean expansion
increased frequency and intensity of storms
Excavation
dredging (canals, pipelines, drainage)
mineral extraction (sand, shell, heavy mins.)
Wetland Destruction
pollutant discharge
traffic
failed reclamation
burning

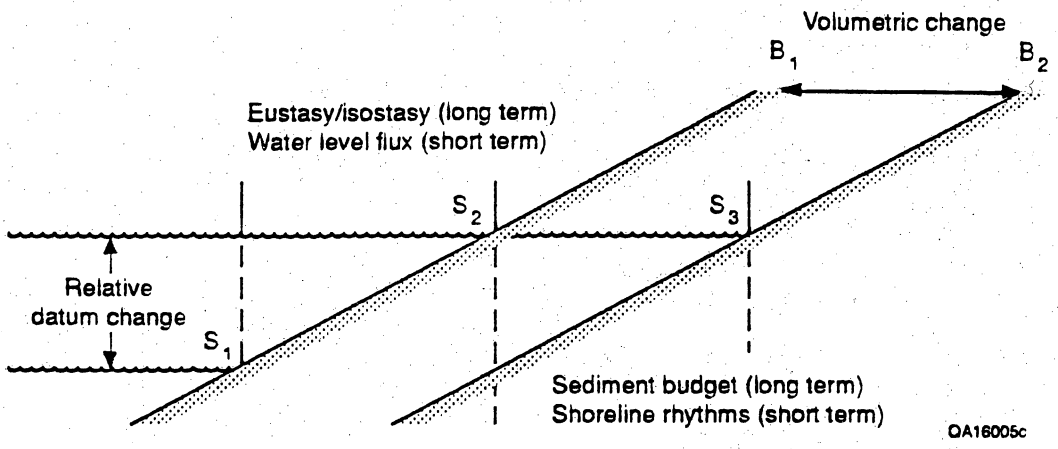

B. Morton
1-21-
4.0.

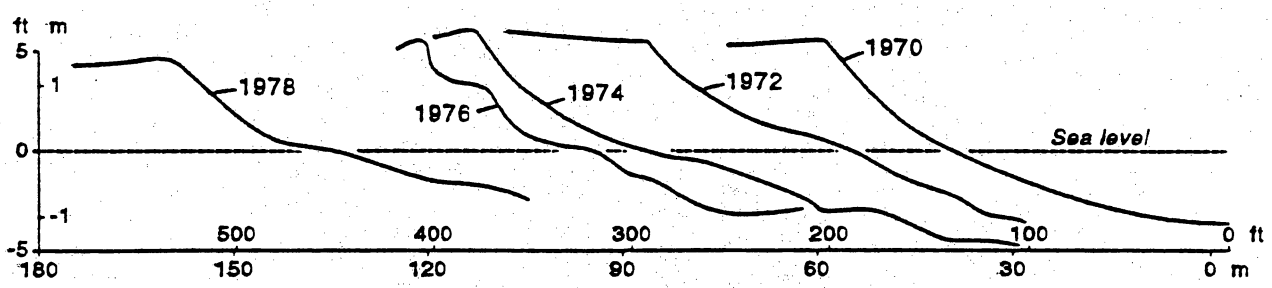

QAa3280c

Morton 1/A P 18/9

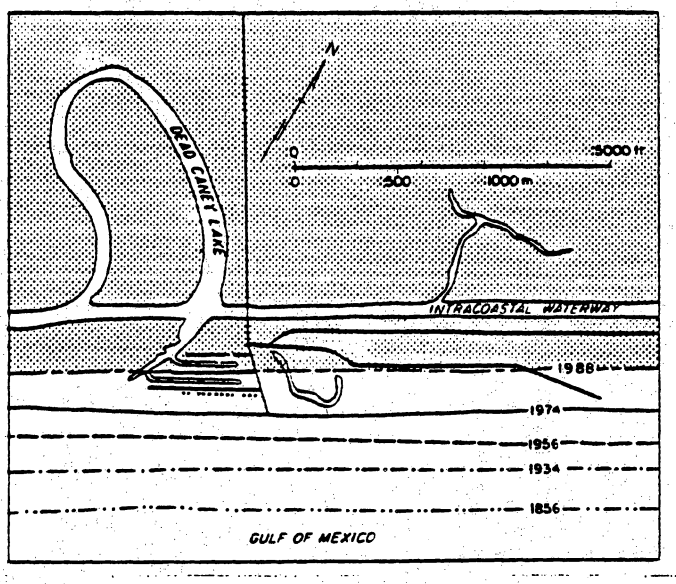
N
0
0
500
1000 m
5000 ft
DEAD CANEY LAKE
INTRACOASTAL WATERWAY
1988
1974
1956
1934
1856
GULF OF MEXICO

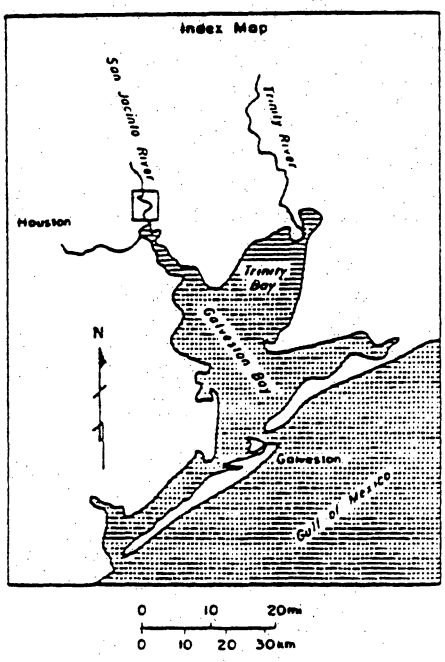

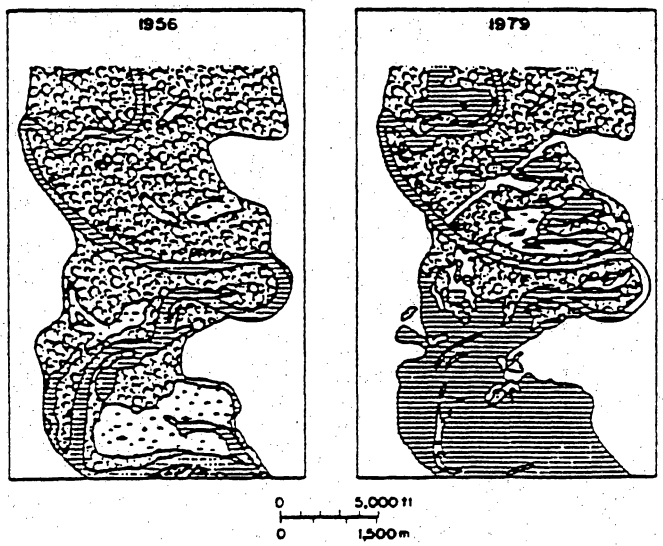

Wetland Map Unit	1956		1979		Net Change	
	Acres	Hectares	Acres	Hectares	Acres	Hectares
Water	875	355	2,295	930	+1,420	+ 575
Fluvial Woodlands & Swamps	3,480	1,410	2,090	845	−1,390	− 565
Fresh to Brackish Marsh	650	265	300	120	− 350	− 145

QA 937

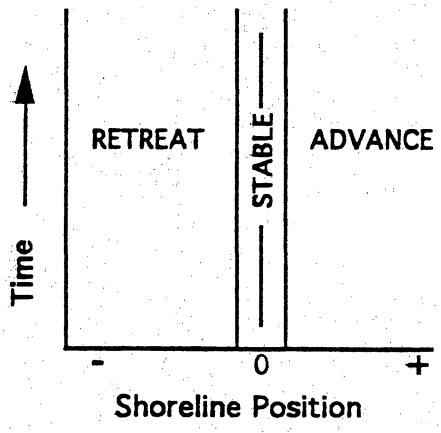
RETREAT
STABLE
ADVANCE
Time
-
0
+
Shoreline Position

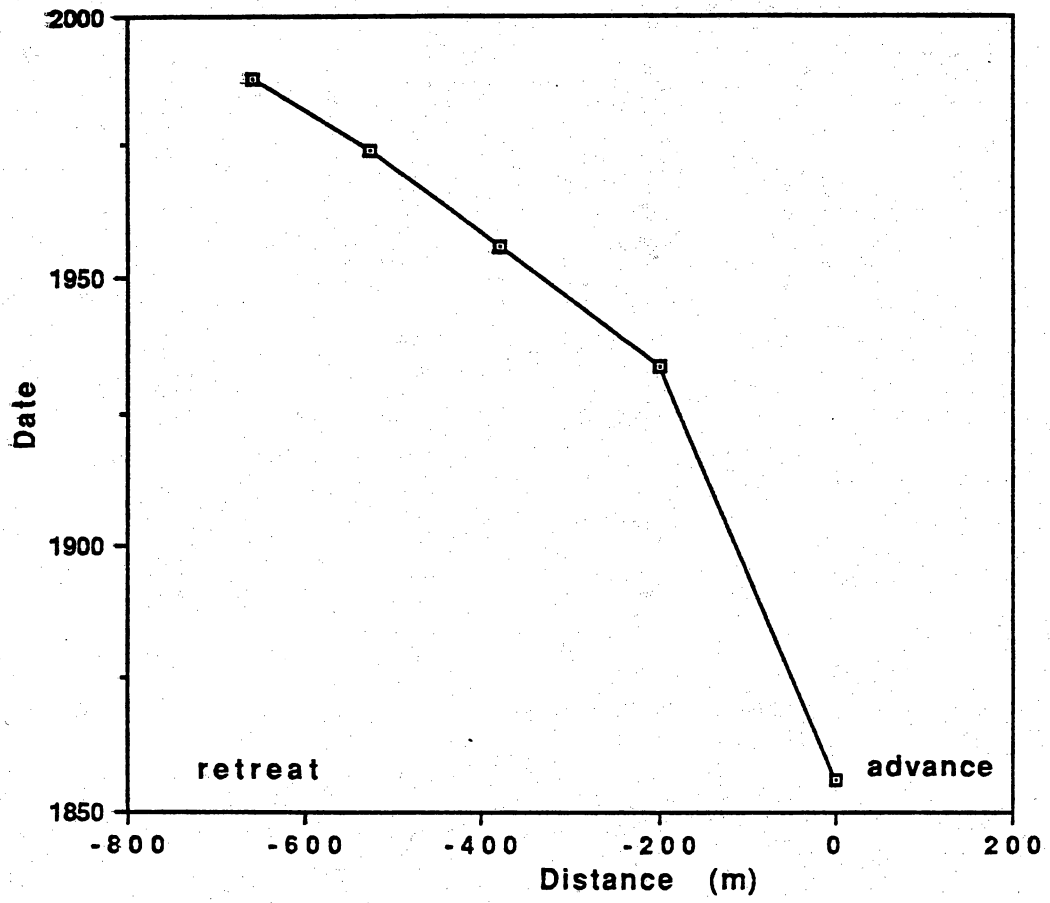
2000
1950
1900
1850
Date
retreat
advance
-800
-600
-400
-200
0
200
Distance (m)

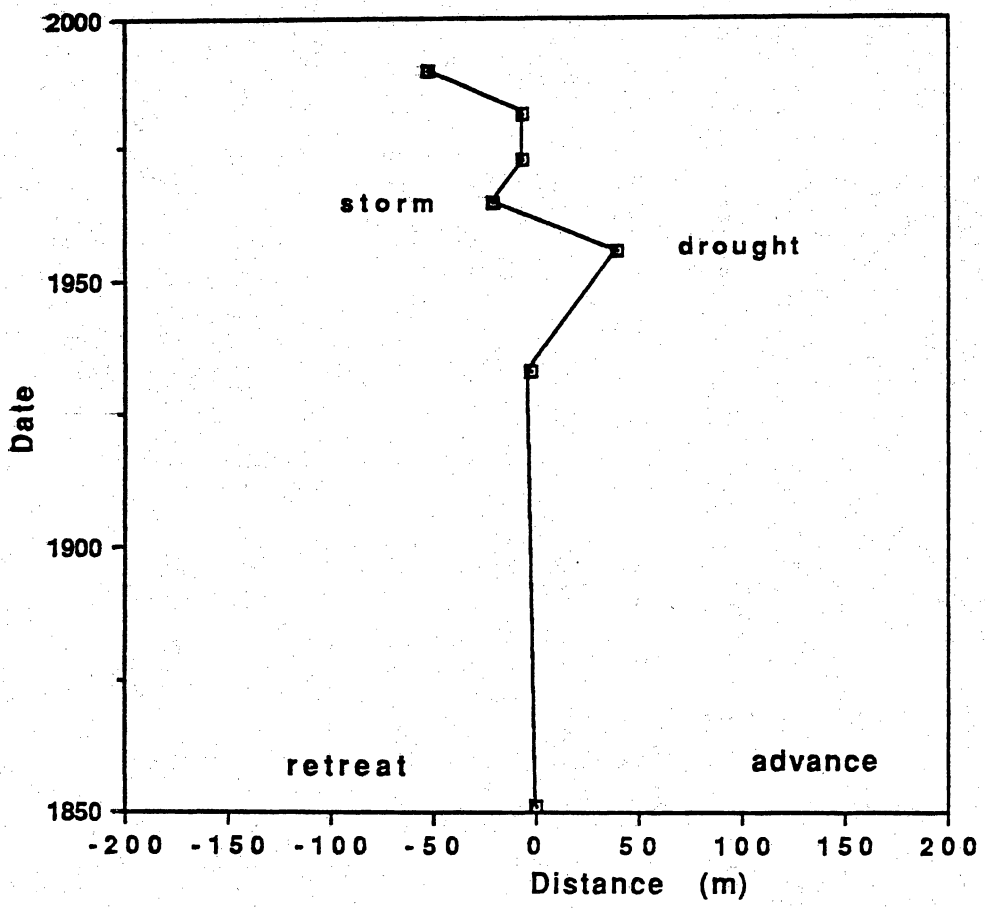
2000
1950
1900
1850
Date
storm
drought
retreat
advance
-200
-150
-100
-50
0
50
100
150
200
Distance (m)

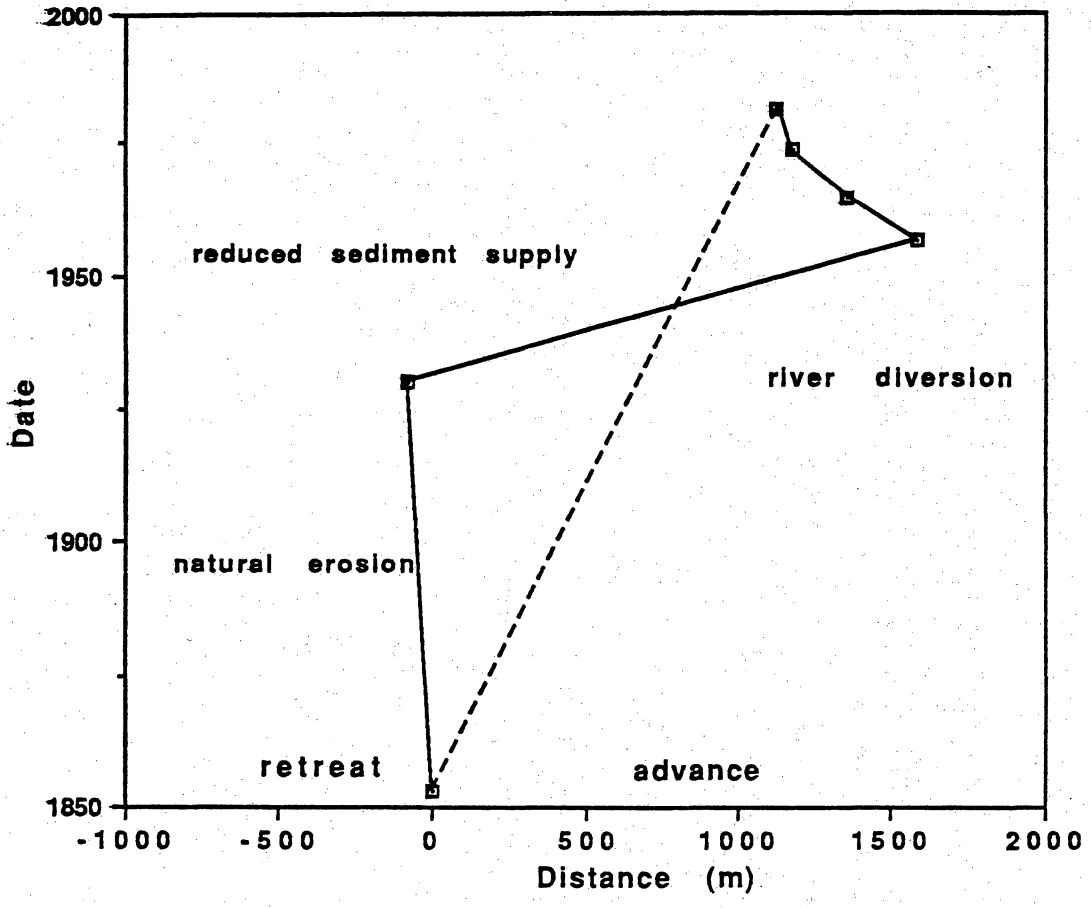
2000
1950
1900
1850
Date
reduced sediment supply
river diversion
natural erosion
retreat
advance
-1000
-500
0
500
1000
1500
2000
Distance (m)